DESIGN OF STABLE INTER-PILLAR SPANS AT TAU LEKOA MINE

Michael John Dunn

A research report submitted to the Faculty of Engineering, University of the Witwatersrand, Johannesburg, in partial fulfilment of the requirements for the degree of Master of Science in Engineering.

Perth, 2007

DECLARATION

I declare that this research report is my own, unaided work. It is being submitted for the Degree of Master of Science in Engineering in the University of the Witwatersrand, Johannesburg. It has not been submitted before for any degree or examination in any other University.

_____ (Student No. 9706012G)

_____ day of _____ 2007

ABSTRACT

Since the commencement of mining at Tau Lekoa Mine in 1991, large geologically controlled falls of ground (FOG) have been problematic. Crush pillars are used to control these instabilities. Limiting of panel spans and cutting of pillars results in practical problems and production constraints which influence labour efficiencies, productivity and ultimately the economics of mining.

This study analysed 81 large FOG that occurred over 1991 to 2001 using statistical methods. Statistical distributions describing the falls of ground, rock mass properties and mining parameters were determined. A probabilistic approach was used to evaluate stable spans and the crush pillar stability.

The probability of large hanging wall instabilities was assessed for several mining situations using a Fault Tree methodology.

Larger spans are possible provided an appropriate internal support system is designed. A probabilistic or risk based design approach is recommended as this is considered more logical than a deterministic approach.

In memory of my grandparents:

Jack Dunn

Thelma Dunn

Desmond Duffey

Rose Duffey

ACKNOWLEDGEMENTS

I would like to thank Professor T.R. Stacey for his advice, guidance and patience throughout the study.

My appreciation is extended to the management of AngloGold Ashanti and Tau Lekoa Mine for permission to conduct this study.

The assistance of the Tau Lekoa Mine Rock Engineering Department in gathering data for this study is gratefully acknowledged. In particular I would like to thank Joggie van Oort, Godwin Hungwe and Ozias Sehlabaka.

The support of Johan Laas is also gratefully acknowledged.

I would especially like to thank my wife Alyson for her patience, understanding and encouragement during this study.

TABLE OF CONTENTS

APPENDICES

LIST OF FIGURES

LIST OF TABLES

GLOSSARY OF ACRONYMS AND SYMBOLS

ACRONYMS

BIC	Bushveld Igneous Complex
CG	Centre gully
FOG	Fall of ground
FOS	Factor of safety
FTA	Fault tree analysis
GCD	Ground control district
KMMA	Klerksdorp Mine Managers Association
MC	Main Channel
MTC	Middle Terrace Conglomerate
MTS	Middle Terrace and Slope
PDF	Probability density function
PEM	Point estimate method
RC	Reworked Channel
RGA	Regional geotechnical area
UT	Upper Terrace
VCR	Ventersdorp Contact Reef
VR	Vaal Reef

SYMBOLS

ν	Poisson's Ratio
σ_1	Major principal stress (MPa)
σ_3	Minor principal stress (MPa)
σ_C	Uniaxial compressive strength
cm	centimetre
E	Young's Modulus
e	Extraction ratio
F	Factor of safety
h	Pillar height
K_c	Confinement strength factor
kN	Kilo Newton
m	metre
m^2	Square metres
m^3	Cubic metres
M_L	Local magnitude
mm	millimetre
MPa	Mega Pascal
S	Span
T	Fallout thickness (m)
w	Pillar width
σ_p	Pillar stress
σ_r	Residual pillar strength
σ_s	Peak pillar strength
σ_v	Vertical stress

1 INTRODUCTION

Extensive hard rock tabular mining is conducted in South Africa, mainly related to the exploitation of the Witwatersrand Basin and the Bushveld Igneous Complex. Mining is conducted from near surface down to a depth of approximately 3.5km. A wide range of support types are used including: pillar systems, backfill, packs, elongates and tendons. In the shallower to intermediate mining environments, various pillar systems are used in conjunction with elongate and pack support whilst in deeper mines, stabilizing pillars and backfill are used with elongates and packs. Tau Lekoa Mine is the subject of this study and falls within the intermediate mining environment.

1.1 Location and Description of Tau Lekoa Mine

Tau Lekoa Gold Mine is one of four mines making up the Vaal River Operations of AngloGold Ashanti. The mine is situated 170 kilometres south west of Johannesburg near the town of Orkney in the North West Province of South Africa (Figure 1.1). The mine exploits the Ventersdorp Contact Reef (VCR) of the Witwatersrand Basin. Shaft sinking operations began in 1986, with production commencing in 1991, and this is currently expected to continue until 2015. About 2 million tons of ore is mined per annum producing approximately 8 tons of gold per annum.

The VCR is a tabular reef and in the Tau Lekoa lease area extends from 800m to 1700m below surface. Shallower and deeper extensions to the orebody are situated to the east and west respectively of the current mining lease area. Two vertical shafts from surface, one for men and material (MM Shaft) and the other for rock and ventilation (RV Shaft) are used to access the orebody. The shaft infrastructure is protected by means of a 500m by 400m elliptical shaft pillar.

Due to the complex geological environment, a scattered mining method is employed with pre-developed access tunnels in the footwall. The pre-developed raises are spaced 120m to 180m apart (Figure 1.2). The main levels are spaced

150m apart, which at the average dip of 27 degrees results in a raise length of 300m. Following ledging of the raises, breast mining is conducted in a strike direction.

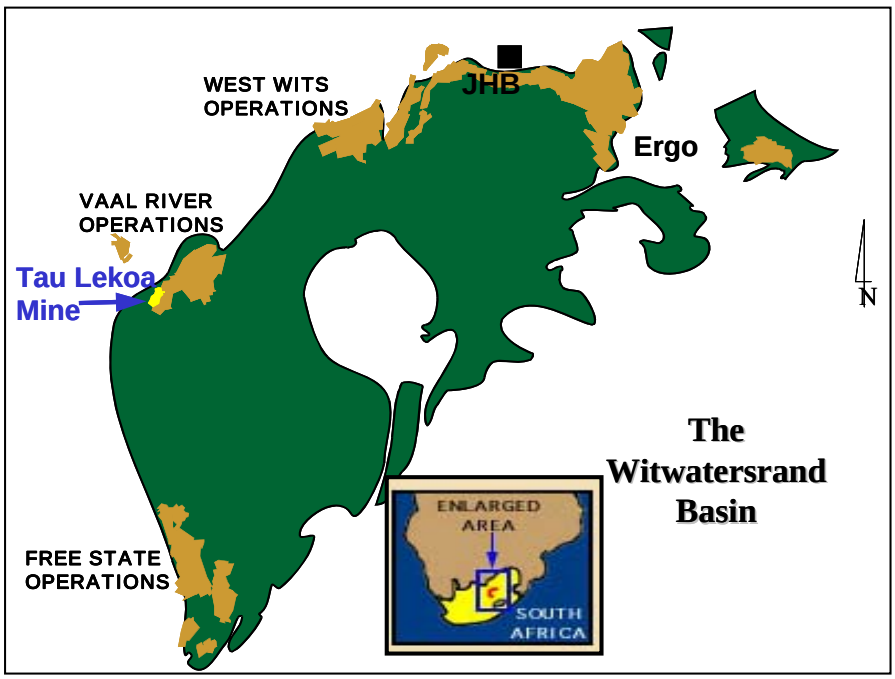

Figure 1.1 Location of Tau Lekoa Mine (not to scale)

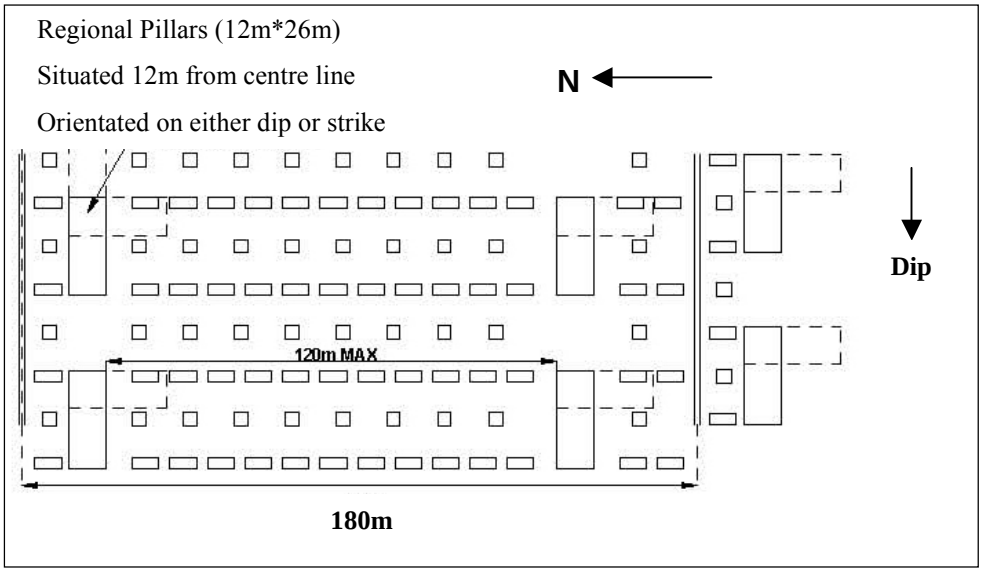

Figure 1.2 Raiseline and pillar layout at Tau Lekoa Mine

1.2 Overview of large hangingwall instabilities on Tau Lekoa Mine

Large falls of ground or hangingwall instabilities have occurred in stope panels at Tau Lekoa Mine since the commencement of production. Between 1991 and the end of 2001, 107 incidents were recorded in a database for large falls of ground. In a number of cases, relatively small falls of ground were included in the database and in some instances the information was incomplete. These records have been filtered out and reasonably reliable and complete data are available for 81 of these large falls of ground (Appendix A). Locally, these large falls of ground are referred to as dome collapses. This terminology is misleading, as three different types of large hangingwall instability have been identified, namely:

- wedge failure;
- dome failure;
- wedge / dome failure.

The scale of these instabilities ranges from a few metres to tens of metres with a mass range of tens to thousands of tons. Structures contributing to the collapse are often extremely difficult to identify in a mining environment where stress induced fracturing of the hangingwall and poor illumination are common. Figures 1.3 and 1.4 are examples of large FOG at Tau Lekoa Mine

Figure 1.3 Dome collapse with part of the dome still intact in the hangingwall

Figure 1.4 Large wedge collapse (a) with vertical jointing (b) and bounded on the upper side by a prominent flat dipping vein (c)

When production commenced in 1991, the initial method was down dip mining leaving crush pillars 30m apart with timber composite packs as internal support (Figure 1.5). The first collapses occurred when the faces had advanced ±30m. In-stope pillars were then introduced at irregular intervals but collapses continued to occur when certain spans were exceeded.

Due to poor efficiencies associated with cutting pillars when mining down dip, the mining method was changed to breast mining with crush pillars left on strike. The maximum stable span was determined to be 20m through back analysis by Harris and Rosenblatt (1993). Pack support was found to be ineffective due to low closure rates and the internal support was changed to a system with a higher initial stiffness. Mine poles were used for stoping widths less than 1.8m and 3m resin bolts at stoping widths greater than 1.8m.

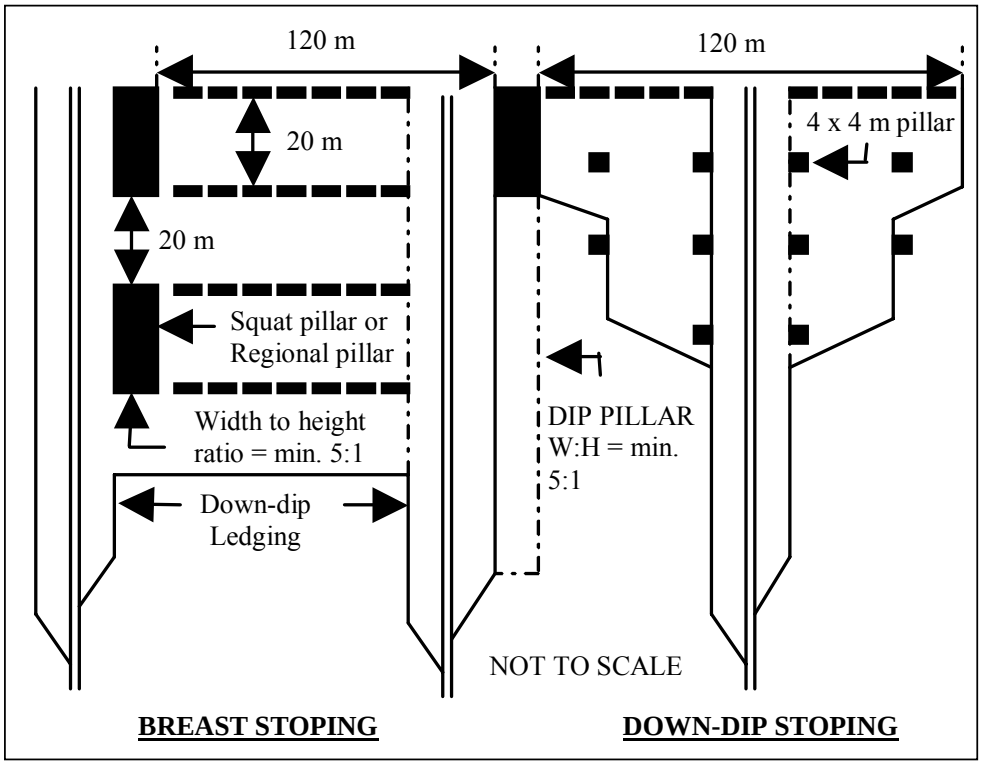

Figure 1.5 Early stoping layouts at Tau Lekoa Mine (Judeel and Laas, 1999)

Collapses continued to occur and mid-panel pillars were left at irregular intervals when problems were identified. Leaving of mid-panel pillars became a standard in

1995. In-stope support was also changed from mine poles to profile props and 1.5m grouted rockbolts replaced resin bolts. Pre-stressing devices on the timber elongates were introduced at the end of 1997 to limit blasting out of support and ensure active support close to the face.

Currently a conventional strike pillar layout with a face length of 20m is used. Mid-panel or in-stope pillars are left every 16m along strike when mining in a northerly direction and every 10m along strike when mining in a southerly direction or at stoping widths greater than 1.8m (Figure 1.6). Three support standards have been designed to cater for the following conditions:

- North mining at a stoping width less than 1.8m
- North mining at a stoping width greater than 1.8m
- South mining at a stoping width less than 1.8m

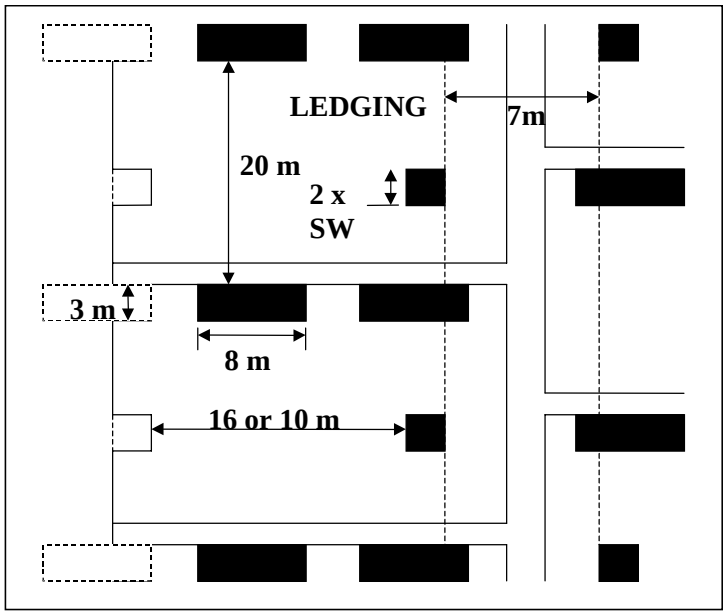

Figure 1.6 Current Tau Lekoa stope panel layout

The maximum span between the crush pillars is based on an empirical relationship between span and fallout thickness based on back analysis of large hangingwall instabilities (Judeel and Laas, 1999). According to this relationship, the fallout

thickness is generally 0.125 times the inter-pillar span. The internal support standards are designed to cater for the thickness of hangingwall instability that could be expected based on this relationship.

1.3 Problem statement

The current Tau Lekoa Mine stope support strategy appears to have been successful in controlling large hangingwall instabilities with a general downward trend in the number of occurrences. However, large hangingwall instabilities still occur occasionally.

The requirement of cutting of regular mid-panel pillars and limiting face length to 20m is problematic from a production perspective negatively influencing face advance and labour efficiencies. Mid-panel pillars also reduce the percentage extraction by approximately four to five percent.

Underground observations of large stable spans indicate that spans could possibly be increased without negative implications. Often large hangingwall instabilities seem to be clustered in certain areas.

The empirical relationship, on which the inter-pillar span design is based, has a poor statistical correlation of approximately 30 to 35 percent. This poor relationship is manifested in large instabilities at relatively small spans and large spans that appear stable.

These observations highlight the problems associated with the current inter-pillar span design and there are concerns that some panels or areas are either being over- or under- supported. The problem can be summarised as follows:

Large hangingwall instabilities at Tau Lekoa pose a threat to both safety and productivity. Leaving crush pillars and limiting spans can successfully control these instabilities. However, the current design does not take cognisance of

specific geological and rock mass conditions, thus either overestimating or underestimating support requirements to the detriment of safety or production or both.

The aim of this research project is the investigation of factors governing the stability of spans in between crush pillars and crush pillar stability on Tau Lekoa Mine. It is hoped that by reviewing the current design and defining various geotechnical relationships, the current design can be optimised with benefits in terms of safety, productivity and increased profitability.

1.4 Objectives of this study

The primary objectives of the research project are to:

- Review the current inter-pillar span and crush pillar design;
- Investigate factors influencing the stability in between pillars;
- Attempt to identify different geotechnical relationships;
- Apply a probabilistic approach to determining stable spans and crush pillar design;
- Assess the risk factors contributing to large hangingwall instabilities.

1.5 Research methodology

An overview of the project approach and methodology is briefly outlined below.

1.5.1 Research context

Stable inter-pillar spans at Tau Lekoa can be defined as the spacing between crush pillars at which large hangingwall instabilities are not likely to occur. Large hangingwall instabilities can be defined as the following:

- An instability that exceeds the capability of support installed in between crush pillars.
- Instability over a large area of a panel, mainly due to structurally controlled instability or rock mass failure.
- Instability, mainly due to instability of one or several crush pillars.

The focus of this research will be major instabilities over a large area of a panel and will include an investigation of stable spans and crush pillar design. The following hypothesis will be tested during this study:

Stable inter-pillar spans are highly dependent on the local geology and rock mass character. A critical review of the design and definition of geotechnical relationships could result in an optimised Stope Support Strategy that would benefit safety, and increase productivity and profitability at Tau Lekoa Mine.

1.5.2 Research approach

The research approach adopted is outlined below.

Literature review

Literature pertaining to pillar systems design has been reviewed with a focus on stable span and crush pillar design approaches and this is covered in Chapter 2.

Data collection

Data have been collected for various aspects that could influence inter-pillar and pillar stability as follows:

- Geotechnical data;
- Large instability investigations;
- Inter-pillar spans and pillar dimensions.

Review of current design

The current design will be reviewed to identify possible shortcomings and potential improvements.

Analysis of large hangingwall instabilities

Data on large falls of ground will be evaluated statistically to establish relationships and determine statistical distributions for contributing mining and geotechnical factors and will be covered in Chapter 4.

Probabilistic evaluation of the pillar system design

A probabilistic approach will be applied to the pillar system design based on a statistical analysis of large hangingwall instabilities. This will include the evaluation of pillar layouts and spans using JBlock (Esterhuizen, 1996) and the application of the Point Estimate Method to crush pillar design. This will be covered in Chapters 5 and 6.

Risk assessment

In Chapter 7 the main factors influencing stable spans and crush pillar stability will be identified and evaluated in terms of risk. This will include the determination of statistical distributions for pillar dimensions and spans.

Discussion, conclusions and recommendations

Results for the study will be discussed in Chapter 8. Conclusions and recommendations arising from the study are covered in Chapter 9.

1.6 Chapter Summary

This chapter provides a brief history of large hangingwall instabilities at Tau Lekoa Mine and the evolution of the stope support strategy. The research methodology for this project has been described.

2 LITERATURE REVIEW

In the previous chapter the problems controlling large geologically defined collapses at Tau Lekoa Mine were outlined. The evolution of the current pillar system design was discussed and some of the weaknesses highlighted in terms of the design approach and the practical implications of applying the current design. This chapter will review literature pertaining to the stable spans and the design of crush pillars.

2.1 Stable inter-pillar spans

According to Swart *et al* (2000) the design methods available for assessing the stability of stopes can be categorised as follows:

- empirical methods;
- analytical methods;
- observational methods.

Empirical methods can be defined as experience based applications of known performance levels. Examples of empirical methods are rock mass classifications and statistical analysis of underground observations.

Analytical methods involve the application of conceptual models with the aim of reproducing behaviour and response. Closed form solutions, numerical methods and structural analysis are examples of analytical methods. These methods are useful for making comparisons and assessing sensitivity for varying input parameters.

Observational methods rely on the monitoring of the rock mass deformation during mining to detect instabilities. This approach is data driven and should start early in the implementation of a design, to allow sufficient data to be generated.

This allows the design to be revised when appropriate. An example of this approach is the New Austrian Tunnelling Method (NATM).

For this study, the focus will be primarily on using empirical and analytical methods with emphasis on a probabilistic approach for the design of a pillar system. This will consider both stable inter-pillar spans and the design of crush pillars.

Various methods have been applied to determine stable stope or panel spans defined as the distance between in-panel pillars. At Tau Lekoa Mine the term inter-pillar stability is often used when referring to stable panel spans. The stability of the span between pillars is a function of the pillar spacing and the ability of the internal support to control or prevent large-scale panel collapses (Haile and Jager, 1995). The design of safe panel spans must take into account:

- variability in the immediate beam thickness;
- intensity, orientation and alteration of hangingwall jointing;
- rock strength;
- horizontal stresses;
- key block failure and block dimensions.

2.1.1 Failure modes

Haile and Jager (1995) identified six different modes of failure in pillar supported hard rock mines within the Bushveld Igneous Complex (BIC). They are as follows:

Keyblock failure

Where two or more mutually intersecting joints are present in the stope hangingwall and create an unstable block geometry.

Wedge failure

Where two major planes of weakness intersect in the stope hangingwall. The areal extent of the failure is generally far greater than that of key block failure.

Buckling failure

When the hangingwall beam buckles and failure is not defined solely by joint geometry.

Beam shear failure

Failure occurs due to slip on widely spaced and sub-vertical planes of weakness or initiated as fractures close to pillars or abutments.

Cooling dome failure

Failure is initiated due to fallout on shallow dipping joints on the periphery of an upside–down basin shaped block of rock. Domes are approximately circular in shape and vary in size from a few square metres to several hundred square metres. They are common across the whole of the BIC.

Unravelling failure

Occurs when the hangingwall of the stope contains a prominent joint set of uniform dip and direction and the hangingwall span between pillars exceeds a certain critical limit.

2.1.2 Failures at Tau Lekoa Mine

With the possible exception of buckling failure, all of the above failure modes have been observed on Tau Lekoa Mine. For dome failures, the upper size limit appears to be tens of square metres as opposed to several hundred square metres. Not all the dome structures are formed by cooling of the lava. In some cases, it appears that flat faulting along the VCR and hangingwall lava contact has deviated from the contact plane and ramped up into the hangingwall resulting in dome structures.

In some cases, more than one failure mode has been observed. For the purposes of this study the focus will be on the more commonly observed types of failure, namely:

- wedge failure;
- dome failure;
- wedge / dome failure.

2.1.3 Design methods for stable spans

Several common approaches to the design of stable spans are outlined below.

Rock mass classification systems

The use of rock mass classification systems appears to be wide spread and has been used in a wide range of mining environments to determine stable spans. Swart *et al* (2000) reviewed several rock mass classification systems and concluded that the following four systems could be considered for evaluating the stability of panel spans:

- The Geomechanics Classification or Rock Mass Rating (RMR) system developed by Bieniawski (1973).
- The Norwegian Geotechnical Institute (NGI), rock quality index or Q-System developed by Barton *et al* (1974).
- The Mining Rock Mass Classification or Modified Rock Mass Rating (MRMR) system developed by Laubscher (1977).
- The Modified Stability Graph Method using the Modified Stability Number (N') developed by Mathews *et al* (1981).

Over the years some of these systems have been modified to suit local conditions. Watson and Noble (1997) reviewed several systems and concluded that the Modified Q-system provided the most accurate description of observed

conditions. However, it did not take into account stress influences and discontinuity orientation.

York *et al*. (1998) reviewed various rock mass rating systems available and found the Impala Platinum Mine adaptation of the Q-system resulted in the best correlation between the rating and actual observed conditions. This system had been adapted to take into account major unfavourable geological structures (Human, 1997) and was applicable to platinum mines exploiting the Merensky Reef (MR).

A Critical Panel Span Design Chart based on an analysis of stable and collapsed panels on the MR was developed. From this work it was concluded that some collapses did not agree with the chart and that a greater understanding of the rock mass was required specifically in terms of stress conditions and discontinuity persistence and orientation.

Recent work by Watson (2004) has resulted in a modified version of the rock mass rating method originally described by Mathews *et al* (1981) and revised by Hutchinson and Diederichs (1996). The new rock mass rating system is termed the 'New Modified Stability Graph'.

From research on various rock mass classification systems, several conclusions were reached and are covered in detail by Swart *et al* (2000). However, in terms of the Tau Lekoa Mine problem, the most applicable was that rock mass classification systems only describe rock mass failure and do not consider other potential failure mechanisms such as beam, block, wedge or dome failures.

Statistical or experience based design

A survey conducted by Haile and Jager (1995) indicated that the design of stope panel spans was primarily based on experience gained in a particular environment over the years. In many cases, the use of unstable versus stable spans statistics forms the basis of stope panel span design.

Harris and Rosenblatt (1993) and Rosenblatt (1994) applied this approach on Tau Lekoa Mine and investigated a number of stable and unstable panels. They concluded that there were no unstable cases at panel spans of 20m or less. This approach was taken further and refined with the establishment of an empirical relationship between panel span and the fallout thickness (Judeel and Laas, 1999). Additional work on this approach has highlighted various shortcomings and the need for an approach that considers all factors influencing panel spans (Dunn, 2000; Dunn 2003; Dunn 2004.)

Analytical methods

Analytical methods include numerical modelling, keyblock analysis and beam analysis.

Beam theory: Swart *et al* (2000) provide a comprehensive overview of beam theory and this will not be repeated. They conclude that elastic beam theory is useful in explaining the deformation and failure of the hangingwall in bedded deposits and can be used to design safe panel spans provided the limitations are understood. However, when sub-vertical jointing is present in the hangingwall, Voussoir beam theory should be applied as tensile strength of the beam is zero. Voussoir beam theory was applied by Akermann (1999) at Amandelbult Platinum Mine. The RMR System (Bieniawski, 1973) was used to determine the rock mass modulus and the design charts developed by Beer and Meek (1982) were applied. Treloar and Steenkamp (2000) applied elastic beam theory in the design of spans at Western Chrome Mines.

Keyblock theory: Stope hangingwall instabilities at Tau Lekoa Mine are often controlled by the presence of geological discontinuities such as joints, veins, faults and lava flow planes. The intersection of these discontinuities can result in the formation of wedges, which can fall or slide out from the hangingwall. This type of environment is suitable for the application of keyblock methods.

The application of keyblock methods is dependent on the correct interpretation of the structural geology and the identification of unstable wedges and blocks. With conventional deterministic keyblock analysis (Goodman and Shi, 1985), the natural scatter is ignored and mean values used. The influence of joint continuity is often disregarded as joint and excavation planes are assumed to be of infinite length.

Probabilistic methods, such as used in JBlock (Esterhuizen, 1996) can be applied to overcome these problems. Esterhuizen and Streuders (1997) applied this approach in a mining environment that included both geological discontinuities and stress fractures. They were able to evaluate different support standards and determine whether keyblocks occur between support units or have potential to fail the support units. The procedure is repeated several thousand times to determine a probability of keyblock failure. It was concluded that this approach was suitable for evaluation of support effectiveness in environments where large numbers of geological discontinuities and stress fracturing are exposed in excavations.

Daehnke et al (1998) evaluated various keyblock models and concluded that a probabilistic approach to keyblock analysis was best suited to keyblock stability analysis. It was shown that as the keyblock size increases the probability of falling out between support units decreases but the probability of failing the support increases. This approach has subsequently been applied in the design of stable spans on various platinum mines (Akermann, 1999; Johnson and Noble, 2004).

Numerical modelling: York et al (1998) used 2-dimensional UDEC modelling to evaluate the stability of a jointed stope hangingwall. Two joint sets were included, a horizontal set and a set with a dip that was varied between 5 and 90 degrees. Various spans were modelled with different joint properties such as friction angles and joint roughnesses. From this modelling a series of design charts were developed for determining stable spans. The influence of support and support spacing was also evaluated. A panel span design methodology using

numerical modelling was outlined. UDEC modelling was used to evaluate stable spans on Amandelbult mine (Mares and Akermann, 1997).

2.2 Crush pillar design

Ozbay and Roberts (1988) described fractured or crush pillars as a subset of yield pillars, which are fractured by face abutment stresses whilst being cut and are formed at their residual strength. A residual strength of 13MPa at a strain of 0.4 was back calculated from underground observations. It was noted that at stoping widths of 1 m to 1.8 m, pillars should not exceed a width-to-height ratio (w:h) of 2:1.

Ryder and Ozbay (1990) provided a design overview of both squat (w:h > 5) and slender (w:h < 5) pillars and a description of pillar behaviour. This included defining a number of correction factors for pillar size, shape, width to height ratio, foundation damage and creep as well as the use of a numerical modelling programme (BEPIL) for the design of pillars. It was noted that the residual strength of a 2:1 pillar was at least 5 to 10 percent of its peak strength.

Ozbay *et al* (1995) reviewed pillar system design practices in the South African hard-rock tabular mining sector and noted that the use of small width to height ratio pillars (w:h < 3) increased with depth where the residual pillar strength was sufficient to meet support resistance requirements. The term “crush pillars” was used for pillars intended to crush while they are still part of the face. It was noted that the design of crush pillars was generally based on using dimensions that had worked elsewhere under similar geotechnical conditions and this was adjusted through observation.

York *et al* (1998) developed a preliminary methodology in the form of a design chart based on numerical modelling. Efforts were also made to instrument and back analyse a crush pillars at Amandelbult and Impala Platinum mines.

Esterhuizen (1993) showed that variability in rock mass properties and mining factors could be taken into consideration for hard-rock pillar design by statistical methods. York and Canbulat (1998) concluded that a probabilistic approach was needed for pillar design to cater for the large variability in material and loading conditions. A probabilistic approach has also been applied in the design of chromitite pillars (Wesseloo and Swart, 2000; Joughin *et al*, 2000) with the application of the Point Estimate Method (PEM).

2.3 Chapter Summary

This chapter has outlined the various approaches that have been taken and can be taken when designing stable spans and crush pillars. It is interesting to note that probabilistic methods have been applied to both stable span and pillar design. The following chapter will describe the geological and geotechnical environment.

3 GEOLOGY AND GEOTECHNICAL OVERVIEW

The previous chapter reviewed literature pertaining to the design of stable spans and crush pillars and highlighted that probabilistic methods have been applied in both cases. This review showed the importance of geological and geotechnical aspects with regard to stable spans and pillars. This chapter will describe the Tau Lekoa Mine geological and geotechnical environment.

3.1 Geological setting

The geological setting is described from a regional, district and mine wide perspective. Tau Lekoa Mine is located in the Klerksdorp goldfield, which is one of several goldfields in the greater Witwatersrand Basin.

3.1.1 The Witwatersrand Basin

The Witwatersrand Basin was a large inland sea in which sedimentation took place some 2.8 billion years ago. The sedimentary sequences that were deposited, comprise intercalated formations of shales, quartzites and conglomerates. The gold bearing reefs of the Witwatersrand Basin vary widely, but the majority are conglomerates, which make up a small portion of the sedimentary column (Ryder and Jager, 2002). This series of sediments is known as the Witwatersrand Supergroup.

The Witwatersrand Basin is the main gold bearing structure in Southern Africa and extends from Evander in the east to Welkom and Klerksdorp in the west. The Witwatersrand Basin is 450km by 300km and is about 7km thick. Sedimentation was halted by the outpouring of lava (Ryder and Jager, 2002).

The gold bearing reefs of the Witwatersrand have been exploited for over a hundred years and during this time seven major goldfields were developed,

namely the: Free State, Klerksdorp, West Wits Line, West Rand, Central Rand, East Rand and Evander goldfields (Ryder and Jager, 2002)

3.1.2 The Klerksdorp Goldfield

Witwatersrand rocks outcrop in and near Klerksdorp and the area emerged as a significant goldfield in 1933 when Western Reefs Exploration and Development Company Limited began a detailed exploration programme. The programme was successful and resulted in the establishment of Western Reef Mine in 1942 (Anon., 1998). There are a number of operations in the Klerksdorp Goldfield and they are listed below:

- AngloGold Ashanti Vaal River Operations consisting of Great Noligwa, Kopanang, Moab Khotsong and Tau Lekoa mines.
- African Rainbow Minerals Limited (formerly Vaal Reefs shafts 1-7).
- Hartebeesfontein, Buffelsfontein and Stilfontein mines.

The Vaal Reef (VR), C-Reef (CR), Elsburg Reefs and the Ventersdorp Contact Reef (VCR) are the main reefs that have been exploited in the Klerksdorp area. The goldfield has a strike length of 35km NE to SW, a maximum width of 23km and an average mining depth of 2km over the last 25 years (Ryder and Jager, 2002).

3.1.3 Tau Lekoa Geology

Tau Lekoa Mine exploits the Ventersdorp Contact Reef (VCR) within the Klerksdorp Goldfield. The VCR lies unconformably on the Gold Estates Formation (GE) of the Central Rand Group and is overlain by the Klipriviersberg Group of the Ventersdorp Supergroup (Fourie, 1999).

A stratigraphic column and section for Tau Lekoa Mine are shown in Figure 3.1 and Figure 3.2 respectively. The tabular VCR dip varies between 25 and 35

degrees to the north-west. The channel width varies between 0.1m and 3m, with an average stoping width of 1.6m (Dunn, 2000).

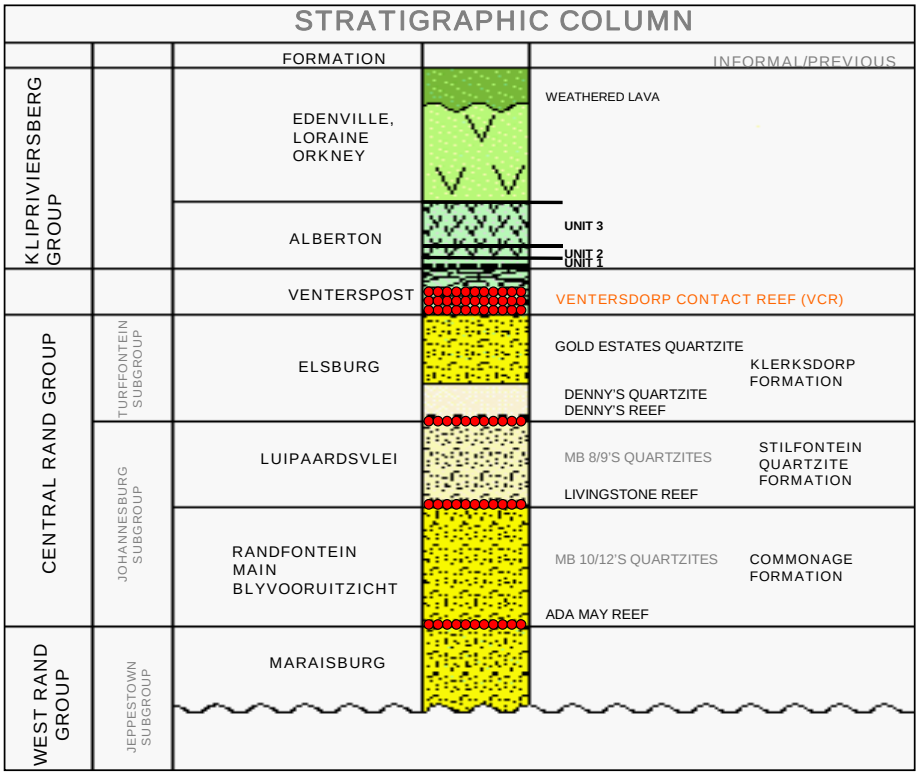

Figure 3.1 Stratigraphic column for Tau Lekoa Mine (De Fries, 2001)

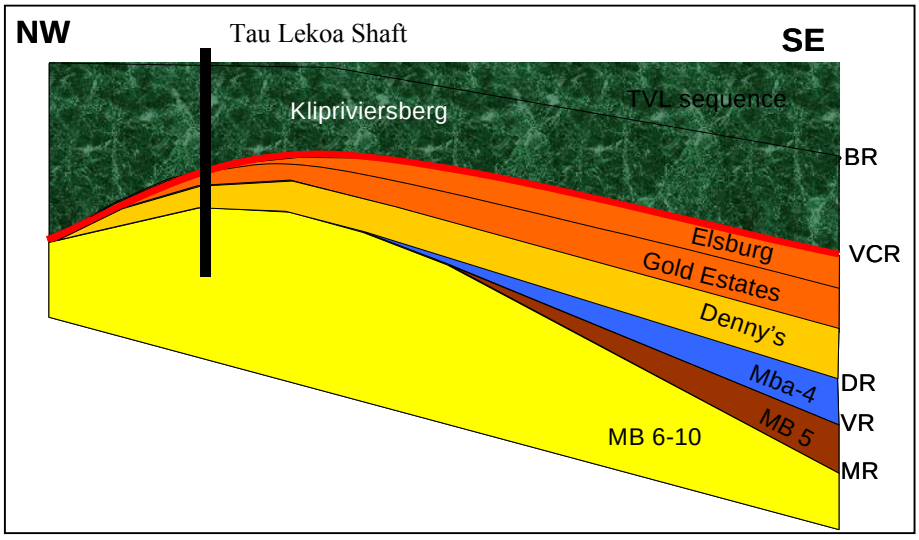

Figure 3.2 Schematic section through Tau Lekoa Mine (De Fries, 2001)

VCR Sedimentology

The VCR was deposited on a major unconformity surface of the underlying Witwatersrand Super Group. This resulted in an irregular palaeo-topography, comprising channels and terraces separated by small slopes. The sedimentary process ceased with the outpouring of lava of the Ventersdorp Supergroup (Ryder and Jager, 2002).

The Tau Lekoa mining lease can be divided into distinct geo-zones based on the palaeo-depositional setting. By using the contact between the Unit 1 and Unit 2 lavas as a datum, a picture of the palaeo-topography was generated across the Tau Lekoa lease (Frith, 1998). Initially four geo-zones were identified namely the: Main Channel, Reworked Channel, Middle Terrace and Slope, and the Upper Terrace areas.

These geo-zones were further refined during 2000 and the Upper Terrace was split into thick conglomerate areas (with a channel width of greater than 40cm), and areas of thin conglomerate (channel width less than 40cm). The Middle Terrace and Slope areas are subdivided based on whether they were adjacent to the Upper Terrace comprising thick or thin conglomerates (Biddulph, 2001). This has resulted in the following geo-zones:

- Main Channel (MC)
- Reworked Channel (RC)
- Middle Terrace Conglomerate (MTC)
- Middle Terrace and Slope (MTS)
- Upper Terrace (UT)
- Upper Terrace Plateau (UTP)

The relative position of the different geo-zones and the spatial distribution of the geo-zones at Tau Lekoa Mine are shown in Figures 3.3 and 3.4 respectively.

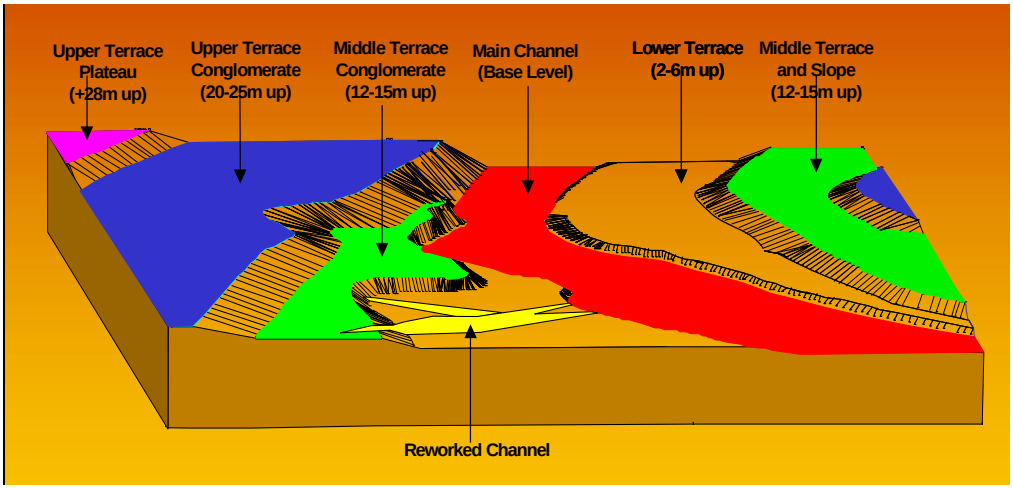

Figure 3.3 Depositional environment showing the relative position of the five geo-zones (Frith, 1998)

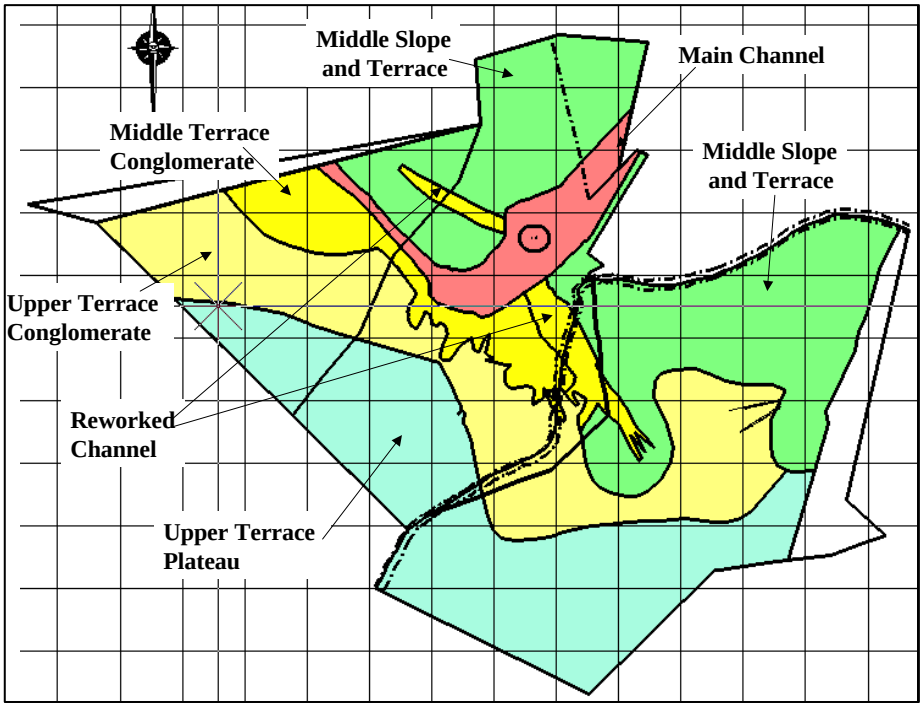

Figure 3.4 Plan showing geo-zones at Tau Lekoa Mine

The VCR underwent various stages of erosion and degradation contemporaneous with a constant sediment supply from the higher lying source area. This process produced the prominent hangingwall undulations (rolls) that are regularly encountered during routine mining operations (Biddulph, 2001). The landscape resultant from the processes described is characterised by a major channel system containing extensive

areas of thick conglomerate, with high lying remnant terraces and undulating slope reef (Figure 3.5).

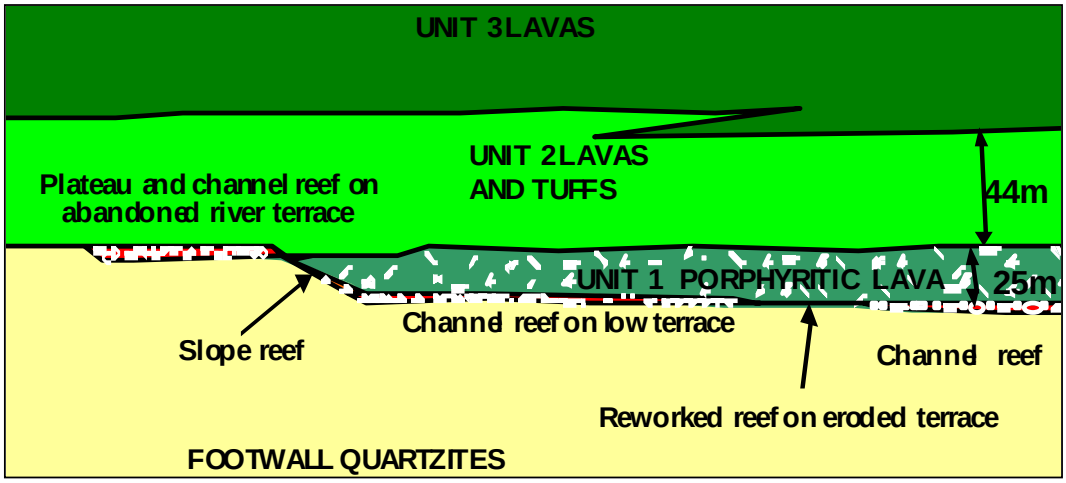

Figure 3.5 Section showing relationship between different reef types and the relative position of the different lava types (Frith, 1998)

Reef rolls

Reef rolls are common and are observed on a variety of scales and were formed as a result of deposition on a palaeosurface with pronounced topographic variations (Roberts and Schweitzer, 1999). Both strike and dip rolls are encountered, and rolls are often associated with strata control problems such as excessive stoping widths.

On-strike down-rolls are considered especially hazardous as mining often proceeds into the VCR hangingwall. The occurrence of a roll and low angle faulting that deviates from the VCR and lava contact can result in the formation of dome structures within the hangingwall.

Faulting

Several major normal faults tending mainly NE-SW and dipping SE and in some cases NW are present (Figure 3.6). There are also numerous smaller faults sympathetic to the major structures as well as faults trending E-W and ENE–WSW. The majority of faults are normal although reverse faults are encountered. Throws range from a few centimetres to hundreds of metres. Low angle thrust faulting is commonly observed along the VCR / lava contact with a mylonite filling present

between the lava and the VCR in some areas (Dunn, 2004). This faulting results in ground control problems.

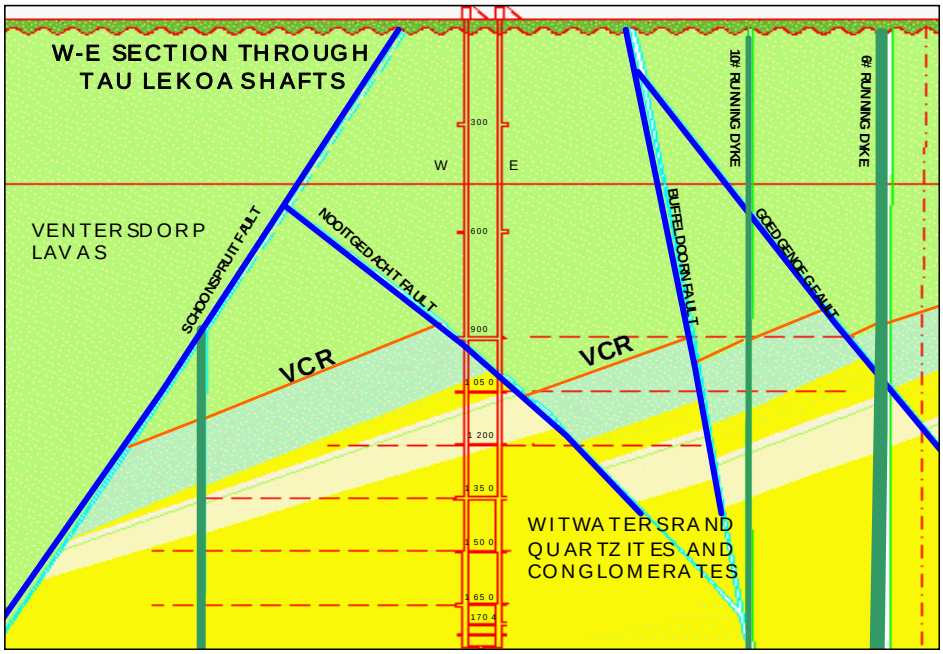

Figure 3.6 West-East section through Tau Lekoa Mine

Dykes

There are several major dykes such as the 6-Shaft Running Dyke and 10-Shaft Running Dyke both trending north–south and the Pick Advance Dyke trending east-west. Numerous smaller dykes sympathetic to the larger dykes are also present. Generally, the dykes are vertical or steeply dipping with some having throws varying from a few centimetres to hundreds of metres. Dyke thickness varies from less than a metre to tens of metres.

Veins and Jointing

Veins of quartzite or calcite and joints are common. The veins are often flat dipping and are especially hazardous. Two broad types of veins are recognised, namely: veins associated with cooling and mineralogical processes that usually have a random orientation; and veins associated with specific joint sets. Van der Heever (1983) identified three joint sets in the Klerksdorp area as described in Table 3.1.

Table 3.1 Joint sets in the Klerksdorp Goldfields

Dip	Dip Direction	Spacing
70°-90°	~335° (~NNW)	2m
50°-70°	~75° (~ENE)	7m-10m
Strata parallel	Strata parallel	1m

Initial joint surveys conducted on 900, 1050 and 1200 levels in 1989 indicated a prominent joint set trending north-south and dipping steeply towards the east (Harris, 1989; Lombard 1989). However, observations over several years indicated that more than one joint set was present but this was never quantified as regular joint surveys are not conducted by the Geology Department.

In mid-2000 the Tau Lekoa Rock Engineering Department began conducting limited joint surveys when visiting stoping panels. These surveys were limited in that the traverse was limited to the face length of a panel, generally 20m and the traverse was only conducted on dip introducing a bias.

Data from 33 panels were analysed making use of the DIPS program and several joint sets were identified (Figures 3.7 to 3.10). The north-south orientated joint set identified previously is the dominant joint set and is clearly visible on the Rosette plot. Four other joint sets have been identified by manually defining joint sets (Figure 3.10).

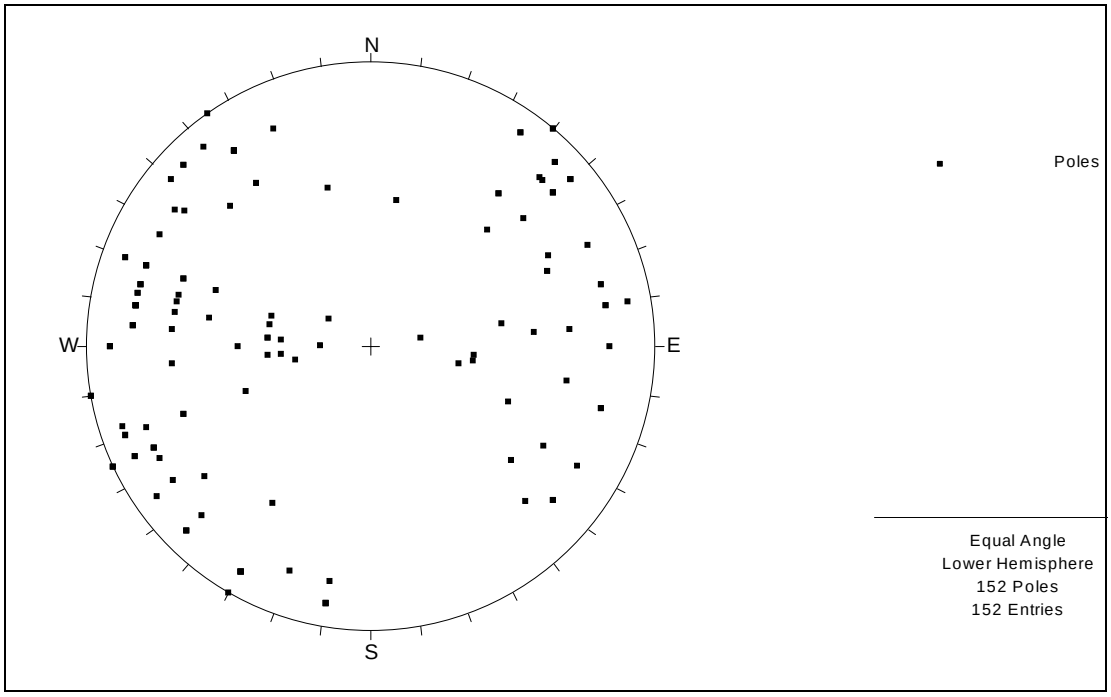

Figure 3.7 Joint poles plotted as dip and dip direction

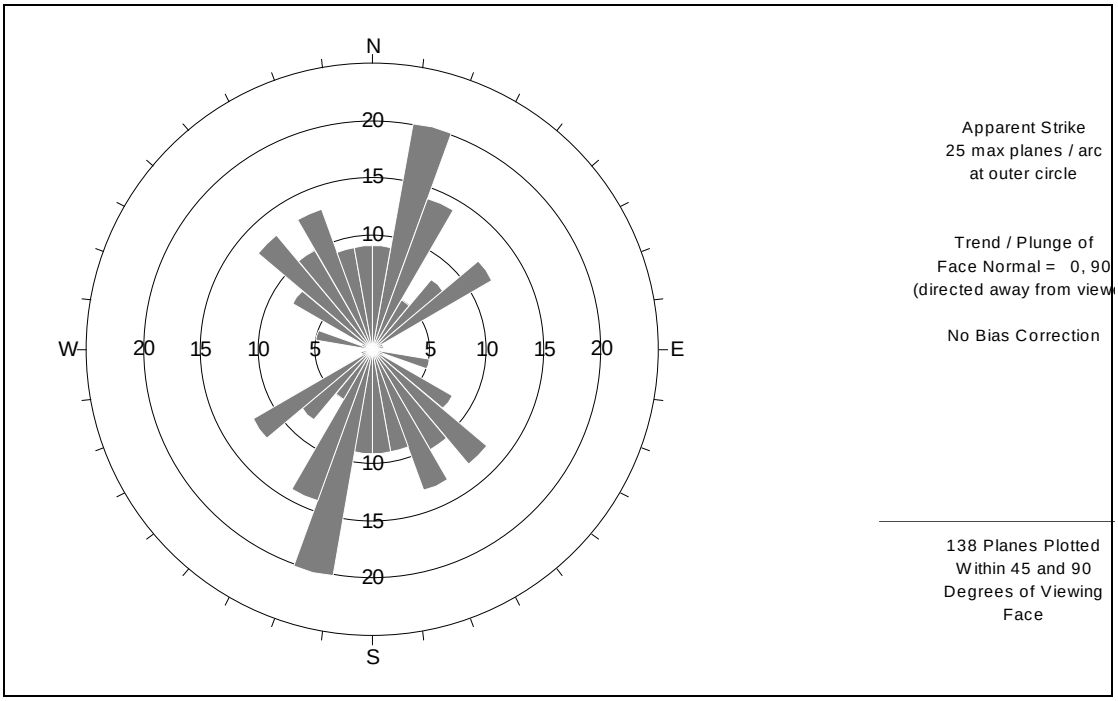

Figure 3.8 Joint rosette plot

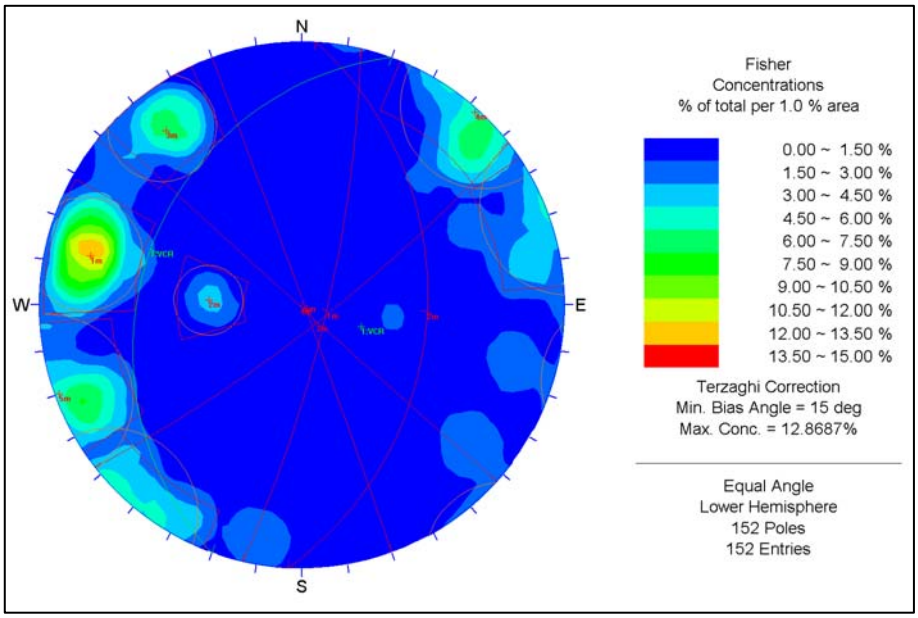

Figure 3.9 Contour plot of joint sets including VCR plane

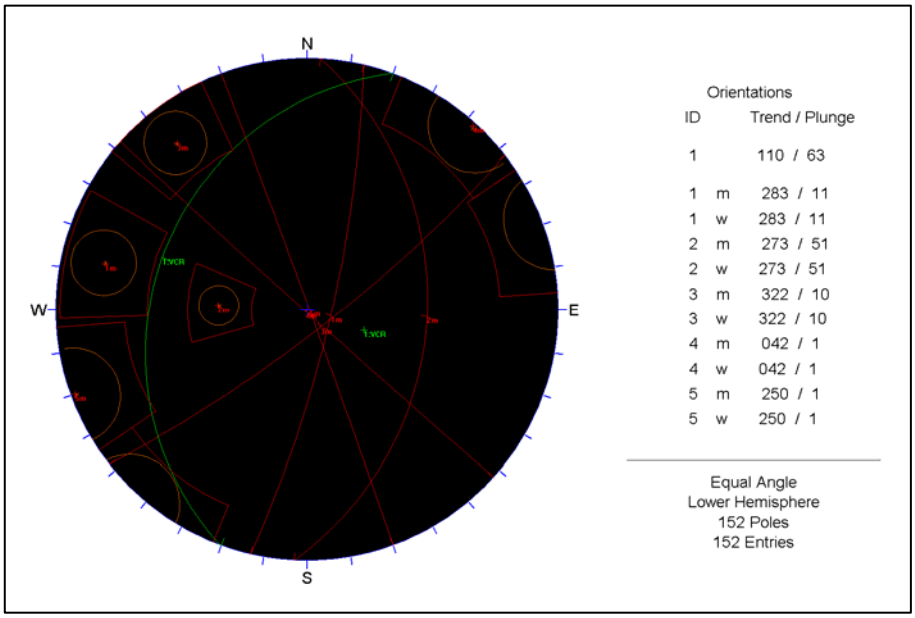

Figure 3.10 Manually defined joint sets based on contours

Utilising the panel joint surveys, an attempt was made to determine the average spacing for the five joint sets. It should be noted that due to the limited nature of the joint surveys this is not a definitive description of the joint spacing. Descriptive statistics have been determined in an attempt to describe the joint spacing and the

probability density function was determined for each set using the @Risk programme (Table 3.2). Figures 3.11 to 3.15 show the probability density functions and cumulative distributions for each joint set.

Table 3.2 Joint information summary

Set	Dip	Dip Dir.	Spacing (m)				Fit
			Mean	Std. Dev	Min.	Max.	
1	79	103	3.17	1.89	0.67	8.37	Logistic
2	39	93	2.70	1.18	1.20	4.80	Beta General
3	80	142	5.04	4.66	1.37	13.30	Pearson 5
4	89	222	0.80	0.49	0.13	1.92	Logistic
5	89	70	1.55	0.80	0.40	3.33	Ext Value

Joint set 2, is the flattest and often has a quartz or calcite infilling forming a prominent vein that is especially hazardous. The thickness of this vein has been observed to vary between a few millimetres to 10cm. This situation is often complicated with flat faulting along the VCR and lava contact. Joint sets 4 and 5 have similar dips close to 90 degrees and it is possible that they are part of the same set.

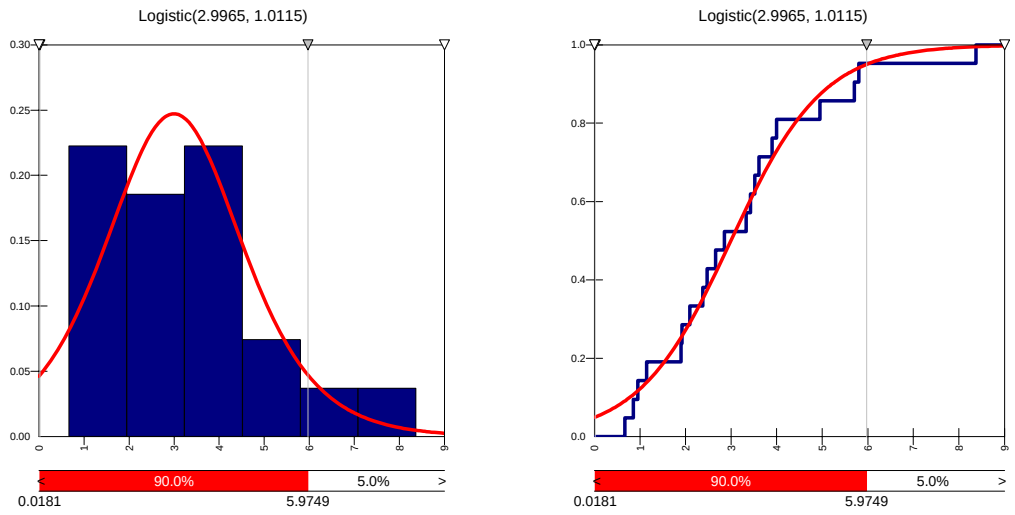

Figure 3.11 PDF and Cumulative distribution for spacing of Joint Set 1

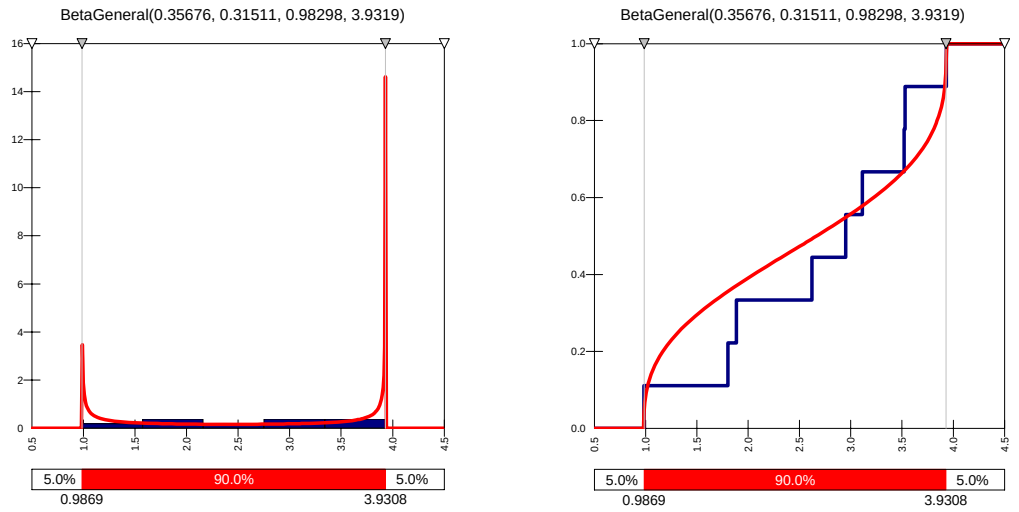

Figure 3.12 PDF and Cumulative distribution for spacing of Joint Set 2

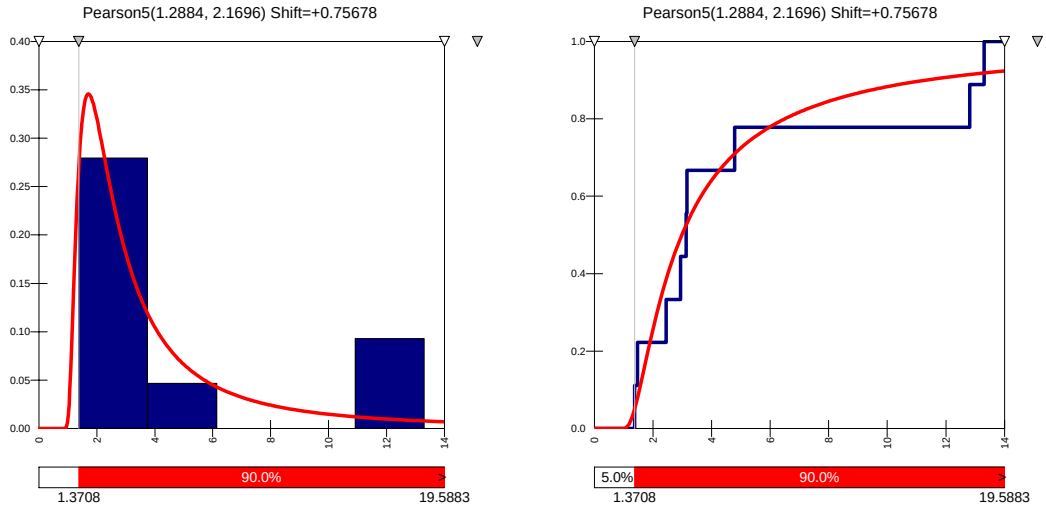

Figure 3.13 PDF and Cumulative distribution for spacing of Joint Set 3

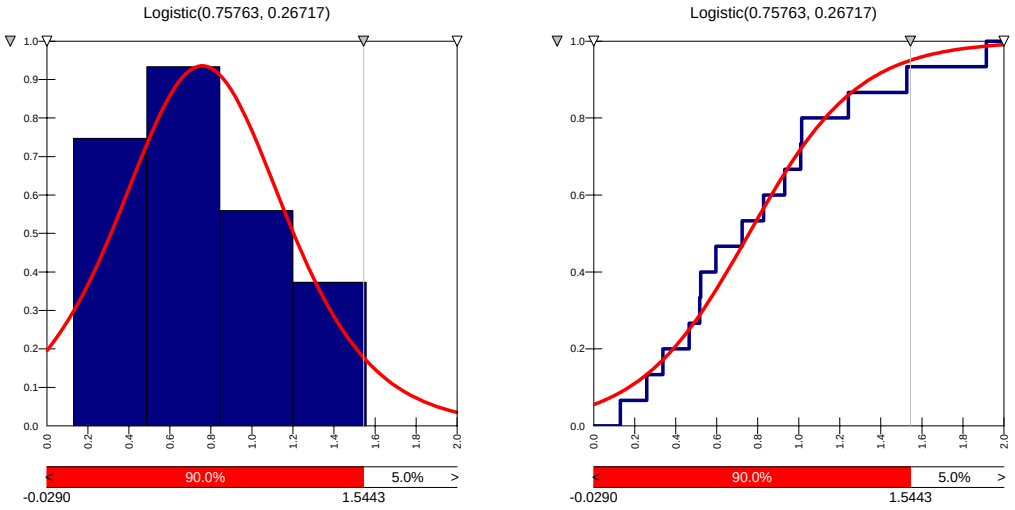

Figure 3.14 PDF and Cumulative distribution for spacing of Joint Set 4

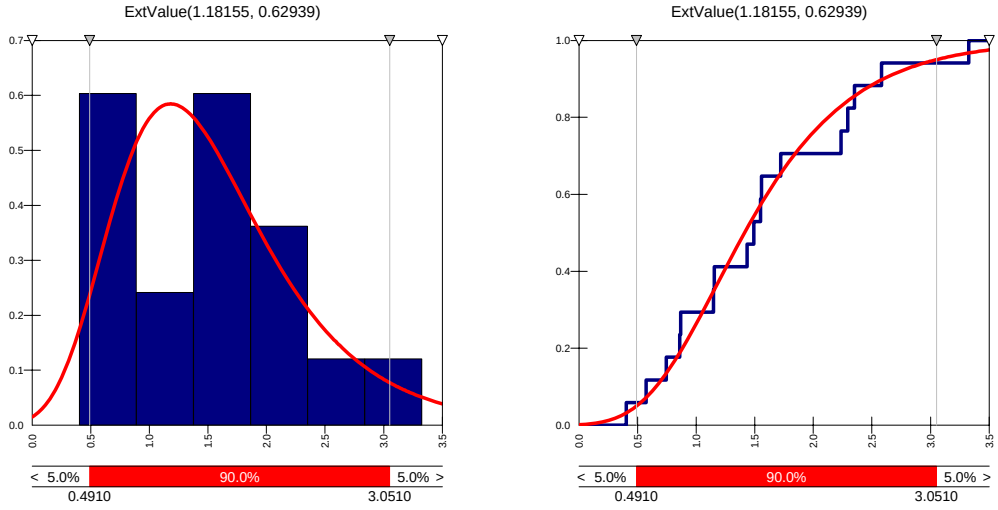

Figure 3.15 PDF and Cumulative distribution for spacing of Joint Set 5

Hangingwall structures

Pilloidal structures (load casts) are observed in the hangingwall (Figure 3.16). Low angle faulting often forms dome like structures when it deviates from the reef / lava contact. Ripouts, or lensoid structures in the VCR hangingwall (Figure 3.17) observed by Berlenbach (1995) in the West Wits area could be responsible for the formation of dome like structures observed at Tau Lekoa Mine. These

structures are related to a stick-slip mechanism along the faulted VCR / lava contact.

Imbricated systems (bedding parallel faults) often splay into imbricated fans or duplex structures (Figure 3.18). These structures can step up forming ramp structures (Roberts *et al*, 1996). This process is another possible mechanism that resulted in the formation of dome like structures observed at Tau Lekoa Mine. The occurrence of ramps in conjunction with steep dipping joints could explain many of the dome collapses observed at Tau Lekoa Mine.

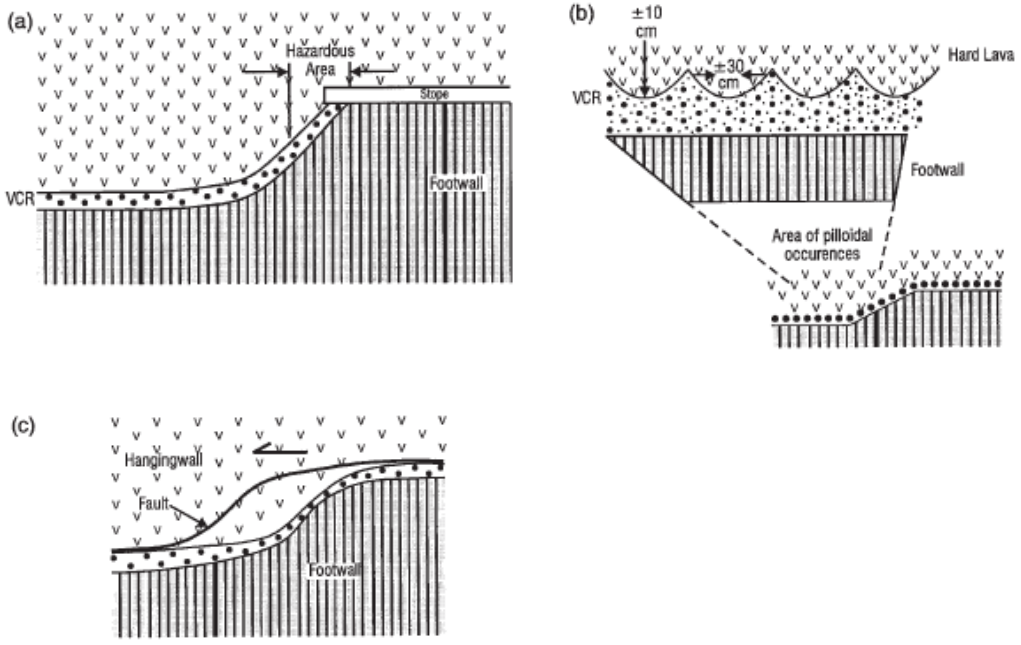

Figure 3.16 Pilloidal structures are often encountered at the terrace/slope transition (a and b). Flat faults between the VCR/ hangingwall contact do not follow the contact but forms a short-cut (c) resulting in hangingwall control problems when mining across rolls (after Roberts and Schweitzer, 1999).

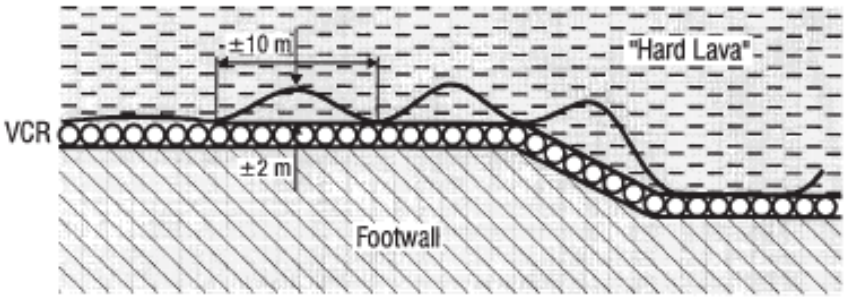

Figure 3.17 Ripouts in a hard lava (Roberts and Schweitzer, 1999**)**

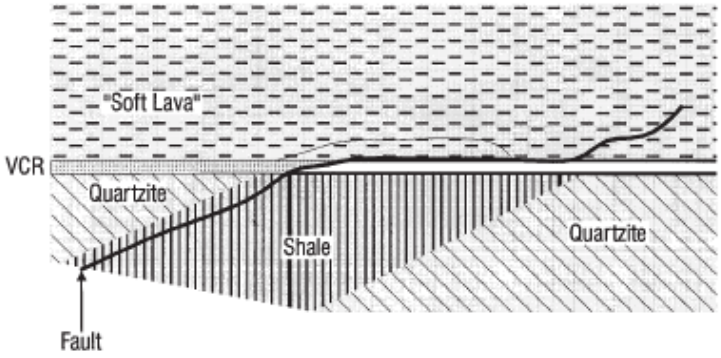

Figure 3.18 Flat faulting ramping into the hangingwall (Roberts and Schweitzer, 1999)

3.2 Geotechnical properties

The geotechnical properties of the hangingwall, VCR and footwall are described in the following sections.

3.2.1 Hangingwall lava strength properties

The Alberton lavas on Tau Lekoa Mine are subdivided into Units 1, 2 and 3 based on petrographical characteristics (De Fries, 2002). Both Unit 1 and Unit 2 lavas are encountered in the immediate hangingwall. In 1988 a suite of triaxial compression tests on samples of lava were done (Briggs, 1988) and the results are

summarised in Table 3.3. The strength parameters were determined to be as follows:

Uniaxial compressive strength (σ_C) = 248MPa
Average Young's Modulus (E) = 85.3GPa
Average Poisson's Ratio (ν) = 0.232
Confinement Strength Factor (K_c) = 12.5

Table 3.3 Triaxial compressive test results for Tau Lekoa lava samples

Sample	σ_1(MPa)	σ_3 (MPa)	E (GPa)	ν
3/1	241	5	80	0.199
3/2	456	10	82	0.246
3/3	459	20	94	0.250

Point Load tests were conducted on core samples from several boreholes to a distance approximately 30m above the reef contact (Lombard, 1989) and indicated σ_C values ranging between 160MPa to 320MPa

Additional uniaxial compressive tests were done in 1993 (Harris and Rosenblatt, 1993) and the following values were derived:

Uniaxial compressive strength (σ_C) = 135MPa
Average Young's Modulus (E) = 77.6GPa
Average Poisson's Ratio (ν) = 0.27

These tests yielded results that were substantially different to those previously obtained. No explanation was given for this difference, although it could possibly have been that samples of an altered lava were used.

Fourie (1999) conducted Point Load testing on 100 lava samples, which were grouped into a number of subclasses based on the physical characteristics of the lava samples. This data was used to determine descriptive statistics (Table 3.4)

and the probability density function (Figure 3.19) for the lava uniaxial compressive strength. Considering the variability in the lava strengths these values correlate reasonably well with previous values.

Table 3.4 Lava strength summary

	Calculated (Excel)	@Risk Fit
Distribution	NA	Logistic
Mean	232.6	227.283
Standard deviation	93.6	94.072
Minimum	70.4	-
Maximum	519.2	-

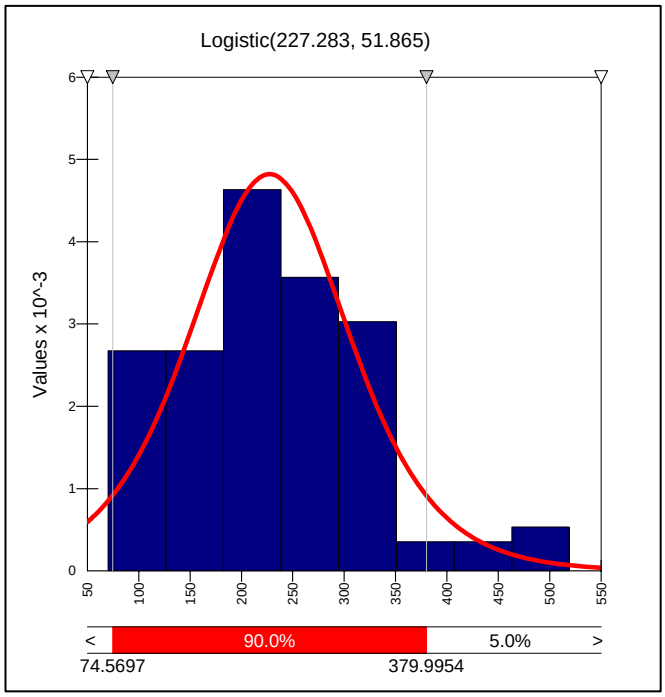

Figure 3.19 Probability density function for lava σ_C (MPa)

3.2.2 Ventersdorp Contact Reef (VCR) strength properties

Unfortunately very few test results are available for the VCR mainly due to the non availability of core which is used for evaluation purposes and difficulties associated with testing conglomerates. However, results from six uniaxial compressive tests are available (Rosenblatt, 1994) and are summarised in Table 3.5 and Figure 3.20 is the probability density function for this data.

Table 3.5 VCR strength and elastic properties summary

	σ_C (MPa)		E (GPa)	ν
	Input (Excel)	@ Risk Fit		
Distribution	-	Logistic	-	-
Mean	182.4	187.094	71.5	0.11
Std Deviation	48.8	44.832	4.6	0.02
Minimum	105.1	-	66.5	0.08
Maximum	236.0	-	78.6	0.12

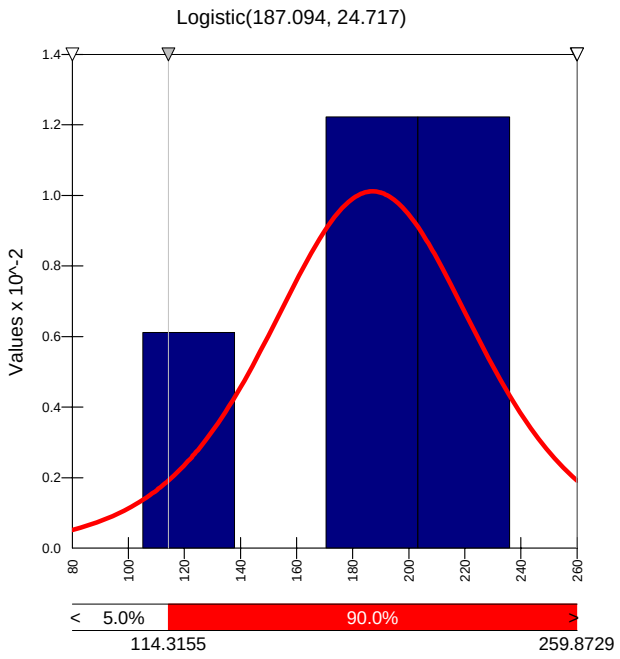

Figure 3.20 Probability density function for VCR σ_C (MPa)

3.2.3 Footwall Quartzites strength properties

Point load tests on footwall samples from several geological boreholes show that the quartzites in a zone to 30m below the VCR have strengths ranging from 135MPa to 200MPa (Lombard, 1989). Uniaxial compressive strength test results (Rosenblatt, 1994) are summarised in Table 3.6 and Figure 3.21 is the probability density function for this data.

Table 3.6 Footwall quartzite strength and elastic properties summary

	σ_C (MPa)		E (GPa)	ν
	Input (Excel)	@ Risk Fit		
Distribution	-	Triang	-	-
Mean	121.1	123.433	121.1	121.1
Std Deviation	22.6	19.634	22.6	22.6
Minimum	86.5	67.899	86.5	86.5
Maximum	151.2	151.200	151.2	151.2

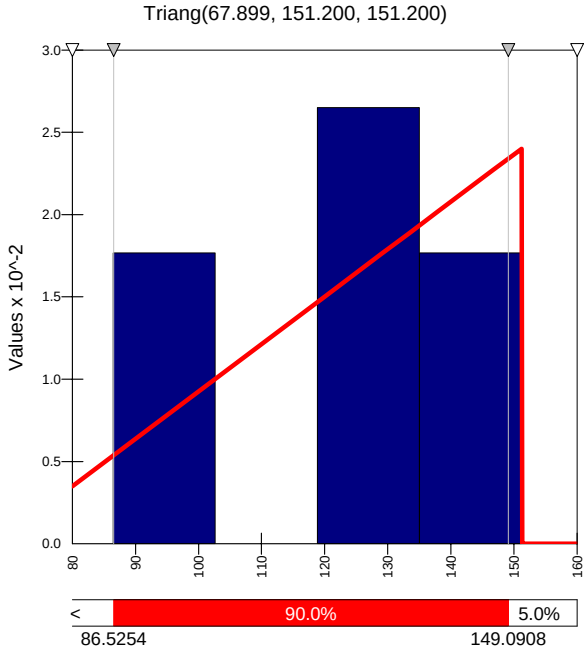

Figure 3. 21 Probability density function for footwall quartzite σ_C (MPa)

3.3 Geotechnical areas

It is necessary to define different geotechnical regions on a mine for rock related Codes of Practice. Guler *et a*l (1998) indicate that a mine should be subdivided firstly into a Regional Geotechnical Areas (RGA) and secondly Ground Control Districts (GCD), also termed local geotechnical areas.

From a RGA perspective Tau Lekoa Mine is considered to fall within the hard lava category defined by Roberts *et al* (1996). Tau Lekoa Mine has not been divided into specific GCD as there is substantially overlap between areas. Several relationships and factors are considered in terms of controlling rock mass behaviour and these are outlined below.

3.3.1 Seismological Setting

Tau Lekoa has historically been regarded as a non-seismic mine for the following reasons:

- relatively shallow mining depth (900m–1650m below surface);
- small mining spans due to complex geology;
- remote from the extensive mining in the Klerksdorp area.

Tau Lekoa Mine was situated outside of the KMMA Regional Seismic Network with the closest sites situated 10km or more away. Under certain circumstances, it was possible to get rough locations (within the mines boundaries) and some idea of magnitude. Two events with an approximate local magnitude of 2.0 were located within the Tau Lekoa boundaries during 1995 and 1998. Between October 2000 and November 2001, the Great Noligwa Mine Seismic Network recorded 18 events in the local magnitude range (M_L) of 1.6 to 2.8 within the Tau Lekoa Mine area. A 6-station seismic network was designed to evaluate seismicity at Tau Lekoa Mine with the first three stations becoming operational in November 2001.

Even with limited seismic coverage, a surprising amount of seismicity was recorded between November 2001 and December 2002 (Table 3.7). Location and sensitivity are reasonable within the network, getting progressively worse with distance from the stations. Generally, the seismicity correlates well with current production and geological structures (Figure 3.22)

Table 3.7 Summary of seismic events at Tau Lekoa Mine

M_L = 0-1	M_L = 1-2	M_L >2
4746	252	11

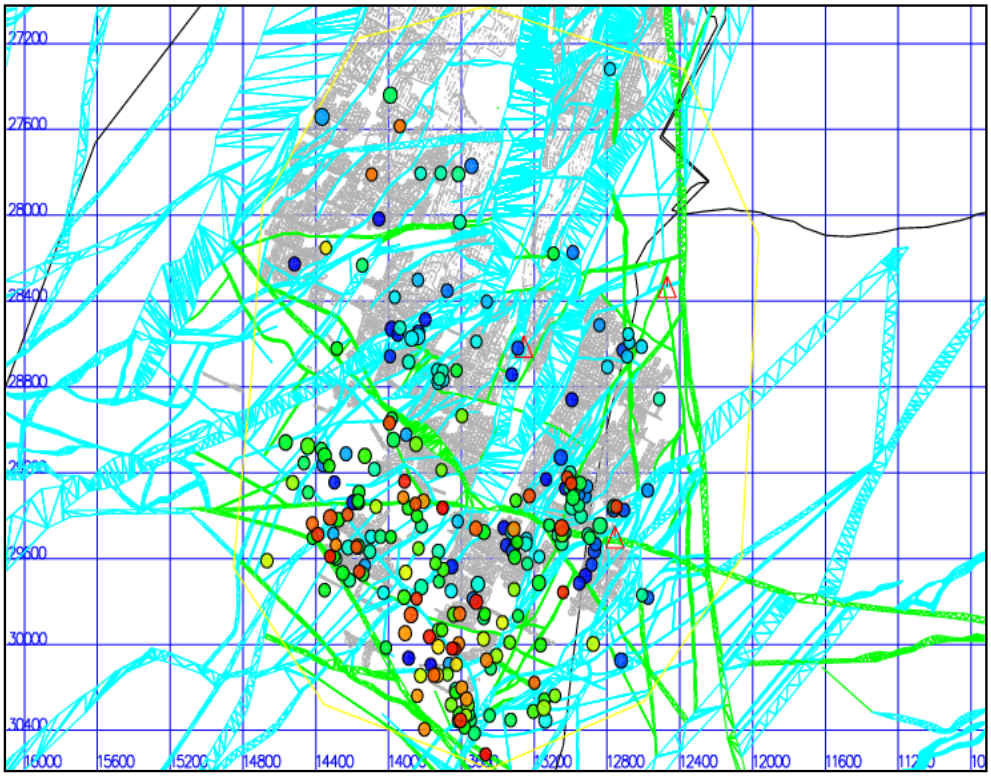

Figure 3.22 Plot showing events of M_L > 1 for the period November 2001 to December 2002

3.3.2 Stress regime

Mining at Tau Lekoa is conducted in an intermediate depth mining environment between 900m to 1650m below surface. Stress measurements conducted on 1200 level (Lombard, 1989) indicated the following:

- A relatively normal near vertical stress of 30-40MPa.
- Relatively high horizontal stress of similar value, acting approximately north to south.
- Low horizontal stress acting approximately east to west.

3.3.3 Closure rates

Generally, closure rates at Tau Lekoa Mine are low due to the relatively shallow mining and small spans as a result of pillars and complex geology. Over several years, basic closure stations were installed in panels across the mine and the average closure rates are summarised in Table 3.8. Closure rates have been plotted against depth and it appears that it does not increase with depth (Figure 3.23). This is probably due to the small spans and any significant difference in closure rate is probably due to differences in span and local geology.

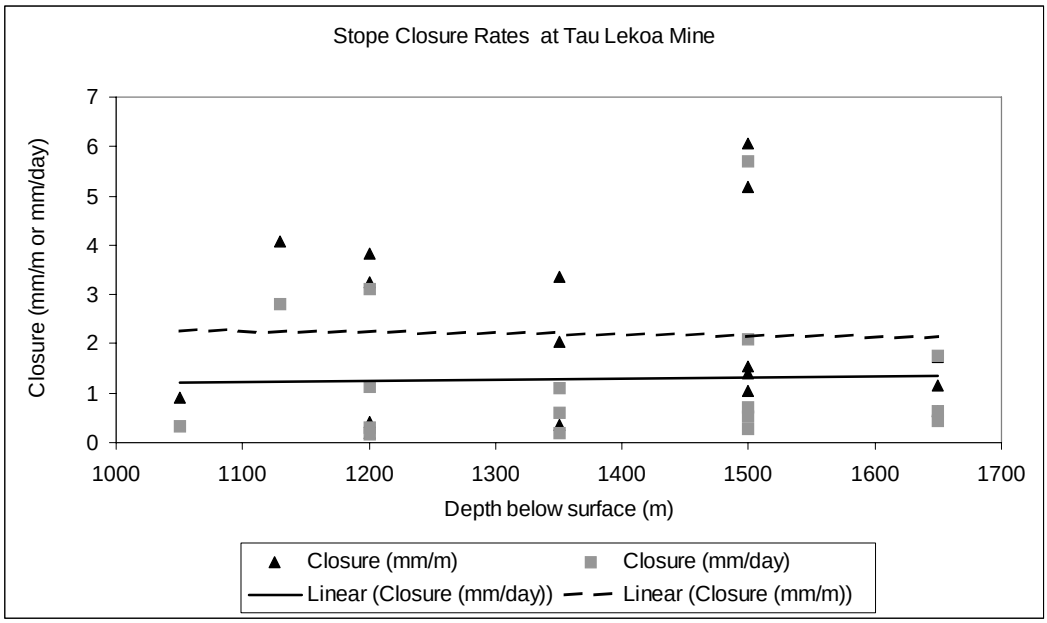

Figure 3.23 Closure rate versus depth

Table 3.8 Closure rate summary

Workingplace	Depth	mm/m	mm/day	Days
1050 S4 Rse 14 P13	1050	0.92	0.32	47
1130 N3 Rse 9A P15	1130	4.09	2.82	38
1200 S3 Rse 12 P5	1200	0.41	0.3	75
1200 S4 Rse 15 P9	1200	3.82	3.12	23
1200 S4 Rse 6 P11	1200	3.26	1.13	91
1200 S4 Rse 8 P11	1200	0.187	0.159	28
1350 N1A Rse 13 P3	1350	2.03	1.1	61
1350 S3 Rse 15 P23	1350	0.35	0.19	64
1350 S3 Rse 21 P28	1350	3.35	0.61	42
1500 S1 Rse 2 P25 (Pillar)	1500	5.19	5.71	7
1500 S1 Rse 2 P25 (Top)	1500	6.05	2.09	33
1500 S1 Rse 9 P17	1500	1.54	0.71	64
1500 S1 Rse 9 P17	1500	1.41	0.52	101
1500 S2 Rse 14 P13	1500	1.05	0.27	35
1650 S3 Rse 18 P22	1650	1.16	0.64	85
1650 S3 Rse 19 P30	1650	1.75	1.77	21
1650 S3 Rse 21 P11	1650	0.64	0.43	9
	Average	2.19	1.29	-
	Std Dev.	1.69	1.38	-

3.3.4 Ground control districts

Several aspects that influence the ground control problems, specifically large collapses have been identified and a brief description follows. These aspects will be dealt with in greater detail in later chapters.

South mining

Experience at Tau Lekoa Mine indicates that more ground control problems, in the form of small and large falls of ground are experienced when mining south. This may be due to unfavourable joint orientations and possibly the direction of

the lava flow. Generally, an attempt is made to mine north where possible, although sometimes due to geological and practical constraints it is necessary to mine south. In these situations, additional care is given to mining sequence and the pillar layout. A detailed discussion and analysis of the ground problems associated with south mining is provided in Chapter 4.

Depositional setting

A number of distinct depositional settings or geo-zones have been identified, each having different characteristics in terms of ground control problems. It was found that when large FOG were superimposed on a geo-zone plan the majority occurred in the Main Channel area. The following factors are considered as possibly contributing to a high incidence of large FOG (Biddulph, 2000):

- The Main Channel is the area on the mine where the thickest channel widths predominate.
- The hanging wall to reef across this entire zone comprises Unit 1 lavas.
- The Main Channel is flanked by major fault structures, the Schoonspruit to the west, and the New Year and Goedgenoeg faults in the east.
- There is a possibility that the Main Channel has and is still being subjected to tensional stresses that may also contribute to the falls of ground that have taken place in the area. This is unproven at this stage and requires further investigation.

The presence of rolls due to erosional channels and slopes results in hangingwall problems when traversing these rolls. The reef generally thins out on slopes and plateaus, and thickens in channels. Reef rolls occur at various scales and vary in dip from 35 to 65 degrees and are predominantly orientated on either dip or strike (Fourie, 2000). The association between the depositional setting and large FOG will be covered in greater detail in Chapter 4.

Channel width

The channel width varies according to the depositional environment with higher channel widths associated with Main Channel and erosional channels, whilst thinner channel widths are encountered on slopes, terraces and plateaus. Experience at Tau Lekoa indicates that there is a higher probability of large hangingwall instability at higher stoping widths.

Two classes have been identified, namely stoping widths that are less than 1.8m and stoping widths greater than 1.8m. This division is arbitrary and is based on the upper limit for the use of timber elongates at Tau Lekoa Mine.

Hangingwall lava variations

The Alberton lavas on Tau Lekoa are subdivided into Units 1, 2 and 3 (Figure 3.5) based on petrographical characteristics (De Fries, 2002). Both Unit 1 and Unit 2 lavas are encountered in the immediate hangingwall. The majority of mining to date has been conducted in areas with Unit 1 as the immediate hangingwall.

The Unit 3 lava is dark grey, homogenous lava with abundant small fresh black and white amygdales and appears to have a porphyritic texture due to the abundance of amygdales. The thickness of the Unit 3 lava is over 80m and the transition to the underlying Unit 2 lava is gradual and normally marked by an agglomerate (De Fries, 2002).

The Unit 2 lava is highly heterogeneous with a greenish tinged succession of lavas and tuffs, predominantly characterised by an abundance of haloed amygdales. The maximum thickness is 44m and the transition to the underlying Unit 1 lava is gradual but in most cases marked by an agglomerate (De Fries, 2002).

The Unit 1 lava is an aphanitic grey lava with fresh black and white amygdales that are in most cases fresh and non-haloed. The most distinguishing characteristic of the unit is the presence of phenocrysts in the lava. White feldspars dominate at the top whereas towards the base these phenocrysts are normally black and

chloritised. The maximum thickness of the Unit 1 lava is between 25 and 28m (De Fries, 2002).

Observations underground indicate that hangingwall conditions can vary quite substantially over a few metres. This is related to the large variation in the uniaxial compressive strength of the lava. Low angle thrust faulting along the VCR / lava contact also results in lower rock mass strength.

3.4 Chapter Summary

In this chapter, the geological and geotechnical environment was described and a brief introduction to some of the geotechnical aspects related to large FOG has been given. Statistical distributions have also been determined for geotechnical data such as joint spacing and rock strength properties. These will be used in later chapters as part of a probabilistic design approach. The following chapter will deal with a comprehensive analysis of large hangingwall instabilities at Tau Lekoa Mine.

4 LARGE FALL OF GROUND ANALYSIS

The previous chapter outlined the geological and geotechnical environment at Tau Lekoa Mine and established the descriptive statistics and probability density functions for use in a probabilistic approach to pillar system design. This chapter will focus on an in depth analysis of large hangingwall instabilities or FOG.

Between 1991 and 2001, 107 incidents were recorded in the Tau Lekoa Large Fall of Ground database. A number of small falls of ground were erroneously entered into the database and some information was incomplete. These incidents were filtered out and fairly reliable and complete data are available for 81 large FOG incidents. Generally, any FOG exceeding $10m^2$ or a mass of about 30 tons is considered large. The database of large hangingwall instabilities is attached as Appendix A.

A statistical approach has been applied in evaluating these large collapses to establish if relationships or trends exist. This analysis includes aspects such as mining direction, mining height, geotechnical areas, mining spans and different periods. The periods considered are as follows:

- 1991-2001
- 1991-1994
- 1995-2001

A major support system change was implemented in 1995 and this has been chosen as an analysis boundary. Using the Microsoft Excel and Palisade @Risk programmes, a statistical analysis was done for a range of parameters. Cumulative distribution curves and probability density functions (PDF) were determined for each parameter for the comparisons purposes and establishing the groundwork for a probabilistic design and risk assessment approach.

4.1 Fallout thickness and pillar span

The design of stable spans between crush pillars at Tau Lekoa Mine is based on a relationship between the fallout thickness and the spans between the crush pillars (Judeel and Laas, 1999; Dunn, 2000; Dunn, 2003; Dunn; 2004). This relationship was determined by plotting the fallout thickness against span and fitting a line using linear regression. The intercept was set at zero, as a FOG is not possible if the span is zero. The following equation describes the relationship:

$T = m * S$

Where T = Fallout thickness; S = Span; m = slope of the line

Generally, the relationship has a low correlation in terms of the coefficient of determination (r^2) value. The trendline is considered reliable when it has an r^2 value approaching 1. An example of a fallout thickness versus span plot is shown in Figure 4.1 and additional plots are included in Appendix B.

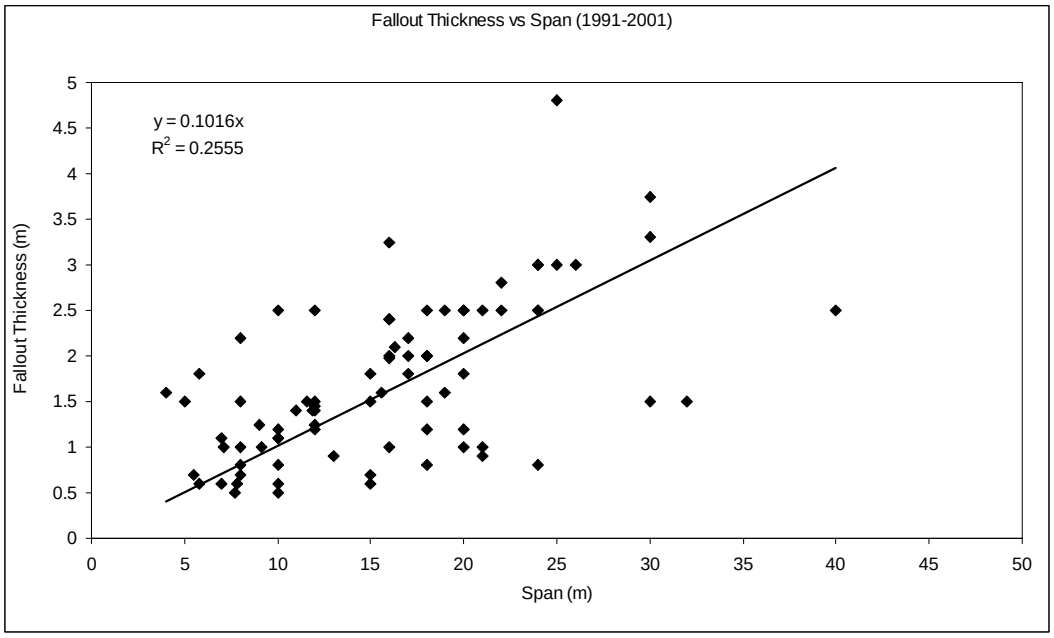

Figure 4.1 Fallout thickness versus span for the period 1991 to 2001

The relationship has been determined for different periods and mining directions and is summarised in Table 4.1. Generally, the relationship between the fallout thickness and span is poor with r^2 values of less than 0.3 in 75 percent of cases considered. Reasonable r^2 values were obtained for north mining between 1991-2001 and 1991-1994 as well as for south mining in 1995-2001 and for centre gullies in 1995-2001.

Table 4.1 Summary of fallout thickness (T) versus span (S) relationships

Period	Number of FOG	Relationship	r^2
All: 1991-2001	81	T = 0.1016 * S	0.2555
All: 1991-1994	18	T = 0.1026 * S	0.1397
All: 1995-2001	63	T = 0.1009 * S	0.1256
North: 1991-2001	34	T = 0.1085 * S	0.3923
North: 1991-1994	4	T = 0.1221 * S	0.729
North: 1995-2001	31	T = 0.1035 * S	0.161
South: 1991-2001	26	T = 0.0888 * S	0.2366
South: 1991-1994	9	T = 0.0813 * S	0.2976
South: 1995-2001	17	T = 0.0951 * S	0.4922
CG: 1991-2001	21	T = 0.108 * S	0.086
CG: 1991-1994	5	T = 0.1136 * S	0.1801
CG: 1995-2001	15	T = 0.1035 * S	0.4976

4.2 Large FOG Dimensions

A statistical analysis was conducted for each period and three different mining situations (north mining, south mining and over centre gullies). The mean, standard deviation, minimum and maximum were determined for the different FOG dimensions. The 95 percent cumulative level was estimated from the data as this is commonly used in stope support design in the South African gold mining industry (Daehnke *et al*, 1998). Probability density functions and cumulative distributions were determined for each case using @Risk. Due to insufficient data, distributions for north mining over the period 1991-1994 could not be determined.

4.2.1 Fallout thickness

Table 4.2 is a summary of the statistical analysis of fallout thickness. The frequency and PDF for large FOG for 1991-2001 are shown in Figure 4.2 and Figure 4.3 respectively. This information for the other situations considered is included in Appendix C.

Table 4.2 Fallout thickness statistical summary

Period	Mean	Std Dev.	Min.	Max.	95% Cum.	Distribution
All: 1991-2001	1.71	0.86	0.5	4.8	3.45	Inverse Gaussian
All: 1991-1994	2.31	1.01	1.0	4.8	4.1	Exponential
All: 1995-2001	1.53	0.73	0.5	3.25	2.45	Beta General
North: 1991-2001	1.67	0.94	0.5	3.75	3.26	Normal
North: 1991-1994	2.99	0.65	2.4	3.75	3.7	-
North: 1995-2001	1.48	0.82	0.5	3.25	2.8	Exponential
South: 1991-2001	1.56	0.65	0.8	3.0	2.45	Log Logistic
South: 1991-1994	1.71	0.62	1.0	2.5	2.48	Beta General
South: 1995-2001	1.49	0.67	0.8	3.0	2.5	Exponential
CG: 1991-2001	1.94	0.93	0.6	4.8	3.0	Ext Value
CG: 1991-1994	2.86	1.26	1.5	4.8	4.45	Beta General
CG: 1995-2001	1.60	0.58	0.6	2.5	2.4	Ext Value

The minimum fallout thickness for all data is 0.5m and the maximum is 4.8m with a mean of 1.71m and a 95 percent cumulative level of 3.45m. The mean fallout thickness for the period 1995-2001 is less than for the period 1991-1994. This reduction ranges from 0.22m to 1.51m and this trend is also reflected in the fallout thickness versus span relationship. This may mean that the more stringent support system adopted in 1995 had the impact of reducing fallout thicknesses.

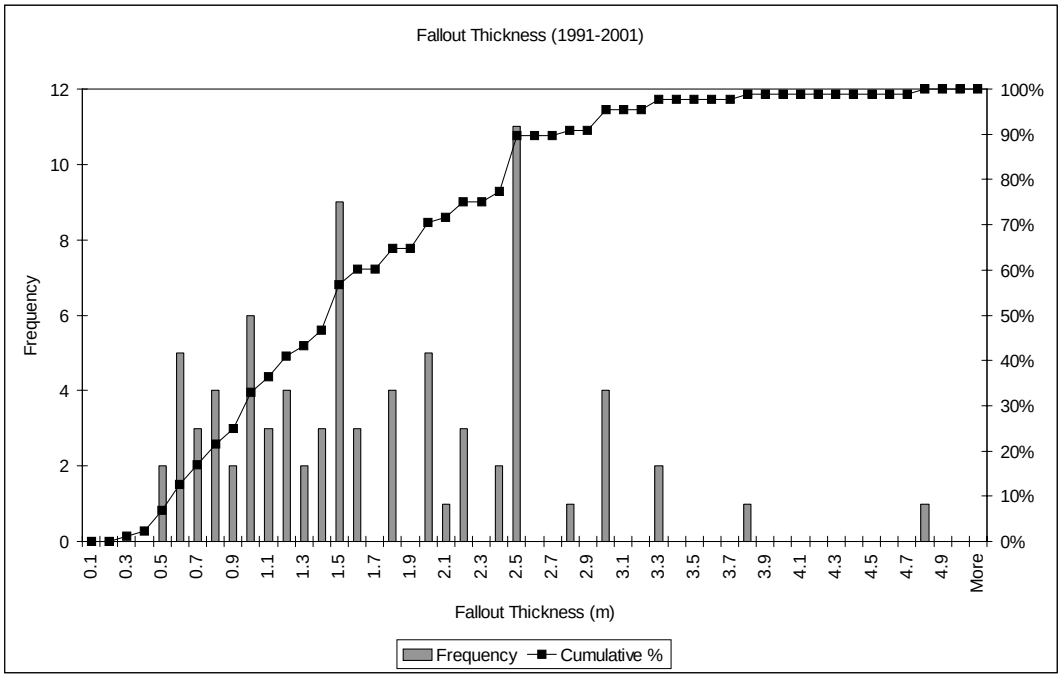

Figure 4.2 Fallout thickness frequency and cumulative percentage for 1991-2001

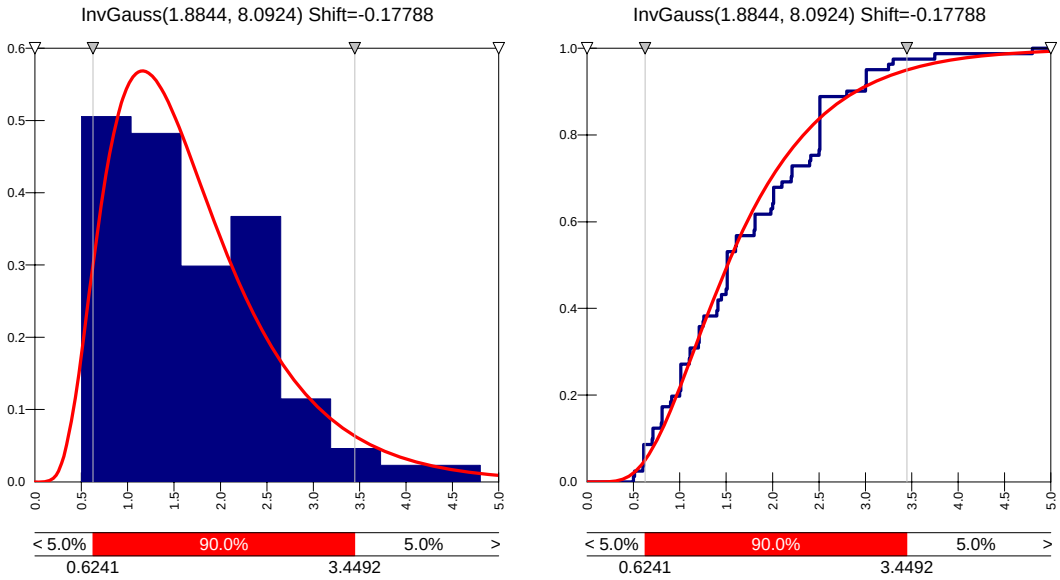

Figure 4.3 Fallout thickness PDF and cumulative distribution for 1991-2001

4.2.2 FOG Length

Table 4.3 is a summary of statistical information for the FOG length for different cases. Figures showing the frequency, cumulative percentage and probability density function for each case are included in Appendix D. The minimum FOG length is 4m and the maximum is 43m with a mean of 15.30m and a 95 percent level of 35m. There does not appear to be any major difference in the FOG length for the different cases although the 95 percent cumulative levels for South 1991-2001, South 1991-1994 and CG 1991-1994 are lower.

Table 4.3 FOG length statistical summary

Period	Mean	Std Dev.	Min.	Max.	95% Cum.	Distribution
All: 1991-2001	15.30	8.77	4	43	35	Ext Value
All: 1991-1994	16.0	7.75	4	36	35	Logistic
All: 1995-2001	14.81	9.03	4.5	43	34.5	Beta General
North: 1991-2001	15.49	9.58	5.8	40	34.5	Pearson 5
North: 1991-1994	26.0	10.46	16	36	37.8	-
North: 1995-2001	13.78	8.74	4.5	40	32.7	Inverse Gaussian
South: 1991-2001	14.53	7.87	4	43	25	Logistic
South: 1991-1994	14.22	4.87	4	19	18.5	Logistic
South: 1995-2001	14.70	9.21	4.5	43	34	Ext Value
CG: 1991-2001	15.93	8.80	5	40	35	Ext Value
CG: 1991-1994	14.80	4.66	8	21	20.5	Beta General
CG: 1995-2001	16.28	9.84	5	40	37.5	Exponential

4.2.3 FOG Width

Table 4.4 is a summary of statistical information for the FOG width for different cases. Figures showing the frequency, cumulative percentage and probability density function for each case are included in Appendix E. The minimum FOG width is 2.5m and the maximum is 30m with a mean of 9.79m and a 95 percent

level of 21.1m. Generally, the maximum FOG widths for south mining and centre gullies are smaller than for north mining. The mean width for north mining 1991-1994 is substantially larger than for the other cases but is based on a small number of occurrences.

Table 4.4 FOG width statistical summary

Period	Mean	Std Dev.	Min.	Max.	95% Cum.	Distribution
All: 1991-2001	9.79	5.94	2.5	30	21.1	Ext Value
All: 1991-1994	11.22	6.26	3	30	20.5	Logistic
All: 1995-2001	9.37	5.84	2.5	24	22	Inverse Gaussian
North: 1991-2001	10.06	7.26	2.5	40	32.5	Pearson 5
North: 1991-1994	19.50	7.55	14	30	27	-
North: 1995-2001	8.63	6.30	2.5	40	24	Log Logistic
South: 1991-2001	9.75	5.22	3	24	19	Log Logistic
South: 1991-1994	9.11	3.37	3	14	13	Beta General
South: 1995-2001	10.09	6.04	3.2	24	20	Inverse Gaussian
CG: 1991-2001	9.39	4.48	3	20	16	Normal
CG: 1991-1994	8.40	3.58	3	12	11.75	Beta General
CG: 1995-2001	9.34	4.73	4	20	17.8	Ext Value

4.2.4 FOG Dimension

Unfortunately, the orientation of the FOG lengths and widths were not noted in the database. It would have been useful to know if these dimensions were orientated on dip or strike. The data for both of these measurements were combined and the statistics were determined for a parameter called the FOG dimension. Figures showing the frequency, cumulative percentage and probability density function for each case are included in Appendix F.

The minimum FOG dimension is 2.5m and the maximum is 43m with a mean of 12.54m and a 95 percent level of 28.9m. Generally, there does not appear to be a

significant difference in FOG dimension with the exception of north mining for 1991-1994, which is substantially larger than for the other cases. This is due to the higher minimum and the small number of occurrences.

Table 4.5 FOG dimension statistical summary

Period	Mean	Std Dev.	Min.	Max.	95% Cum.	Distribution
All: 1991-2001	12.54	7.96	2.5	43	28.9	Log Normal 2
All: 1991-1994	14.11	7.54	3	36	24.8	Logistic
All: 1995-2001	12.09	8.05	2.5	43	25	Inverse Gaussian
North: 1991-2001	12.77	8.87	2.5	40	32.5	Log Logistic
North: 1991-1994	22.75	9.13	14	36	35	-
North: 1995-2001	11.02	7.99	2.5	40	24	Exponential
South: 1991-2001	12.14	7.04	3	43	23.9	Log Logistic
South: 1991-1994	12.00	4.83	3	19	18.1	Ext Value
South: 1995-2001	12.40	8.02	3.2	43	24.5	Log Logistic
CG: 1991-2001	12.66	7.65	3	40	23	Ext Value
CG: 1991-1994	11.60	5.17	3	21	20.5	Beta General
CG: 1995-2001	12.65	8.45	4	40	31	Inverse Gaussian

4.3 Geotechnical relationships

The large FOG were analysed in terms of the following:

- Stoping width
- Depositional setting
- Mining direction

4.3.1 Stoping width

Higher channel widths and the associated stoping widths have been identified as being more hazardous (Judeel and Laas, 1999). It was found that there was a

higher relative incidence of large FOG at stoping widths greater than 1.8m even though the bulk of stoping was at a lower stoping width. The 1.8m stoping width was chosen as a boundary because this is the upper limit for the timber elongate support used at Tau Lekoa Mine. When this stoping width limit is exceeded, the support is changed to rock bolts and spans are reduced to 10m.

Table 4.6 is a summary of the stoping widths for the FOG considered in this study. The minimum stoping width is 110cm and the maximum is 350cm with a mean of 180.9cm and a 95 percent cumulative level of 260cm. The frequency and cumulative percentage and PDF for all large FOG for 1991-2001 are shown in Figures 4.4 and 4.5 respectively with additional figures included in Appendix G.

Table 4.6 FOG Stoping width statistical summary

Period	Mean	Std Dev.	Min.	Max.	95% Cum.	Distribution
All: 1991-2001	180.9	43.9	110	350	260	Gamma
All: 1991-1994	193.8	50.3	121	287	276	Uniform
All: 1995-2001	177.2	41.6	110	350	230	Logistic
North: 1991-2001	185.4	44	114	350	241	Logistic
North: 1991-1994	214.8	53.4	172	287	250	-
North: 1995-2001	182	41.5	114	350	237	Logistic
South: 1991-2001	172	43.6	110	284	258	Beta General
South: 1991-1994	193.7	57.9	121	284	275	Beta General
South: 1995-2001	150.5	29.7	110	200	195	Beta General
CG: 1991-2001	184.8	44.6	135	300	264	Ext Value
CG: 1991-1994	177.4	33.6	147	228	220	Beta General
CG: 1995-2001	187.1	50	135	300	293	Log Logistic

The cumulative percentage graph in Figure 4.4 shows that 64.2 percent of large FOG occurred at a stoping width of 1.8m or less. The @Risk PDF (Figure 4.5) shows that 55.7 percent of large FOG occurred at a stoping width of 1.8m or less. This means that approximately 40 percent of large FOG occurred at a stoping

width of greater than 1.8m. Generally, between 10 and 15 percent of mining at Tau Lekoa Mine, takes place at a stoping width greater than 1.8m.

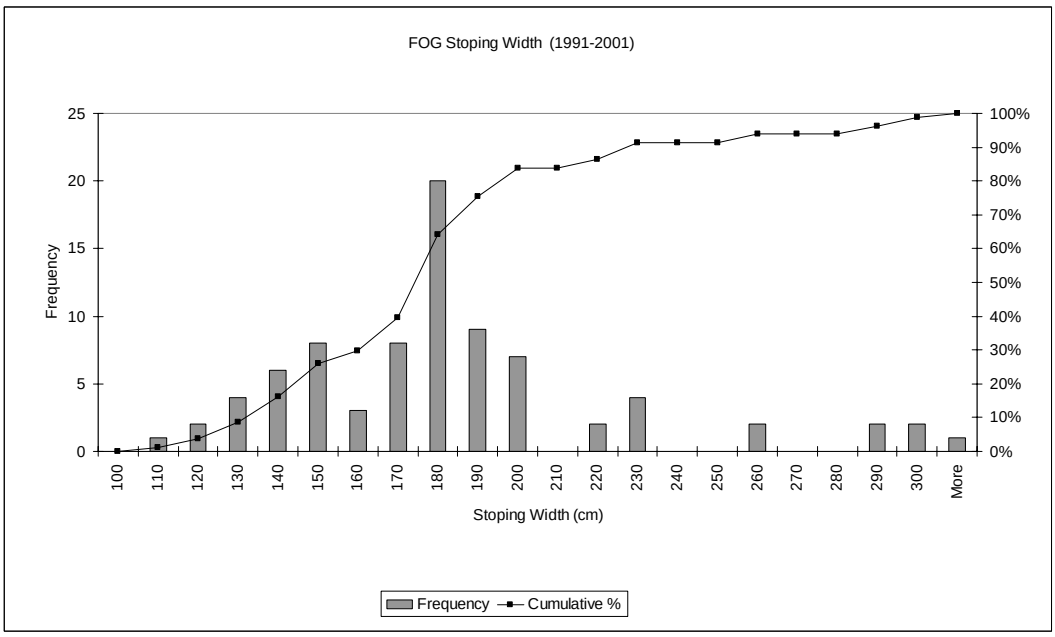

Figure 4.4 FOG stoping width frequency and cumulative percentage for 1991-2001

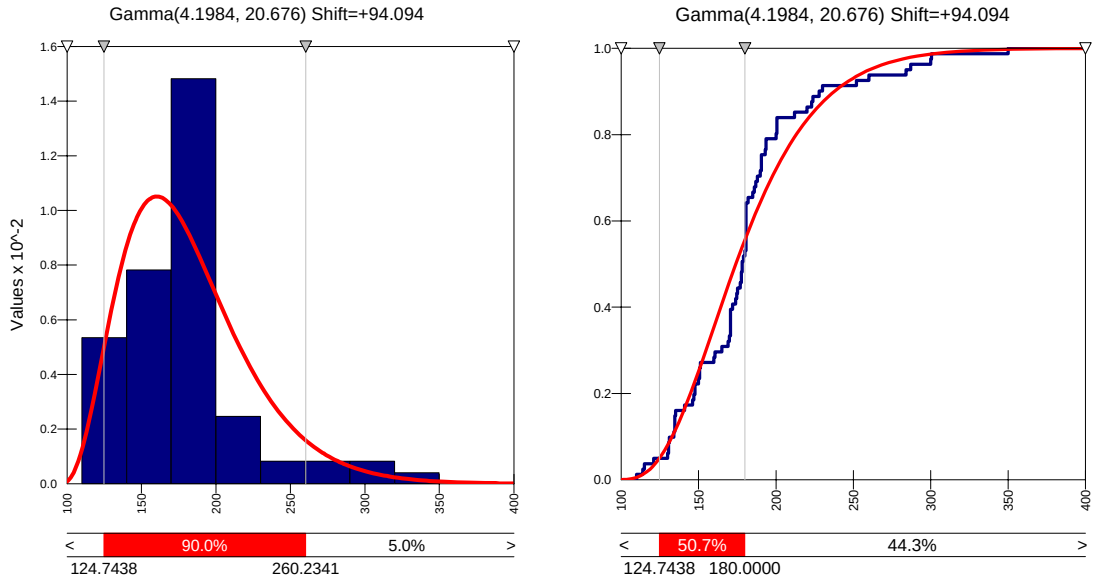

Figure 4.5 FOG stoping width probability density function and cumulative distribution for 1991-2001

4.3.2 Depositional setting

Biddulph (2000) investigated the spatial distribution of large FOG by superimposing the data for the period 1991 to 1999, on the geological model plan. It was concluded that the majority of these occurred within the Main Channel (Figure 4.6). It was postulated that this could be due to the Unit 1 lavas that overlay the Main Channel or possibly due to tensional stresses related to the large structures flanking these areas or the human element. The following two factors need to be considered with respect to this analysis:

- a large proportion of the early mining was in the Main Channel;
- support standards prior to 1995 were different.

Figure 4.6 Spatial distribution of large FOG over part of Tau Lekoa Mine

This study has been reviewed and updated to include data from 2001 and 2002. Table 4.7 summarises the breakdown of large FOG and their spatial occurrence

relative to the different geo-zones. The period 1996-2001 has been analysed because production figures per geo-zone are available for this period. Prior to this no breakdown in production per geo-zone was available.

Table 4.7 FOG (actual and percentage %) per Geo-zone

Geo-zone	1991-2001		1991-1994		1995-2001		1996-2001	
	Act.	%	Act.	%	Act.	%	Act.	%
Main Channel (MC)	62	77	18	100	44	70	39	67
Reworked Channel (RC)	8	10	0	0	8	13	8	14
Middle Terrace Conglomerate (MTC)	5	6	0	0	5	8	5	9
Middle Terrace & Slope (MTS)	5	6	0	0	5	8	5	9
Upper Terrace (UT)	1	1	0	0	1	1	1	2

Table 4.8 Annual production (m2) breakdown per geo-zone (1996-2001)

	1996	1997	1998	1999	2000	2001	Total	%
MC	134912	117999	60815	12027	14295	53848	393896	20
RC	93755	136980	131770	70228	69995	39871	542599	31
MTC	86892	93737	79563	90657	103052	173385	627286	27
MTS	0	13829	76806	75038	44198	15520	225391	11
UT	0	0	3677	40194	77914	94780	216565	11
Total	315559	362545	352631	288144	309454	377404	2005737	100

From Table 4.8 it can be seen that mining in the Main Channel makes up 20 percent of all mining for the period considered. If the cumulative production (2012361m^2) for the period 1991-1995 is included and it is assumed that 80 percent of this mining was in the Main Channel, then mining in the Main Channel constitutes 44 percent of the area mined up until the end of 2001. Table 4.9 is a breakdown of large FOG per geo-zone normalised relative to production. The Main Channel appears to be significantly more hazardous in terms of large FOG.

Table 4.9 Breakdown of large FOG per geo-zone normalised against production for 1996 to 2001

Geo-zone	Act	%	m^2/ FOG
MC	39	67	10100
RC	8	14	67825
MTC	5	9	125457
MTS	5	9	45078
UT	1	2	216565
Total	58	100	34582

4.3.3 Mining direction

Mining in a southerly direction has been regarded as problematic at Tau Lekoa for many years (Siebert, 1997; Judeel and Laas, 1999). According to Judeel (1998) the chances of a large FOG in a south mining panel are double that of a north mining panel. It has been postulated this is due to the unfavourable dip of discontinuities in relation to the south mining faces. To cater for this, more stringent support standards were developed and implemented.

Dunn and Hungwe (2003) conducted a study using the Modified Q-system (Kirsten, 1988) and concluded that the average Q value for north mining panels was 1.7 (Poor) and the average value for south mining panels was lower at 0.9 (Very Poor).

South mining generally makes up about 35 percent of the mining at Tau Lekoa. Table 4.10 shows the actual large FOG and the expected large FOG normalised to the production levels south mining panels. For the period 1991-2001, there are 44 percent more large FOG than what was theoretically expected. For 1991-1994, there are 450 percent more than expected but this is based on a much smaller sample size. For 1995-2001, there is no difference and this is possibly related to better support standards implemented for south mining. Generally, there is a

higher chance of having a large FOG in a south mining panel but this risk can be reduced by appropriate standards.

Table 4.10 South mining versus north mining FOG

	1991-2001		1991-1994		1995-2001	
	North	South	North	South	North	South
Actual	34	26	4	9	30	17
Normalised	-	18	-	2	-	17
% Increase	-	44	-	450	-	0

4.4 Mining depth

The influence of depth on the occurrence of large FOG was investigated. Figure 4.7 shows the frequency and cumulative percentage of the depths at which large FOG occurred for the period 1991-2001. Figure 4.8 is the probability density function and the cumulative distribution. The majority of large FOG occurred on 1200 and 1350 levels, which are 1200m and 1350m below surface.

This exercise was repeated for the periods 1991-1994 and 1995-2001. Figures 4.9 and 4.10 show that for 1991-1994, the majority of large FOG occurred on 1200 level. For 1995-2001 the majority of large FOG occurred in 1350 level stopes (Figures 4.11 and 4.12).

For the period 1991-1994, the majority of mining was on the upper levels and possibly this is why there is a concentration of large FOG on 1200 level. As mining progressed deeper, the mean depth of large FOG increased. However, it should be noted that there are relatively few occurrences of large FOG below 1350 level and there are two possible explanations for this. Firstly, most of the deeper mining took place after the new standards were introduced in 1995 and personnel were probably more adept at identifying wedge or dome structures in the hangingwall. Secondly, it is possible as the mining depth increased, stress induced fracturing became the driving mechanism instead of geological

discontinuities. Based on this analysis it is not possible to reach any firm conclusions about the relationship between depth and large FOG and this is an area requiring further investigation.

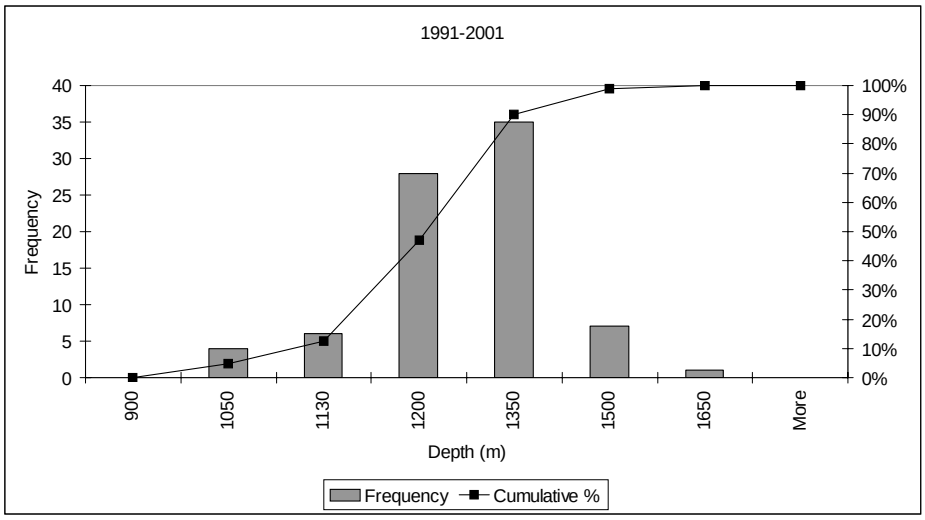

Figure 4.7 Large FOG depth frequency and cumulative percentage (1991-2001)

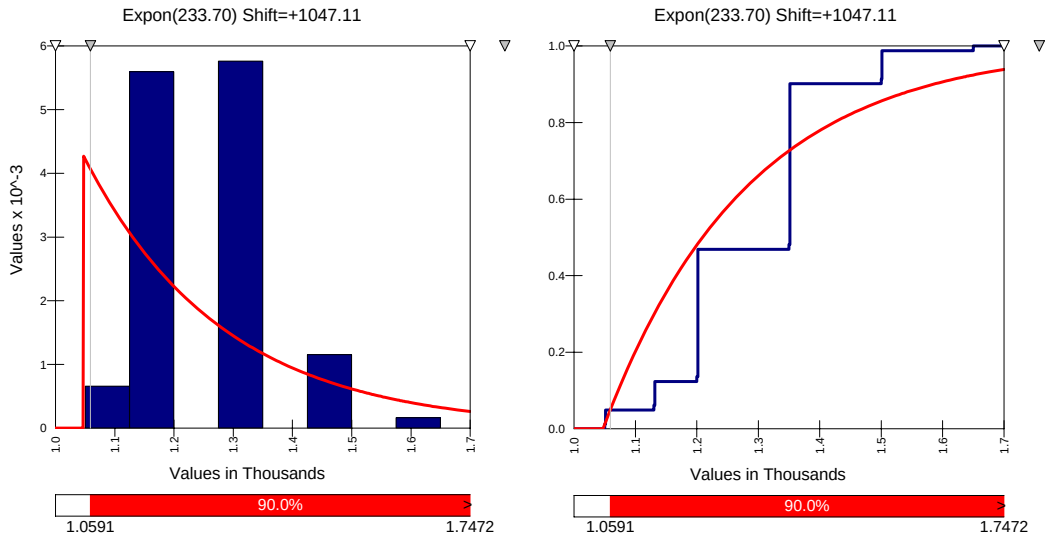

Figure 4.8 Large FOG depth PDF and cumulative distribution (1991-2001)

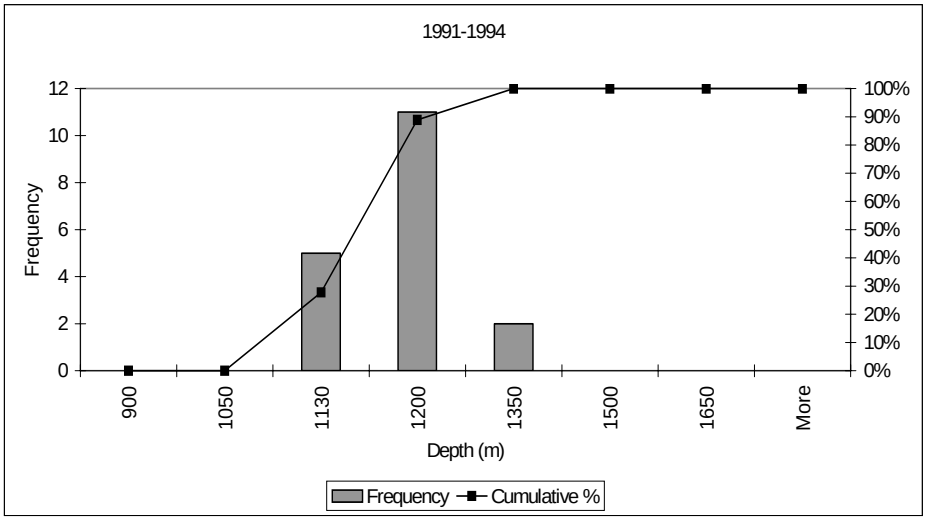

Figure 4.9 Large FOG depth frequency and cumulative percentage (1991-1994)

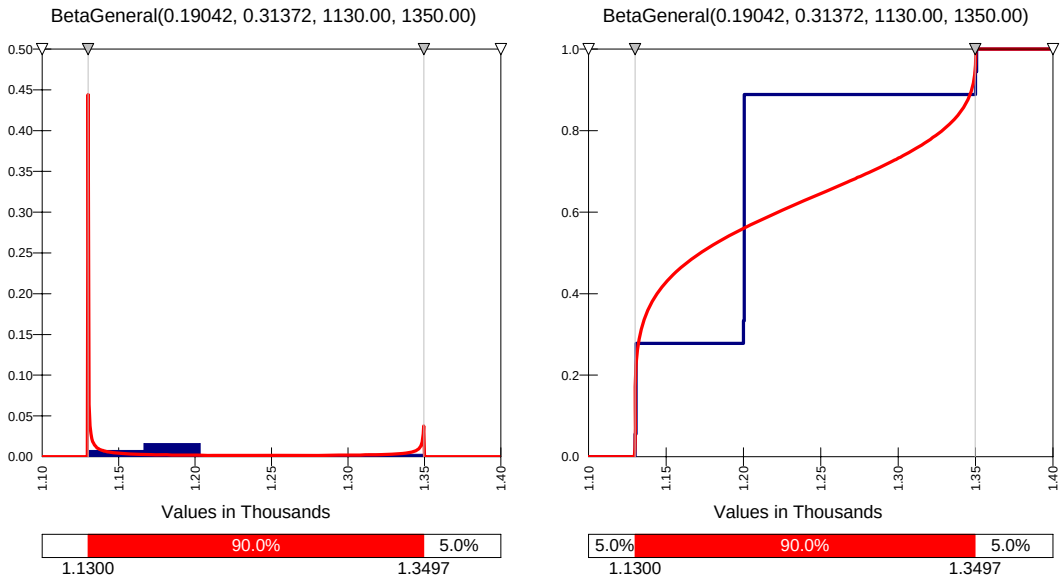

Figure 4.10 Large FOG depth PDF and cumulative distribution (1991-1994)

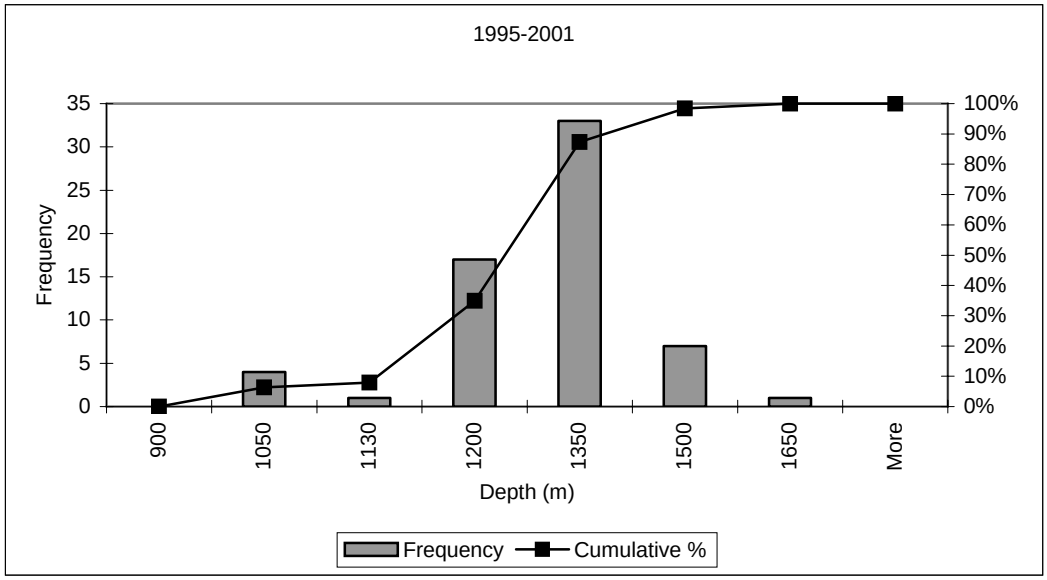

Figure 4.11 Frequency and cumulative percentage of the depth of large FOG (1995-2001)

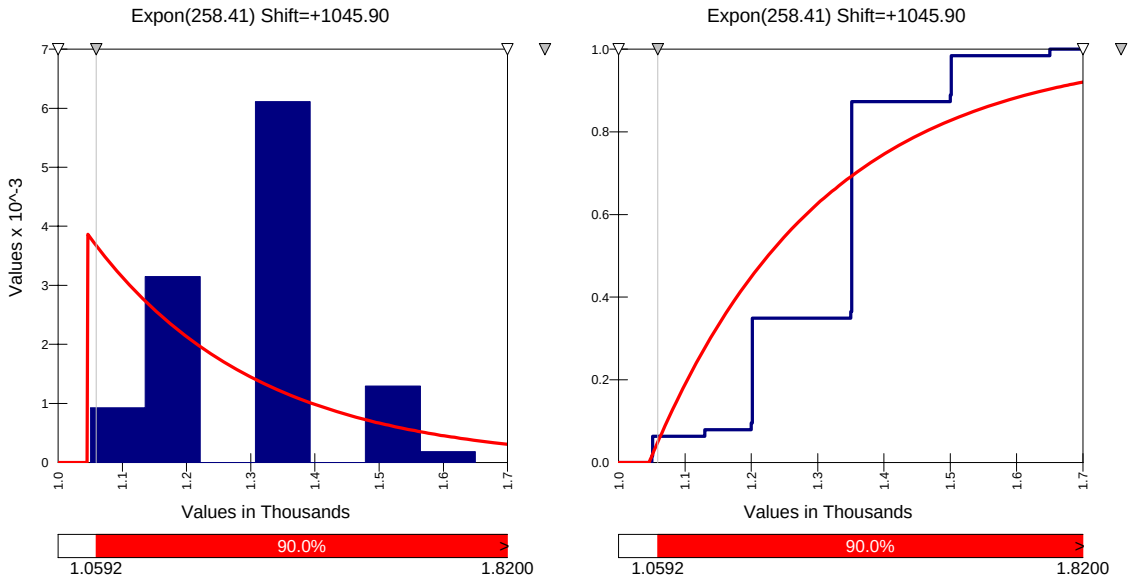

Figure 4.12 Large FOG depth PDF and cumulative distribution (1995-2001)

4.5 Spans for large FOG

This section considers the spans between pillars for large FOG in panels or across centre gullies. Table 4.11 is a statistical summary for the different cases and supporting figures are attached in Appendix H. From the statistical analysis, it can be seen that the mean spans often exceed the standard requirements of 10m or 16m.

Table 4.11 Large FOG span statistical summary

Period	Mean	Std Dev.	Min.	Max.	95% Cum.	Distribution
All: 1991-2001	15.80	7.15	4	40	27.35	Logistic
All: 1991-1994	21.61	7.5	12	40	33.95	Normal
All: 1995-2001	14.15	6.16	4	32	25	Weibull
North: 1991-2001	14.66	7.23	4	30	24.1	Triangular
North: 1991-1994	24	7.12	16	30	28.8	-
North: 1995-2001	13.20	6.37	4	24	23	Triangular
South: 1991-2001	16.66	6.83	7	40	24.5	Normal
South: 1991-1994	19	8.49	12	40	32.6	Beta General
South: 1995-2001	15.42	5.67	7	24	22	Uniform
CG: 1991-2001	16.61	7.48	7	32	30	Ext Value
CG: 1991-1994	24.4	5.13	16	30	28.5	Logistic
CG: 1995-2001	13.72	6.35	7	32	25.2	Ext Value

Table 4.12 is a summary of the percentage occurrences when the spans exceeded the current minimum span requirements. Prior to 1995, the standards changed several times but since 1995, they have been consistent. Cases where non-conformance to the standards was a factor have been indicated with shading. It can be seen that in some cases the non-adherence to standards is substantial.

Table 4.12 Percentage of 1995 standard spans exceeded

Period	10m spans exceeded (%)	16m spans exceeded (%)
All: 1991-2001	79.2	55.6
All: 1991-1994	100	77.3
All: 1995-2001	71.5	34
North: 1991-2001	64	36
North: 1991-1994	100	75
North: 1995-2001	56.9	27.2
South: 1991-2001	83.5	53.8
South: 1991-1994	100	53.7
South: 1995-2001	78.8	47.4
CG: 1991-2001	82.9	45.7
CG: 1991-1994	100	95
CG: 1995-2001	74.1	25.6

4.6 Chapter summary

This chapter presented results of a statistical analysis of large FOG between 1991 and 2001 at Tau Lekoa Mine. The analysis considered FOG dimensions, the geotechnical environment and mining factors such as mining direction, depth stoping width and spans. The following chapter will focus on an analysis of spans using probabilistic keyblock modelling.

5 STABLE SPANS

The previous chapter presented results from a statistical analysis of large falls of ground which considered the dimensions, stoping width, depositional environment, mining direction as well as mining depth and spans. This chapter will present results from an analysis of spans using JBlock software (Esterhuizen, 1996) to conduct probabilistic keyblock analyses.

5.1 JBlock software

JBlock was developed to evaluate the potential for gravity driven rock falls. Due to the extent of mining in large tabular mines, it is not possible to map all discontinuities underground. A probabilistic method is used to determine potential keyblock dimensions and their interaction with support (Esterhuizen, 1996; Esterhuizen and Streuders 1998).

Using information such as the spacing, orientation and length of discontinuities, it is possible to simulate blocks in the hangingwall (Esterhuizen and Streuders, 1998). Keyblock analysis methods (Shi and Goodman, 1985) are used to evaluate whether blocks are removable and whether the chosen support will be sufficient to ensure stability.

JBlock allows the user to conduct a single block analysis or a multi-block analysis. For a multi-block analysis, discontinuity information is used to generate a number of blocks independently of each other. The length of discontinuities limits the size of the blocks (Esterhuizen and Streuders 1998). It is possible to generate a set of blocks and evaluate stability for different support layouts.

5.2 Modelling approach

A number of models were run using different block sets, mining directions, pillar spans and support standards. JBlock can only model the stability of individual

keyblocks and large collapses made up of several blocks are not considered. Dome structures are also not taken into account although it could be argued that the dome structures approximate a tetrahedral shaped block. While this modelling only caters for blocks formed by discontinuities and does not explicitly consider dome structures, it does allow for comparison between different pillar layouts as well as assessing the impact of increasing spans.

5.2.1 Block generation

JBlock allows the user to generate a set of hangingwall blocks that can be saved and reused to assess different support layouts. The joint information from Table 3.2 was used to generate 10000 keyblocks (Figure 5.1). The discontinuity length was based on the mean, minimum and maximum of the FOG dimension. Joint set 2 was defined as a parting as this set generally overlies the stopes and often has a quartz or calcite infilling. This forms a prominent vein, which is often the upper boundary of large FOG. The first keyblock set generated was named "Normal Blocks".

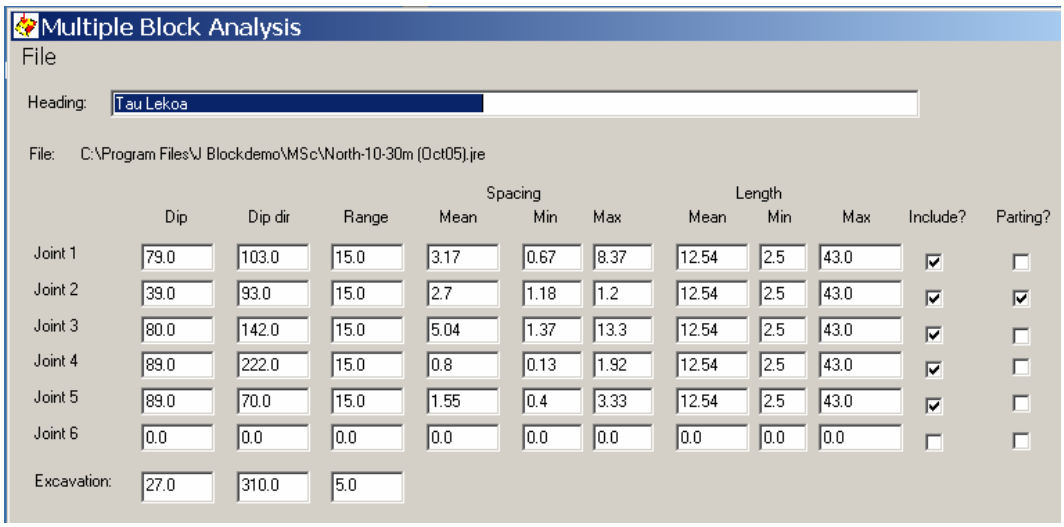

Figure 5.1 Discontinuity input properties for the Normal Block set

From the first set of keyblocks generated, it was noticed the majority of keyblocks were substantially smaller than the large FOG observed. Two further keyblock sets of 10000 keyblocks each were generated and named Large Blocks-1 and

Large Blocks-2. For Large Blocks-1 the mean and minimum joint lengths were increased (Figure 5.2) whilst for Large Blocks-2 the joint spacing was also increased (Figure 5.3) to facilitate the creation of larger keyblocks.

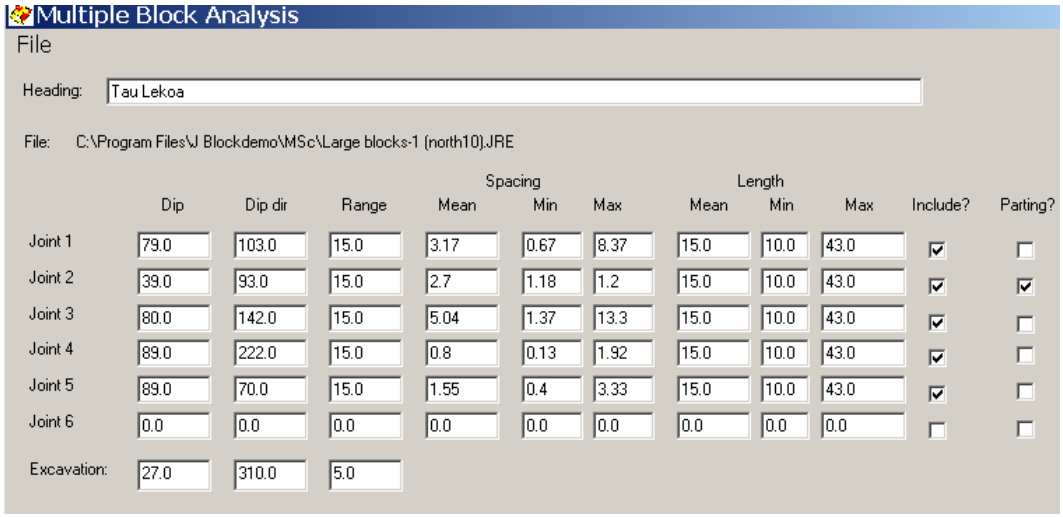

Figure 5.2 Discontinuity input properties for Large Blocks-1

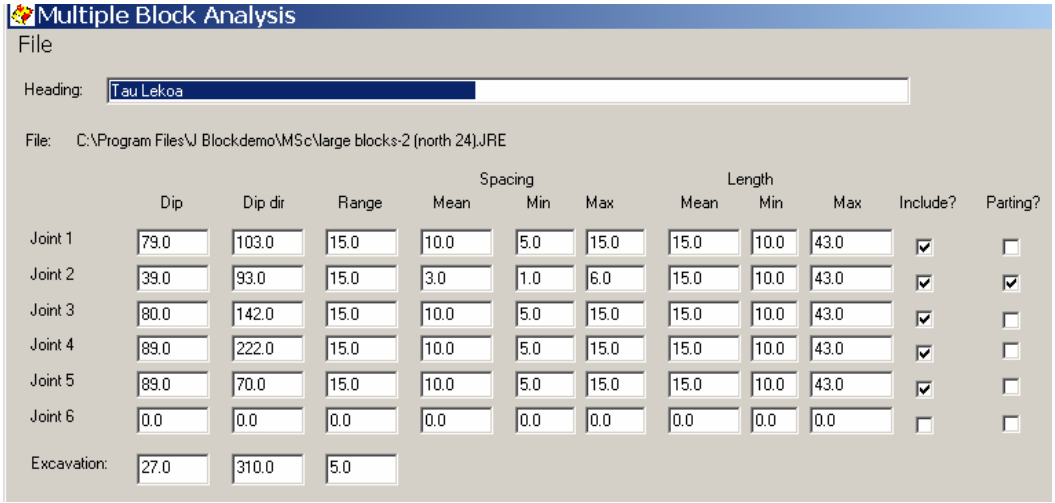

Figure 5.3 Discontinuity input properties for Large Blocks-2

Figure 5.4 shows the block volume frequency for the three different block sets. For Large Blocks-1 and Large Blocks-2, it can be seen that a number of larger blocks have been generated. The larger blocks are still smaller than the largest FOG that has been recorded at Tau Lekoa Mine. Figure 5.5 shows that approximately 65 percent of large FOG have a volume of 300m^3 or less.

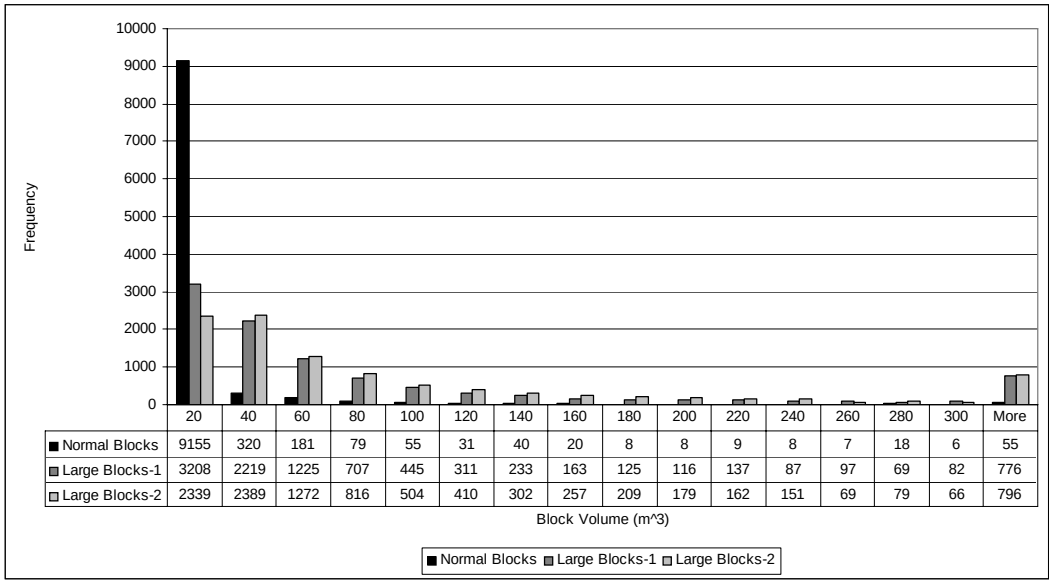

	20	40	60	80	100	120	140	160	180	200	220	240	260	280	300	More
Normal Blocks	9155	320	181	79	55	31	40	20	8	8	9	8	7	18	6	55
Large Blocks-1	3208	2219	1225	707	445	311	233	163	125	116	137	87	97	69	82	776
Large Blocks-2	2339	2389	1272	816	504	410	302	257	209	179	162	151	69	79	66	796

Figure 5.4 Distribution of keyblock volumes determined from JBlock

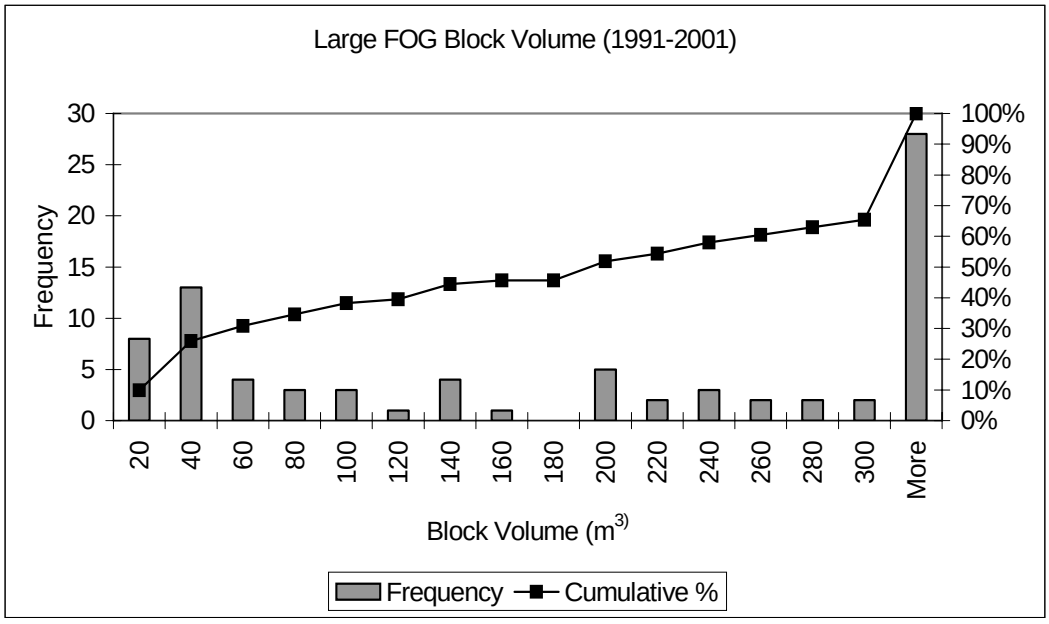

Figure 5.5 Block volumes for large FOG at Tau Lekoa (1991-2001)

The number of larger keyblocks generated by JBlock is relatively small. However, over 10 years of mining, less than 100 large FOG have been observed. During this period, 2.78 million square metres (2 776 245 m^2) were mined and the total area of large FOG during that period is 15 338m^2. This equates to 0.55 percent of the

total area mined indicating that the small percentage of large keyblocks generated by JBlock is not unrealistic.

5.2.2 Panel layouts modelled

Ten different panel layouts were modelled and these considered mining direction and span. Elongates were used as the internal support and these were assigned a peak load of 150kN. This is substantially lower than the peak loads generated by the 180-200mm diameter profile props under laboratory conditions. The peak load was downgraded to take into account the lower loading rates, elongate variability and deterioration over time as several large FOG occurred in back areas. The elongate spacing was 1.5m on strike and 2m on dip as per the mine standards.

The different mining layouts are summarised in Table 5.1. Face length describes span between strike pillars and the mid-panel span is the span between mid-panel pillars. The current standards were used as a base and the effect of increasing mid-panel span and face length were evaluated for both north and south mining.

Table 5.1 Panel layout summary

Description	Standard	Direction	Face length (m)	Mid-panel span (m)
North 10	Yes	North	20	10
North 10-30	No	North	30	10
North 16	Yes	North	20	16
North 16-30	No	North	30	16
North 24	No	North	20	24
North 24-30	No	North	30	24
South 10	Yes	South	20	10
South 10-30	No	South	30	10
South 15	No	South	20	15
South 15-30	No	South	30	15

5.3 Modelling results

The results are presented in terms of the probabilities of support failure by various sizes of keyblocks and various hazard indicators provided as a JBlock output.

5.3.1 Probabilities of support failure by keyblocks

Table 5.2 shows the probability of support failure for the Normal Blocks set. The probabilities are quite low and do not exceed 5 percent. Generally, there is an increase in the probability of support failure as spans are increased as would be expected. As block size increases there is a reduced likelihood that they will fall in between pillars and the probability of support failure decreases. For some keyblock volumes, the probabilities of support failure are higher for south mining.

Table 5.3 shows the results for Large Blocks-1 and the same trends are apparent with slightly higher probabilities of failure although none exceed 5 percent. The results from the analysis using Large Blocks-2 are shown in Table 5.4. Higher probabilities of support failure are indicated with a couple of cases exceeding 10 percent. The failure probability increases with increasing pillar spans. Mining south does not appear to be more hazardous.

Table 5.2 Probabilities of support failure by keyblocks (Normal Blocks)

Volume	North -10	North 10-30	North 16	North 16-30	North 24	North 24-30	South 10	South 10-30	South 15	South 15-30
20	0.63	0.62	0.69	0.67	0.69	0.74	0.60	0.58	0.63	0.72
40	0.96	0.78	1.80	2.45	2.54	2.34	1.33	1.48	1.88	2.19
60	1.31	0.35	1.24	1.13	2.25	1.75	1.72	2.63	1.61	1.44
80	0.00	0.53	0.00	0.00	1.15	0.32	0.00	0.69	0.00	0.00
100	0.00	0.00	1.06	1.50	4.26	0.00	0.00	0.00	0.00	0.00
120	0.00	0.00	1.28	0.00	0.86	2.40	0.00	0.00	0.00	0.00
140	0.00	0.00	0.00	2.02	0.85	1.46	0.00	0.00	4.05	2.27
160	0.00	0.00	0.00	0.00	0.00	0.00	0.00	0.00	0.00	0.00
180	0.00	0.00	0.00	0.00	0.00	0.00	0.00	0.00	0.00	0.00
200	0.00	0.00	0.00	0.00	0.00	0.00	0.00	0.00	0.00	0.00

Table 5.3 Probabilities of support failure by keyblocks (Large Blocks-1)

Volume	North 10	North 10-30	North 16	North 16-30	North 24	North 24-30	South 10	South 10-30	South 15	South 15-30
20	3.12	3.47	3.92	4.05	4.82	4.68	2.41	2.26	3.66	3.85
40	0.80	0.75	0.86	0.91	0.86	1.06	0.47	0.84	0.98	0.94
60	0.38	0.16	0.14	0.44	0.40	0.44	0.22	0.17	0.44	0.63
80	0.86	1.04	1.06	0.75	0.97	1.05	0.84	0.67	0.97	1.14
100	1.14	1.45	1.89	1.43	1.81	1.30	1.62	2.59	1.41	2.22
120	2.11	2.70	0.88	1.94	1.83	1.75	0.00	1.31	1.25	2.15
140	1.10	0.74	0.96	0.63	0.99	0.34	0.00	0.00	1.22	0.91
160	0.00	0.00	0.00	0.00	0.00	0.00	0.00	0.00	0.00	0.00
180	0.00	0.00	0.00	0.00	0.00	0.00	0.00	0.00	0.00	0.00
200	0.00	0.00	0.00	0.36	0.00	0.00	0.00	0.00	0.00	0.00
220	0.00	0.00	0.00	0.46	1.10	0.61	0.00	0.00	1.11	1.41
240	0.00	0.00	0.00	0.00	0.00	0.00	0.00	0.00	0.00	0.00
260	0.00	0.00	0.00	0.00	0.00	0.00	0.00	0.00	0.00	0.00

Table 5.4 Probabilities of support failure by keyblocks (Large Blocks-2)

Volume	North -10	North 10-30	North 16	North 16-30	North 24	North 24-30	South 10	South 10-30	South 15	South 15-30
20	8.42	7.60	10.05	10.62	10.06	10.54	7.32	7.96	9.12	9.21
40	5.10	5.13	8.09	7.40	7.63	8.57	3.01	3.73	6.70	6.46
60	2.59	3.02	4.33	5.43	6.49	5.66	1.22	1.41	3.43	3.78
80	2.37	3.80	4.65	5.07	5.72	5.35	1.90	0.96	4.05	4.12
100	0.41	1.61	4.73	4.70	4.94	5.86	0.00	0.58	3.53	2.20
120	3.24	5.36	3.67	4.30	4.72	6.12	2.52	3.47	3.67	4.27
140	0.00	2.41	5.45	5.33	3.81	5.44	0.00	3.70	0.51	1.65
160	1.04	0.71	4.85	5.11	6.91	9.04	1.54	0.00	3.80	8.70
180	1.72	0.00	2.25	4.84	6.84	4.91	0.00	2.56	1.92	2.55
200	0.00	3.85	3.48	4.66	8.50	9.12	0.00	0.00	0.00	2.65
220	0.00	1.61	0.88	2.03	0.54	1.57	0.00	0.00	0.00	2.70
240	0.00	2.00	0.00	0.69	0.57	0.86	0.00	0.00	0.00	0.00
260	0.00	0.00	2.08	4.76	1.49	4.58	0.00	0.00	0.00	0.00
280	0.00	0.00	0.00	0.00	1.72	0.00	0.00	0.00	2.78	0.00
300	0.00	0.00	0.00	1.59	4.88	5.26	0.00	0.00	0.00	0.00

The various models were compared by adding the probabilities of support failure by keyblocks and the results are shown in Figure 5.6. The summed probabilities shown are indicative only and not the real probabilities of failure, which are shown in Tables 5.2, 5.3 and 5.4 for different block sizes. From this it can be seen that the probability of support failure increases with increasing span for all three keyblock sets. From this modelling, it appears that south mining is less hazardous although the spans used were slightly different.

The results using the Large Blocks-2 set are probably the most realistic. An additional 10 models were run to assess the impact of increasing the elongate support peak load to 300kN for this keyblock set. Figure 5.6 shows that the summed probabilities of failure are substantially reduced by superior support.

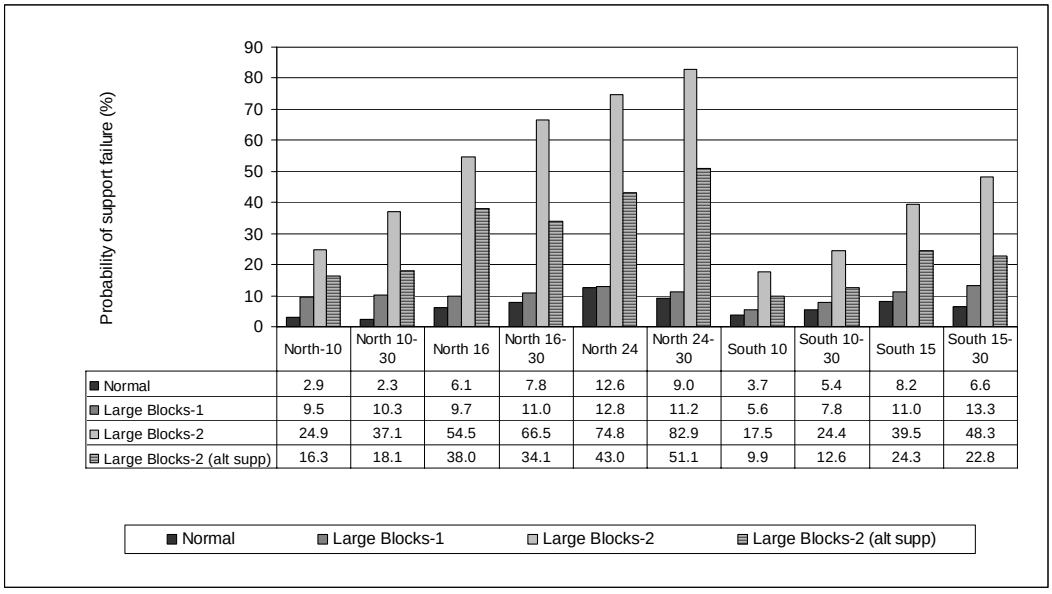

	North-10	North 10-30	North 16	North 16-30	North 24	North 24-30	South 10	South 10-30	South 15	South 15-30
Normal	2.9	2.3	6.1	7.8	12.6	9.0	3.7	5.4	8.2	6.6
Large Blocks-1	9.5	10.3	9.7	11.0	12.8	11.2	5.6	7.8	11.0	13.3
Large Blocks-2	24.9	37.1	54.5	66.5	74.8	82.9	17.5	24.4	39.5	48.3
Large Blocks-2 (alt supp)	16.3	18.1	38.0	34.1	43.0	51.1	9.9	12.6	24.3	22.8

Figure 5.6 Summed probabilities of support failure by keyblocks for all keyblock sets including results from additional modelling with Large Blocks-2 and superior support

5.3.2 Fall of ground hazard indicators

JBlock calculates a number of hazard indicators that can be used to compare different panel and support layouts. The following were used in this analysis:

- the sum of all the hazard units (tothaz);
- the volume of failure (failvol);
- the maximum percentage failure found in the area of interest grid (failtotmax%);
- the maximum hazard value found in the area of interest grid (haztotmax).

The rockfall hazard calculated by JBlock is based on fatal accidents statistics from deep level gold mining and considers both the block size and personnel exposure. The hazard value is calculated at different points and is normalised per 1000m^2. The sum of all the hazard units is also determined. This does not have a real meaning and should only used for comparative purposes (Esterhuizen, 1996).

Table 5.5 shows the results for the 40 models conducted using the three different keyblock sets. The results have been ranked in ascending order based on the total hazard. For the Normal Blocks set analysis, the South 15 and North 24 panel layout options are the most hazardous. For the Large Blocks-1 and Large Blocks-2 analyses, North 16-30, North 16, North 24 and North 24-30 are the most hazardous due to the larger spans. The option of using superior support can reduce the hazard by approximately 50 percent.

This analysis indicates that span rather than mining direction is the driving factor in influencing the hazard level and that it is possible to reduce the hazard by installing superior support. A cost-benefit analysis should be conducted in terms of optimising spans and the internal support standard. An acceptable hazard level needs to be defined as part of this process.

Table 5.5 Hazard summary with options ranked in ascending order based on the Total Hazard (Tothaz)

	Panel Layout	Tothaz	Failvol	Failtotmax%	Haztotmax
Normal Blocks	North 10-30	1.37E+03	1.66E+03	2.67	1.08E+00
	South 10-30	2.15E+03	2.07E+03	2.24	1.23E+00
	South 10	2.44E+03	1.76E+03	2.37	1.61E+00
	North 10	2.72E+03	1.64E+03	2.40	1.78E+00
	North 16	3.32E+03	2.57E+03	2.74	1.70E+00
	South 15-30	4.34E+03	3.45E+03	4.34	2.17E+00
	North 16-30	4.38E+03	3.44E+03	3.68	1.69E+00
	North 24-30	4.65E+03	4.43E+03	4.41	1.61E+00
	South 15	5.21E+03	3.06E+03	3.61	2.43E+00
	North 24	6.10E+03	4.28E+03	4.67	2.51E+00
Large Blocks-1	South 10	2.18E+04	4.29E+03	1.14	6.93E+00
	South 10-30	2.24E+04	5.41E+03	1.18	5.40E+00
	North 10	4.55E+04	6.63E+03	1.49	9.64E+00
	North 10-30	5.20E+04	8.56E+03	1.49	7.30E+00
	South 15	7.68E+04	1.01E+04	2.18	1.03E+01
	South 15-30	7.71E+04	1.28E+04	2.39	8.72E+00
	North 16	1.05E+05	1.26E+04	2.12	1.03E+01
	North 16-30	1.14E+05	1.79E+04	2.55	9.21E+00
	North 24	1.19E+05	1.74E+04	2.81	9.90E+00
	North 24-30	1.38E+05	2.69E+04	2.79	7.58E+00
Large Blocks-2	South 10	6.32E+04	6.90E+03	1.36	9.76E+00
	South 10-30	6.79E+04	9.26E+03	1.49	8.01E+00
	North 10-30	2.86E+05	1.96E+04	2.89	1.72E+01
	North 10	3.44E+05	1.66E+04	3.29	2.53E+01
	South 15	6.46E+05	2.93E+04	4.73	2.81E+01
	South 15-30	7.30E+05	4.17E+04	5.16	2.38E+01
	North 16	1.29E+06	4.28E+04	6.72	4.13E+01
	North 16-30	1.31E+06	5.94E+04	6.86	3.10E+01
	North 24	1.93E+06	7.24E+04	9.04	4.07E+01
	North 24-30	2.11E+06	1.01E+05	8.00	2.81E+01
Large Blocks-2 (alt supp)	South 10-30	3.00E+04	5.84E+03	1.12	6.06E+00
	South 10	3.08E+04	4.57E+03	0.97	7.01E+00
	North 10-30	1.57E+05	1.31E+04	2.18	1.26E+01
	North 10	1.72E+05	1.10E+04	2.16	1.62E+01
	South 15-30	3.11E+05	2.48E+04	3.43	1.51E+01
	South 15	3.31E+05	1.95E+04	3.44	2.04E+01
	North 16-30	6.38E+05	3.76E+04	5.12	2.28E+01
	North 16	6.87E+05	3.06E+04	4.51	2.83E+01
	North 24	9.74E+05	4.83E+04	6.22	2.80E+01
	North 24-30	1.03E+06	6.65E+04	5.90	2.06E+01

5.4 Chapter summary

This chapter presented results from JBlock modelling comparing panel layouts. Different spans, mining directions and support types were evaluated and it was found that spans and support type have the largest influence on panel stability. The following chapter will present results from an analysis of crush pillar stability.

6 CRUSH PILLAR STABILITY

The previous chapter presented results from an analysis of spans using probabilistic keyblock methods and JBlock. This chapter will cover crush pillar design at Tau Lekoa Mine. This will include the application of probabilistic methods to cater for the variability in rock mass properties and mining factors such as pillar dimensions and spans.

6.1 Crush pillar design

Ozbay and Roberts (1988) described fractured or crush pillars as a subset of yield pillars, which are fractured by face abutment stresses whilst being cut and are formed at their residual strength. A residual strength of 13MPa at a strain of 0.4 was back calculated from underground observations. It was noted that at stoping widths of 1m to 1.8m pillars should not exceed a width-to-height ratio (w:h) of 2:1.

Ryder and Ozbay (1990) provided a design overview of both squat (w:h > 5) and slender (w:h < 5) pillars and a description of pillar behaviour. This included defining a number of correction factors for pillar size, shape, width-to-height ratio, foundation damage and creep as well as the use of a numerical modelling programme (BEPIL) for the design of pillars. It was noted that the residual strength of a 2:1 pillar was at least 5 to 10 percent of its peak strength.

Ozbay *et al* (1995) reviewed pillar system design practices in the South African hard-rock tabular mining sector and noted that the use of small width-to-height ratio pillars (w:h < 3) increased with depth where the residual pillar strength was sufficient to meet support resistance requirements. The term “crush pillars” was used for pillars intended to crush while they are still part of the face. It was noted that the design of crush pillars was generally based on using dimensions that had worked elsewhere under similar geotechnical conditions and this was adjusted through observation.

York *et al* (1998) developed a preliminary methodology in the form of a design chart based on numerical modelling. Efforts were also made to instrument and back analyse crush pillars at Amandelbult and Impala Platinum mines.

Roberts *et al* (2005) used underground stress measurements and numerical modelling to determine the residual strength of 19MPa for width-to-height ratio of 2:1 for a Merensky Reef crush pillar. They concluded that the residual strength of the crush pillars lies in the range of 13MPa to 25MPa.

Recent SIMRAC research (Canbulat *et al*, 2006) concluded that:

- crush pillars tend to behave in a broadly similar manner in similar mining environments, irrespective of what reef is being mined;
- it is impractical to develop universally applicable design charts.

6.2 Crush pillar design at Tau Lekoa Mine

The design of crush pillars at Tau Lekoa Mine is based on the methodology outlined by Ryder and Ozbay (1990), and considers the pillar shape, width-to-height ratio, foundation damage and creep. Strike pillars of 8m by 3m and mid-panel pillars of 4m by 4m, were designed using a mean VCR strength of 183MPa and a width-to-height ratio of 1.5 (Harris and Rosenblatt, 1993; Rosenblatt, 1994).

The peak pillar strength was calculated to be 80MPa with an estimated residual strength of 10MPa, although it is not clear how this value was derived. Numerical modelling (BESOL) was used to determine the face stress and a pillar factor of safety of 0.8 was determined and was considered sufficient to ensure pillar fracturing (Harris and Rosenblatt, 1993; Rosenblatt, 1994).

Generally, crush pillar behaviour at Tau Lekoa Mine has been as expected. Occasionally pillars will scale excessively due to an inadequate width-to-height ratio or a locally weaker rock mass. The most common reason for undersized

pillar would be over mining. Scraper and water-jet action also contribute to pillar scaling.

In some cases, pillars have totally disintegrated creating a larger effective span, which is considered hazardous. Undersized pillars are usually excessively fractured which can lead to excessive scaling and eventual pillar failure. Undersized or under designed pillars are also unable to provide the support load required thus increasing the demand on internal support elements and increasing the possibility of failure of the entire support system.

Only one case of pillar bursting has been observed at Tau Lekoa Mine. This was associated with dynamic loading from a distant seismic event on a geological structure and an oversized pillar that was partially positioned within a dyke which has a higher strength than the VCR.

6.3 Probability based crush pillar design

The design approach adopted at Tau Lekoa Mine used typical values for the uniaxial compressive strength and the pillar width-to-height ratio, whereas in reality both vary considerably and this variation should be considered during the design process. Esterhuizen (1993) showed that variability in rock mass properties and mining factors could be taken into consideration for hard-rock pillar design by statistical methods and the application of Rosenblueth's Point Estimate Method (Harr, 1987).

York and Canbulat (1998) concluded that a probabilistic approach was needed for pillar design to cater for the large variability in material and loading conditions. Subsequently, a probabilistic approach has also been applied in the design of chromitite pillars (Wesseloo and Swart, 2000; Joughin *et al*, 2000) with the application of the Point Estimate Method (PEM).

Probabilistic methods such as Monte Carlo simulation (MCS) or Latin Hypercube sampling (LHS) could be applied in the design of pillars. Pine and Thin (1993) evaluated various probabilistic analysis methods including MCS, LHS and PEM for risk assessment in mine pillar design and concluded that PEM provides comparable results to MCS and LHS with much less computation. This method will not be described in detail as it is well documented by Harr (1987) and in the literature referred to previously. This approach has been applied in revisiting crush pillar design at Tau Lekoa Mine to account for variability in pillar strength and the loading system.

6.3.1 Pillar strength

The pillar peak (σ_s) and residual (σ_r) strengths were estimated using the approach outlined by Ryder and Ozbay (1990) as follows:

$\sigma_s = \sigma_c * F1 * F2 * F3 * F4 * F5 * F6$

where:

F1 Strength adjustment to downgrade σ_c to the pillar rock mass strength, (typically 0.2 to 0.5 is used).

F2 Shape correction: Square pillar = 1; Rectangle (1*2) = 1.1; Rectangle (1*4) = 1.2; Rectangle (1*large) = 1.3

F3 Width-to-height ratio adjustment for laboratory specimen to a unit cube (1.3)

F4 Pillar width-to-height ratio adjustment: 1 (w:h = 1); 1.2 (w:h = 2); 1.4 (w:h = 3); 1.6 (w:h = 4)

F5 Foundation damage (a value of 1 is used unless there is contrary evidence).

F6 Creep (a value of 1 is used unless there is contrary evidence).

Peak pillar strength

The peak pillar strength was determined for both the rectangular strike pillars and the square mid-panel pillars by applying the PEM to the Ryder and Ozbay (1990) relationship. The rock strength (σ_c) and the pillar width-to-height ratio are considered as the main variables in this analysis.

A mean σ_c of 187.1 ± 44.8MPa as determined in section 3.2.2 was used as an input. Pillar width-to-height ratio input was based on distributions and descriptive statistics of pillar measurements over a 20 month period and is covered in greater detail in Chapter 7. A summary of the variable input parameters is shown in Table 6.1 with the relevant adjustment factors.

Table 6.1 Variable input parameters used to determine pillar strength

Parameter	Mean	Std Deviation	+	_
σ_c	187.2 (MPa)	44.8 (MPa)	231.9 (MPa)	142.3(MPa)
w:h	1.8	0.72	2.52	1.09
F4	-	-	1.3	1

Results of the PEM analysis for peak pillar strength are shown in Table 6.2. The peak strength for a strike pillar is 123.1 ± 33.8MPa and for a mid-panel pillars it is 111.9 ± 30.7MPa.

Residual pillar strength

Based on the 5 to 10 percent range outlined by Ozbay and Ryder (1990) the residual pillar strength has been estimated as eight percent of the peak pillar strength using the following relationship:

$$\sigma_r = 0.08 * \sigma_s$$

The residual strengths determined for the rectangular strike pillars (9.8 ± 2.7MPa) and the square mid-panel pillars (9.0 ± 2.5MPa) were similar and close to the

original estimate of 10MPa (Harris and Rosenblatt, 1993; Rosenblatt, 1994) but lower than the 13MPa to 25MPa range stated by Roberts *et al* (2005).

Table 6.2 Results of PEM analysis of peak pillar strength

	Strike pillars F1 = 0.4; F2 = 1.1; F3 = 1.3; F5 & F6 = 1		Mid-panel pillars F1 = 0.4; F2 = 1; F3 = 1.3; F5 & F6 = 1	
Combination of parameters	σ_s (MPa)	$(\sigma_s)^2$	σ_s (MPa)	$(\sigma_s)^2$
+ +	172.4	29735.8	156.8	24575.1
+ -	132.6	17595.2	120.6	14541.5
- +	105.8	11196.7	96.2	9253.4
- -	81.4	6625.2	74.0	5475.4
Sum	492.3	65152.9	447.5	53845.4
Expected	123.1	16288.2	111.9	13461.3
Std Deviation	33.8	-	30.7	-

6.3.2 Average pillar stress

Average pillar stresses (σ_p) have been estimated using tributary-area theory as numerical modelling was not included in the scope of this project. The purpose is to demonstrate how pillar stress can vary with depth and the local extraction ratio. In the original design, a single face stress value of 103MPa was used to estimate the average pillar stress (Harris and Rosenblatt, 1993; Rosenblatt, 1994).

Mining at Tau Lekoa Mine is carried out at between 900m to 1650m below surface. The pre-mining vertical stress (σ_v) on each mining level was assumed to be equivalent to the overburden stress, estimated to be 27MPa per kilometre depth. At Tau Lekoa Mine the mining level is approximately the depth below surface and Table 6.3 summarises the vertical virgin stress for each mining level.

Table 6.3 Vertical stress per mining level

Mining Level	σ_v (MPa)
900	24.3
1050	28.4
1200	32.4
1350	36.5
1500	40.5
1650	44.6
Mean	34.4
Std Dev	7.6

To apply tributary-area theory, the local extraction ratio (e) was estimated based on measurements over a 20 month period of pillar width-to-height ratios and spans in between pillars. Descriptive statistics and distributions were compiled for these data and are covered in Chapter 7. A summary of the variable input parameters is shown in Table 6.4.

Table 6.4 Variable input parameters used to determine pillar stress (input data in brackets)

Parameter	Mean	Std Deviation	+	_
w:h	1.8	0.72	2.52	1.09
Span (m)	12.5 (12.0)	6.65 (2.89)	19.15 (14.89)	5.85 (9.11)
σ_v (MPa)	34.4	7.6	42	26.8

Tributary-area theory assumes that each pillar carries an equal share of the overburden and ideally should only be applied to regular pillar layouts and at mining spans at least equal to the mining depth. At depth, this method tends to over estimate the pillar stresses as the effects of abutments and large regional pillars are ignored. To counteract this, the local extraction ratio was downgraded by 20 percent to account for un-mined ground in the form of geological losses and regional pillars.

The average pillar stress was determined using the following equation:

$\sigma_p = \sigma_v / (1 - e)$

The extraction ratio (e) was determined using the tributary-area based on point estimates of span and pillar width. Results of the PEM analysis of pillar stress using the input data are summarised in Table 6.5. Similar results were obtained when the descriptive statistics from the @ Risk fit were used.

Table 6.5 Results of PEM analysis of average pillar stress

	Strike pillars		Mid-panel pillars	
Combination of parameters	σ_p (MPa)	$(\sigma_p)^2$	σ_p (MPa)	$(\sigma_p)^2$
+ + +	124.9	15596.9	182.9	33452.4
+ + -	157.3	24733.1	202.9	41169.1
+ - +	105.9	11220.3	139.9	19571.3
- + +	79.7	6350.5	116.7	13620.7
- - +	67.6	4568.5	89.3	7968.7
+ - -	138.6	19222.8	183.0	33477.5
- + -	100.4	10070.5	129.5	16762.6
- - -	88.5	7826.9	116.8	13630.9
Sum	862.8	99589.5	1160.9	179653.2
Expected	107.9	12448.7	145.1	22456.6
Std Deviation	28.6	-	37.4	

6.3.3 Pillar factor of safety

The peak pillar strength and average pillar stress were used to determine the pillar factor of safety (F) as follows:

$F = \sigma_s / \sigma_p$

The PEM was applied in determining the factor of safety for both strike and mid-panel pillars and the results of this analysis are shown in Table 6.6. Crush pillars are designed to be in a failed state with factors of safety of 1 or slightly less.

This analysis shows that it is possible to have factors of safety greater than 1, which could result in pillars not crushing, increasing the risk of unstable pillar failure. Very low factors of safety especially for mid-panel pillars, are a real possibility and could result in excessive pillar scaling and ultimately total pillar failure. This is in line with observations that scaling of mid-panel pillars is often a problem. Strapping these pillars with scraper rope is a mine standard that was implemented to reduce this problem.

Results from the probabilistic analysis provide better insight into how pillars could behave compared to the deterministic approach originally applied.

Table 6.6 Results of PEM analysis of pillar FOS

	Strike pillars		Mid-panel pillars	
Combination of parameters	FOS	$(FOS)^2$	FOS	$(FOS)^2$
+ +	1.15	1.32	0.78	0.61
+ -	1.98	3.91	1.32	1.75
- +	0.65	0.43	0.44	0.20
- -	1.13	1.27	0.75	0.57
Sum	4.91	6.93	3.30	3.13
Expected	1.23	1.73	0.83	0.78
Std Deviation	0.48	-	0.32	

6.4 Chapter Summary

This chapter presented a brief overview of deterministic crush pillar design at Tau Lekoa Mine. The Point Estimate Method (Harr, 1987) was applied to cater for variability in rock strength, pillar dimensions and spans. This demonstrated how

pillar strength and loading environment can vary and that a probabilistic approach provides a better insight into possible pillar behaviour. The following chapter will focus on risk assessment in an attempt to include geotechnical and mining aspects.

7 LARGE HANGINGWALL INSTABILITY RISK ASSESSMENT

The previous chapter covered crush pillar design at Tau Lekoa Mine and included a probabilistic approach with the application of the Point Estimate Method. This demonstrated how pillar strength and pillar stress vary due to the rock mass, pillar dimensions, span and depth variations. This chapter will cover a risk assessment of large hangingwall instabilities.

7.1 Risk Assessment at Tau Lekoa Mine

A qualitative Baseline Risk Assessment on rock related hazards at Tau Lekoa Mine in 1999 identified large hangingwall instabilities or FOG in the form of wedges or domes, as a hazard related to excessive spans. Crush pillar failure related to either undersized or oversized pillars was also identified as a hazard. Undersized pillars and subsequent failure of these pillars were noted as a potential contributor to excessive spans. Oversized pillars have the potential to burst and could result in excessive spans.

In 2002 a hazard identification and risk assessment workshop was conducted at Tau Lekoa Mine for the purposes of ranking rock related hazards and the relative risk for different excavation types. A qualitative / probabilistic approach based on the opinions of the workshop attendees and using the simplified scale shown in Table 7.1 was applied. The probability of occurrence for large hangingwall instabilities was assessed to be 0.01 or 1 percent (Hanekom, 2003).

Table 7.1 Simplified rating scale

Qualitative Likelihood	Probability of Occurrence
Certain	0.1
Often	0.01
Seldom	0.001
Very scarce	0.00001
Never	0.0000001

7.2 Risk Assessment and Hazard Identification

Risk assessment is a process which includes the identification of hazards and the assessment of risk and prioritisation for action. This process can be either quantitative or qualitative and various techniques or methodologies can be used. It should be conducted in a systematic manner and be used to reduce risk to people, property or business. The following definitions have been used in this assessment (Stacey, 2001; Swart, 2003).

Hazard A source of potential harm or a situation with a potential to cause loss.

Probability The likelihood of a specific event or outcome expressed as a number between 0 and 1, with 0 representing an impossible event and 1 indicating a certain event.

Risk Any event that could prevent an entity from achieving its objectives and is measured by likelihood (probability or frequency) of occurrence and the consequence of a specific event. Risk can be expressed as follows:
Risk = (Probability of an event) * (Consequence of occurrence)

This study considers the risk associated with large hangingwall instabilities in stope panels. The possible consequences of such an event range from negligible when it occurs in a back area to catastrophic when the result is multiple fatalities. Production losses would generally be low to moderate as only a portion of a stoping panel would normally be affected. However, repeated incidents or a multiple fatality have the potential to result in significant production losses.

The focus is on quantifying the probability of occurrence for large hangingwall instabilities by incorporating various factors that contribute to the occurrence of these instabilities.

7.3 Conditions for a Large Hangingwall Instability

For a large hangingwall instability to occur, a number of conditions must be satisfied as follows:

- Presence of a large dome or wedge structure within the hangingwall.
- Freedom of ejection i.e. a dome or wedge must fall within the span between crush pillars, although cantilever rotational failure is possible if there is limited overlap of a crush pillar (Figure 7.1).
- Dome or wedge demand exceeds the internal support system capacity.

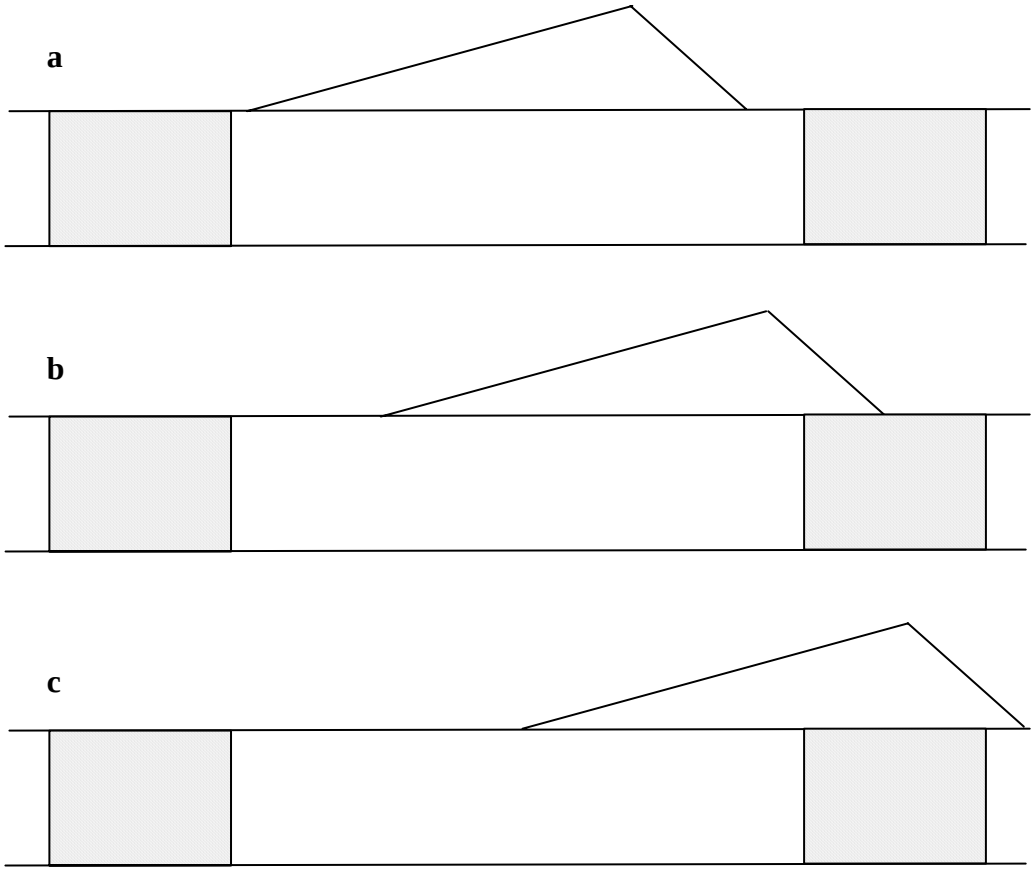

Figure 7.1 Schematic showing potential for a large hangingwall instability: (a) high probability as wedge occurs in between pillars; (b) cantilever failure possible; (c) wedge failure unlikely

7.4 Fault Tree Analysis

Conditions for large hangingwall instabilities can be depicted using a Fault Tree as shown in Figure 7.2. Fault Tree Analysis (FTA) is a quantitative or qualitative approach by which conditions and factors that can contribute to a specified undesired incident are identified and organised in systematic manner (Stacey, 2001). This technique is described in detail by Stacey (2001) therefore only the basic definitions are covered in this report.

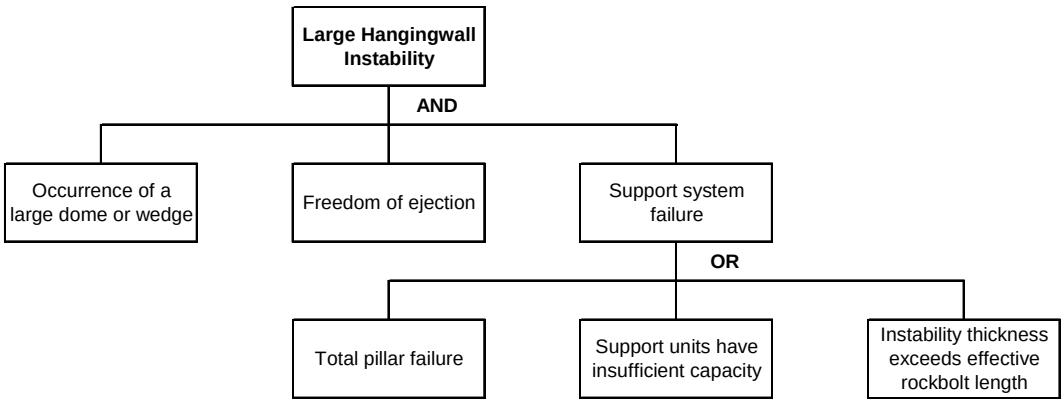

Figure 7.2 Cause tree showing factors that contribute to large hangingwall instabilities

The tree shown in Figure 7.2 depicts the logic and relationships between various factors contributing to the top fault, in this case a large hangingwall instability. The levels below the top fault are called the primary and secondary faults and in this form the tree is referred to as a "cause tree". Once the probabilities of occurrence or likelihood have been incorporated for the primary and secondary faults it is termed a "fault tree" and it is possible to calculate the probability of occurrence for the top fault.

7.4.1 Calculating probabilities of occurrence

Two types of gates are used when calculating the probability of occurrence within the "fault tree". The following descriptions have been taken from Stacey (2001).

AND Gates

Are used where faults are statistically dependent i.e. when it is necessary for *n* secondary faults to occur in order for a primary fault to result, then the probability of occurrence is represented by:

p[primary fault] = p[secondary fault 1] * p[secondary fault 2] * …* p[secondary fault n]

OR Gates

Are used where faults are statistically independent i.e. if a primary fault can result as a consequence of the occurrence of any *n* secondary faults, then the probability of occurrence is determined from the calculation as follows:

p[primary fault] = 1 - (1 – p[secondary fault 1])(1 – p[secondary fault 2]) ……. (1 – p[secondary fault n])

7.4.2 Allocation of probabilities of occurrence

If data is available on the probability of occurrence of specific faults this can be used as an input for the fault tree or they can be estimated using the qualitative description shown in Table 7.2. Another option would be to use simulation techniques and sample from a probability density function.

Previous chapters covered a number of factors that influence and contribute to large hangingwall instabilities. This section will attempt to evaluate these factors in terms of probability of occurrence for the various faults shown in Figure 7.2.

Table 7.2 Probability of occurrence (Stacey, 2001)

Qualitative likelihood of occurrence	Probability of occurrence
Certain	1
Very High	10^{-1}
High	10^{-2}
Medium	10^{-3}
Low	10^{-4}
Very Low	10^{-5}
Extremely Low	10^{-6}
Practically Zero	10^{-7}

7.5 Factors Influencing Large Hangingwall Instabilities at Tau Lekoa

A number of factors influence large hangingwall instabilities and a discussion of these follows.

7.5.1 Occurrence of large dome or wedge structures

It is difficult to assess the frequency of large dome or wedge structures at Tau Lekoa Mine as they are not routinely mapped. Probabilistic keyblock modelling using JBlock is able to provide some idea of the size range and relative proportion of joint defined blocks that could be formed. This analysis is covered in Chapter 5 and Figure 7.3 is a summary of the cumulative percentage of block volumes for the different block sets.

The size of the blocks created in JBlock is influenced by the joint spacing. Figure 7.3 show a higher proportion of smaller blocks in the Normal block set with only eight percent of blocks exceeding $20m^3$. The minimum joint spacing was increased when generating the other two block sets (Large Blocks-1 and Large Blocks-2) and they have a higher proportion of large blocks.

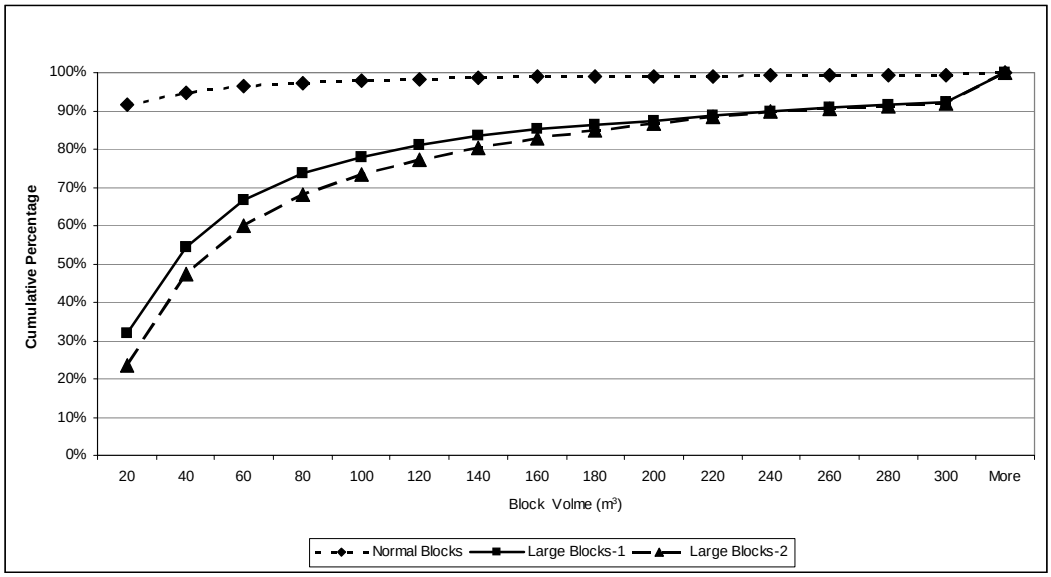

Figure 7.3 Cumulative percentage of block volume for different block sets

From this data it can be inferred that large joint defined blocks are relatively common although they are not necessarily unstable. Limited data is available on the frequency and size of dome structures at Tau Lekoa Mine. Ripouts, ramps and duplex structures are common in the lavas forming the VCR hangingwall (Roberts and Schweitzer, 1999); and it is likely that domes in a range of sizes are common at Tau Lekoa Mine.

7.5.2 Freedom of ejection

For this study, freedom of ejection is defined as the appearance of a potentially unstable block (dome or wedge) within the span between the crush pillars. For a block to have potential to fallout in between the crush pillars, the block dimensions must be less than the spans between pillars. Even if a discreet block occurs within the span it is not necessarily unstable. Block stability is influenced by the frictional properties of the discontinuities forming the block and the stress normal to these planes.

Span and potential instabilities

In Chapter 4 it was shown that span standards were exceeded for many of the large FOG recorded at Tau Lekoa Mine. Spans are measured on a monthly basis by the Survey Department and plotted on the mine plans which are reviewed monthly by the Rock Engineering Department and incorporated into a panel rating (Judeel and Laas, 1999).

Span measurements over a twenty month period (March 2000 to November 2001) were used to determine the probability density functions and cumulative distributions and are summarised in Table 7.3 with the cumulative distribution for all spans shown in Figure 7.4. It can be seen that there is a difference between the statistical parameters determined using the @Risk fit to those determined directly from the input data (shown in brackets).

Table 7.3 Statistical summary for spans

	Fit	Mean (m)	Std Dev (m)	95% (m)	% > 10m	% >16m
All Spans	Uniform	12.5 (12.0)	6.65 (2.89)	23.1 (16.7)	60.9 (64.2)	34.8 (6.1)
South	Uniform	11.0 (10.0)	5.22 (2.54)	19.1 (15.0)	55.5 (48.1)	22.3 (3.0)
North <1.8m	Uniform	12.5 (12.5)	6.66 (2.96)	22.6 (16.0)	60.8 (71.2)	34.8 (5.2)
North >1.8m	Uniform	11.5 (12.3)	4.95 (2.78)	19.4 (29)	58.7 (71.2)	23.8 (8.2)

From this analysis it can be inferred that span standards are often exceeded (shaded cells in Table 7.3). A large proportion of the observed large FOG occurred at spans that exceeded the standard. As the span is increased the probability of a wedge or dome occurring between crush pillars is also increased. A large span also increases the probability of larger potential instabilities. This

results in an increased probability of failure and this as shown by the JBlock modelling described in Chapter 5.

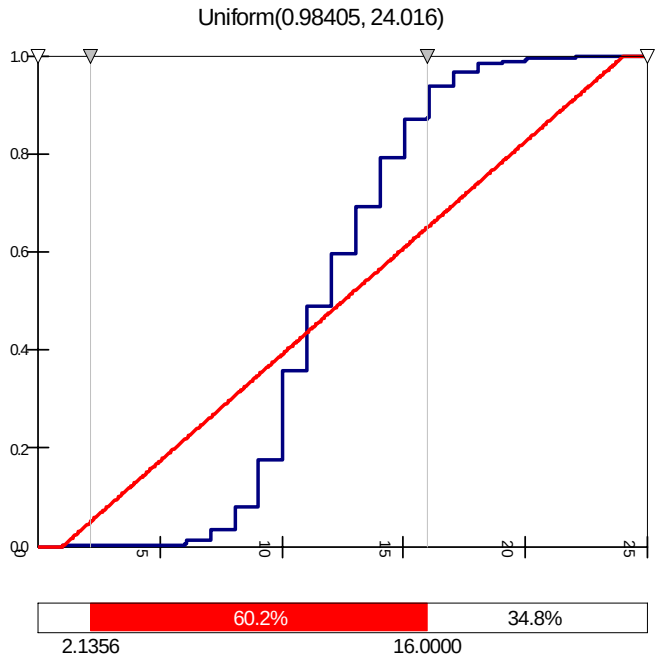

Figure 7.4 Cumulative distribution for span (statistical fit and input data)

Dome and wedge dimensions

Figure 7.5 shows the distribution and cumulative percentage for block dimensions (length and width) generated using JBlock (Large Blocks-2). Ninety-six percent of the block dimensions are less than 16m and 79 percent are less than 10m. Whilst it is difficult to determine the real distribution of large dome or wedge structures in space, JBlock modelling showed that they can occur quite regularly in between pillars.

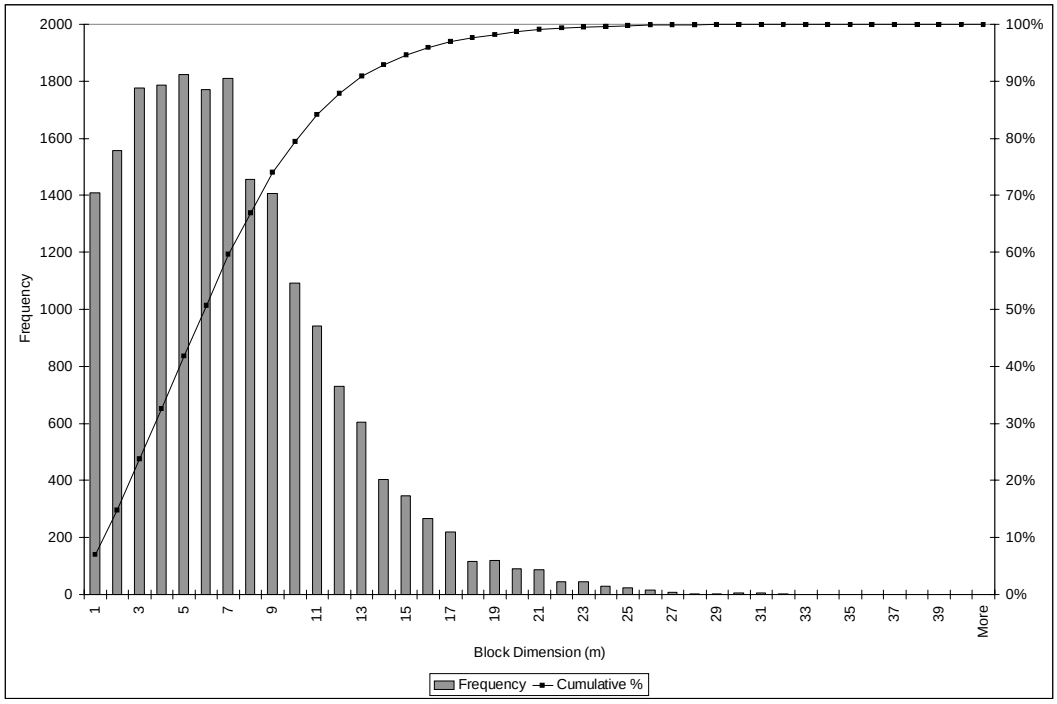

Figure 7.5 Block dimension distribution and cumulative percentage from JBlock modelling (Large Blocks-2)

Depositional setting

In Chapter 4 it was indicated that large FOG were more likely to occur within the Main Channel. There does not appear to be any logical reason why the lava above the Main Channel should have a higher incidence of dome or wedge structures.

The Main Channel is characterised by higher stoping widths as a result of the thicker channel and it is more likely that rock bolts would be used in these areas. The effectiveness of timber elongates is reduced at higher stoping widths and is possibly one the reasons why a greater proportion of large FOG occur in the Main Channel.

Mining direction

The large FOG data indicates that there is a higher risk when mining south. However, the JBlock analysis does not support this finding. A possible explanation is the mining direction relative to the dip direction of joints. When mining south joint set 2 dips away from the face, making it difficult to identify

wedge structures in the hangingwall. When mining north, joint set 2 dip towards the face and potential wedges can be identified earlier. A mid-panel pillar can then be left to support the wedge.

7.5.3 Support system failure

The mass of a potential hangingwall instability is determined by its length, width, height and shape; and the rock density. The demand on the support system is a function of the mass of the potential instability and gravity. The support system capacity is a function of the load-deformation characteristics of the individual support units, unit density and installation quality. In the case of pillars the mining quality is important. Support system failure occurs when the demand from the hangingwall instability exceeds the capacity of the support system.

The stope support system at Tau Lekoa Mine is based on an empirical relationship between the fallout thickness and the span between crush pillars. The internal support is designed to control a potential instability thickness derived from this empirical relationship with a poor statistical correlation.

Pillar failure

The crush pillars were designed at a width-to-height ratio of 1.5, a residual pillar strength of 10MPa and a factor of safety of 0.8. In Chapter 6 it was demonstrated that the crush pillar residual strength varies due to rock strength and width-to-height variability.

Pillar widths and heights are measured on a monthly basis by the Survey Department and plotted on the mine plans which are reviewed monthly by the Rock Engineering Department and incorporated into a panel rating (Judeel and Laas, 1999).

Measurements over a twenty month period (March 2000 to November 2001) were used to determine a mean width-to-height ratio of 1.8±0.72 for both strike and mid-panel pillars. Figure 7.6 shows the cumulative distribution for strike pillars.

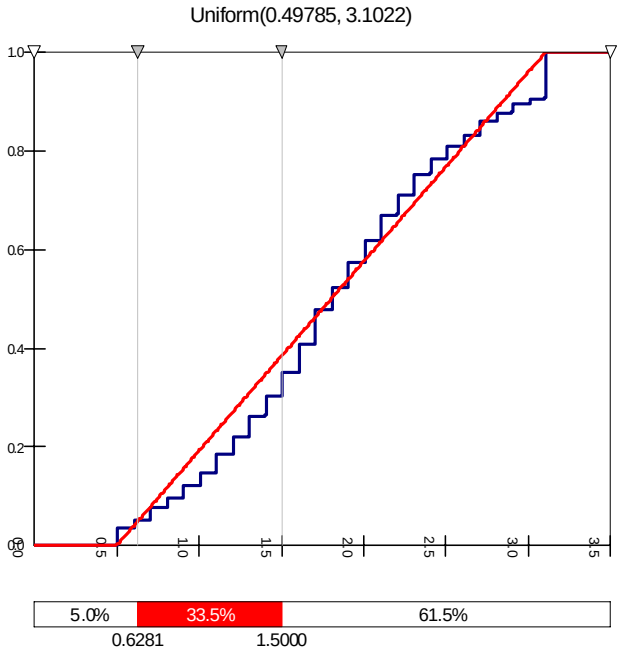

Figure 7.6 Cumulative distribution for strike pillar width-to-height ratio

From this it can be inferred that there is a 38.5 percent chance of having a width-to-height ratio of less than 1.5 and a 20 percent chance of a width-to-height ratio of less than 1. A crush pillar with a width-to-height ratio of 1 has a residual strength of 6 to 7MPa and is unlikely to fail due to loading by a dome or wedge.

At a low width-to-height ratio of less than 0.5 it is possible that a crush pillar could fail. Based on the distribution of measured pillar width-to height ratios this is unlikely with less than 5 percent of width-to-height ratios below 0.5

Internal support capacity exceeded

The potential fallout thickness at Tau Lekoa Mine is estimated to be 0.125 times the span and internal support is required to support a thickness of 1.25m and 2m

for spans of 10m and 16m respectively. The support resistance requirements are shown in Table 3.4.

Table 7.4 Back area support resistance requirements

Span (m)	Potential fallout thickness (m)	SR requirement (kN/m^2)
10m	1.25	33
16m	2	53

To satisfy this at stoping widths of less than 1.8m, profile props with a peak capacity of 250kN are used at a spacing of 1.5m on strike and 2m on dip. This provides a support resistance of 83kN/m^2 sufficient to support a thickness of 3.1m.

In reality it is unlikely that this support resistance is achieved underground as the in situ loads achieved by timber profile props are lower due to the slower loading rate. Timber is also highly variable and markedly influenced by moisture content, presence of cracks and stoping height. The unit performance and quality of support installation and actual installed spacing determines the real support resistance. For the JBlock analysis, the unit loads were down graded to 150kN to account for these factors.

Figure 7.7 shows the height distribution and cumulative percentage for blocks generated using JBlock. Eighty-two percent of the blocks have a height in excess of 3m although many of these blocks are stable.

The above factors indicate that it is quite possible that the internal support capacity can be exceeded. This was shown in the JBlock analysis which indicted that support failure by keyblocks occurred quite often and the probability of support failure increased with increasing span.

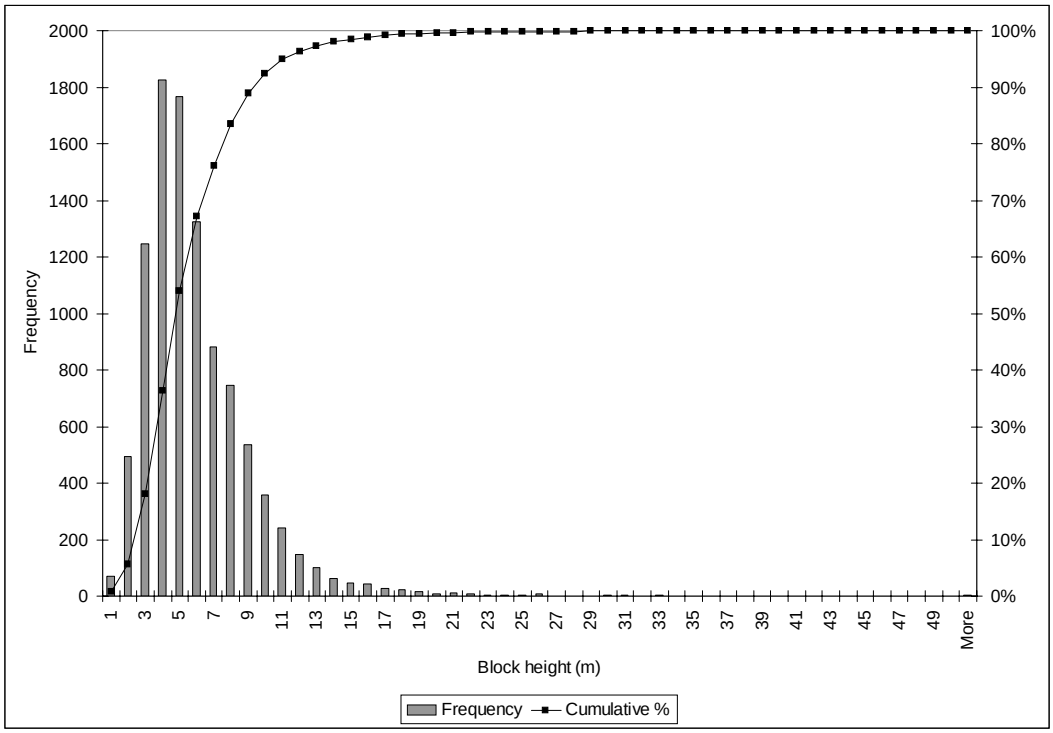

Figure 7.7 Block height distribution and cumulative percentage from JBlock

Instability thickness exceeds effective rock bolt length

For stoping widths greater than 1.8m the span is reduced to 10m and 1.5m long end anchored rock bolts with a capacity of 170kN are used at a spacing of 1.5m on strike and 2m on dip providing a support resistance of 57kN/m^2.

Based on the fallout thickness versus span relationship the rock bolts have to cater for a thickness of 1.25m and the standard exceeds the support resistance requirement shown in Table 7.4. This design relies on suspension as a mechanism and end anchored bolts are only able to support rock situated below the end anchor.

With a perfect installation at 90 degrees to the hangingwall it would be possible to support a 1.4m thickness. In reality the bolts are installed at about 70 degrees and are only able to support a thickness of about 1.3m. The spacing of bolts also has an impact on the capacity of the support system.

Figure 7.8 shows the deviation from the thickness predicted using the empirical relationship and the actual thickness measured for the 81 large FOG. This shows that the predicted thickness is exceeded 27 percent of the time and the effective bolt length of 1.3m is exceeded 20 percent of the time.

Figure 7.7 indicates that 95 percent of the blocks generated in JBlock have heights exceeding the thickness the support is capable of supporting although many of the blocks generated are stable.

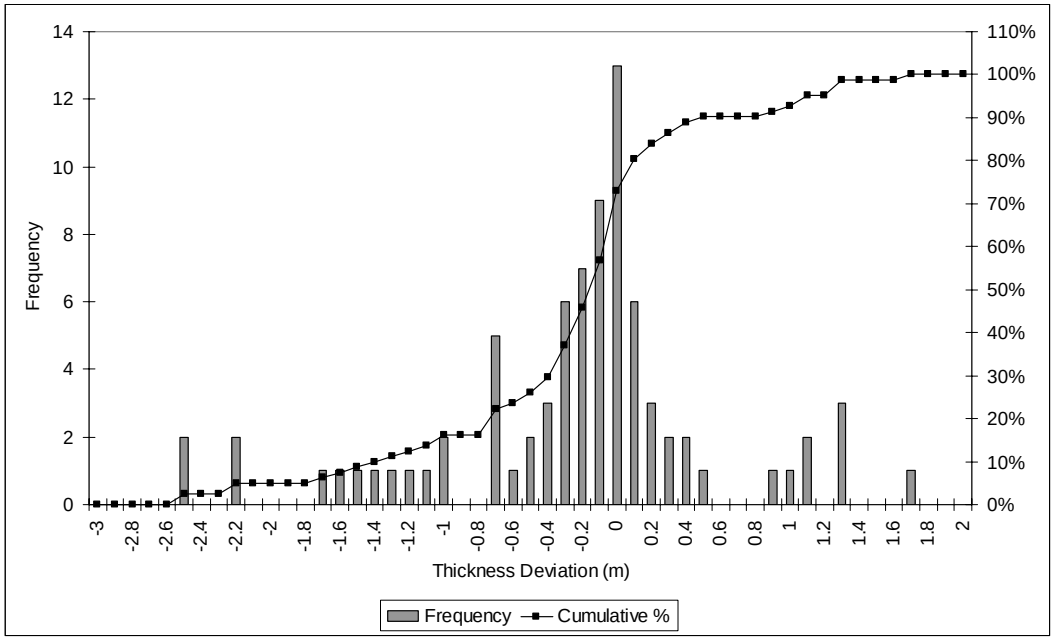

Figure 7.8 Deviation of actual thickness from predicted thickness for large FOG (1991-2001)

7.6 Assessing Probability of Occurrence at Tau Lekoa Mine

The cause tree shown in Figure 7.2 was used to evaluate the probability of occurrence for a large hangingwall instability. It is possible to possible to further refine this tree by breaking down the primary and secondary faults into a number of components which were discussed in section 7.5.

For this study the simplified fault tree was used. Table 7.2 was used to allocate probabilities to the various faults. The probability of occurrence for large hangingwall instabilities is 0.01 percent (Figure 7.9) which is low according to the qualitative likelihood of occurrence scale outlined by Stacey (2001). This is considerably lower than the previous estimate (Hanekom, 2003) which was based on the opinion of the workshop attendees, whilst this assessment considers and attempts to quantify several contributing factors.

This approach can be used to assess the impact of changing factors that influence the freedom of ejection and the support system capacity. For this analysis it was assumed that the probability of occurrence for large domes and wedges remains constant and was allocated a value of 0.1 (10 percent) or "very high" (Stacey, 2001). The effect of varying the following was assessed:

- Increased support capacity
- Increased freedom of ejection due to increased span
- Increased freedom of ejection due to south mining
- Increased freedom of ejection due to south mining and increased span

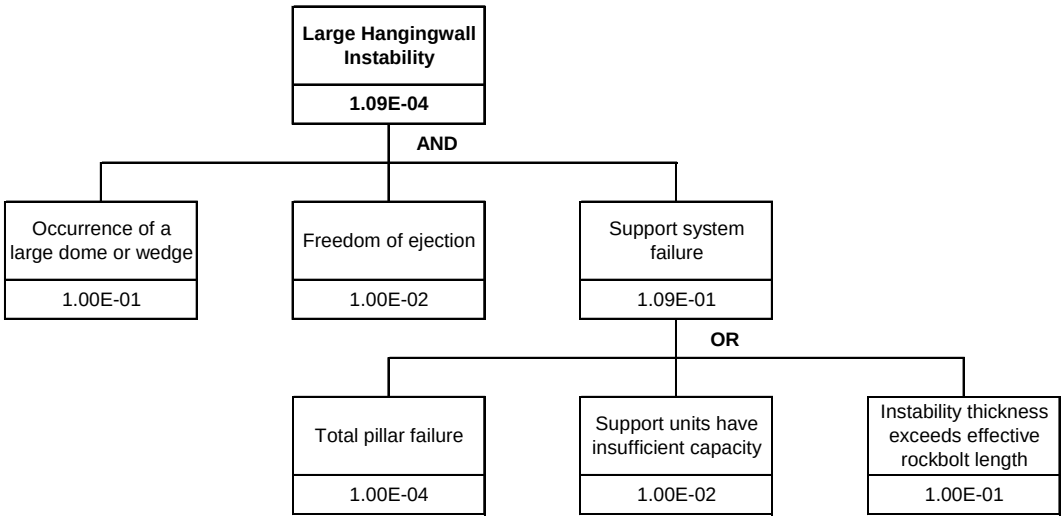

Figure 7.9 Large hangingwall instability fault tree analysis

The results of this analysis are shown in Table 7.5 and indicate that the probability of occurrence increases with an increased span but is decreased with increased internal support capacity. It is possible to obtain the same large hangingwall instability probability of occurrence as the base case by increasing the span but also increasing the internal support capacity.

This approach could be used in a cost-benefit analysis to determine the optimum approach to dealing with large hangingwall instabilities in terms of safety and profitability. It is possible to further develop and refine the fault tree and use a more sophisticated approach to assessing the probabilities of occurrence.

Table 7.5 Large hangingwall instability probability of occurrence

Description	Probability of Occurrence				
	Freedom of ejection	Support system failure			**Large HW Instability**
		Pillar failure	Insufficient support capacity	Thickness exceeds bolt length	
Base case	0.01	0.0001	0.01	0.1	**0.0001 (Low)**
Increased support	0.01	0.0001	0.001	0.01	**0.00001 (Very Low)**
Span increased	0.1	0.0001	0.01	0.1	**0.001 (Medium)**
South mining	0.1	0.0001	0.01	0.1	**0.001 (Medium)**
Increased support & span	0.1	0.0001	0.001	0.01	**0.0001 (Low)**
South mining & increased span	0.19	0.0001	0.01	0.1	**0.002 (Medium)**

7.7 Large Hangingwall Instability Risk Assessment

The analysis outlined in section 7.6 does not consider exposure and the severity of the consequences. Hanekom (2003) calculated people exposure as 4.34E-02 for a $2m^2$ fall of ground in the face area (9m back from the face). This was based on

1500 people exposed for 5 hours in 80 panels with a face length of 20m and is calculated as follows:

$$\text{Exposure} = \text{No. of people} * (\text{Time}_{\text{Stope}} / \text{Time}_{\text{Total}}) * (\text{Area}_{\text{FOG}} / \sum\text{Area}_{\text{Stope face}})$$
$$= 1500 * (5 / 24) *(2 / [80*20*9])$$
$$= 4.34\text{E-}02$$

As the FOG area increases, the chance of coincidence increases resulting in an increase in personnel exposure. For a $20m^2$ FOG the personnel exposure is 4.34E-01 and for a $100m^2$ FOG it is 2.17E+00. If a fatality is given a severity value of one, the risk of a fatality incident due to a large FOG can be calculated as outlined in section 7.2. The probability of the event is the product of the probability of occurrence and exposure.

The following is an example for a $100m^2$ FOG.

$$\text{Risk} = (1.00\text{E-}04 *2.17\text{E}00) * 1$$
$$= 2.17\text{E-}04 \text{ (or } 0.0217\%)$$

This can be compared to acceptable life time probabilities shown in Table 7.6. In this example, the degree of risk falls in the “slight chance” category. This exercise could be repeated for different exposures and consequences to obtain a better understanding of the risk associated with large hangingwall instabilities.

Table 7.6 Acceptable lifetime probabilities (%) of total losses (Cole, 1993)

Degree of risk	Life	Property	Money
Very risky	70	700	7000
Risky	7	70	700
Some risk	0.7	7	70
Slight chance	0.07	0.7	7
Unlikely	0.007	0.07	0.7
Very unlikely	0.0007	0.007	0.07
Practical impossible	0.00007	0.0007	0.007

7.8 Chapter Summary

This chapter attempted to quantify the probability of occurrence for a large hangingwall instability using a fault tree approach and results from the previous chapters. It was demonstrated that this approach could be used to evaluate different support and mining options. The risk of a fatality was assessed for a hangingwall instability with a face area of $100m^2$ and this could be repeated for other sizes. The next chapter will discuss results for the various analyses conducted as part of this study.

8 DISCUSSION OF RESULTS

The previous chapter outlined an assessment of the probability of occurrence for large hangingwall instabilities using the fault tree methodology. The impact of increasing spans and upgrading support on the probability of occurrence was evaluated. An attempt was made to assess the risk of a fatality due to a large hangingwall instability. This chapter will discuss results of various analyses undertaken in this study.

8.1 Fallout Thickness and Span

The design of stope support at Tau Lekoa Mine is based on a relationship between the fallout thickness and span. The relationship has a poor statistical correlation due to the scatter of the data. This relationship was defined for different periods and mining situations but generally the correlation remained poor.

For recorded instabilities, the thickness predicted using the thickness versus span relationship was exceeded 27 percent of time. For blocks generated using JBlock, the percentage of blocks exceeding the prediction is much higher although not all blocks are unstable.

The empirical relationship between fallout thickness and span does not adequately reflect specific underlying geological conditions associated with larger hangingwall instabilities and is unable to account for internal support and variations in the quality of that support.

There is some logic in the assumption that as span increases the thickness of potential instability increases although caution should be exercised when using this approach. Possibly the design should be based on catering for a specific percentage cumulative thickness for large hangingwall instabilities. A 95 percent cumulative thickness is commonly used in South African tabular mining.

Ultimately the risk tolerance of various stakeholders would determine what cumulative percentage should be used.

Another approach could be to consider the 95 percent cumulative level for the factor relating fallout thickness to span as shown in Figure 8.1. At an 80 percent cumulative level, thicknesses of 1.3m and 2.1m would have to be supported for 10m and 16m spans respectively. For a 95 percent cumulative level, thicknesses of 2.5m and 4m would have to be supported for 10m and 16m spans respectively.

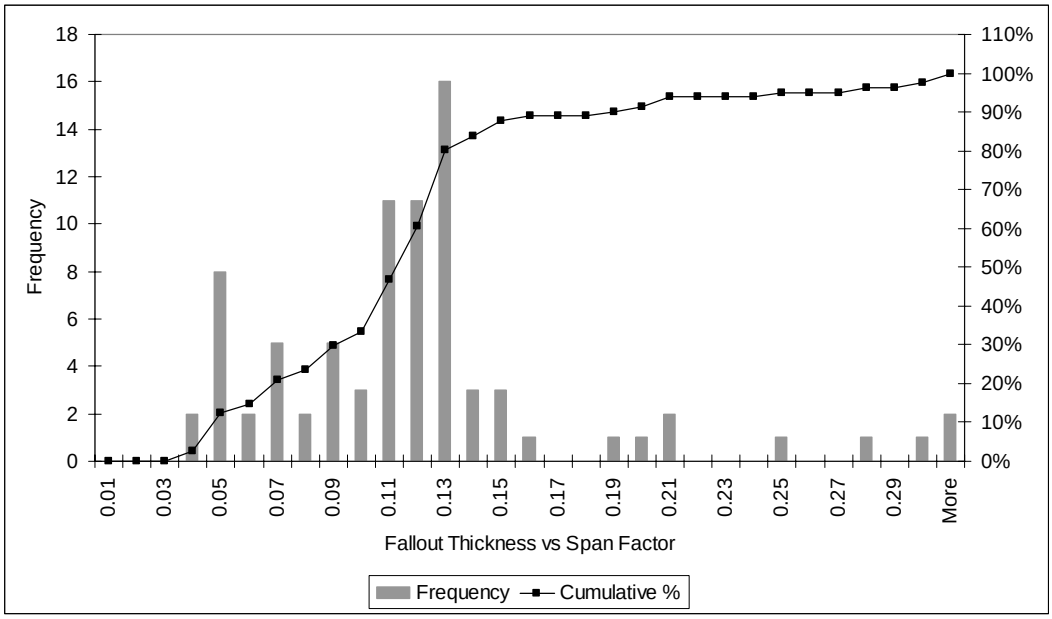

Figure 8.1 Cumulative fallout thickness versus span factor

8.2 Large FOG Statistical Analysis

Various parameters describing large FOG and influencing factors were analysed and a discussion follows.

8.2.1 Large FOG dimensions and spans

Generally, large FOG dimensions have decreased since new standards were introduced in 1995. This could be due to a reduction in spans and improved

adherence to standards. Seventy-seven percent of large FOG occurred at spans in excess of 16m for the period 1991-1994, whilst for the period 1995-2001 only 34 percent of large FOG occurred at spans exceeding 16m.

Span measurements over a twenty month period (March 2000 to November 2001) indicate that a low percentage of panels have spans greater than 16m. Adherence to the 10m spans for south mining and north mining at a stoping widths exceeding 1.8m is problematic with non-conformances of 48 percent and 71 percent respectively.

8.2.2 Geotechnical relationships

Stoping width appears to be a contributing factor to large FOG as about 64 percent of large FOG occurred at stoping widths exceeding 1.8m, which only makes up about 15 percent of all stoping. From this it could be inferred that there is a higher risk at higher stoping widths. This statement should be treated with caution as there is no logical reason why there would be a higher probability of occurrence of large dome or wedge structures in areas with thicker channels.

The higher occurrence of large FOG in thicker channel width areas is most likely to be associated with the support systems applied in these areas. The efficiency of timber elongates is reduced at higher stoping widths and the alternative 1.5m long rock bolts used at Tau Lekoa Mine are often inadequate with the effective length exceeded by the fallout thickness in 20 percent of occurrences.

Spatially, the majority of large FOG occurred in the Main Channel areas of Tau Lekoa Mine. This zone is characterised by thicker channels and was generally mined at a higher stoping width. There does not appear to be any geological reason why there should be a greater occurrence of large domes or wedges within the hangingwall lavas covering these areas. It is likely that the higher proportion of large FOG in the Main Channel areas is associated with the support systems used for higher stoping widths.

When production first commenced at Tau Lekoa Mine it was mostly within the Main Channel. Initially there was limited understanding of the problem and the current pillar and support standards were only introduced in 1995. Prior to 1996 all large FOG occurred within the Main Channel.

Evidence suggests that mining in a southerly direction is more hazardous than mining north. This increased hazard is associated with the unfavourable direction of discontinuities relative to the panel face. An analysis using JBlock indicated that there was little difference between north and south mining panels and that spans are a more significant factor.

The majority of large FOG have taken place below the 1130 level down to the 1350 level with very few large FOG observed below 1350 level. It is suggested that this could be due to a change in the geotechnical environment and a change in the failure mechanism with increasing depth. Geological discontinuities control failure in the shallower areas with stress fracturing becoming the dominant factor as the mining depth increases.

The apparent depth relationship is also linked to the distribution of the Main Channel and the vertical distribution of mining over time. Mining commenced on the upper levels and by the time it reached the 1500 and 1650 levels the new standards had been introduced and personnel were familiar with the ground control problems. Based on this it is difficult to reach a firm conclusion relating to mining depth and large FOG and this is an area requiring further investigation.

8.3 JBlock Modelling

JBlock was used to assess the stability of blocks formed by discontinuities with a focus on larger blocks. Normally JBlock is used to assess smaller blocks in relation to internal or local support spacing. In this study it was demonstrated that

JBlock could be used to model larger blocks that can arise from various discontinuities.

Although JBlock is unable to generate domes it is reasonable to assume that a tetrahedral block approximates a dome structure. Another weakness of this approach is that JBlock only considers individual blocks and cannot account for large FOG made up of several blocks. Whilst JBlock modelling has weaknesses it was useful in comparing different spans, pillar layouts, internal support systems and mining directions.

It was not possible to confirm that mining direction has a major influence on hangingwall instability at Tau Lekoa Mine. This may be due to the presence of flat southerly dipping structures that are not picked up during mapping. The higher occurrence of large instabilities in south mining panels may be due to an inability to recognise dome or wedge structures when mining south. This would be due to flat structures dipping away from the advancing stope face.

The span between crush pillars was shown to be a major factor as would be expected. It was also shown that it is possible to negate the affect of an increased span by increasing the internal support capacity. Overall this analysis showed promise and should be expanded on.

8.4 Crush Pillar Design

Generally, crush pillar behaviour has not been a problem at Tau Lekoa Mine. Pillar failure has only been experienced when pillars have been cut with a very low width-to-height ratio. Failure due to increased pillar stress due to larger spans has not been observed.

The crush pillar design was revisited and a probabilistic approach was applied to account for variability of various parameters such as rock strength, pillar dimensions and loading conditions. The original design used an average rock

mass strength, loading conditions expected at a depth of 1200m and a different pillar layout to that currently in use.

Measurements of actual span and pillar dimensions were used to assess the range of pillar strength and pillar stress that could be anticipated. The application of the Point Estimate Method demonstrated how the peak and residual pillar strengths varied due to variations in rock strength and actual pillar dimensions. The expected pillar strength calculated using this approach is similar to that determined previously (Harris and Rosenblatt, 1993; Rosenblatt, 1994) although there is a 28 percent variation about the expected value.

The same approach was applied when determining the pillar stress using tributary area theory based on actual measured spans. Consideration was also given to the variation in vertical stress due to different mining depths. Determining pillar stress in this manner caters for a range of conditions. Using variable pillar strengths and pillar stresses it was possible to evaluate the crush pillar factor of safety for various conditions.

A number of assumptions were made in this analysis and it could be improved by developing numerical models to estimate pillar stresses. The approach was useful in demonstrating the impact of variations in both material properties and mining practices and is considered superior to a design that only considers mean values.

8.5 Support Strategy Performance

Figure 8.2 shows the number of large FOG normalised with production (m^2). Overall there appears to have been an improvement with the frequency of large FOG and normalised FOG decreasing over time. This trend can be broken down into a number of episodes. There was a drastic improvement between 1992 and 1994 and this is related to the evolution of the support system and the change from composite packs to timber elongates. A better understanding of the ground conditions by mine personnel probably also contributed to this improvement.

There was a regression over 1995, 1996 and 1997 with an increased number of large FOG although the rate tapered off in 1997. This regression is disappointing and puzzling as more stringent standards were introduced in 1995. The majority of the large FOG over 1996 and 1997 occurred in the Main Channel. Adherence to span standards seems to have been particularly poor during this period with 68 percent non-adherence. Subsequent to 1997 there has been a continued improvement with a reduction in the number of large FOG per 1000m^2 mined.

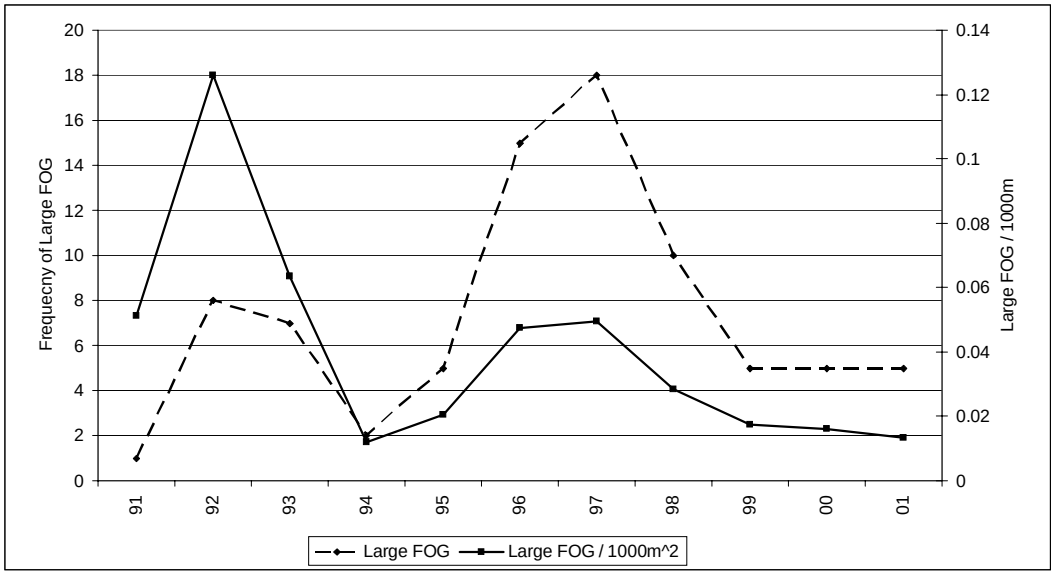

Figure 8.2 Large FOG per year (frequency and rate per 1000m^2)

8.6 Alternative Internal Support Options

There is potential to increase spans at Tau Lekoa Mine and possibly omit mid-panel pillars provided an appropriate internal support standard is used. Larger spans and the omission of mid-panel pillars are likely to have a positive impact on mining rates and percentage extraction and should increase the mining economics for the operation.

The impact of increased support resistance was evaluated during the JBlock analysis. It was shown that by increasing the support resistance through using

support with a higher load capacity it was possible to reduce the probability of a large FOG even when spans were increased.

Profile props with a diameter of 180-200mm are used as internal support at Tau Lekoa Mine. These elongate units are relatively cheap and have been widely used in South African gold and platinum mines. The profile props used at Tau Lekoa Mine have a peak load of 250kN and a limited yield capacity. They are prone to buckling failure when the ratio between the length and the diameter of the profile prop exceeds 10. This limits the stoping width at which they can be used.

There are a number of alternative elongates on the market with a higher load capacity and a more reliable yielding mechanism. These units are generally less prone to bucking failure and can be used at higher stoping widths. It is possible to upgrade the internal support resistance at Tau Lekoa Mine by using superior elongates and / or reducing the spacing between elongates. The unit price of superior elongates is generally significantly more than that of profile props.

Various types of pack support could be considered to increase the internal support resistance at Tau Lekoa Mine. When mining first commenced in 1991 composite packs were used and were found to be too soft. There are a number of stiffer pack options available and it is possible that pack support could be applied at Tau Lekoa Mine. Unfortunately Tau Lekoa Mine is a low grade operation and relies on efficient mining to be economical. Pack mining requires more labour and is more expensive than elongates and is unlikely to be economic at Tau Lekoa Mine.

During the risk assessment it was shown that there is a relatively high probability of the wedge or block height exceeding the effective length of the 1.5m rock bolts used at Tau Lekoa Mine. Due to the practical constraints of installing longer rock bolts effectively in narrow stoping widths this option should not be considered as a viable alternative.

By using the information from this study and a rigorous design approach it is possible to design an internal support system that is capable of controlling and limiting the majority of potential hangingwall instabilities. The design should include a comprehensive cost-benefit analysis taking into account different pillar layouts, increased spans and various support types.

8.7 Risk Assessment

In Chapter 7 an attempt was made to bring together the various components of this study through a risk assessment. A fault tree methodology was applied and it was demonstrated how different factors influence large hangingwall instabilities. This was an initial attempt and this aspect of the study can be expanded and should be incorporated into the design process. Whilst it is not possible to control the occurrence of large dome or wedge structures it is possible to design alternative support systems. The use of the fault tree methodology as part of a cost-benefit analysis will assist in optimising the Tau Lekoa Mine support standards.

8.8 Chapter Summary

This Chapter briefly discussed results from the various aspects covered in this study. Part of this discussion focused on alternatives to the current support and it is suggested that further work is required to optimise the Tau Lekoa Mine support standards. The final chapter will outline the conclusions and recommendations arising from this study.

9 CONCLUSIONS AND RECOMMENDATIONS

The previous chapter briefly discussed the results of various analyses conducted for this study. This chapter covers the conclusions and recommendations arising from this study.

9.1 Conclusions

The following conclusions were drawn from this study.

9.1.1 Fallout thickness versus span relationship

The relationship between fallout thickness and span was found to be poor for all periods and mining situations considered. Whilst this relationship can be used as a guide there is a 27 percent chance that the predicted thickness will be under estimated.

This is considered high and a more appropriate approach would be to consider the 95 percent cumulative thickness for large FOG and design support standards to cater for this. Alternatively a risk based approach could be used to determine appropriate design criteria.

9.1.2 Statistical analysis

The following conclusions arise from the statistical analysis of large FOG.

FOG dimensions

Statistical information on the FOG dimensions could be used in a risk based or probabilistic design approach. This would assist in the design of appropriate support standards.

Mean dimensions for large FOG deceased slightly since the implementation of new standards in 1995.

Depositional setting

Mining in the Main Channel and at stoping widths greater than 1.8m appears to be more hazardous in terms of large FOG. There is no logical reason why these factors would influence the distribution of large dome or wedge structures. The higher occurrence of instability is more likely to be associated with ineffectiveness of support used at higher stoping widths. The efficiency of profile props is diminished at higher stoping widths and the 1.5m long rock bolts currently used are inadequate for a high proportion of dome and wedge structures.

Mining direction

The statistical analysis indicated that mining in a southerly direction was more hazardous than mining in a northerly direction. This finding was not supported by the results of a probabilistic keyblock analysis using JBlock. Further investigation is required and special attention must be given to the mapping of flat dipping structures within the hangingwall.

Mining depth

The majority of large FOG occurred above 1350 Level and this could mean that the mode of hangingwall failure changes from geologically controlled to stress driven with depth. Further investigation is required to confirm this preliminary conclusion.

9.1.3 Stable spans

JBlock modelling indicated that span has a greater influence on hangingwall instabilities than mining direction. This modelling also highlighted that in-stope support with a superior load capacity could reduce the probability of hangingwall instability. This should be explored further by means of a cost-benefit analysis

that considers alternative support and span options in terms of increased recoveries or improved labour efficiencies for a similar or better risk profile.

9.1.4 Crush pillar design

The application of the point estimate method was useful in demonstrating the variability in pillar strength and pillar stress with the expected values correlating reasonably well with the original design.

Crush pillars are designed to have a factor of safety of 1 or slightly less. This analysis demonstrated that it was possible to obtain low factors of safety which could result in pillar failure. This has been observed at Tau Lekoa Mine in the form of excessive scaling of crush pillars and ultimately total pillar loss.

This analysis could be improved by conducting three dimensional numerical modelling to determine pillar stresses for different pillar layouts and mining depths.

9.1.5 Risk assessment

By using the Fault Tree Analysis methodology it was possible to link various aspects of the study together for risk assessment purposes. Using a simplified fault tree the probability of occurrence for large hangingwall instabilities was evaluated for various pillar layouts and support options. This approach could be expanded on and used as part of the design process.

An attempt was made to assess the risk of a fatality due to a large hangingwall instability. This was found to fall in the “slight chance” category (Cole, 1993). This is preliminary work and further analysis is needed.

9.1.6 General

The following general conclusions are drawn:

- Adherence to pillar standards is problematic and management should focus efforts on improving this aspect.
- From this study it is clear that none of the design approaches can be used in isolation and empirical, analytical and probabilistic approaches should be complementary.
- The use of mean values in design is limited and a risk based or probabilistic approach provides more insight into the range of possibilities.
- This work has provided a basis for probabilistic design in terms of establishing a database and determining statistical distributions for a number of parameters.
- A probabilistic approach to stope support design at Tau Lekoa Mine is considered to be more meaningful and logical than a deterministic approach.

9.2 Recommendations

The following recommendations arise from this study:

- Adherence to standards should be improved and this could be facilitated by training and improved understanding of the role of pillars at Tau Lekoa Mine.
- A more stringent methodology is required to determine the potential thickness of large hangingwall instabilities. A probabilistic or risk based approach is suggested.
- The continued use of 1.5m long rock bolts should be rigorously investigated.
- Information of flat dipping structures should be collected to gain a better understating of their distribution and influence on large hangingwall instabilities.

- The relationship between large hangingwall instabilities and mining depth should be investigated further with specific attention given to a possible change in failure mechanisms.
- An increase in the span between crush pillars or the omission of mid-panel pillars is possible provided an appropriate internal support system is designed. It is suggested that a cost-benefit approach be adopted to quantify the impact of higher percentage extraction and labour efficiencies against increased support costs.
- Further work is required on the design of crush pillars as the mining depth increases. This should include three dimensional stress modelling and must consider variations in the rock mass and loading environment.
- A formal design approach should be adopted for the design of pillars and internal support standards. It is suggested that a probabilistic approach be adopted.
- A comprehensive risk assessment should be conducted as part of the design process.

10 REFERENCES

Ackermann, K.A. (1999) A support design methodology for shallow scattered environments. *Successful support systems for safe and efficient mining.* SAIMM Colloquium.

Anon. (1998) Mandatory Code of Practice to Combat Rockfall and Rockburst accidents in Terms of the Mine Health and Safety Act of 1996. Revision 2. Vaal River Operations. *Internal AngloGold Document.*

Barton, N., Lien, R., and Lunde, J. (1974) Engineering classifications of rock masses for the design of tunnel support. *Rock Mechanics*. 6 (4): 189-236.

Beer, G. & Meek, J.J. (1982) Design curves for roofs and hangingwalls in bedded rocks based on 'voussior' beam and plate solutions. *Trans. Instn. Min. Metall.* 91: A18-A22.

Berlenbach, J.W. (1995) Aspects of bedding-parallel faulting associated with Ventersdorp Contact Reef on the Kloof Gold Mine. *S.Afr. J. Geol.,* vol. 98, no. 4, pp. 335-348.

Biddulph, M.N. (2000) *Implications of the geological model on safety at Tau Lekoa Mine.* Internal AngloGold Report.

Biddulph, M.N. (2001) *Geological Model (insert in LOM book).* Internal AngloGold Report.

Bieniawski, Z.T. (1973) Engineering classification of rock masses. *Trans. S. African Institute Civil Eng.* 15: pp. 335-344.

Briggs, D.J. (1988) *The mechanical properties of the dolerite dyke and Ventersdorp lava material from 10-shaft Vaal Reefs gold mine.* COMRO Consultancy report R2/88.

Canbulat, I., Grodner, M., Lightfoot, N., Ryder, J., Essrich, E., Dlokweni, T.,Wilkinson, A., Krog C. and Prohaska G. (2006) *The determination of loading conditions for crush pillars and the performance of crush pillars under dynamic loading.* SIM 040302 project report. SIMRAC.

Cole, K. (1993) Building over abandoned shallow mines. Paper 1: Considerations of risk and reliability. *Ground Engng.* vol. 26, no. 1, pp. 34-37.

Daehnke, A., Andersen, L.M., de Beer, D., Esterhuizen, G.S., Glisson, F.J., Grodner, M.W, Hagan, T.O., Jaku, E.P, Kuijpers, J.S., Peake, A.V., Piper, P.S., Quaye, G.B., Reddy, N., Roberts, M.K.C., Schweitzer, J.K., Stewart, D.R. and Wallmach, T. (1998) *Stope face support systems.* GAP 330 project report. SIMRAC.

De Vries, P.R. (2001) *VCR Geology at Tau Lekoa Mine.* Internal AngloGold Presentation.

De Vries, P.R. (2002) *Characterisation of the Upper Terrace Channel Facies on Goedgenoeg, Tau Lekoa, and Weltevreden.* Internal AngloGold Report.

Dunn, M.J. (2000) Review of Tau Lekoa Mine's Stope Support Strategy and Geotechnical Environment. *Proc. South African National Institute of Rock Engineers Symposium: Keeping it in the Bushveld and Advances in Support Technology.* Rustenburg, South Africa.

Dunn, M.J. (2003) The determination of stable inter-pillar spans at Tau Lekoa Mine. *Technology Roadmap for Rock Mechanics. Proc. 10th ISRM Congress, Johannesburg, 8-12 September 2003.* SAIMM.

Dunn, M.J. (2004) A probabilistic approach to determining stable inter-pillar spans on Tau Lekoa Mine. In: Villaescusa, E. & Potvin, Y. eds. *Proc. 5th International Symposium on Ground Support in Mining and Underground Construction.* Perth.

Dunn, M.J. & Hungwe, G. (2004) The application of a rock mass rating system at Tau Lekoa Mine. In: Villaescusa, E. & Potvin, Y. eds. *Proc. 5th International Symposium on Ground Support in Mining and Underground Construction.* Perth.

Esterhuizen, G.S. (1993) Variability considerations in hard rock pillar design. *Proc. SANGORM Symposium: Rock Engineering problems related to Hard Rock Mining at Shallow to Intermediate depth.* Rustenburg, South Africa.

Esterhuizen, G.S. (1996) JBlock User's Manual and Technical Reference.

Esterhuizen, G.S. & Streuders, S.B. (1998) Rockfall hazard evaluation using probabilistic keyblock analysis. *Jour. S.Afr. Inst. Min. Metall.,* vol. 98, no. 2, pp. 59-63.

Esterhuizen, G.S. (1999) *Review of Stope Support System - Tau Lekoa Mine.* SRK Consultancy Report for Tau Lekoa Mine.

Fourie, C. (1999) *Implications of variable lava strengths on the hangingwall stability at Tau Lekoa.* Internal AngloGold Report.

Fourie, C. (2000) *Characteristics of the VCR outside of the Main channel.* Internal AngloGold Report.

Frith, I. (1998) *Developments to the VCR facies model at Tau Lekoa Mine.* Presentation for the AngloGold Senior Geologists Conference.

Goodman, R.E. & Shi, G. (1985) *Block theory and its application in rock engineering.* Prentice Hall.

Güler, G, Quaye, G.B., Jager, A.J., Schweitzer, J.K., Grodner, M, Reddy, N, Andersen, L, Milev, A & Wallmach, T. (1998) *A methodology for the definition of geotechnical areas within the South African gold and platinum stoping horizons.* GAP 416 project report. SIMRAC.

Haile, A.T. & Jager, A.J. (1995) *Develop guidelines for the design of pillar systems for shallow and intermediate depth, tabular, hard rock mines and provide a methodology for assessing hangingwall stability and support requirements between pillars.* GAP 024 project report. SIMRAC.

Hanekom, J.W.L. (2003) I*dentification of rock related hazards and the assessment of the risks involved with these hazards.* SRK consultancy report for AngloGold Ashanti.

Harr, M.E. (1987) *Reliability-based design in civil engineering*. McGraw-Hill, New York, 290p.

Harris, B.A (1989) *Stereographic projections and preliminary interpretations – 10 Shaft.* Internal AngloGold Report.

Harris, B.A. & Rosenblatt, M. (1993) *No. 10 Shaft support strategy.* Internal AngloGold Report.

Human, L. (1997) *A Guideline for the use of the Q System on Impala Mine.* Internal Impala Platinum Report.

Hungwe, G. & Dunn, M.J. (2003) *Rock mass ratings in stopes on Tau Lekoa Mine.* Internal AngloGold Report.

Hutchinson, J.D. and Diederichs, M.S. (1996) *Cablebolting in Underground Mine*s, BiTech Publishers Ltd, Richmond, Canada.

Johnson, R.A. & Noble, K.R. (2004) Support Design Methodolgy. *Mechanized Mining and Support in the Bushveld Complex.* SAIMM Colloquium. Randburg, South Africa.

Judeel, G. (1998) *Progress report on the 10-Shaft fall of ground project.* Internal AngloGold Report.

Judeel, G. & Laas, J.J. (1999) An empirical method for the determination of the fall out height versus span between crush pillars at AngloGold – Tau Lekoa Mine. In: Hagan T.O. ed. *Implementing rock engineering knowledge. Proc. 2nd Southern Africa Rock Engineering Symposium.* Johannesburg

Joughin, W.C., Swart, A.H. & Wesseloo, J. (2000) Risk based chromitite pillar design - Part 2: Non-linear modelling. *Proc. South African National Institute of Rock Engineers Symposium: Keeping it in the Bushveld and Advances in Support Technology.* Rustenburg, South Africa.

Kirsten, H.A.D. (1988) Norwegian Geotechnical Institute or Q System by N Barton. Discussion contribution. In Louis Kirkaldie (ed.) *Rock classification Systems for Engineering Purposes, ASTM STP 984*. 85-88. Philadelphia

Laubscher, D.H. & Taylor, H.W. (1976) The importance of geomechanics classification of jointed rock masses in mining operations. In Z.T. Bieniawski (ed.) *Proc. symp. On exploration for Rock Engineering.* Johannesburg.

Laubscher, D.H. (1977) Geomechanics classification of jointed rock masses – mining applications. *Trans. Instn. Min. Metall.* vol. 86, pp. A1-A8.

Leach, A. R. (1998) *Siting of regional pillars and effect on gully stability at Vaal Reefs 10 Shaft.* Itasca consultancy report for AngloGold.

Lombard, J.J. (1989) *Rock Mechanics strategy for 10 Shaft.* Internal AngloGold Report.

Mathews, K.E., Hoek, E., Wyllie, D.C. & Stewart, S.B.V. (1981) *Prediction of stable excavation for mining at depth below 1000m in hard rock.* CANMET Report. DSS Serial No. OSQ80-00081, DSS File 17 SQ 23440-0-9020. Ottawa: Dept. Energy, Mines and Resources.

Mares, L & Akermann, K. (1997) *On-reef support design at RPM, Amandelbult section.* COP to Combat Rockfall Accidents-Rustenburg Platinum Mines, Amandelbult Section.

Ozbay, M.U. & Roberts, M.K.C. (1988) Yield Pillars in stope support. *Rock Mechanics in Africa.* Swaziland.

Ozbay, M.U., Ryder, J.A. & Jager, A.J. (1995) The design of pillar systems as practised in shallow hard-rock tabular mines in South Africa. *Jour. S.Afr. Inst. Min. Metall.,* vol. 95, no. 1, pp. 7-18.

Pine, R. Thin, I. (1993) Probabilistic risk assessment in mine pillar design. *Proc. Int. Cong. Mine Design,* Kingston, Canada, August 1993, pp. 363-373.

Roberts, M.K., Güler, G, Quaye, G.B., Schweitzer, J.K. & Eve, R. (1996) *Improved support design by an increased understanding of rock mass behaviour around the Ventersdorp Contact Reef.* GAP 102 project report. SIMRAC, Johannesburg.

Roberts, M.K. & Schweitzer, J.K. (1999) Geotechnical areas associated with the Ventersdorp contact Reef, Witwatersrand Basin, South Africa. *Jour. S. Afr. Inst. Min. Metall.,* Vol. 99, pp 157-166.

Roberts, D.P., M.K.C. Roberts, A.J. Jager and S. Coetzer. (2005). The determination of the residual strength of hard rock crush pillars with a width to height ratio of 2:1. *Jour. S.Afr. Inst. Min. Metall.,* vol 105, no. 6, pp. 401-408.

Rosenblatt, M. (1994) *Support strategy – Vaal Reefs No. 10 Shaft.* Internal AngloGold Report.

Ryder, J.A. & Jager, A.J. (2002) *A Textbook on Rock Mechanics for Tabular Hard Rock Mines.* SIMRAC, Johannesburg.

Ryder, J.A. & Ozbay, M.U. (1990) A methodology for designing pillar layouts for shallow mining. *Proc. ISRM Symposium: Static and Dynamic Considerations in Rock Engineering.* Swaziland.

Siebert, C. (1997) Mining south on Vaal Reefs 10-Shaft. *Internal AngloGold Report.*

Stacey, T.R. (2001) *Best practice rock engineering handbook for "other" mines.* OTH 602 project report. SIMRAC, Johannesburg..

Streuders, S.B. & Treloar, M.L. (1997) Rock engineering experiences with innovative stope support systems and practical mine layouts on the Samancor Chrome Mines. In G. G. Gurtunca. & T.O. Hagan (eds), *Implementing rock engineering knowledge. Proc. 1st Southern African Rock Engineering Symposium, Johannesburg, 15-17 September 1997.* Johannesburg, South Africa.

Swart, A.H. (2003) *Fault-Event Tree Analysis Technique*. SRK consultancy report for AngloGold Ashanti.

Swart, A.H., Stacey, T.R., Wesseloo, J. Joughin, W.C., Le Roux. K., Walker, D. & Butcher, R. (2000) *Investigation of factors governing the stability/instability of stope panels in order to define a suitable design methodology for near surface and shallow mining operations.* OTH 501 project report. SIMRAC, Johannesburg..

Treloar, M.L. & Steenkamp. C.J. (2000) Design Guidelines and Practical Considerations for Shallow Chrome Mining at SAMANCOR -Western Chrome Mines. *Proc. South African National Institute of Rock Engineers Symposium: Keeping it in the Bushveld and Advances in Support Technology.* Rustenburg, South Africa.

Van Der Heever, P. (1983) *The influence of Geological Structure on Seismicity and Rockbursts in the Klerksdorp Goldfield.* MSc Thesis. Rand Afrikaans University, Johannesburg..

Watson, B.P, & Akerman, K. (1999) *Comparison between geotechnical areas on the Bushveld Complex platinum mines to identify critical spans and suitable in-panel support.* COP to Combat Rockfall Accidents-Rustenburg Platinum Mines, Amandelbult Section

Watson, B.P. & Noble, K.R. (1997) Comparison between geotechnical areas on the Bushveld Igneous Complex platinum mines, to identify critical spans and suitable in-panel support. In G. G. Gurtunca. & T.O. Hagan (eds), *Implementing rock engineering knowledge. Proc. 1st Southern African Rock Engineering Symposium, Johannesburg, 15-17 September 1997.* Johannesburg, South Africa.

Watson B.P. & Roberts D. 1999. A new approach to designing safe panel spans on the Merensky Reef. In: T. O. Hagan (ed.), Implementing rock engineering knowledge. *Proc. 2nd Southern Africa Rock Engineering Symposium, Johannesburg, 1999*. Johannesburg, South Africa.

Watson, B.P. (2004) A rock mass rating system for evaluating stope stability on the Bushveld Platinum mines. *Jour. S.Afr. Inst. Min. Metall.,* vol. 104, no. 4, pp. 229-238.

Wesseloo, J. & Swart, A.H. (2000). Risk based chromitite pillar design - Part 1: Application of locally empirically derived pillar formula. *Proc. South African National Institute of Rock Engineers Symposium: Keeping it in the Bushveld and Advances in Support Technology.* Rustenburg, South Africa.

York, G., Canbulat, I. Kabeya, K.K. Le Bron, K. Watson, B.P. & Williams, S.B. (1998) *Develop guidelines for the design of pillar systems for shallow and intermediate depth, tabular, hard rock mines and provide a methodology for assessing hangingwall stability and support requirements for panels between pillars.* GAP 334 project report. SIMRAC , Johannesburg.

York, G. & Canbulat, I. (1998) The scale effect, critical rock mass strength and pillar system design. *Jour. S.Afr. Inst. Min. Metall.,* vol. 98, no. 1, pp. 23-37.

APPENDIX A

LARGE FOG DATABASE FOR TAU LEKOA MINE

Table A1

Large FOG in stopes at Tau Lekoa Mine (1991-2001)

No.	ID	Date	Workingplace	SW (cm)	Length (m)	Width (m)	Thickness (m)	Mass (tons)	Weigth (kN)	Span (m)
1	40	1991	1200 N1 Rse 1	187	8	3	1.5	82	808	30.0
2	41	1992	1130 N1A Rse 12	178	15	9	3	927	9090	25.0
3	42	1992	1200 N1 Rse 12 P2C	260	12	12	2.5	824	8080	20.0
4	43	1992	1200 N1 Rse 1B P1/2	228	16	12	3	1318	12928	26.0
5	2	1992	1130 N1A Rse 12 P2B	252	18	14	2.4	1384	13575	16.0
6	3	1992	1200 N1 Rse 11 P1	287	36	30	3.75	9266	90903	30.0
7	4	1992	1200 N1 Rse 12 P2	284	16	12	2.5	1098	10774	40.0
8	5	1992	1200 N1 Rse 11 P2/2A	179	17	8	1.8	560	5495	15.0
9	6	1992	1130 N1A Rse 13 P5-8	147	14	7	2	448	4399	16.0
10	7	1993	1200 N1 Rse 4 P7	172	34	20	2.5	3890	38157	20.0
11	8	1993	1200 N1 Rse 9 P8	169	19	6	1.2	313	3071	20.0
12	9	1993	1350 N1 Rse 10 P22	131	14	9	1	288	2828	20.0
13	11	1993	1130 N1A Rse 13 P5	177	16	14	2.4	1230	12067	16.0
14	12	11/01/93	1200 N1 Rse 11 P1	223	18	14	3.3	1903	18665	30.0
15	44	21/07/93	1130 N1A Rse 13 P5/6	147	21	11	4.8	2537	24887	25.0
16	14	1993	1200 S1 Rse 4 P8	121	18	10	1.5	618	6060	12.0
17	15	11/03/94	1200 S1 Rse 2 P16	170	4	3	1.45	40	391	12.0
18	18	12/94	1350 N1 Rse 6 P24	177	10	8	1	183	1796	16.0
19	16	11/03/95	1200 N1 Rse 9	147	40	20	1.8	3295	32321	20.0
20	19	10/95	1350 N1 Rse 7 P17	190	22	19	2.8	2678	26270	22.0
21	20	28/08/95	1200 N3 Rse 4	212	17	16	2.5	1556	15263	19.0
22	21	13/04/95	1200 N3 Rse 4 P18	134	14	11	1.5	529	5185	18.0
23	56	1995	1200 N3 Rse 4 P18	134	10	10	1	229	2245	21.0
24	22	1996	1050 N1 Rse 11 P2	180	14	7	2	448	4399	18.0
25	23	1996	1200 N1 Rse 9 P8	193	12	9	2.2	544	5333	20.0
26	31	1996	1350 N1 Rse 10 P21	224	24	24	3	3954	38785	24.0
27	32	1996	1350 N1 Rse 10 P23	115	14	14	1.6	718	7039	19.0
28	33	1996	1350 N1 Rse 8 P28	151	25	24	2.5	3432	33668	24.0
29	34	1996	1350 N1 Rse 1 Ledge	150	7	4	1.2	77	754	12.0
30	35	1996	1350 N1 Rse 6 P21	150	24	21	2.5	2883	28281	22.0
31	36	1996	1350 N1 Rse 6 P19	170	13	8	1.5	357	3501	15.0
32	37	1996	1350 N1 Rse 6 P19	170	9	6	1.2	148	1454	10.0
33	38	1996	1350 N1 Rse 6 P21	150	16	13	2.2	1047	10271	17.0
34	26	1996	1200 S1 Rse 2 P6	188	24	24	3	3954	38785	24.0
35	27	10/07/96	1050 N2B Rse 16	193	20	8	1.25	458	4489	12.0
36	28	26/09/96	1500 N1 Rse 6	135	23	12	1.4	884	8673	12.0
37	58	10/96	1200 N Rse 4 P18	134	14	11	1.2	423	4148	18.0
38	63	05/01/96	1200 N3 Rse 4 P18	134	14	7	2	448	4399	18.0
39	64	26/06/97	1200 N3A Rse 9A P8	130	9	9	1.1	204	2000	10.0
40	25	06/03/97	1050 N2B Rse 15	186	21	15	2.5	1802	17676	21.0
41	65	1997	1350 S1 Rse 3 P15	185	13	6.5	1.5	290	2845	11.6
42	66	1997	1350 N1 Rse 10 C/G	146	14.6	10.2	1.6	545	5348	15.6
43	67	1997	1350 S1 Rse 9 P23	114	13.1	8.8	1	264	2587	9.1
44	68	1997	1350 S1 Rse 9 P21	174	7	3	1.6	77	754	4.0
45	69	1997	1350 S1 Rse 9 P19	141	16.8	8	2.2	677	6637	8.0
46	70	1997	1350 N1 Rse 1 C/G	174	13.2	10.3	2.1	653	6408	16.3
47	71	05/08/97	1200 S1 Rse 4 P2	200	43	15	2	2952	28954	17.0
48	72	09/97	1350 S1 Rse 1 P11	130	40	24	0.9	1977	19393	21.0
49	73	09/97	1350 N1 Rse 6 P15	180	6	4.5	0.7	43	424	8.0
50	74	09/97	1350 N1 Rse 6 P17	170	6	5.3	0.6	44	428	7.8
51	75	09/97	1130 N3A Rse12 P12	190	14	6	0.8	154	1508	18.0
52	77	09/97	1200 N1A Rse 15 P2	110	6	5.9	0.9	73	715	13.0
53	78	09/97	1500 N1 Rse 1 P20	175	8	8	0.8	117	1149	8.0
54	79	31/10/97	1350 N1 Rse 6 C/G	180	13.7	12.6	1.4	553	5424	11.9
55	80	18/11/97	1200 S3 Rse 10 P16	130	11.4	3.2	1	83	819	7.1
56	82	02/12/97	1200 N1 Rse 4 P7	193	5.8	5.7	1.8	136	1336	17.0
57	83	08/01/98	1350 S1 Rse 9 P13	170	14.6	4.6	1.98	304	2985	16.0
58	85	22/04/98	1350 S1 Rse 1 P16	200	4.5	3.5	1.1	40	389	7.0
59	86	03/98	1350 S1 Rse 10 P15+17	350	33	13	2.5	2454	24073	24.0
60	87	04/98	1350S1R3P33	230	14.3	4	0.7	92	899	15.0
61	81	19/05/98	1500 S1 Rse 2 P15	160	8	5.4	0.6	59	582	15.0
62	88	05/98	1350S1R7P19	190	10.2	5.8	0.6	81	797	5.8
63	89	06/98	1350S1R3P27	200	6.3	3.4	0.5	25	240	7.7
64	90	06/98	1350 S1 Rse 7 P19	220	12	9.8	1.8	484	4751	5.8
65	91	07/98	1350 S1 Rse 3 P31	180	9.5	3	0.5	33	320	10.0
66	92	08/98	1350 S1 Rse 3 P33	190	6	5.6	0.7	54	528	5.5
67	93	1999	1500 S1 Rse 1Ledge (top)	180	8	5	1.1	101	988	10.0
68	60	1999	1500 N1 Rse 6 P6 Ledge	160	12	7	2.5	480	4714	12.0
69	94	1999	1500 S1 Rse 1Ledge (bot.)	180	5	4	1	46	449	8.0
70	95	25/08/99	1350 S1 Rse 8 P17	178	8	3	1.25	69	673	9.0
71	96	09/99	1350 S1 Rse 3 P21	180	30	16	2.5	2746	26934	18.0
72	98	21/2/00	1350 S1 Rse 5 P5	200	6	2.5	1.5	51	505	5.0
73	99	13/03/00	1500 S1 Rse 8 C/G	300	11	5	1.5	189	1852	8.0
74	100	27/03/00	1350 S1 Rse 3 C/G	300	35	8	2.5	1602	15712	10.0
75	102	20/10/00	12 S4 Rse 11 P14	165	19	12	1.4	730	7165	11.0
76	103	01/09/00	1350 Rse 18 P15	182	10	5	0.6	69	673	10.0
77	62	2001	1200 N1A Rse 16 P9	177	8	4	0.8	59	575	24.0
78	105	18/05/01	1650 S3 Rse 19 P26	180	8	6	0.8	88	862	10.0
79	106	20/07/01	1200 S4 Rse 8E C/G	180	14	13	1.5	625	6128	32.0
80	107	22/08/01	1200 S3 Rse 9 C/G	170	6	5	0.6	41	404	7.0
81	108	15/11/01	1050 S4 Rse 15 P11	180	17	8	3.25	1011	9921	16.0
			AVERAGE	180.90	15.30	9.79	1.71	952.37	9342.73	15.80
			STD DEVIATION	43.90	8.77	5.94	0.86	1408.59	13818.23	7.15

Table A2

Large FOG in North mining stopes at Tau Lekoa Mine (1991-2001)

No.	ID	Date		Workingplace	SW (cm)	Length (m)	Width (m)	Thickness (m)	Mass (tons)	Weigth (kN)	Span (m)
1	3	1992	1992	1200 N1 Rse 11 P1	287	36	30	3.75	9266	90903	30
2	7	1993	1993	1200 N1 Rse 4 P7	172	34	20	2.5	3890	38157	20
3	11	1993	1993	1130 N1A Rse 13 P5	177	16	14	2.4	1230	12067	16
4	12	11/01/93	1993	1200 N1 Rse 11 P1	223	18	14	3.3	1903	18665	30
5	19	10/95	1995	1350 N1 Rse 7 P17	190	22	19	2.8	2678	26270	22
6	31	1996	1996	1350 N1 Rse 10 P21	224	24	24	3	3954	38785	24
7	32	1996	1996	1350 N1 Rse 10 P23	115	14	14	1.6	718	7039	19
8	35	1996	1996	1350 N1 Rse 6 P21	150	24	21	2.5	2883	28281	22
9	36	1996	1996	1350 N1 Rse 6 P19	170	13	8	1.5	357	3501	15
10	37	1996	1996	1350 N1 Rse 6 P19	170	9	6	1.2	148	1454	10
11	38	1996	1996	1350 N1 Rse 6 P21	150	16	13	2.2	1047	10271	17
12	65	1997	1997	1350 S1 Rse 3 P15	185	13	6.5	1.5	290	2845	11.6
13	67	1997	1997	1350 S1 Rse 9 P23	114	13.1	8.8	1	264	2587	9.1
14	68	1997	1997	1350 S1 Rse 9 P21	174	7	3	1.6	77	754	4
15	69	1997	1997	1350 S1 Rse 9 P19	141	16.8	8	2.2	677	6637	8
16	72	09/97	1997	1350 S1 Rse 1 P11	130	40	24	0.9	1977	19393	21
17	73	09/97	1997	1350 N1 Rse 6 P15	180	6	4.5	0.7	43	424	8
18	74	09/97	1997	1350 N1 Rse 6 P17	170	6	5.3	0.6	44	428	7.8
19	81	19/05/98	1998	1500 S1 Rse 2 P15	160	8	5.4	0.6	59	582	15
20	82	02/12/97	1997	1200 N1 Rse 4 P7	193	5.8	5.7	1.8	136	1336	17
21	83	08/01/98	1998	1350 S1 Rse 9 P13	170	14.6	4.6	1.98	304	2985	16
22	86	03/98	1998	1350 S1 Rse 10 P15+17	350	33	13	2.5	2454	24073	24
23	87	04/98	1998	1350 S1 Rse 3 P33	230	14.3	4	0.7	92	899	15
24	88	05/98	1998	1350 S1 Rse 7 P19	190	10.2	5.8	0.6	81	797	5.8
25	89	06/98	1998	1350 S1 Rse 3 P27	200	6.3	3.4	0.5	25	240	7.7
26	90	06/98	1998	1350 S1 Rse 7 P19	220	12	9.8	1.8	484	4751	5.8
27	91	07/98	1998	1350 S1 Rse 3 P31	180	9.5	3	0.5	33	320	10
28	92	08/98	1998	1350 S1 Rse 3 P33	190	6	5.6	0.7	54	528	5.5
29	95	25/08/99	1999	1350 S1 Rse 8 P17	178	8	3	1.25	69	673	9
30	96	09/99	1999	1350 S1 Rse 3 P21	180	30	16	2.5	2746	26934	18
31	98	21/2/00	2000	1350 S1 Rse 5 P5	200	6	2.5	1.5	51	505	5
32	103	01/09/00	2000	1350 Rse 18 P15	182	10	5	0.6	69	673	10
33	62	2001	2001	1200 N1A Rse 16 P9	177	8	4	0.8	59	575	24
34	108	15/11/01	2001	1050 S4 Rse 15 P11	180	17	8	3.25	1011	9921	16
				AVERAGE	185.35	15.49	10.06	1.67	1152.05	11301.59	14.66
				STD DEVIATION	44.00	9.58	7.26	0.94	1853.52	18183.03	7.23

Table A3

Large FOG in South mining stopes at Tau Lekoa Mine (1991-2001)

No.	ID	Date	Workingplace	SW (cm)	Length (m)	Width (m)	Thickness (m	Mass (tons)	Weigth (kN)	Span (m)
1	2	1992	1130 N1A Rse 12 P2B	252	18	14	2.40	1384	13575	16
2	4	1992	1200 N1 Rse 12 P2	284	16	12	2.50	1098	10774	40
3	5	1992	1200 N1 Rse 11 P2/2A	179	17	8	1.80	560	5495	15
4	42	1992	1200 N1 Rse 12 P2C	260	12	12	2.50	824	8080	20
5	8	1993	1200 N1 Rse 9 P8	169	19	6	1.20	313	3071	20
6	9	1993	1350 N1 Rse 10 P22	131	14	9	1.00	288	2828	20
7	14	1993	1200 S1 Rse 4 P8	121	18	10	1.50	618	6060	12
8	15	11/03/94	1200 S1 Rse 2 P16	170	4	3	1.45	40	391	12
9	18	12/94	1350 N1 Rse 6 P24	177	10	8	1.00	183	1796	16
10	21	13/04/95	1200 N3 Rse 4 P18	134	14	11	1.50	529	5185	18
11	56	1995	1200 N3 Rse 4 P18	134	10	10	1.00	229	2245	21
12	22	1996	1050 N1 Rse 11 P2	180	14	7	2.00	448	4399	18
13	23	1996	1200 N1 Rse 9 P8	193	12	9	2.20	544	5333	20
14	26	1996	1200 S1 Rse 2 P6	188	24	24	3.00	3954	38785	24
15	33	1996	1350 N1 Rse 8 P28	151	25	24	2.50	3432	33668	24
16	58	10/96	1200 N Rse 4 P18	134	14	11	1.20	423	4148	18
17	63	05/01/96	1200 N3 Rse 4 P18	134	14	7	2.00	448	4399	18
18	64	26/06/97	1200 N3A Rse 9A P8	130	9	9	1.10	204	2000	10
19	71	05/08/97	1200 S1 Rse 4 P2	200	43	15	2.00	2952	28954	17
20	75	09/97	1130 N3A Rse12 P12	190	14	6	0.80	154	1508	18
21	77	09/97	1200 N1A Rse 15 P2	110	6	5.9	0.90	73	715	13
22	78	09/97	1500 N1 Rse 1 P20	175	8	8	0.80	117	1149	8
23	80	18/11/97	1200 S3 Rse 10 P16	130	11.4	3.2	1.00	83	819	7.1
24	85	22/04/98	1350 S1 Rse 1 P16	200	4.5	3.5	1.10	40	389	7
25	102	20/10/00	12 S4 Rse 11 P14	165	19	12	1.40	730	7165	11
26	105	18/05/01	1650 S3 Rse 19 P26	180	8	6	0.80	88	862	10
			AVERAGE	171.96	14.53	9.75	1.56	759.79	7453.53	16.66
			STD DEVIATION	43.55	7.87	5.22	0.65	1051.96	10319.70	6.83

Table A4

Large FOG in Centre Gullies at Tau Lekoa Mine (1991-2001)

No.	ID	Date	Workingplace	SW (cm)	Length (m)	Width (m)	Thickness (m)	Mass (tons)	Weigth (kN)	Span (m)
1	6	1992	1130 N1A Rse 13 P5-8	147	14	7	2	448	4399	16
2	16	11/03/95	1200 N1 Rse 9	147	40	20	1.8	3295	32321	20
3	20	28/08/95	1200 N3 Rse 4	212	17	16	2.5	1556	15263	19
4	25	06/03/97	1050 N2B Rse 15	186	21	15	2.5	1802	17676	21
5	27	10/07/96	1050 N2B Rse 16	193	20	8	1.25	458	4489	12
6	28	26/09/96	1500 N1 Rse 6	135	23	12	1.4	884	8673	12
7	34	1996	1350 N1 Rse 1 Ledge	150	7	4	1.2	77	754	12
8	40	1991	1200 N1 Rse 1	187	8	3	1.5	82	808	30
9	41	1992	1130 N1A Rse 12	178	15	9	3	927	9090	25
10	43	1992	1200 N1 Rse 1B P1/2	228	16	12	3	1318	12928	26
11	44	21/07/93	1130 N1A Rse 13 P5/6	147	21	11	4.8	2537	24887	25
12	60	1999	1500 N1 Rse 6 P6 Ledge	160	12	7	2.5	480	4714	12
13	66	1997	1350 N1 Rse 10 C/G	146	14.6	10.2	1.6	545	5348	15.6
14	70	1997	1350 N1 Rse 1 C/G	174	13.2	10.3	2.1	653	6408	16.3
15	79	31/10/97	1350 N1 Rse 6 C/G	180	13.7	12.6	1.4	553	5424	11.9
16	93	1999	1500 S1 Rse 1Ledge (top)	180	8	5	1.1	101	988	10
17	94	1999	1500 S1 Rse 1Ledge (bot.)	180	5	4	1	46	449	8
18	99	13/03/00	1500 S1 Rse 8 C/G	300	11	5	1.5	189	1852	8
19	100	27/03/00	1350 S1 Rse 3 C/G	300	35	8	2.5	1602	15712	10
20	106	20/07/01	1200 S4 Rse 8E C/G	180	14	13	1.5	625	6128	32
21	107	22/08/01	1200 S3 Rse 9 C/G	170	6	5	0.6	41	404	7
			AVERAGE	184.76	15.93	9.39	1.94	867.51	8510.24	16.61
			STD DEVIATION	44.61	8.80	4.48	0.93	872.36	8557.81	7.48

Table A5

Large FOG in stopes at Tau Lekoa (1991-1994)

No.	ID	Date	Workingplace	SW (cm)	Length (m)	Width (m)	Thickness (m)	Mass (tons)	Weigth (kN)	Span (m)
1	40	1991	1200 N1 Rse 1	187	8	3	1.5	82	808	30.0
2	41	1992	1130 N1A Rse 12	178	15	9	3	927	9090	25.0
3	42	1992	1200 N1 Rse 12 P2C	260	12	12	2.5	824	8080	20.0
4	43	1992	1200 N1 Rse 1B P1/2	228	16	12	3	1318	12928	26.0
5	2	1992	1130 N1A Rse 12 P2B	252	18	14	2.4	1384	13575	16.0
6	3	1992	1200 N1 Rse 11 P1	287	36	30	3.75	9266	90903	30.0
7	4	1992	1200 N1 Rse 12 P2	284	16	12	2.5	1098	10774	40.0
8	5	1992	1200 N1 Rse 11 P2/2A	179	17	8	1.8	560	5495	15.0
9	6	1992	1130 N1A Rse 13 P5-8	147	14	7	2	448	4399	16.0
10	7	1993	1200 N1 Rse 4 P7	172	34	20	2.5	3890	38157	20.0
11	8	1993	1200 N1 Rse 9 P8	169	19	6	1.2	313	3071	20.0
12	9	1993	1350 N1 Rse 10 P22	131	14	9	1	288	2828	20.0
13	11	1993	1130 N1A Rse 13 P5	177	16	14	2.4	1230	12067	16.0
14	12	11/01/93	1200 N1 Rse 11 P1	223	18	14	3.3	1903	18665	30.0
15	44	21/07/93	1130 N1A Rse 13 P5/6	147	21	11	4.8	2537	24887	25.0
16	14	1993	1200 S1 Rse 4 P8	121	18	10	1.5	618	6060	12.0
17	15	11/03/94	1200 S1 Rse 2 P16	170	4	3	1.45	40	391	12.0
18	18	12/94	1350 N1 Rse 6 P24	177	10	8	1	183	1796	16.0
			AVERAGE	193.83	17.00	11.22	2.31	1494.93	14665.25	21.61
			STD DEVIATION	50.28	7.75	6.26	1.01	2167.30	21261.21	7.50

Table A6

Large FOG in North Mining stopes at Tau Lekoa (1991-1994)

No.	ID	Date	Workingplace	SW (cm)	Length (m)	Width (m)	Thickness (m)	Mass (tons)	Weigth (kN)	Span (m)
1	3	1992	1200 N1 Rse 11 P1	287	36	30	3.75	9266	90903	30.0
2	7	1993	1200 N1 Rse 4 P7	172	34	20	2.5	3890	38157	20.0
3	11	1993	1130 N1A Rse 13 P5	177	16	14	2.4	1230	12067	16.0
4	12	11/01/93	1200 N1 Rse 11 P1	223	18	14	3.3	1903	18665	30.0
			AVERAGE	214.75	26.00	19.50	2.99	4072.18	39948.11	24.00
			STD DEVIATION	53.36	10.46	7.55	0.65	3642.24	35730.37	7.12

Table A7

Large FOG in South Mining stopes at Tau Lekoa (1991-1994)

No.	ID	Date	Workingplace	SW (cm)	Length (m)	Width (m)	Thickness (m)	Mass (tons)	Weigth (kN)	Span (m)
1	42	1992	1200 N1 Rse 12 P2C	260	12	12	2.5	824	8080	20.0
2	2	1992	1130 N1A Rse 12 P2B	252	18	14	2.4	1384	13575	16.0
3	4	1992	1200 N1 Rse 12 P2	284	16	12	2.5	1098	10774	40.0
4	5	1992	1200 N1 Rse 11 P2/2A	179	17	8	1.8	560	5495	15.0
5	8	1993	1200 N1 Rse 9 P8	169	19	6	1.2	313	3071	20.0
6	9	1993	1350 N1 Rse 10 P22	131	14	9	1	288	2828	20.0
7	14	1993	1200 S1 Rse 4 P8	121	18	10	1.5	618	6060	12.0
8	15	11/03/94	1200 S1 Rse 2 P16	170	4	3	1.45	40	391	12.0
9	18	12/94	1350 N1 Rse 6 P24	177	10	8	1	183	1796	16.0
			AVERAGE	193.67	14.22	9.11	1.71	589.74	5785.40	19.00
			STD DEVIATION	57.91	4.87	3.37	0.62	444.52	4360.70	8.49

Table A8

Large FOG in Centre Gullies at Tau Lekoa (1991-1994)

No.	ID	Date	Workingplace	SW (cm)	Length (m)	Width (m)	Thickness (m)	Mass (tons)	Weigth (kN)	Span (m)
1	40	1991	1200 N1 Rse 1	187	8	3	1.5	82	808	30.0
2	41	1992	1130 N1A Rse 12	178	15	9	3	927	9090	25.0
3	43	1992	1200 N1 Rse 1B P1/2	228	16	12	3	1318	12928	26.0
4	6	1992	1130 N1A Rse 13 P5-8	147	14	7	2	448	4399	16.0
5	44	21/07/93	1130 N1A Rse 13 P5/6	147	21	11	4.8	2537	24887	25.0
			AVERAGE	177.40	14.80	8.40	2.86	1062.46	10422.69	24.40
			STD DEVIATION	33.55	4.66	3.58	1.26	948.07	9300.58	5.13

Table A9

Large FOG in North Mining stopes at Tau Lekoa (1995-2001)

No.	ID	Date	Workingplace	SW (cm)	Length (m)	Width (m)	Thickness (m)	Mass (tons)	Weigth (kN)	Span (m)
1	19	10/95	1350 N1 Rse 7 P17	190	22	19	2.8	2678	26270	22.0
2	31	1996	1350 N1 Rse 10 P21	224	24	24	3	3954	38785	24.0
3	32	1996	1350 N1 Rse 10 P23	115	14	14	1.6	718	7039	19.0
4	35	1996	1350 N1 Rse 6 P21	150	24	21	2.5	2883	28281	22.0
5	36	1996	1350 N1 Rse 6 P19	170	13	8	1.5	357	3501	15.0
6	37	1996	1350 N1 Rse 6 P19	170	9	6	1.2	148	1454	10.0
7	38	1996	1350 N1 Rse 6 P21	150	16	13	2.2	1047	10271	17.0
8	65	1997	1350 S1 Rse 3 P15	185	13	6.5	1.5	290	2845	11.6
9	67	1997	1350 S1 Rse 9 P23	114	13.1	8.8	1	264	2587	9.1
10	68	1997	1350 S1 Rse 9 P21	174	7	3	1.6	77	754	4.0
11	69	1997	1350 S1 Rse 9 P19	141	16.8	8	2.2	677	6637	8.0
12	72	09/97	1350 S1 Rse 1 P11	130	40	24	0.9	1977	19393	21.0
13	73	09/97	1350 N1 Rse 6 P15	180	6	4.5	0.7	43	424	8.0
14	74	09/97	1350 N1 Rse 6 P17	170	6	5.3	0.6	44	428	7.8
15	82	02/12/97	1200 N1 Rse 4 P7	193	5.8	5.7	1.8	136	1336	17.0
16	83	08/01/98	1350 S1 Rse 9 P13	170	14.6	4.6	1.98	304	2985	16.0
17	86	03/98	1350 S1 Rse 10 P15+17	350	33	13	2.5	2454	24073	24.0
18	87	04/98	1350S1R3P33	230	14.3	4	0.7	92	899	15.0
19	81	19/05/98	1500 S1 Rse 2 P15	160	8	5.4	0.6	59	582	15.0
20	88	05/98	1350S1R7P19	190	10.2	5.8	0.6	81	797	5.8
21	89	06/98	1350S1R3P27	200	6.3	3.4	0.5	25	240	7.7
22	90	06/98	1350 S1 Rse 7 P19	220	12	9.8	1.8	484	4751	5.8
23	91	07/98	1350 S1 Rse 3 P31	180	9.5	3	0.5	33	320	10.0
24	92	08/98	1350 S1 Rse 3 P33	190	6	5.6	0.7	54	528	5.5
25	95	25/08/99	1350 S1 Rse 8 P17	178	8	3	1.25	69	673	9.0
26	96	09/99	1350 S1 Rse 3 P21	180	30	16	2.5	2746	26934	18.0
27	98	21/2/00	1350 S1 Rse 5 P5	200	6	2.5	1.5	51	505	5.0
28	103	01/09/00	1350 Rse 18 P15	182	10	5	0.6	69	673	10.0
29	62	2001	1200 N1A Rse 16 P9	177	8	4	0.8	59	575	24.0
30	108	15/11/01	10950 S4 Rse 15 P11	180	17	8	3.25	1011	9921	16.0
			AVERAGE	181.43	14.09	8.80	1.50	762.70	7482.05	13.41
			STD DEVIATION	42.11	8.71	6.34	0.83	1097.31	10764.58	6.37

Table A10

Large FOG in South Mining stopes at Tau Lekoa (1995-2001)

No.	ID	Date	Workingplace	SW (cm)	Length (m)	Width (m)	Thickness (m)	Mass (tons)	Weigth (kN)	Span (m)
1	21	13/04/95	1200 N3 Rse 4 P18	134	14	11	1.5	529	5185	18.0
2	56	1995	1200 N3 Rse 4 P18	134	10	10	1	229	2245	21.0
3	22	1996	1050 N1 Rse 11 P2	180	14	7	2	448	4399	18.0
4	23	1996	1200 N1 Rse 9 P8	193	12	9	2.2	544	5333	20.0
5	33	1996	1350 N1 Rse 8 P28	151	25	24	2.5	3432	33668	24.0
6	26	1996	1200 S1 Rse 2 P6	188	24	24	3	3954	38785	24.0
7	58	10/96	1200 N Rse 4 P18	134	14	11	1.2	423	4148	18.0
8	63	05/01/96	1200 N3 Rse 4 P18	134	14	7	2	448	4399	18.0
9	64	26/06/97	1200 N3A Rse 9A P8	130	9	9	1.1	204	2000	10.0
10	71	05/08/97	1200 S1 Rse 4 P2	200	43	15	2	2952	28954	17.0
11	75	09/97	1130 N3A Rse12 P12	190	14	6	0.8	154	1508	18.0
12	77	09/97	1200 N1A Rse 15 P2	110	6	5.9	0.9	73	715	13.0
13	78	09/97	1500 N1 Rse 1 P20	175	8	8	0.8	117	1149	8.0
14	80	18/11/97	1200 S3 Rse 10 P16	130	11.4	3.2	1	83	819	7.1
15	85	22/04/98	1350 S1 Rse 1 P16	200	4.5	3.5	1.1	40	389	7.0
16	102	20/10/00	12 S4 Rse 11 P14	165	19	12	1.4	730	7165	11.0
17	105	18/05/01	1650 S3 Rse 19 P26	180	8	6	0.8	88	862	10.0
			AVERAGE	160.47	14.70	10.09	1.49	849.81	8336.66	15.42
			STD DEVIATION	29.69	9.21	6.04	0.67	1267.05	12429.74	5.67

Table A11

Large FOG in Centre Gullies at Tau Lekoa (1995-2001)

No.	ID	Date	Workingplace	SW (cm)	Length (m)	Width (m)	Thickness (m)	Mass (tons)	Weigth (kN)	Span (m)
1	16	11/03/95	1200 N1 Rse 9	147	40	20	1.8	3295	32321	20.0
2	20	28/08/95	1200 N3 Rse 4	212	17	16	2.5	1556	15263	19.0
3	27	10/07/96	1050 N2B Rse 16	193	20	8	1.25	458	4489	12.0
4	34	1996	1350 N1 Rse 1 Ledge	150	7	4	1.2	77	754	12.0
5	28	26/09/96	1500 N1 Rse 6	135	23	12	1.4	884	8673	12.0
6	66	1997	1350 N1 Rse 10 C/G	146	14.6	10.2	1.6	545	5348	15.6
7	70	1997	1350 N1 Rse 1 C/G	174	13.2	10.3	2.1	653	6408	16.3
8	25	06/03/97	1050 N2B Rse 15	186	21	15	2.5	1802	17676	21.0
9	79	31/10/97	1350 N1 Rse 6 C/G	180	13.7	12.6	1.4	553	5424	11.9
10	93	1999	1500 S1 Rse 1Ledge (top)	180	8	5	1.1	101	988	10.0
11	60	1999	1500 N1 Rse 6 P6 Ledge	160	12	7	2.5	480	4714	12.0
12	94	1999	1500 S1 Rse 1Ledge (bot.)	180	5	4	1	46	449	8.0
13	99	13/03/00	1500 S1 Rse 8 C/G	300	11	5	1.5	189	1852	8.0
14	100	27/03/00	1350 S1 Rse 3 C/G	300	35	8	2.5	1602	15712	10.0
15	106	20/07/01	1200 S4 Rse 8E C/G	180	14	13	1.5	625	6128	32.0
16	107	22/08/01	1200 S3 Rse 9 C/G	170	6	5	0.6	41	404	7.0
			AVERAGE	187.06	16.28	9.69	1.65	806.59	7912.60	14.18
			STD DEVIATION	48.26	9.84	4.78	0.60	870.84	8542.90	6.40

Table A12 FOG and geozones

Large FOG in stopes at Tau Lekoa Mine (1991-2001)

No.	ID	Date	Workingplace	SW (cm)	Length (m)	Width (m)	Thickness (m)	Mass (tons)	Weigth (kN)	Span (m)
1	40	1991	1200 N1 Rse 1	187	8	3	1.5	82	808	30.0
2	41	1992	1130 N1A Rse 12	178	15	9	3	927	9090	25.0
3	42	1992	1200 N1 Rse 12 P2C	260	12	12	2.5	824	8080	20.0
4	43	1992	1200 N1 Rse 1B P1/2	228	16	12	3	1318	12928	26.0
5	2	1992	1130 N1A Rse 12 P2B	252	18	14	2.4	1384	13575	16.0
6	3	1992	1200 N1 Rse 11 P1	287	36	30	3.75	9266	90903	30.0
7	4	1992	1200 N1 Rse 12 P2	284	16	12	2.5	1098	10774	40.0
8	5	1992	1200 N1 Rse 11 P2/2A	179	17	8	1.8	560	5495	15.0
9	6	1992	1130 N1A Rse 13 P5-8	147	14	7	2	448	4399	16.0
10	7	1993	1200 N1 Rse 4 P7	172	34	20	2.5	3890	38157	20.0
11	8	1993	1200 N1 Rse 9 P8	169	19	6	1.2	313	3071	20.0
12	9	1993	1350 N1 Rse 10 P22	131	14	9	1	288	2828	20.0
13	11	1993	1130 N1A Rse 13 P5	177	16	14	2.4	1230	12067	16.0
14	12	11/01/93	1200 N1 Rse 11 P1	223	18	14	3.3	1903	18665	30.0
15	44	21/07/93	1130 N1A Rse 13 P5/6	147	21	11	4.8	2537	24887	25.0
16	14	1993	1200 S1 Rse 4 P8	121	18	10	1.5	618	6060	12.0
17	15	11/03/94	1200 S1 Rse 2 P16	170	4	3	1.45	40	391	12.0
18	18	12/94	1350 N1 Rse 6 P24	177	10	8	1	183	1796	16.0
19	16	11/03/95	1200 N1 Rse 9	147	40	20	1.8	3295	32321	20.0
20	19	10/95	1350 N1 Rse 7 P17	190	22	19	2.8	2678	26270	22.0
21	20	28/08/95	1200 N3 Rse 4	212	17	16	2.5	1556	15263	19.0
22	21	13/04/95	1200 N3 Rse 4 P18	134	14	11	1.5	529	5185	18.0
23	56	1995	1200 N3 Rse 4 P18	134	10	10	1	229	2245	21.0
24	22	1996	1050 N1 Rse 11 P2	180	14	7	2	448	4399	18.0
25	23	1996	1200 N1 Rse 9 P8	193	12	9	2.2	544	5333	20.0
26	31	1996	1350 N1 Rse 10 P21	224	24	24	3	3954	38785	24.0
27	32	1996	1350 N1 Rse 10 P23	115	14	14	1.6	718	7039	19.0
28	33	1996	1350 N1 Rse 8 P28	151	25	24	2.5	3432	33668	24.0
29	34	1996	1350 N1 Rse 1 Ledge	150	7	4	1.2	77	754	12.0
30	35	1996	1350 N1 Rse 6 P21	150	24	21	2.5	2883	28281	22.0
31	36	1996	1350 N1 Rse 6 P19	170	13	8	1.5	357	3501	15.0
32	37	1996	1350 N1 Rse 6 P19	170	9	6	1.2	148	1454	10.0
33	38	1996	1350 N1 Rse 6 P21	150	16	13	2.2	1047	10271	17.0
34	26	1996	1200 S1 Rse 2 P6	188	24	24	3	3954	38785	24.0
35	27	10/07/96	1050 N2B Rse 16	193	20	8	1.25	458	4489	12.0
36	28	26/09/96	1500 N1 Rse 6	135	23	12	1.4	884	8673	12.0
37	58	10/96	1200 N Rse 4 P18	134	14	11	1.2	423	4148	18.0
38	63	05/01/96	1200 N3 Rse 4 P18	134	14	7	2	448	4399	18.0
39	64	26/06/97	1200 N3A Rse 9A P8	130	9	9	1.1	204	2000	10.0
40	25	06/03/97	1050 N2B Rse 15	186	21	15	2.5	1802	17676	21.0
41	65	1997	1350 S1 Rse 3 P15	185	13	6.5	1.5	290	2845	11.6
42	66	1997	1350 N1 Rse 10 C/G	146	14.6	10.2	1.6	545	5348	15.6
43	67	1997	1350 S1 Rse 9 P23	114	13.1	8.8	1	264	2587	9.1
44	68	1997	1350 S1 Rse 9 P21	174	7	3	1.6	77	754	4.0
45	69	1997	1350 S1 Rse 9 P19	141	16.8	8	2.2	677	6637	8.0
46	70	1997	1350 N1 Rse 1 C/G	174	13.2	10.3	2.1	653	6408	16.3
47	71	05/08/97	1200 S1 Rse 4 P2	200	43	15	2	2952	28954	17.0
48	72	09/97	1350 S1 Rse 1 P11	130	40	24	0.9	1977	19393	21.0
49	73	09/97	1350 N1 Rse 6 P15	180	6	4.5	0.7	43	424	8.0
50	74	09/97	1350 N1 Rse 6 P17	170	6	5.3	0.6	44	428	7.8
51	75	09/97	1130 N3A Rse12 P12	190	14	6	0.8	154	1508	18.0
52	77	09/97	1200 N1A Rse 15 P2	110	6	5.9	0.9	73	715	13.0
53	78	09/97	1500 N1 Rse 1 P20	175	8	8	0.8	117	1149	8.0
54	79	31/10/97	1350 N1 Rse 6 C/G	180	13.7	12.6	1.4	553	5424	11.9
55	80	18/11/97	1200 S3 Rse 10 P16	130	11.4	3.2	1	83	819	7.1
56	82	02/12/97	1200 N1 Rse 4 P7	193	5.8	5.7	1.8	136	1336	17.0
57	83	08/01/98	1350 S1 Rse 9 P13	170	14.6	4.6	1.98	304	2985	16.0
58	85	22/04/98	1350 S1 Rse 1 P16	200	4.5	3.5	1.1	40	389	7.0
59	86	03/98	1350 S1 Rse 10 P15+17	350	33	13	2.5	2454	24073	24.0
60	87	04/98	1350S1R3P33	230	14.3	4	0.7	92	899	15.0
61	81	19/05/98	1500 S1 Rse 2 P15	160	8	5.4	0.6	59	582	15.0
62	88	05/98	1350S1R7P19	190	10.2	5.8	0.6	81	797	5.8
63	89	06/98	1350S1R3P27	200	6.3	3.4	0.5	25	240	7.7
64	90	06/98	1350 S1 Rse 7 P19	220	12	9.8	1.8	484	4751	5.8
65	91	07/98	1350 S1 Rse 3 P31	180	9.5	3	0.5	33	320	10.0
66	92	08/98	1350 S1 Rse 3 P33	190	6	5.6	0.7	54	528	5.5
67	93	1999	1500 S1 Rse 1Ledge (top)	180	8	5	1.1	101	988	10.0
68	60	1999	1500 N1 Rse 6 P6 Ledge	160	12	7	2.5	480	4714	12.0
69	94	1999	1500 S1 Rse 1Ledge (bot.)	180	5	4	1	46	449	8.0
70	95	25/08/99	1350 S1 Rse 8 P17	178	8	3	1.25	69	673	9.0
71	96	09/99	1350 S1 Rse 3 P21	180	30	16	2.5	2746	26934	18.0
72	98	21/2/00	1350 S1 Rse 5 P5	200	6	2.5	1.5	51	505	5.0
73	99	13/03/00	1500 S1 Rse 8 C/G	300	11	5	1.5	189	1852	8.0
74	100	27/03/00	1350 S1 Rse 3 C/G	300	35	8	2.5	1602	15712	10.0
75	102	20/10/00	12 S4 Rse 11 P14	165	19	12	1.4	730	7165	11.0
76	103	01/09/00	1350 Rse 18 P15	182	10	5	0.6	69	673	10.0
77	62	2001	1200 N1A Rse 16 P9	177	8	4	0.8	59	575	24.0
78	105	18/05/01	1650 S3 Rse 19 P26	180	8	6	0.8	88	862	10.0
79	106	20/07/01	1200 S4 Rse 8E C/G	180	14	13	1.5	625	6128	32.0
80	107	22/08/01	1200 S3 Rse 9 C/G	170	6	5	0.6	41	404	7.0
81	108	15/11/01	1050 S4 Rse 15 P11	180	17	8	3.25	1011	9921	16.0
			AVERAGE	180.90	15.30	9.79	1.71	952.37	9342.73	15.80
			STD DEVIATION	43.90	8.77	5.94	0.86	1408.59	13818.23	7.15

	Main Channel
	Reworked Channel
	Middle Terrace Conglomerate
	Middle Terrace Slope
	Upper Terracte

APPENDIX B

FALLOUT THICKNESS VERSUS SPAN PLOTS (FIGURES B1-B11)

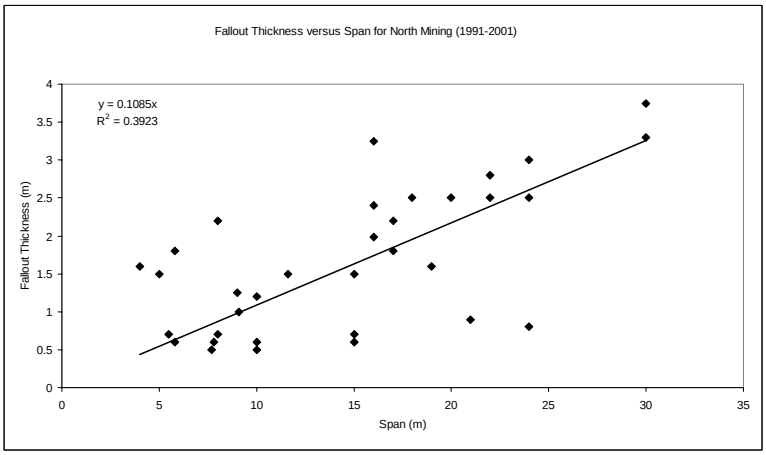

Figure B1 Fallout thickness versus span for north mining (1991-2001)

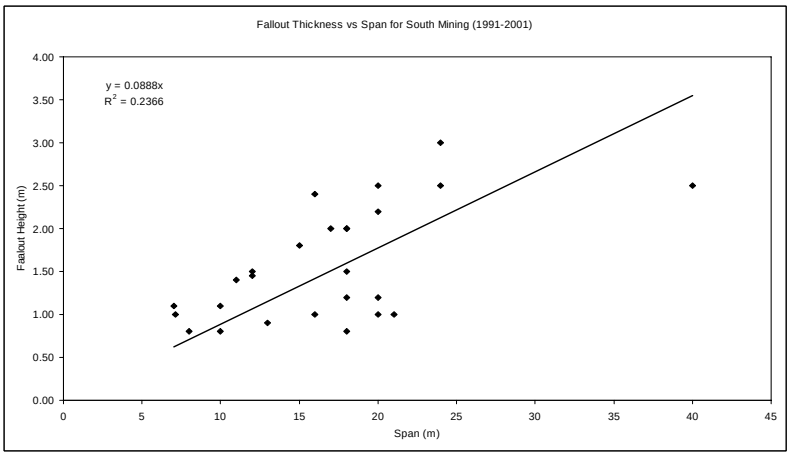

Figure B2 Fallout thickness versus span for south mining (1991-2001)

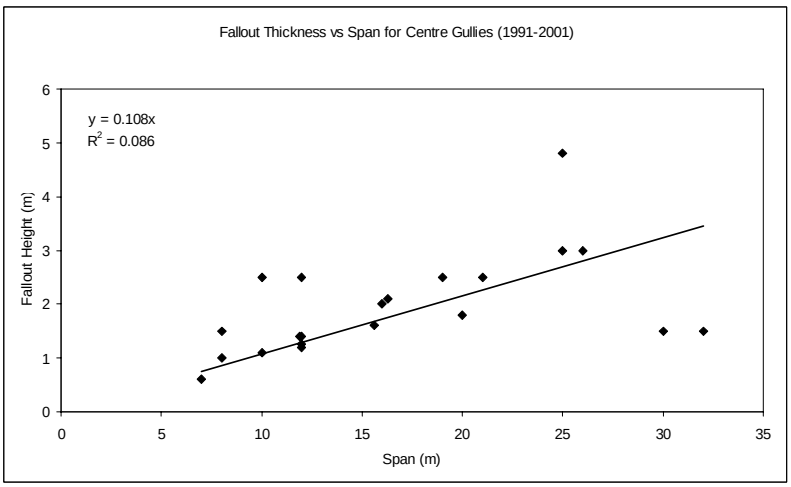

Figure B3 Fallout thickness versus span for centre gullies (1991-2001)

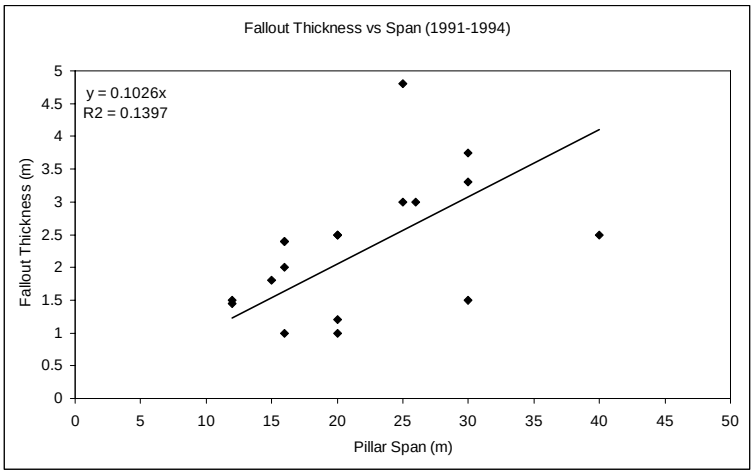

Figure B4 Fallout thickness versus span (1991-1994)

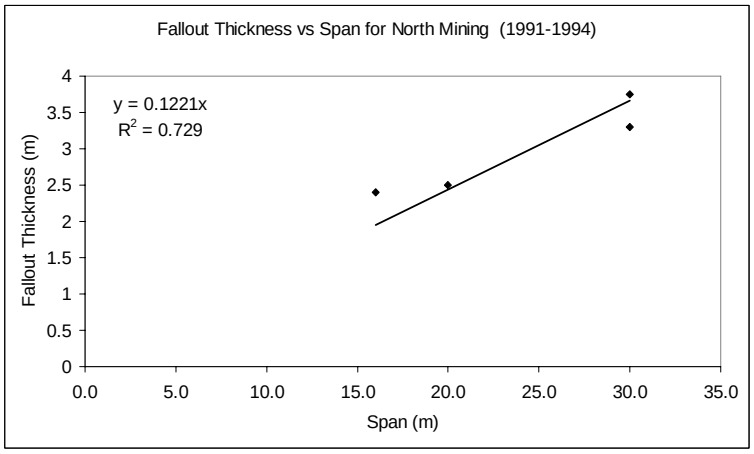

Figure B5 Fallout thickness versus span for north mining (1991-1994)

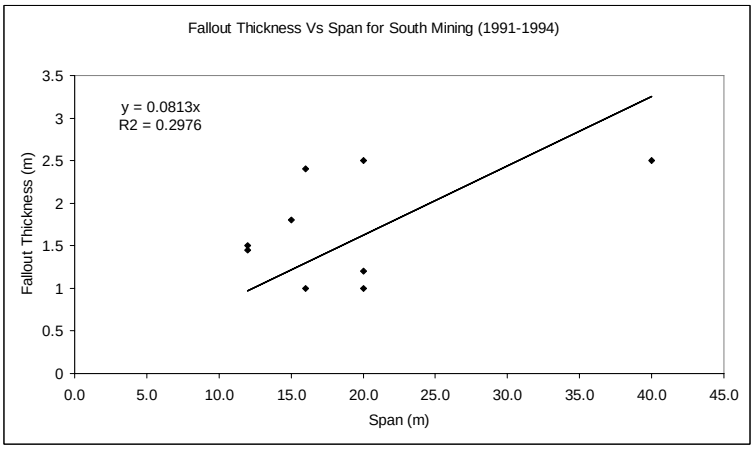

Figure B6 Fallout thickness versus span for south mining (1991-1994)

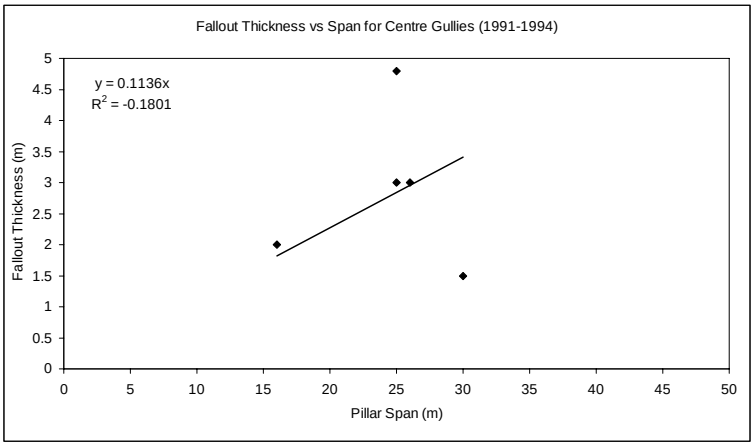

Figure B7 Fallout thickness versus span for centre gullies (1991-1994)

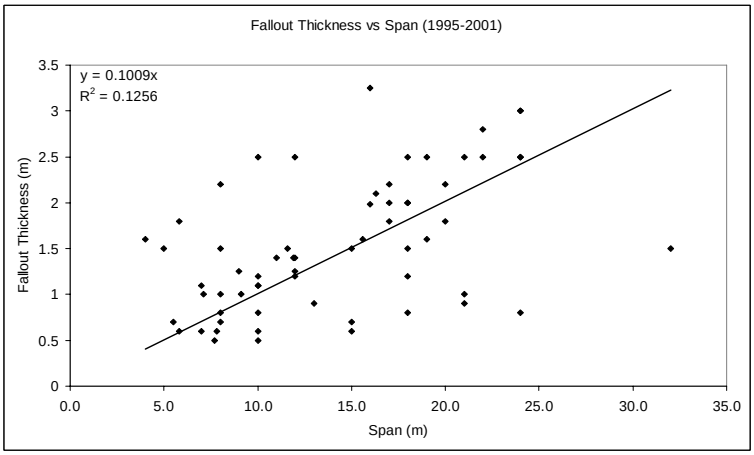

Figure B8 Fallout thickness versus span (1995-2001)

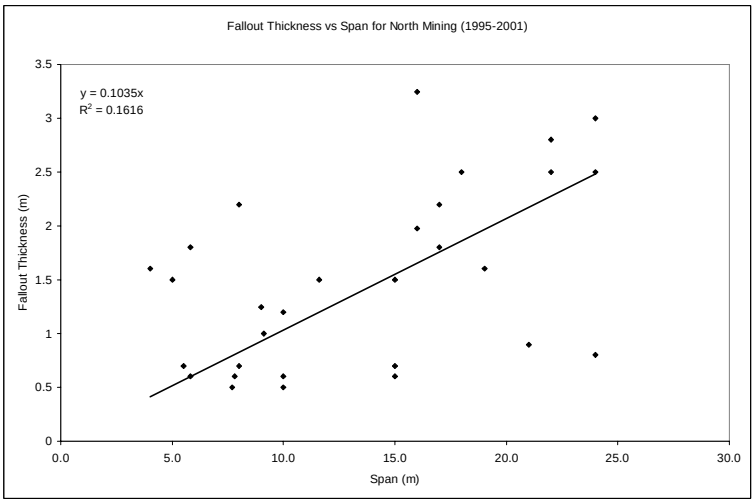

Figure B9 Fallout thickness versus span for north mining (1995-2001)

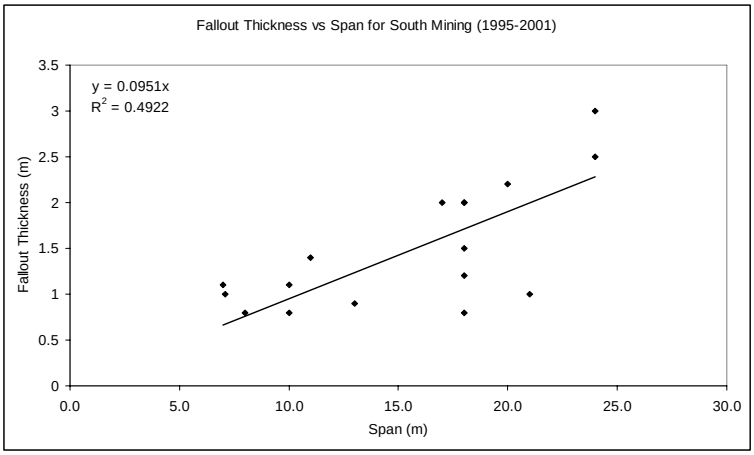

Figure B10 Fallout thickness versus span for south mining (1995-2001)

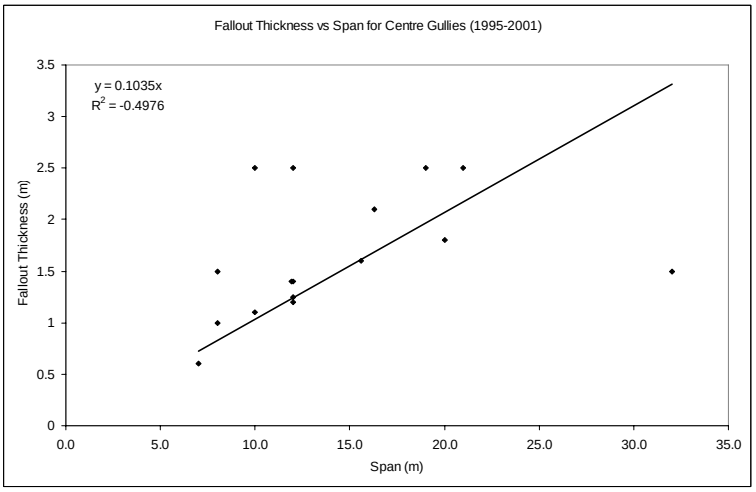

Figure B11 Fallout thickness versus span for centre gullies (1995-2001)

APPENDIX C

FALLOUT THICKNESS (FIGURES C1-C21)

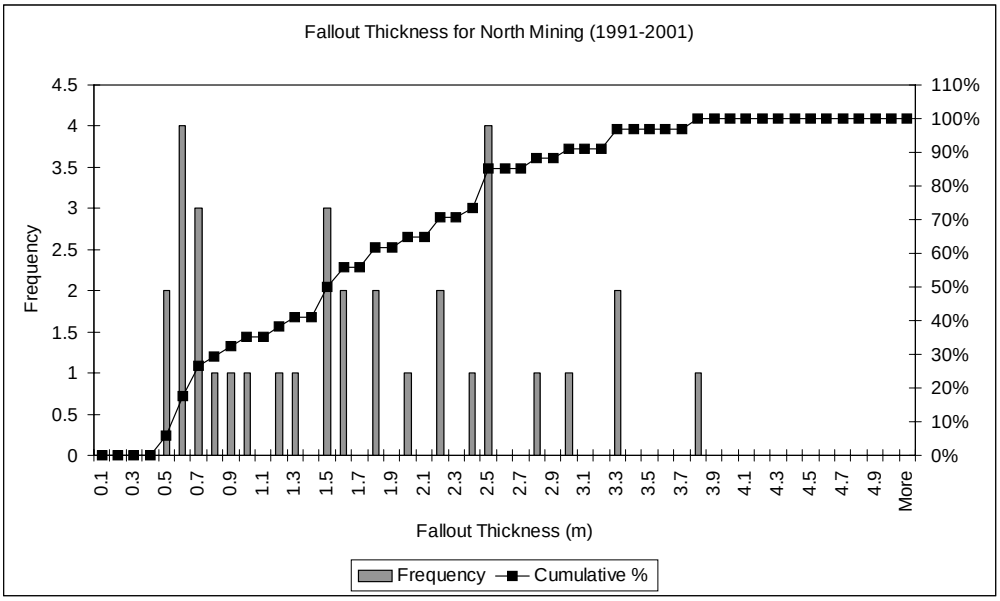

Figure C1 Fallout thickness frequency and cumulative percentage for north mining (1991-2001)

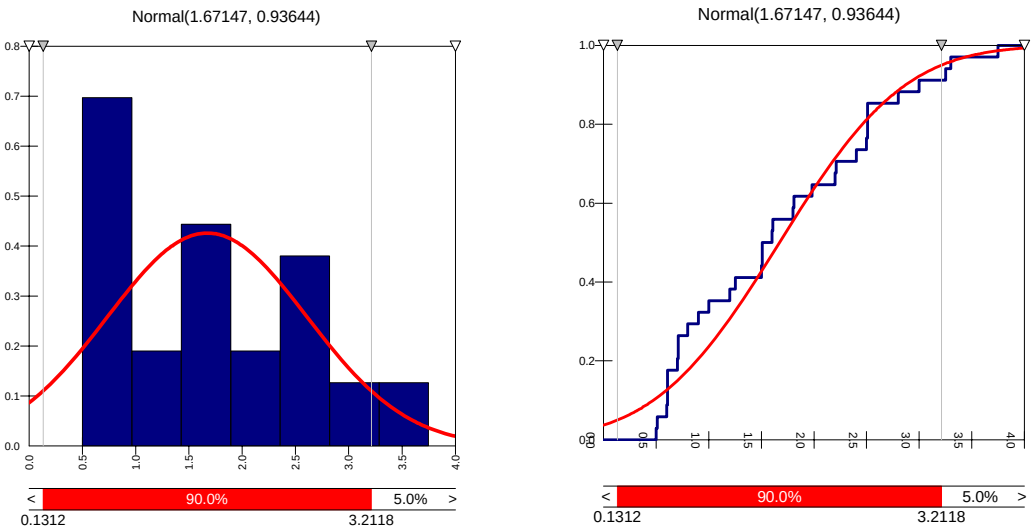

Figure C2 Fallout thickness PDF and cumulative distribution for north mining (1991-2001)

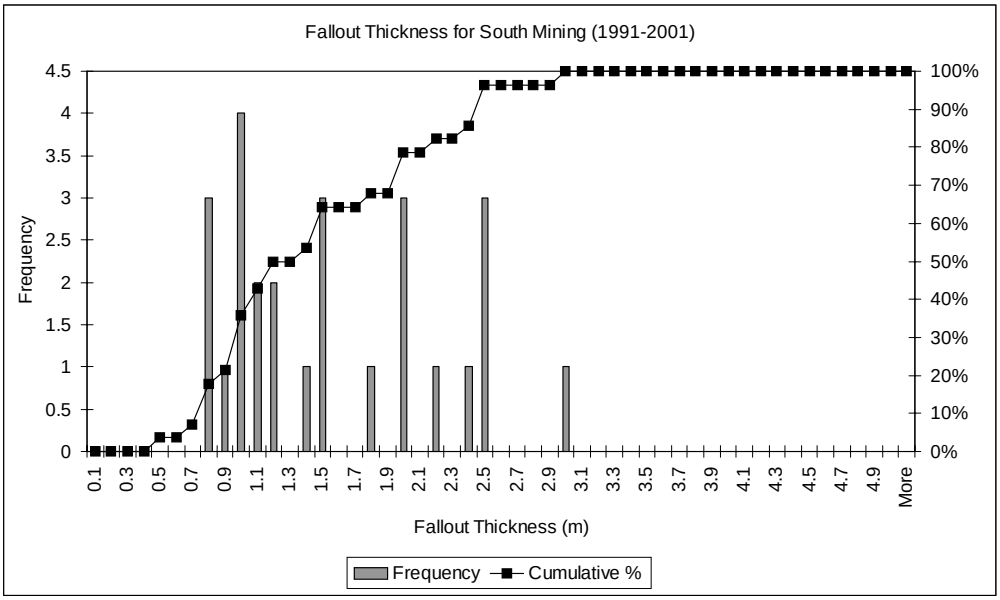

Figure C3 Fallout thickness frequency and cumulative percentage for south mining (1991-2001)

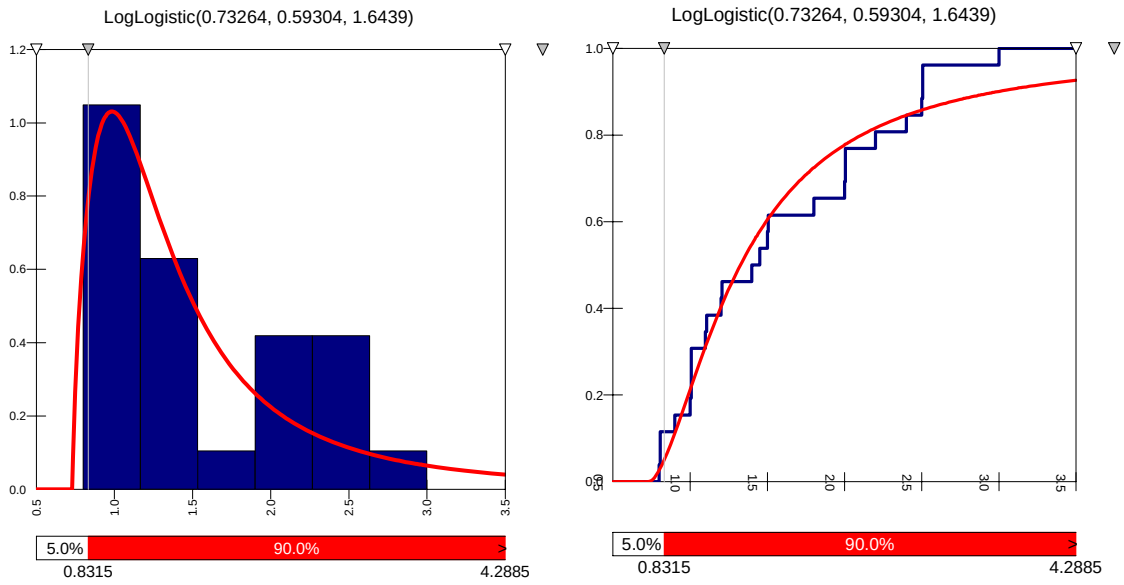

Figure C4 Fallout thickness PDF and cumulative distribution for south mining (1991-2001)

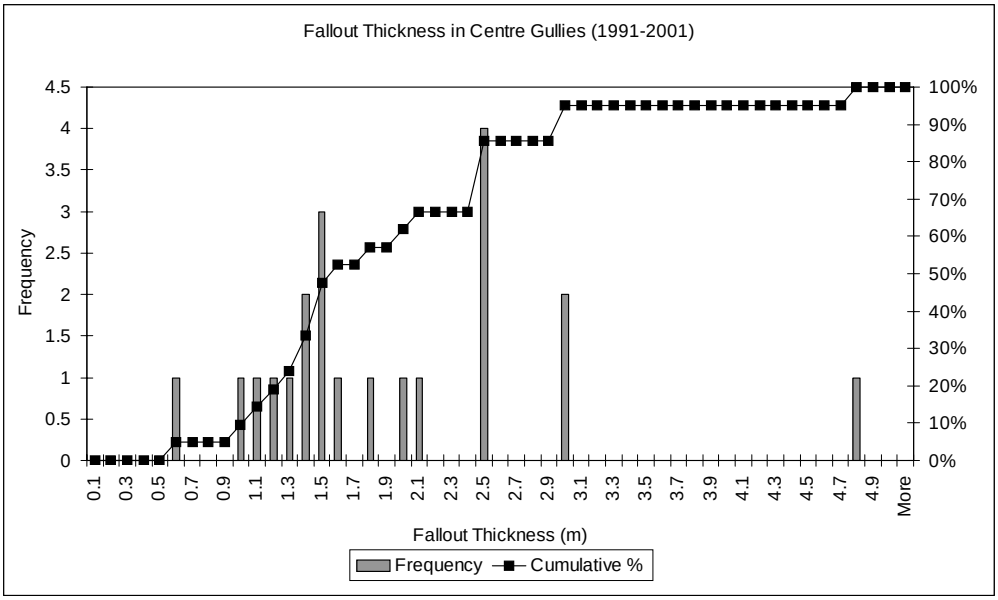

Figure C5 Fallout thickness frequency and cumulative percentage for centre gullies (1991-2001)

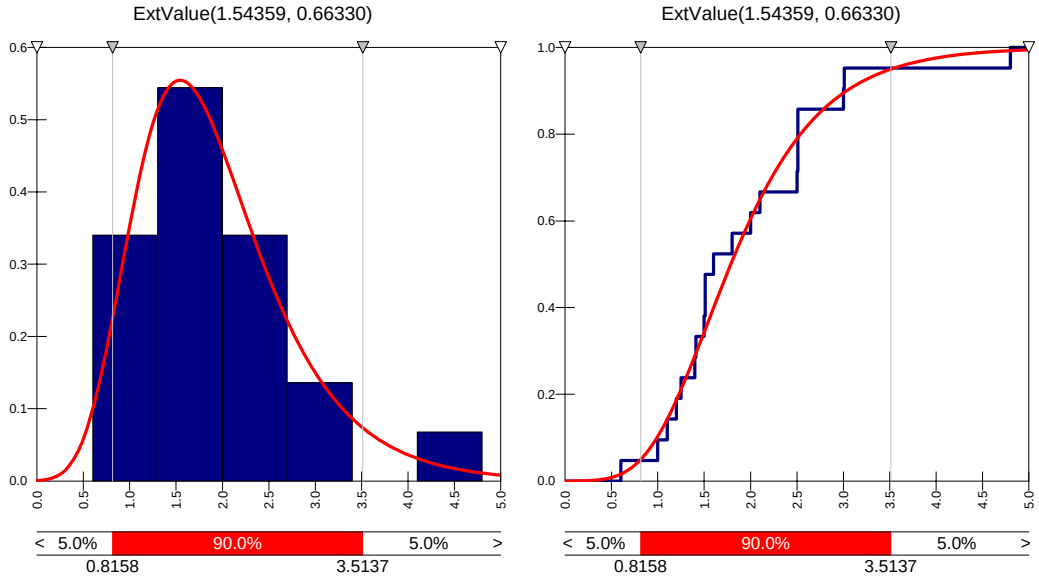

Figure C6 Fallout thickness PDF and cumulative distribution for centre gullies (1991-2001)

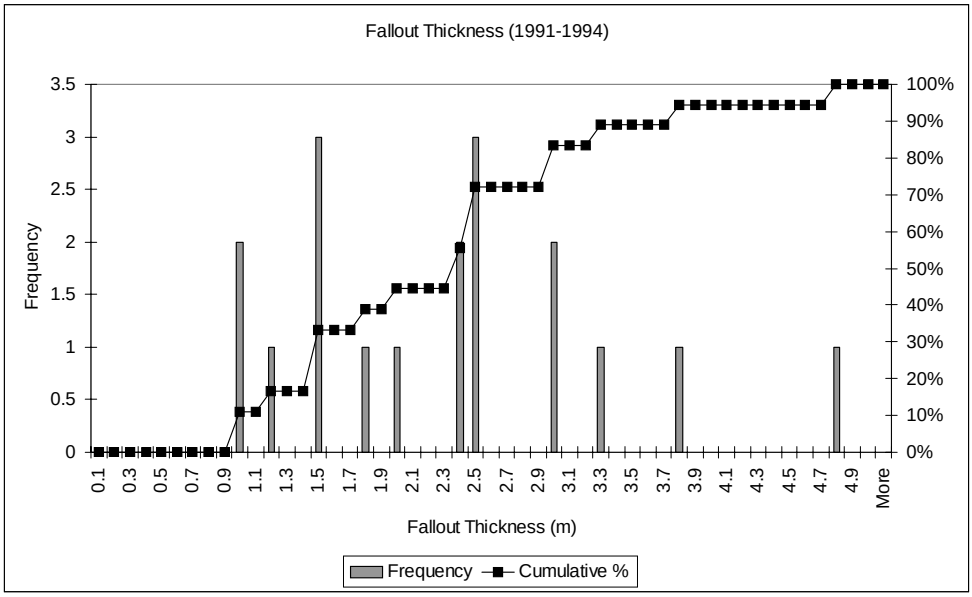

Figure C7 Fallout thickness frequency and cumulative percentage (1991-1994)

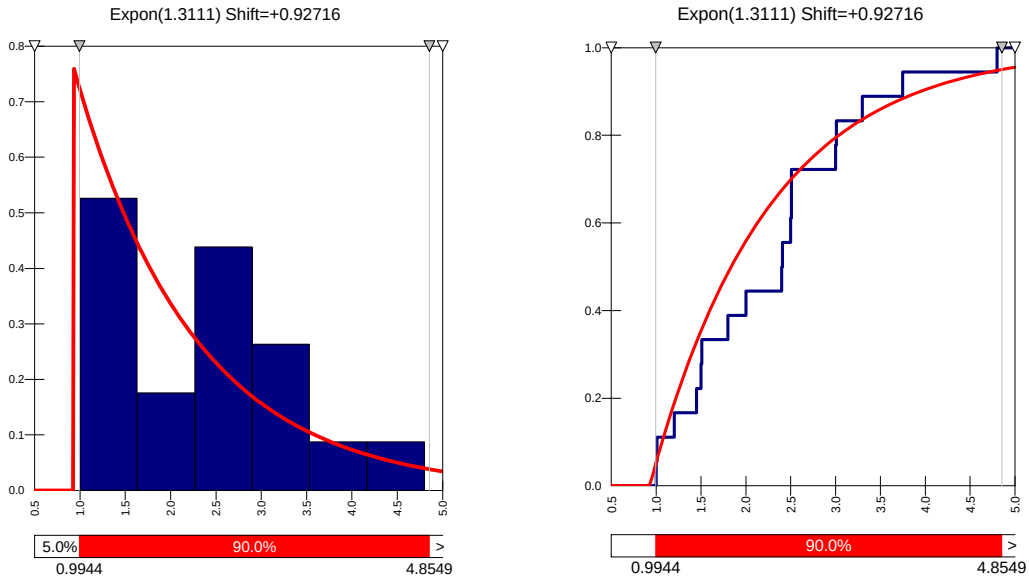

Figure C8 Fallout thickness PDF and cumulative distribution (1991-1994)

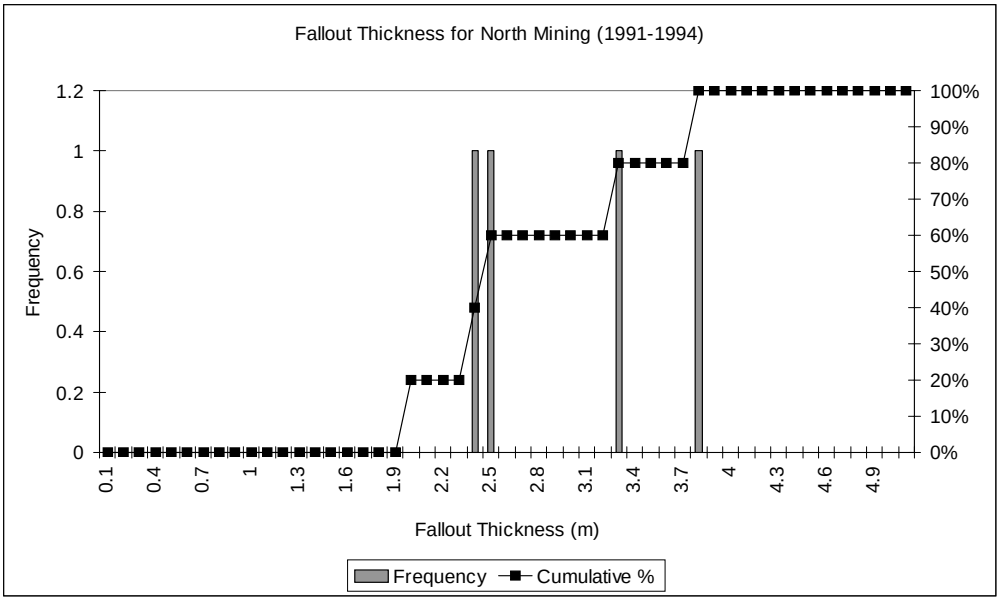

Figure C9 Fallout thickness frequency and cumulative percentage for north mining (1991-1994)

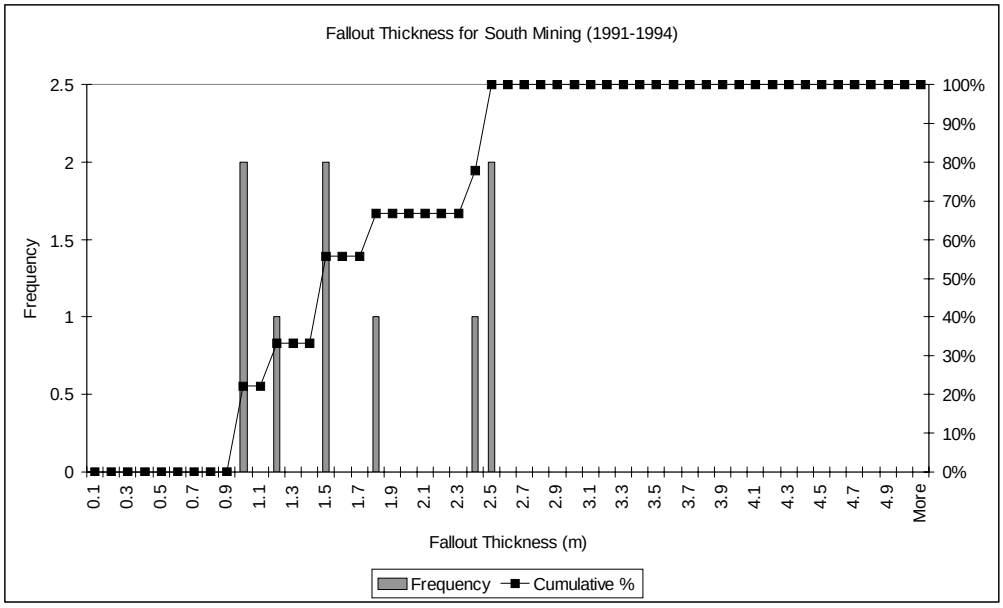

Figure C10 Fallout thickness frequency and cumulative percentage for south mining (1991-1994)

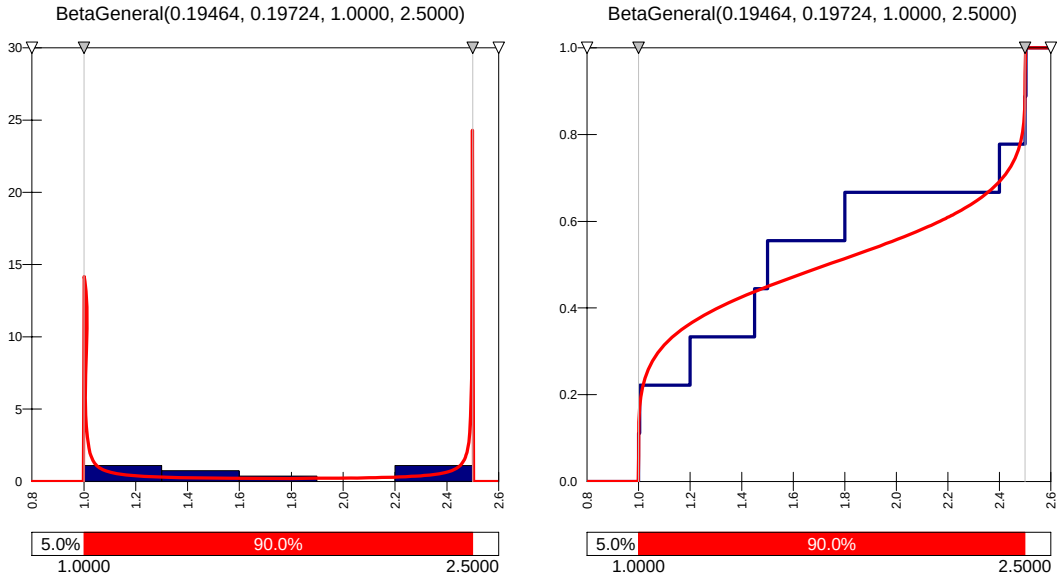

Figure C11 Fallout thickness PDF and cumulative distribution for south mining (1991-1994)

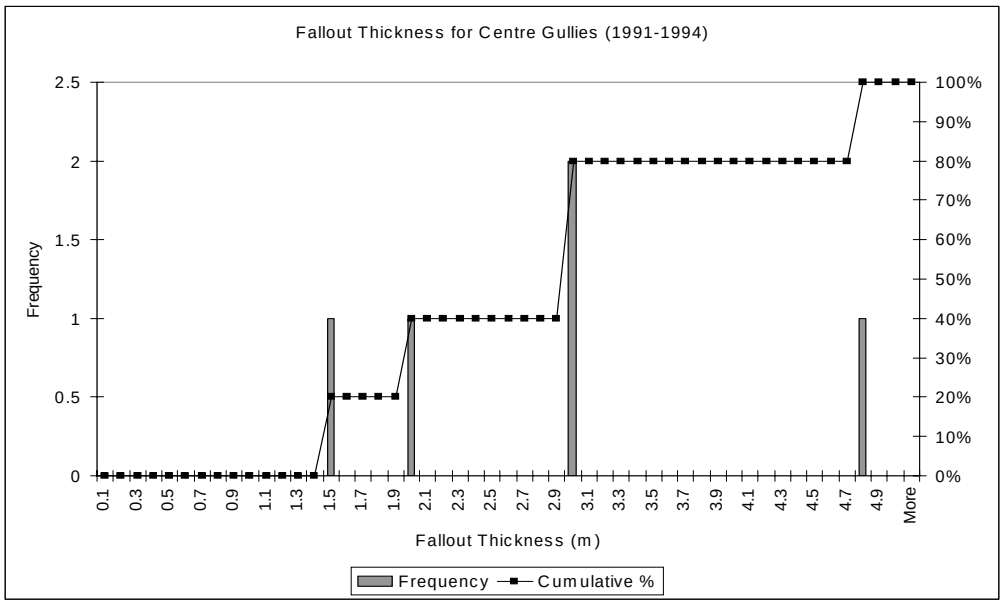

Figure C12 Fallout thickness frequency and cumulative percentage for centre gullies (1991-1994)

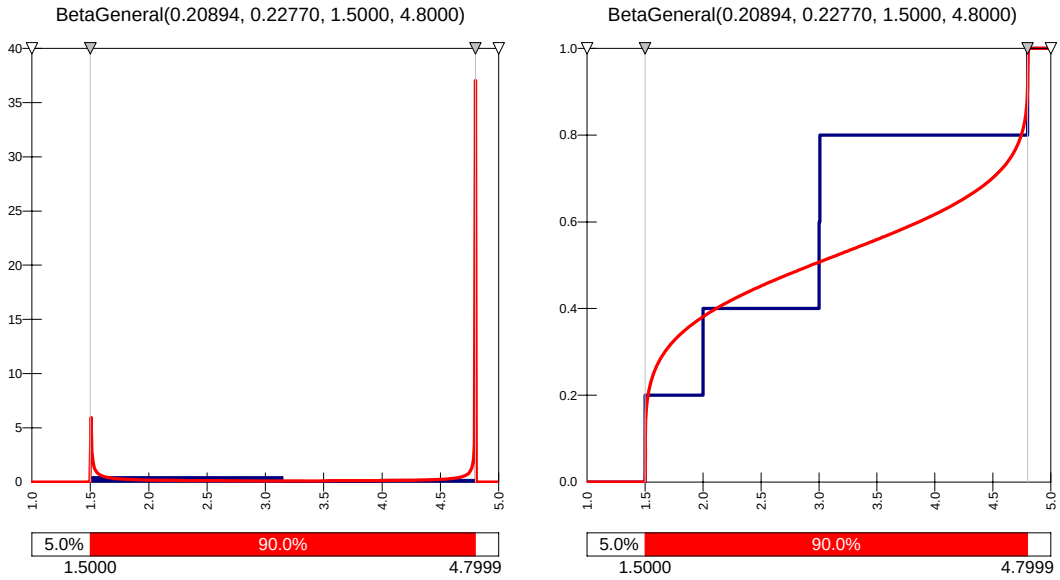

Figure C13 Fallout thickness PDF and cumulative distribution for centre gullies (1991-1994)

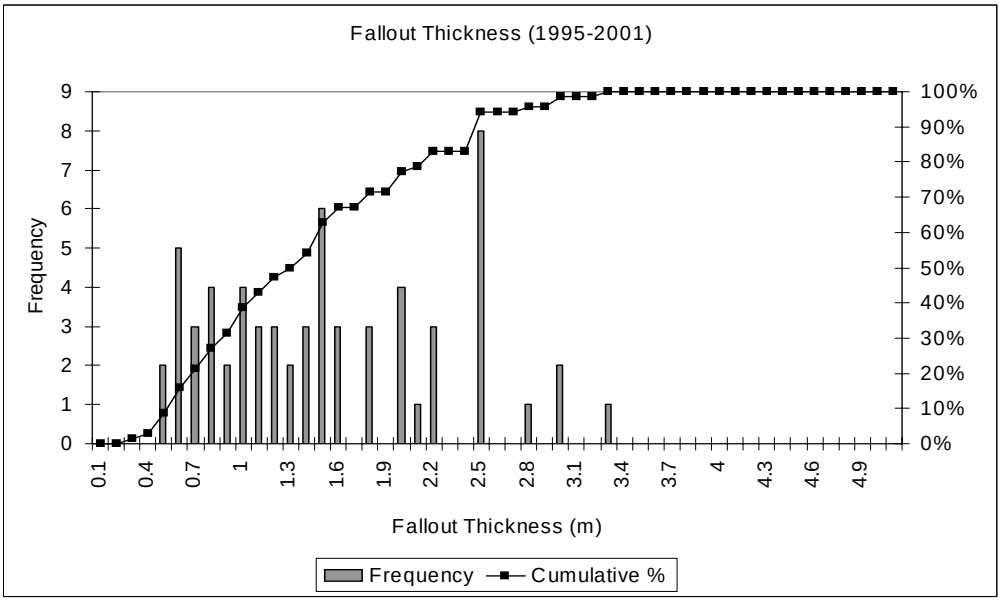

Figure C14 Fallout thickness frequency and cumulative percentage (1995-2001)

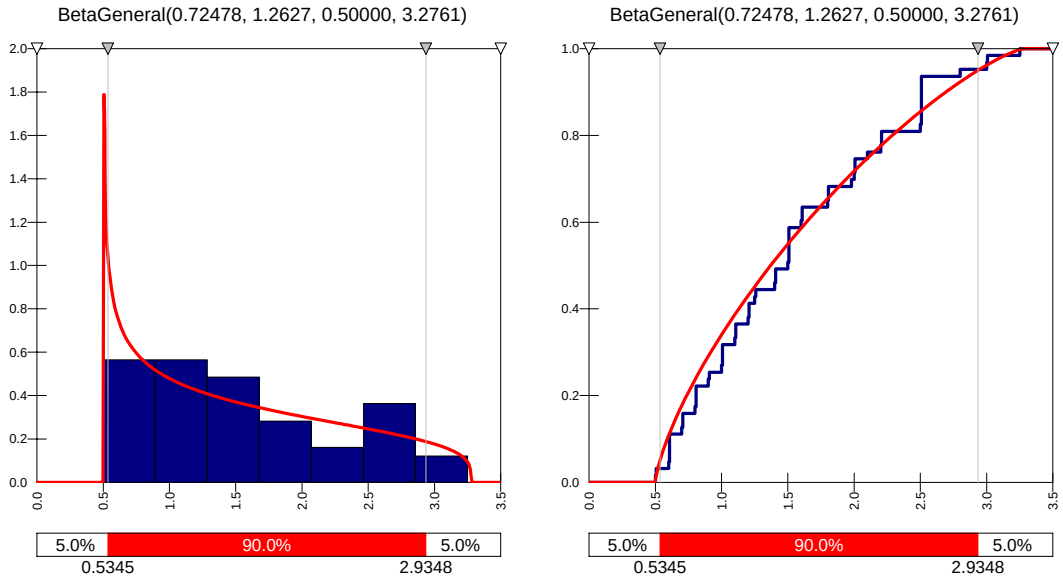

Figure C15 Fallout thickness PDF and cumulative distribution (1995-2001)

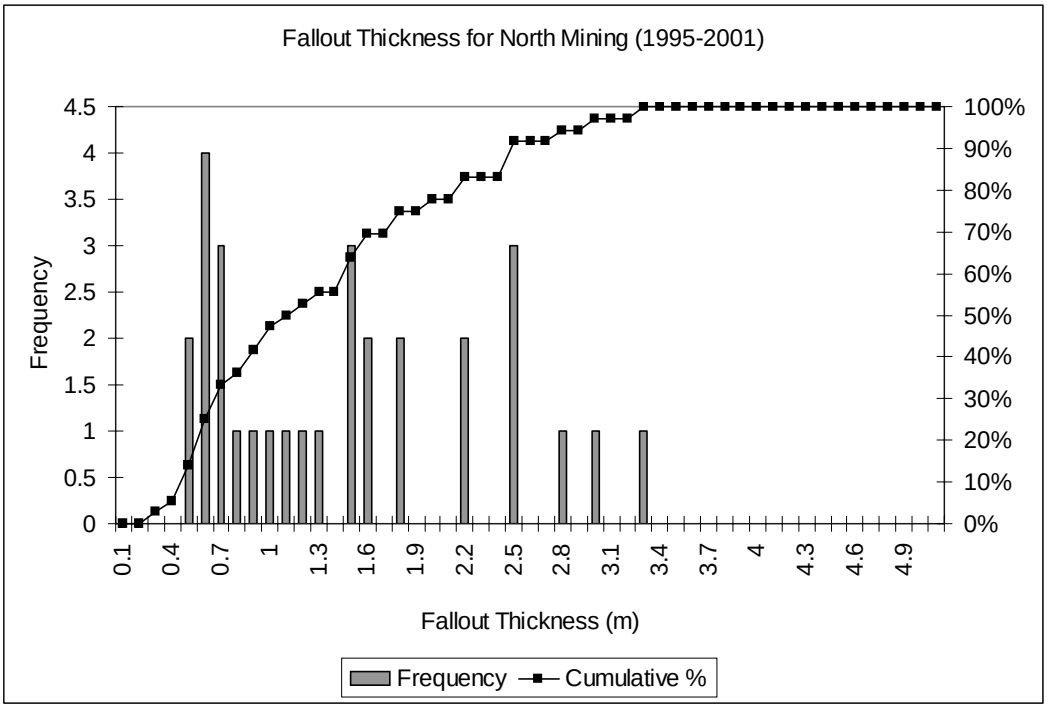

Figure C16 Fallout thickness frequency and cumulative percentage for north mining (1995-2001)

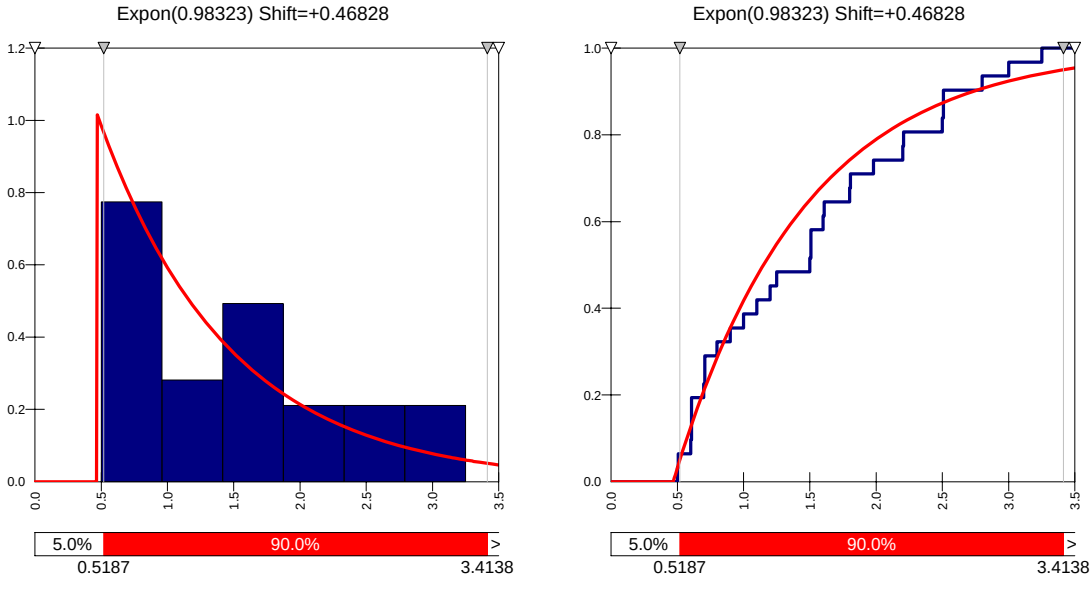

Figure C17 Fallout thickness PDF and cumulative distribution for north mining (1995-2001)

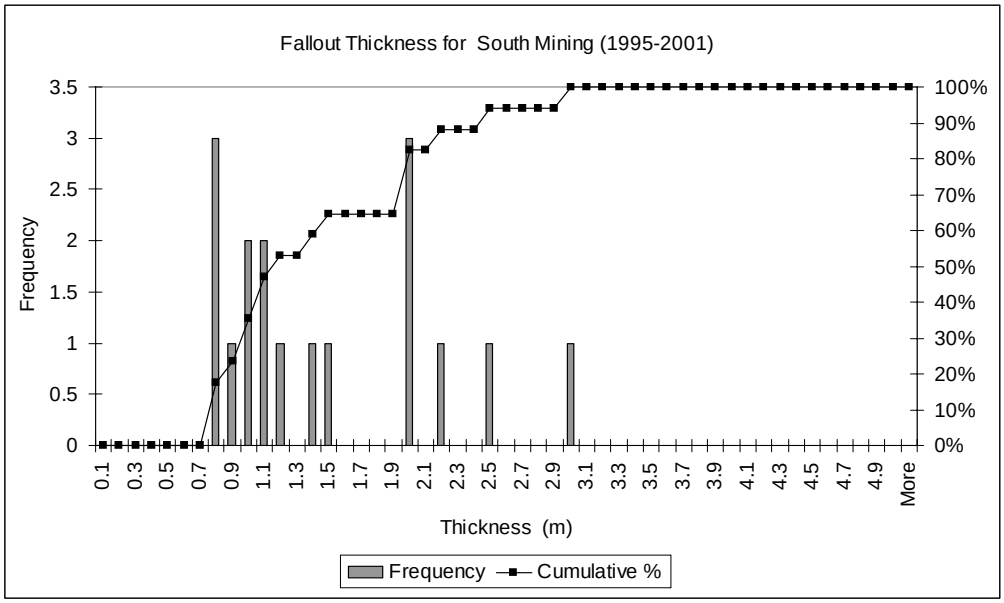

Figure C18 Fallout thickness frequency and cumulative percentage for south mining (1995-2001)

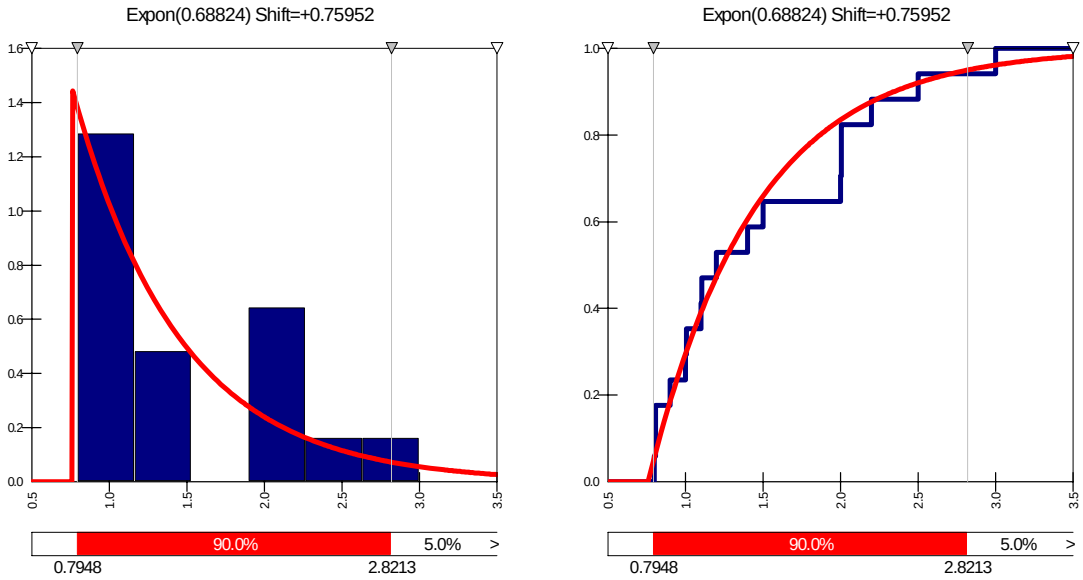

Figure C19 Fallout thickness PDF and cumulative distribution for south mining (1995-2001)

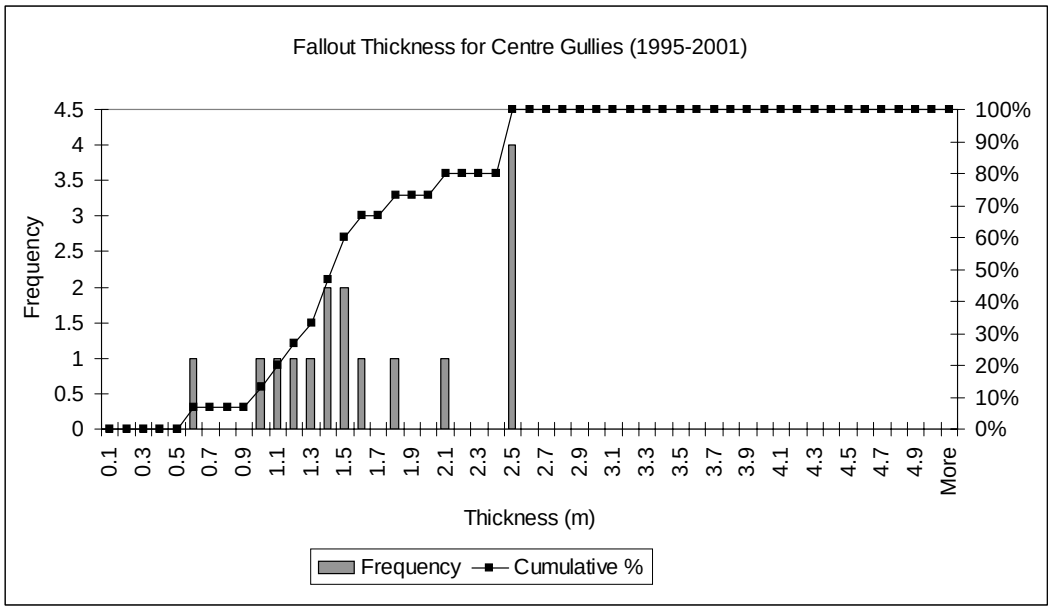

Figure C20 Fallout thickness frequency and cumulative percentage for centre gullies (1995-2001)

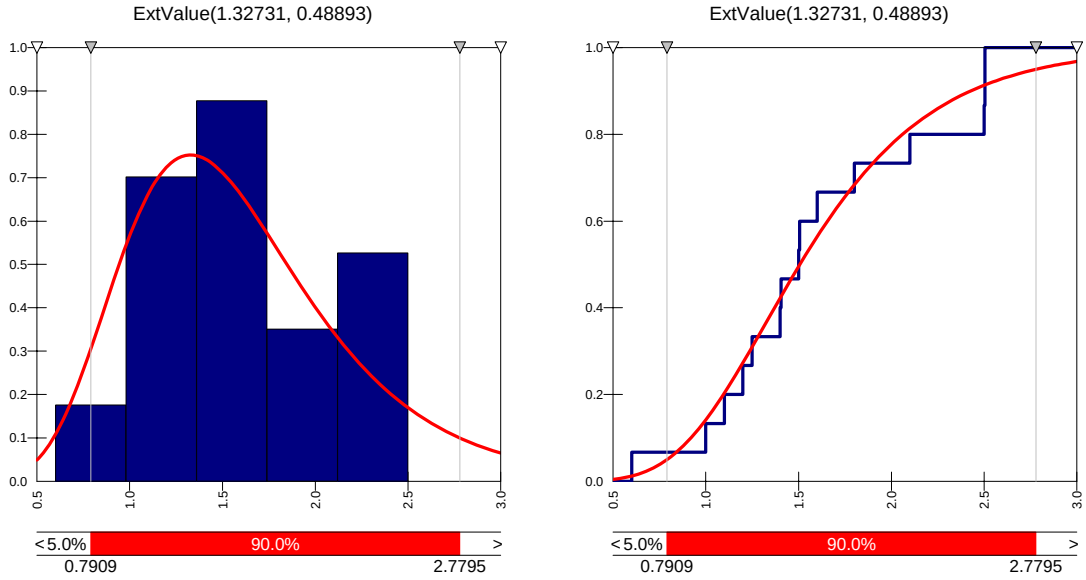

Figure C21 Fallout thickness PDF and cumulative distribution for centre gullies (1995-2001)

APPENDIX D

FOG LENGTH (FIGURES D1-D23)

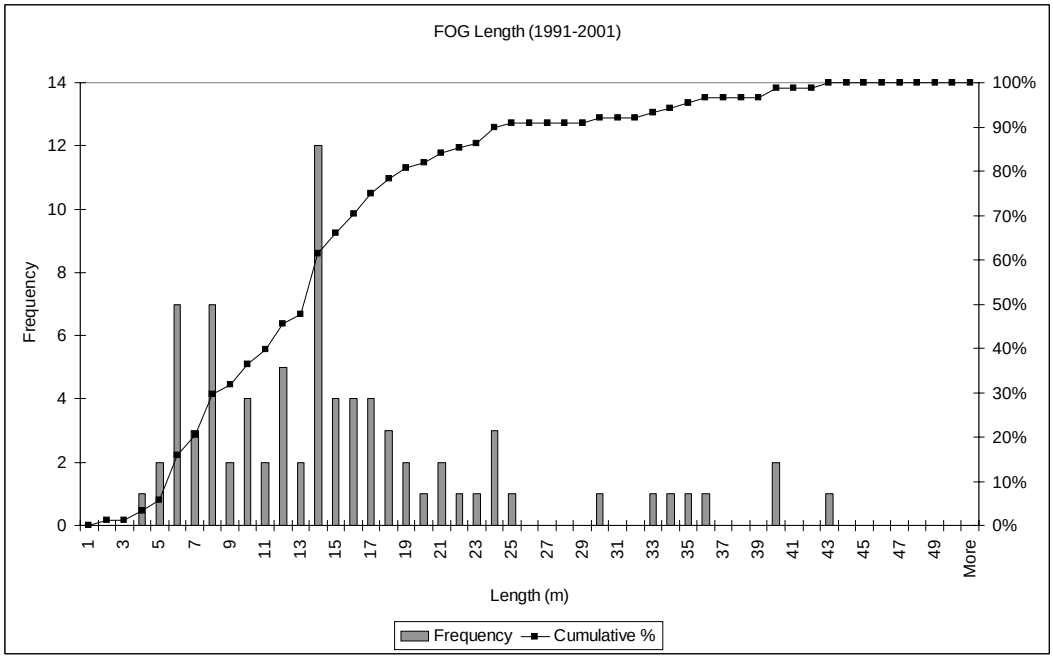

Figure D1 FOG length frequency and cumulative percentage (1991-2001)

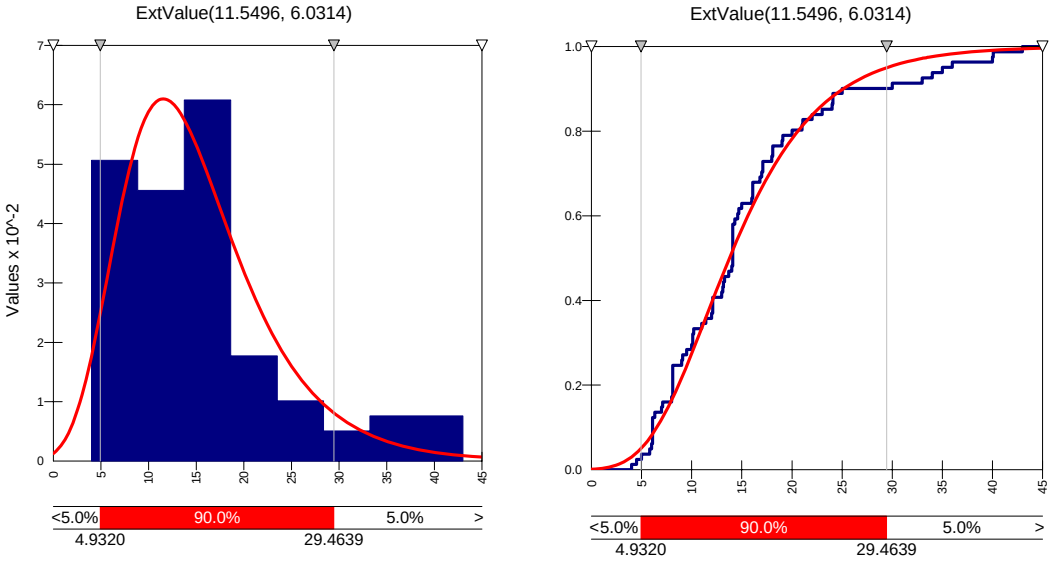

Figure D2 FOG length PDF and cumulative distribution (1991-2001)

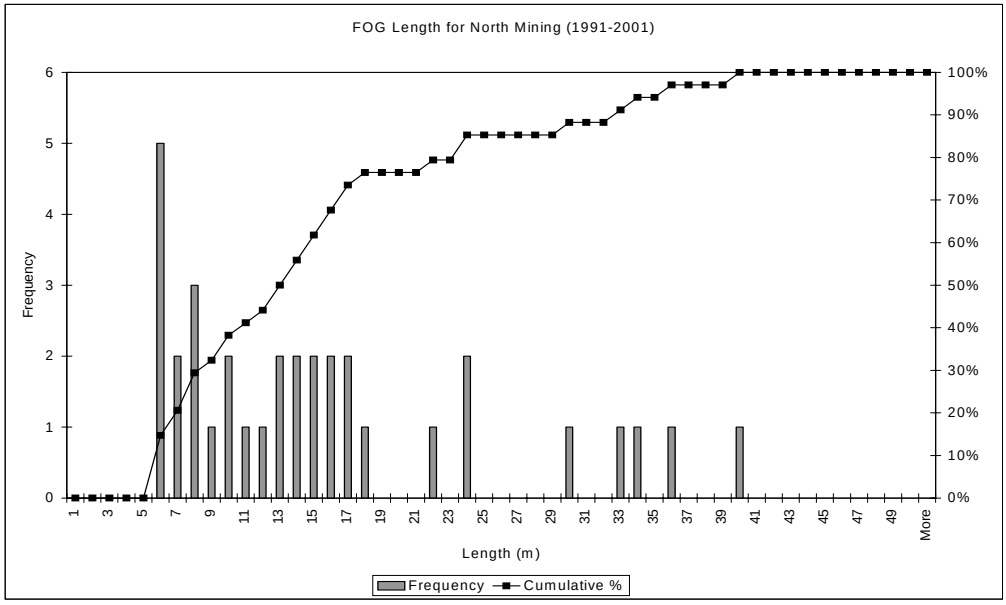

Figure D3 FOG length frequency and cumulative percentage for north mining (1991-2001)

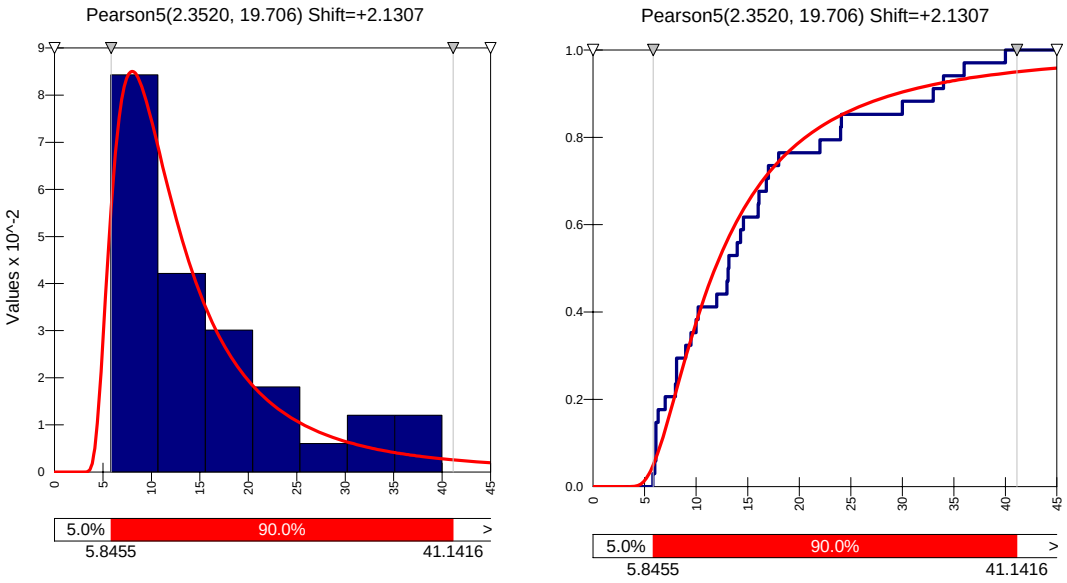

Figure D4 FOG length PDF and cumulative distribution for north mining (1991-2001)

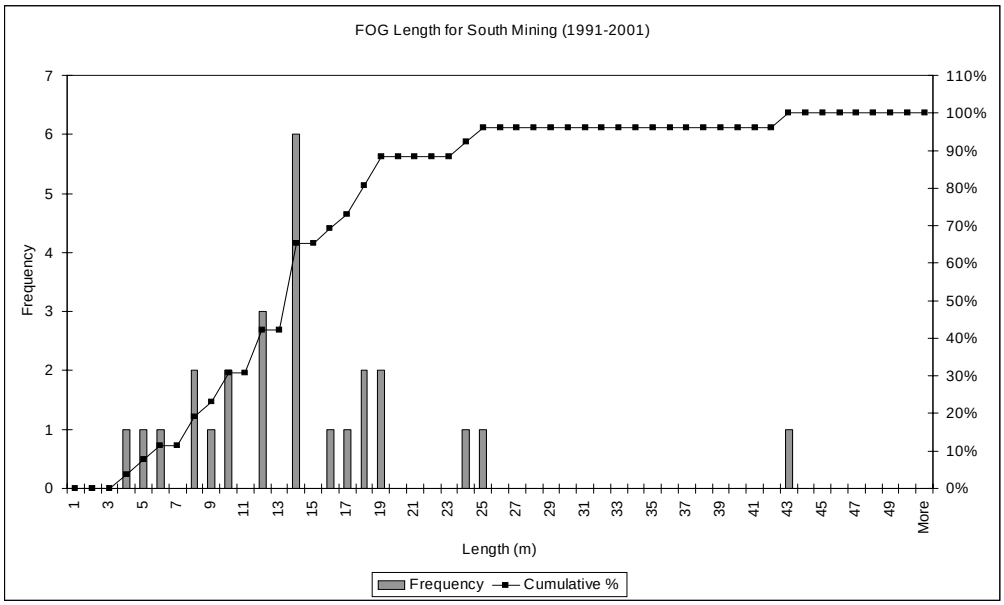

Figure D5 FOG length frequency and cumulative percentage for south mining (1991-2001)

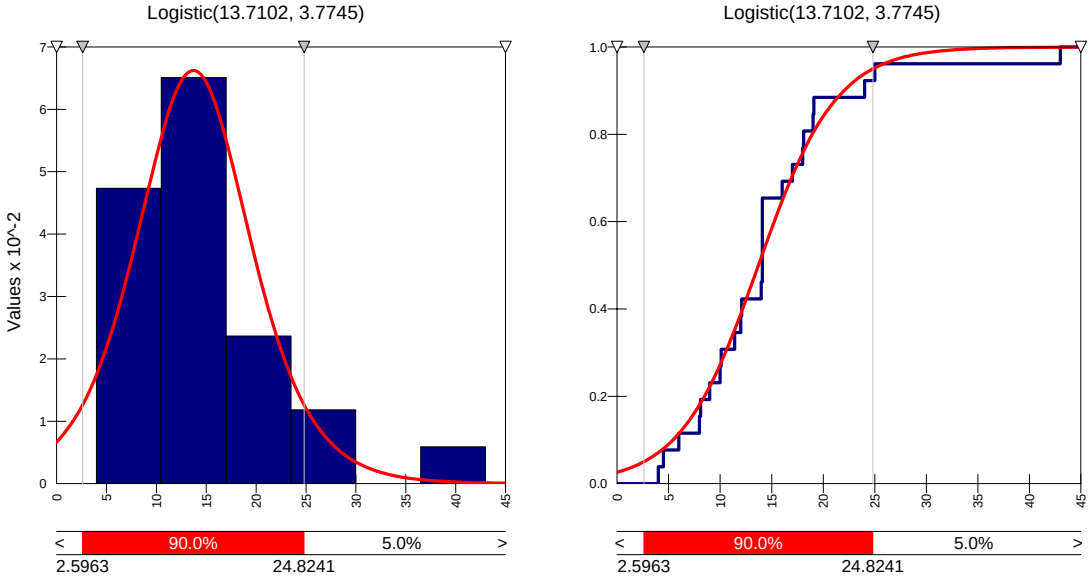

Figure D6 FOG length PDF and cumulative distribution for south mining (1991-2001)

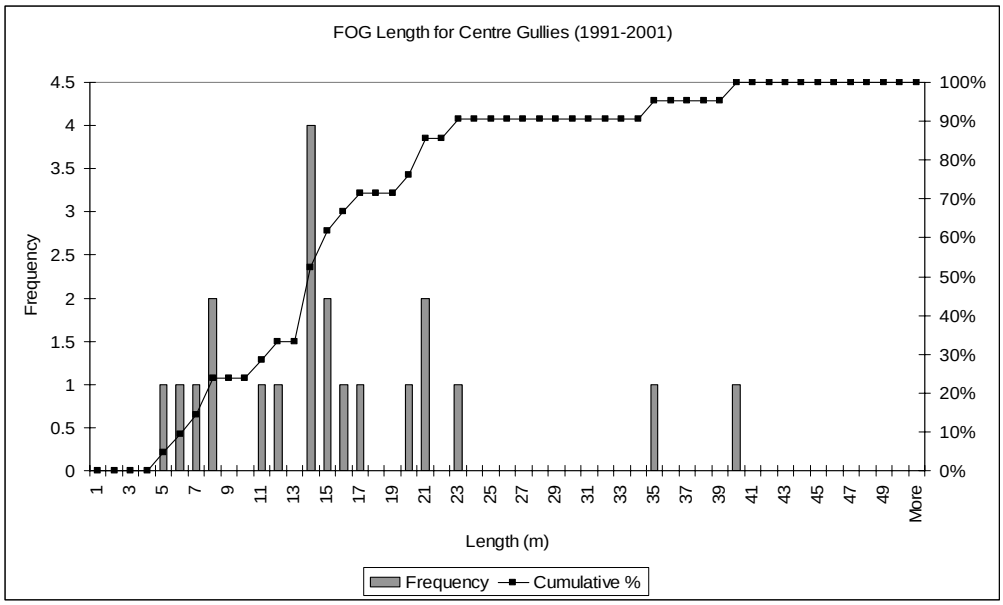

Figure D7 FOG length frequency and cumulative percentage for centre gullies (1991-2001)

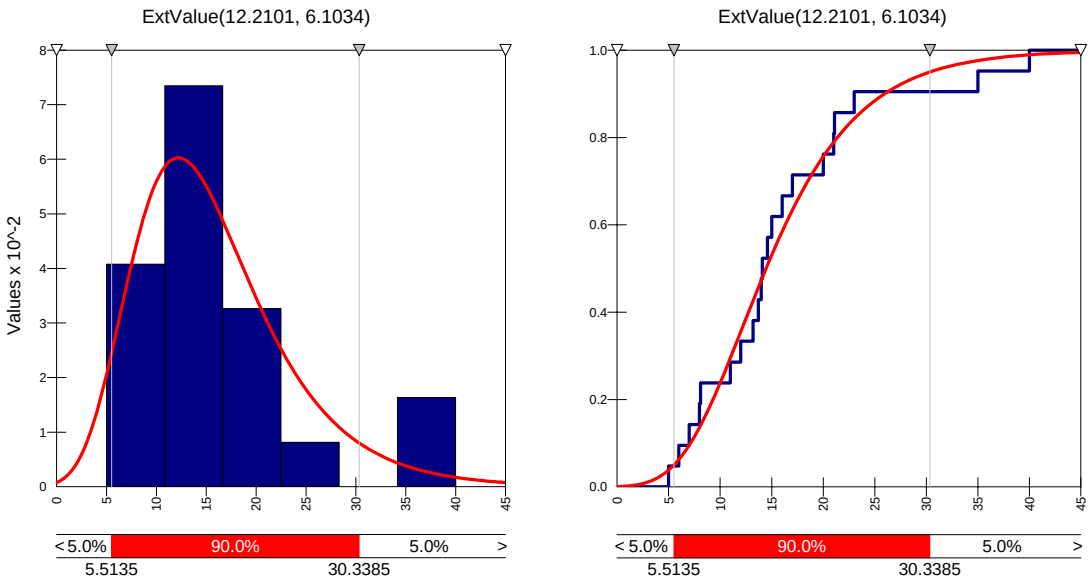

Figure D8 FOG length PDF and cumulative distribution for centre gullies (1991-2001)

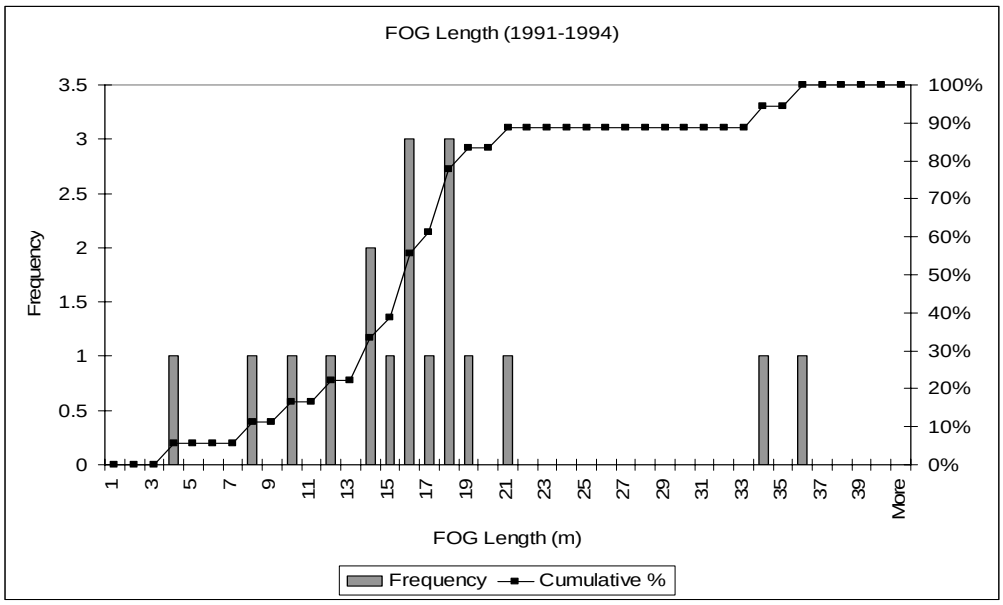

Figure D9 FOG length frequency and cumulative percentage (1991-1994)

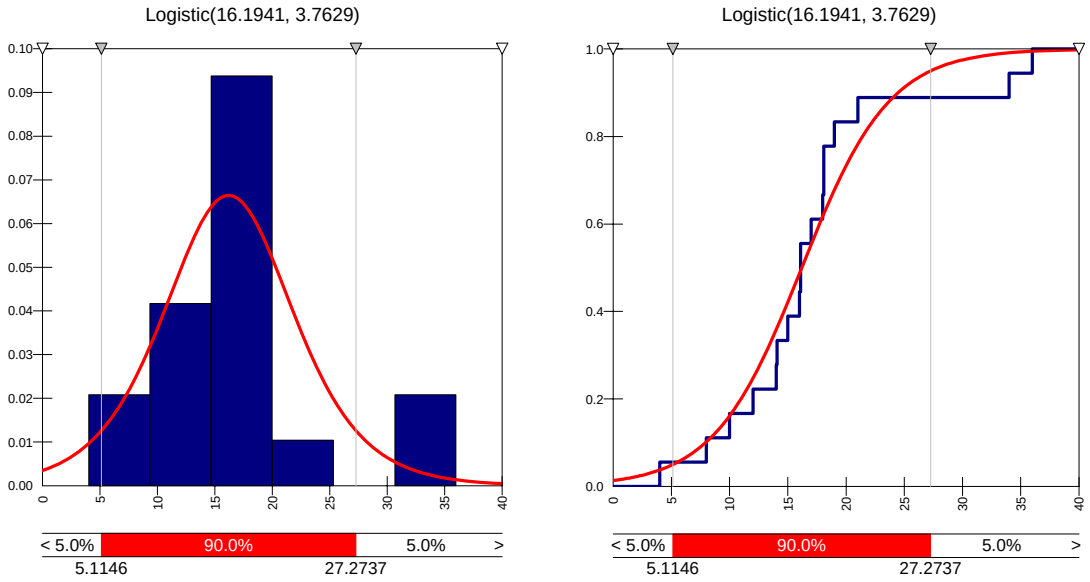

Figure D10 FOG length PDF and cumulative distribution (1991-1994)

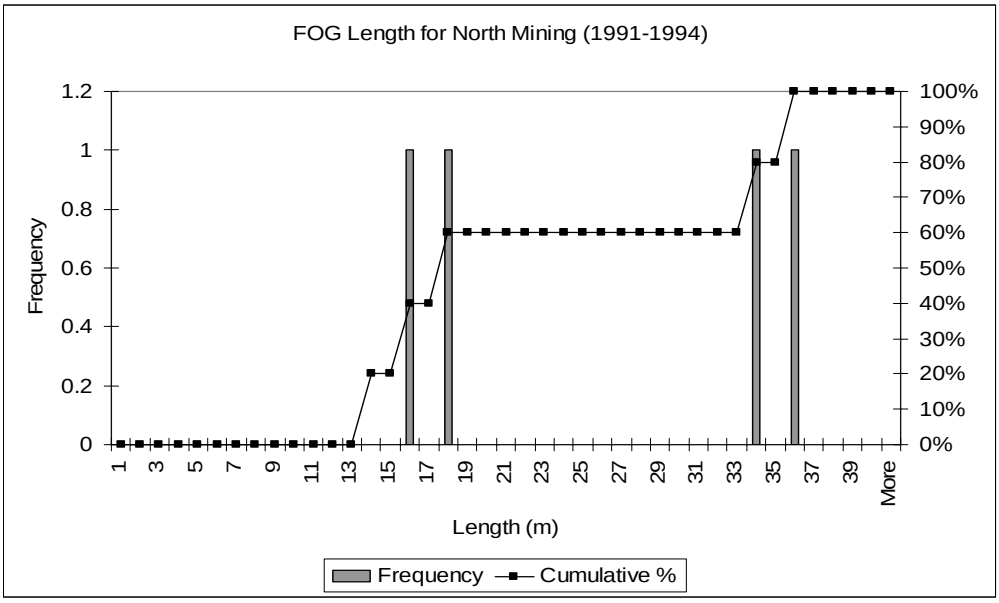

Figure D11 FOG length frequency and cumulative percentage for north mining (1991-1994)

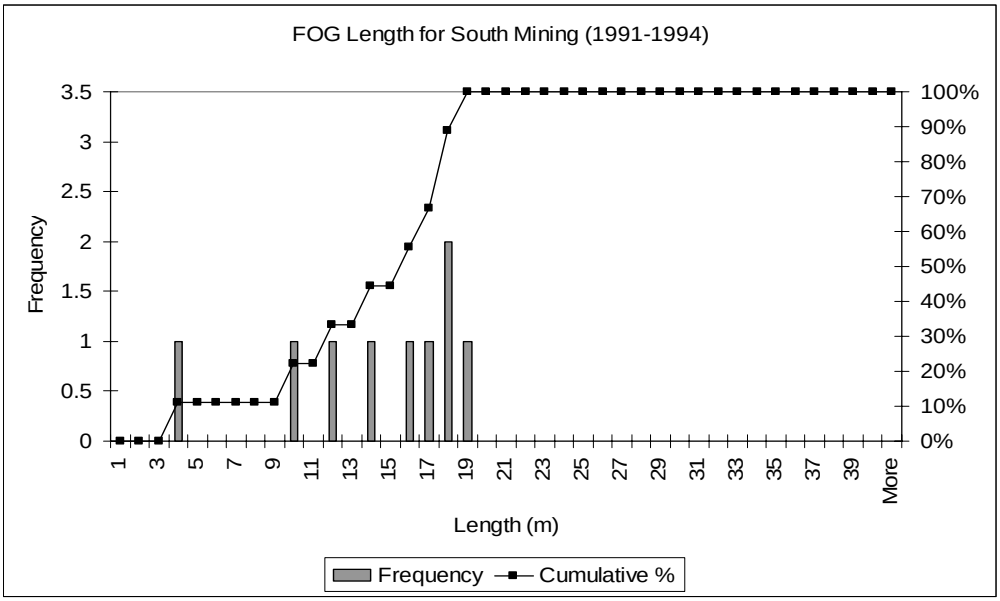

Figure D12 FOG length frequency and cumulative percentage for south mining (1991-1994)

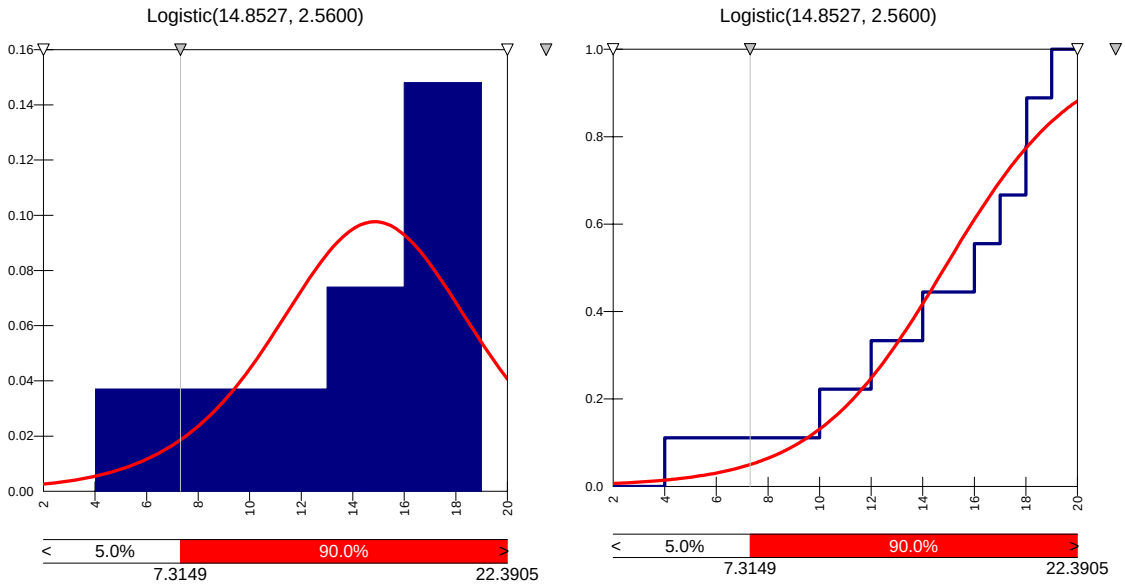

Figure D13 FOG length PDF and cumulative distribution for south mining (1991-1994)

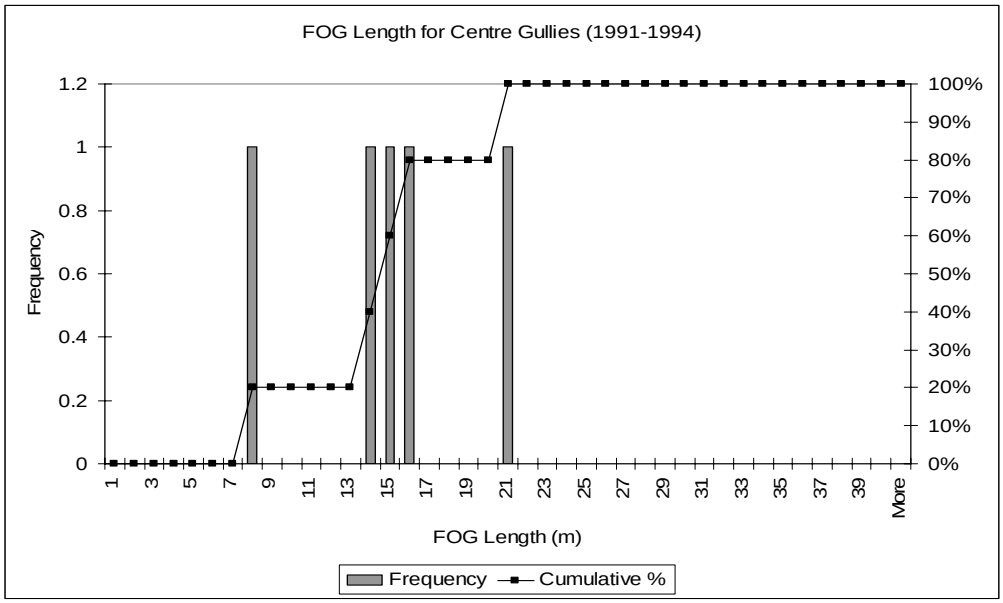

Figure D14 FOG length frequency and cumulative percentage for centre gullies (1991-1994)

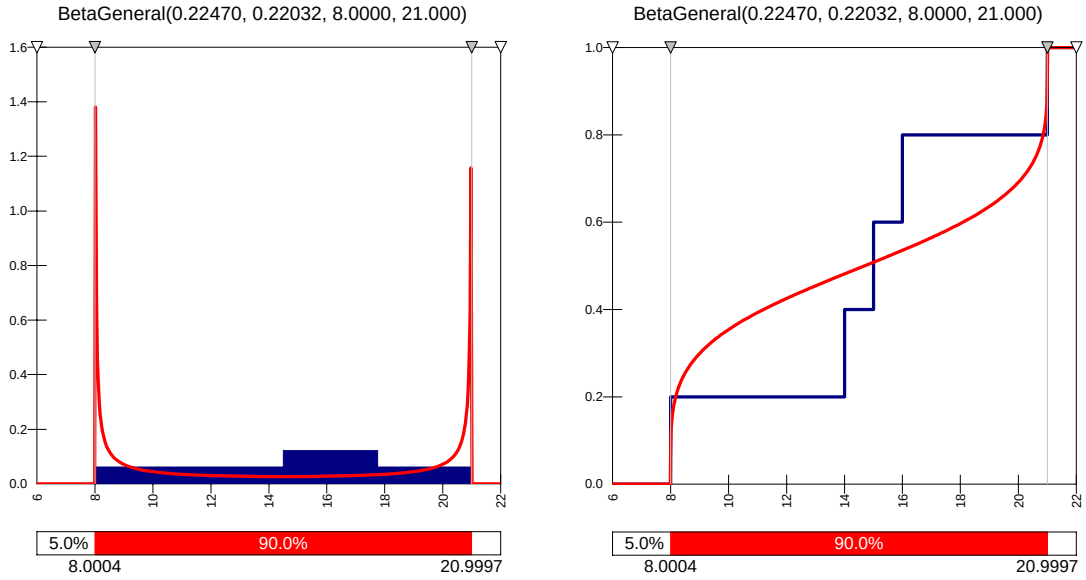

Figure D15 FOG length PDF and cumulative distribution for centre gullies (1991-1994)

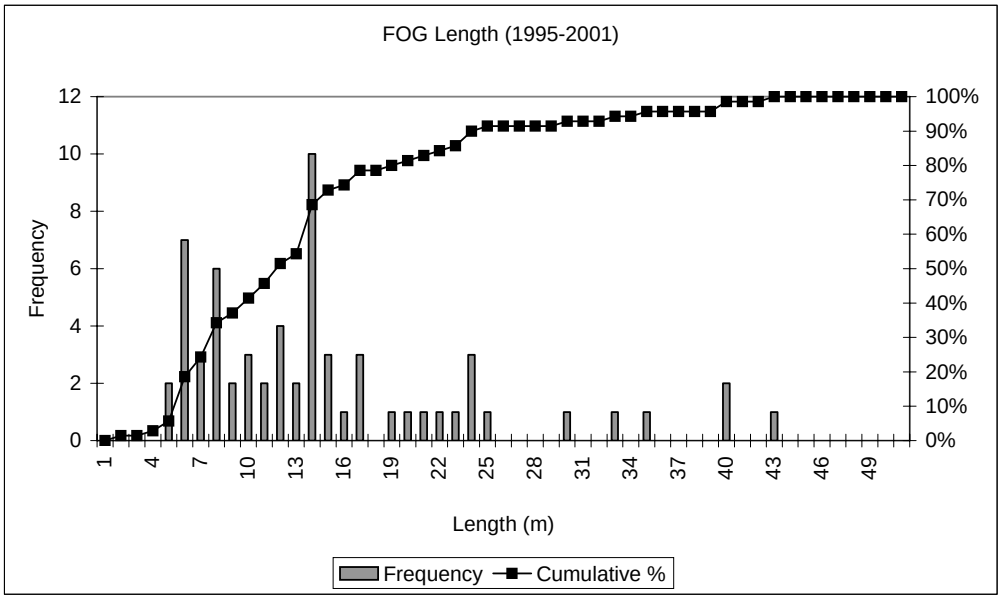

Figure D16 FOG length frequency and cumulative percentage (1995-2001)

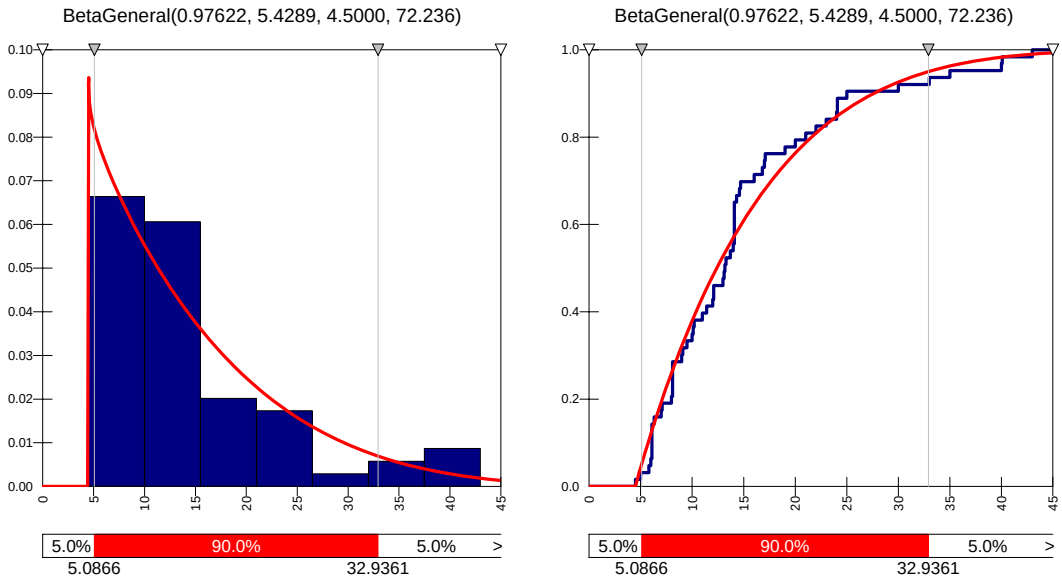

Figure D17 FOG length PDF and cumulative distribution (1995-2001)

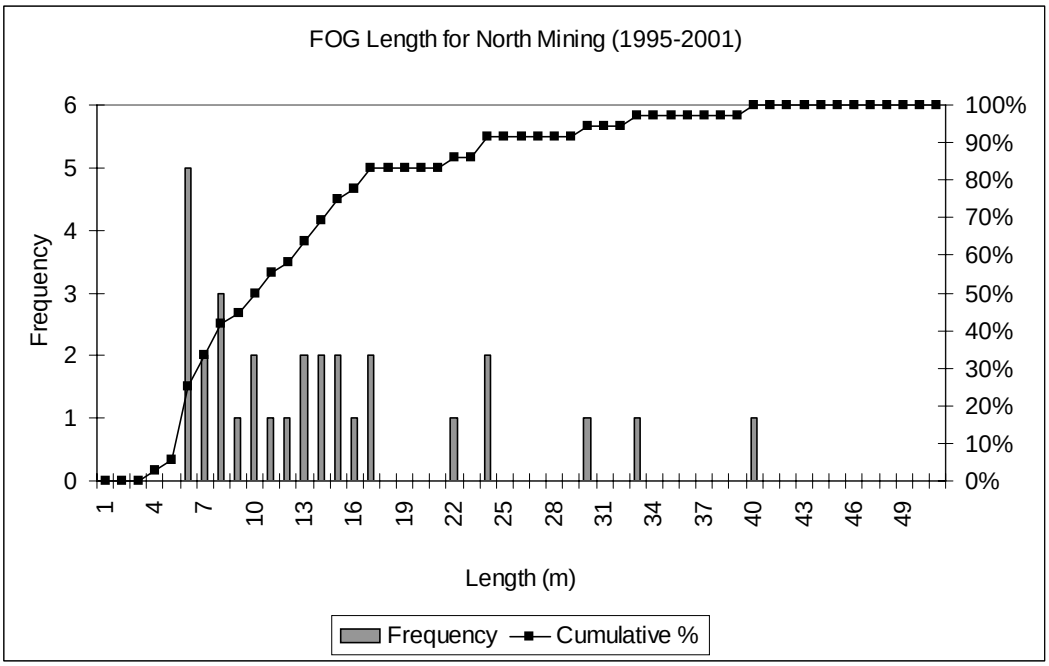

Figure D18 FOG length frequency and cumulative percentage for north mining (1995-2001)

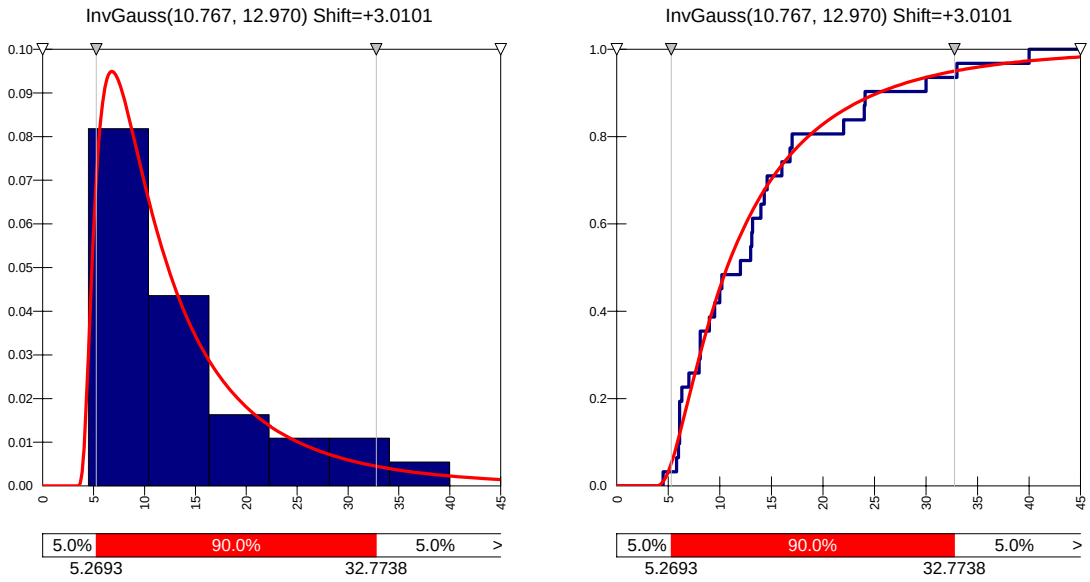

Figure D19 FOG length PDF and cumulative distribution for north mining (1995-2001)

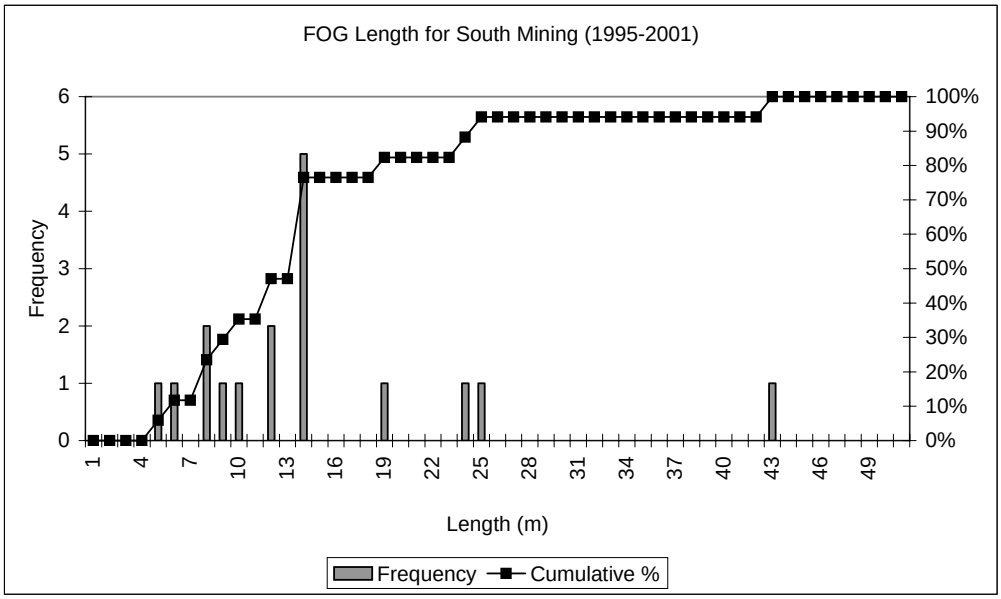

Figure D20 FOG length frequency and cumulative percentage for south mining (1995-2001)

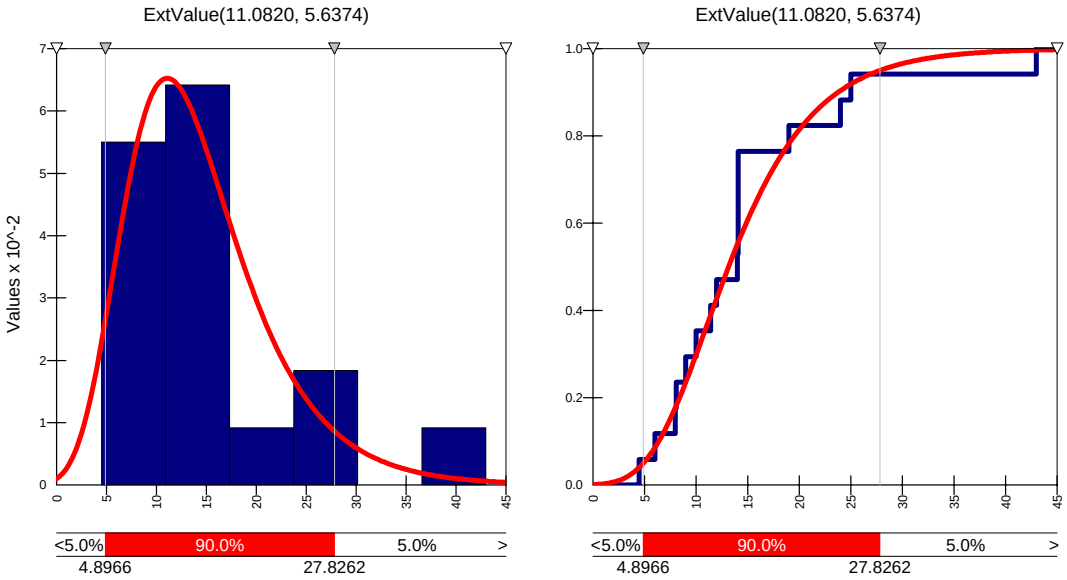

Figure D21 FOG length PDF and cumulative distribution for south mining (1995-2001)

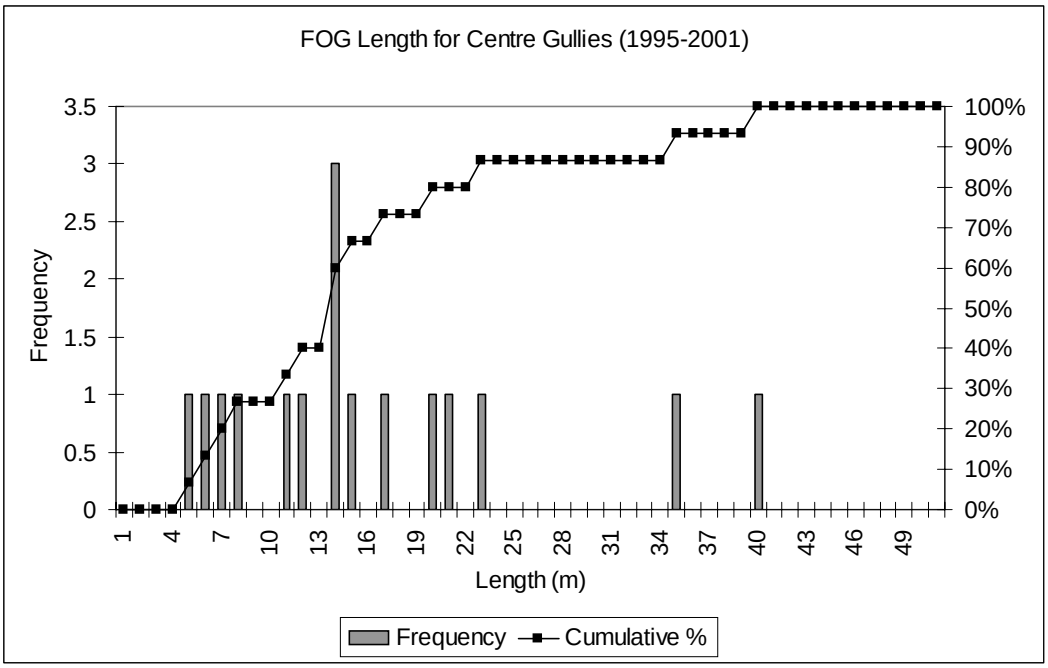

Figure D22 FOG length frequency and cumulative percentage for centre gullies (1995-2001)

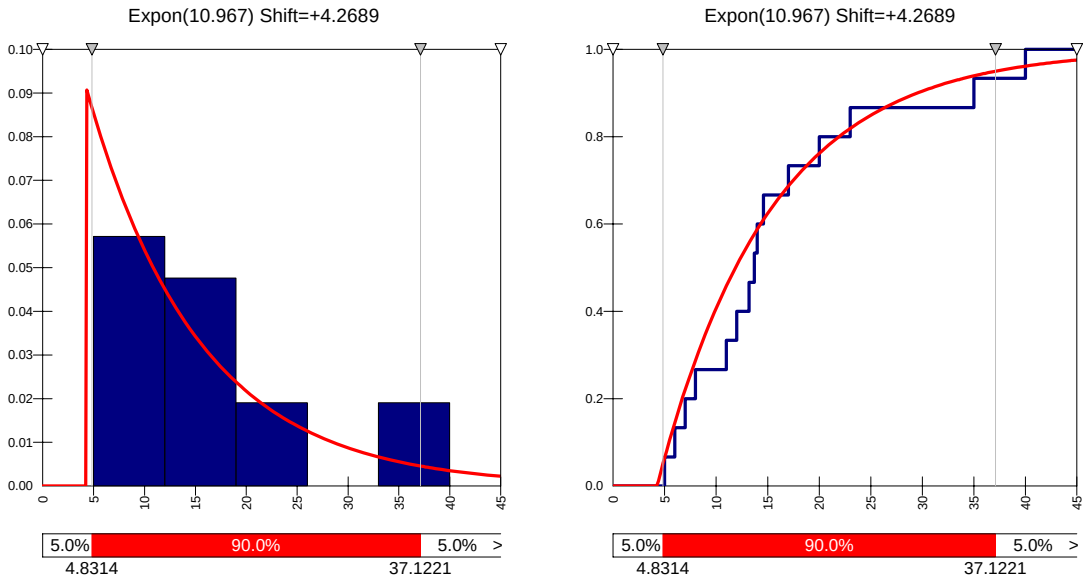

Figure D23 FOG length PDF and cumulative distribution for centre gullies (1995-2001)

APPENDIX E

FOG WIDTH (FIGURES E1-E23)

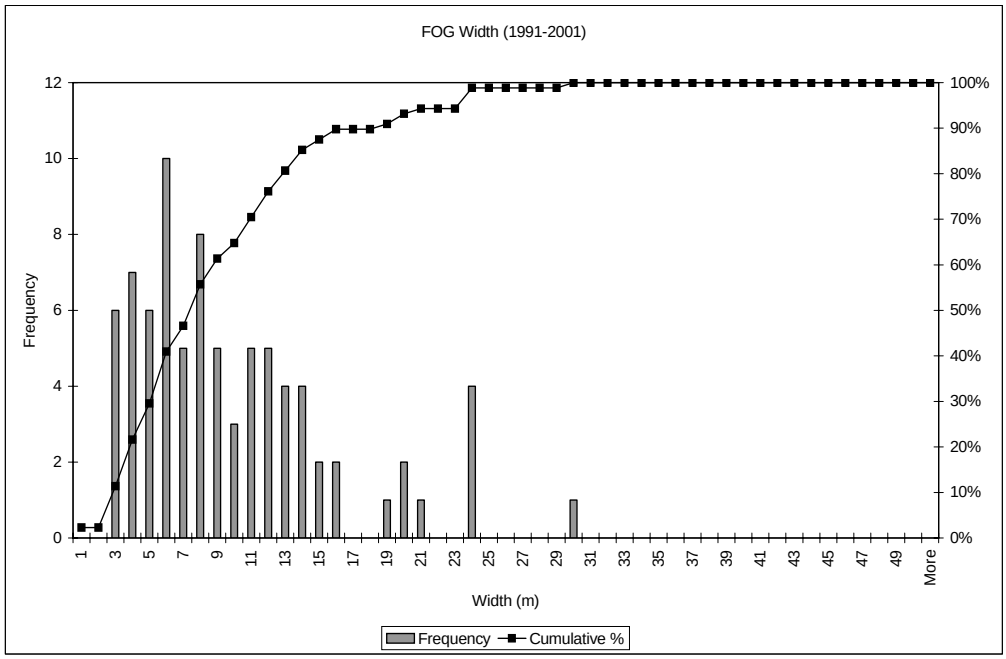

Figure E1 FOG width frequency and cumulative percentage (1991-2001)

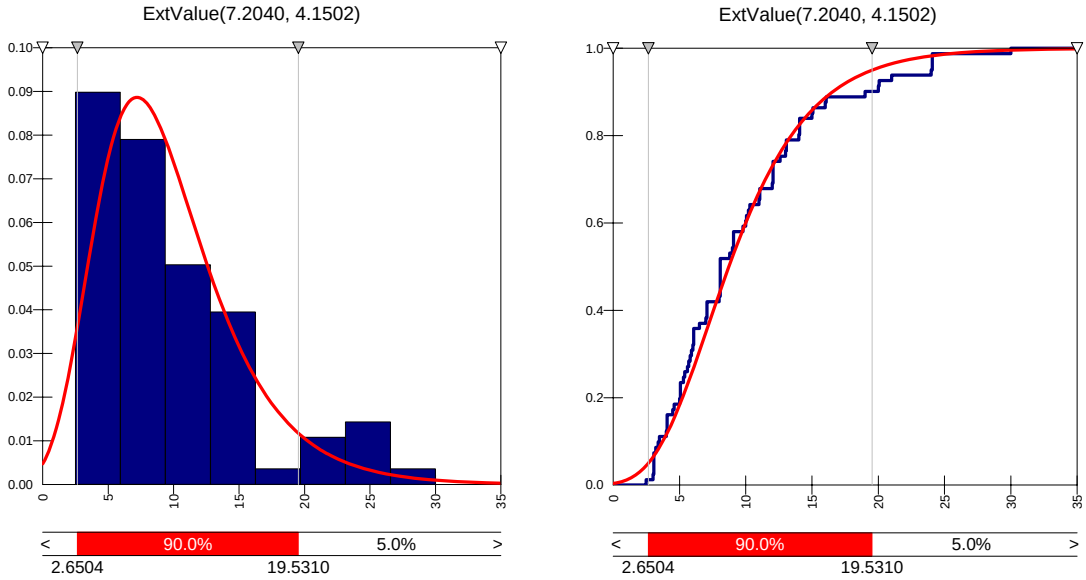

Figure E2 FOG width PDF and cumulative distribution (1991-2001)

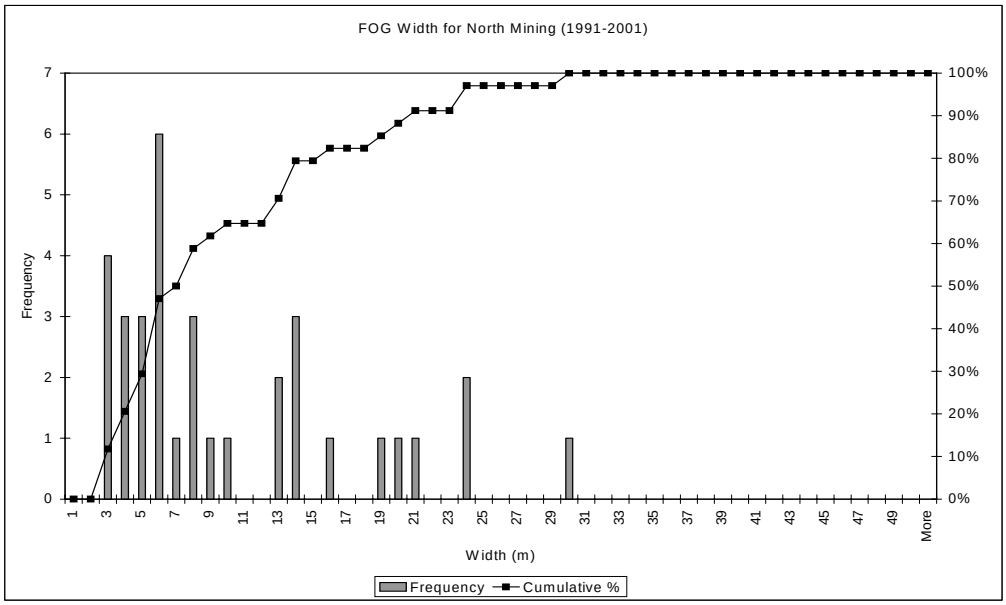

Figure E3 FOG width frequency and cumulative percentage for north mining (1991-2001)

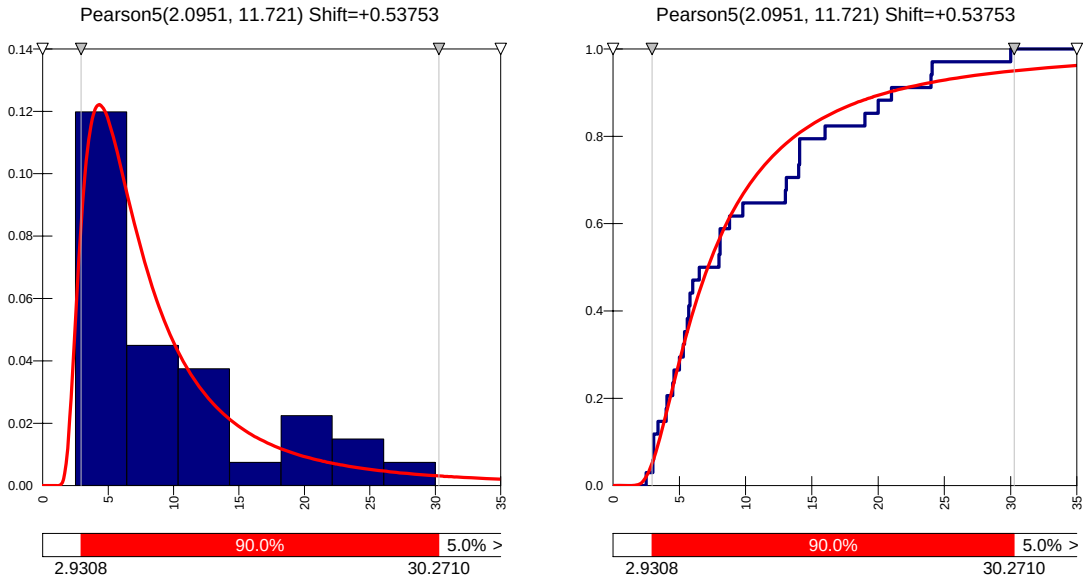

Figure E4 FOG width PDF and cumulative distribution for north mining (1991-2001)

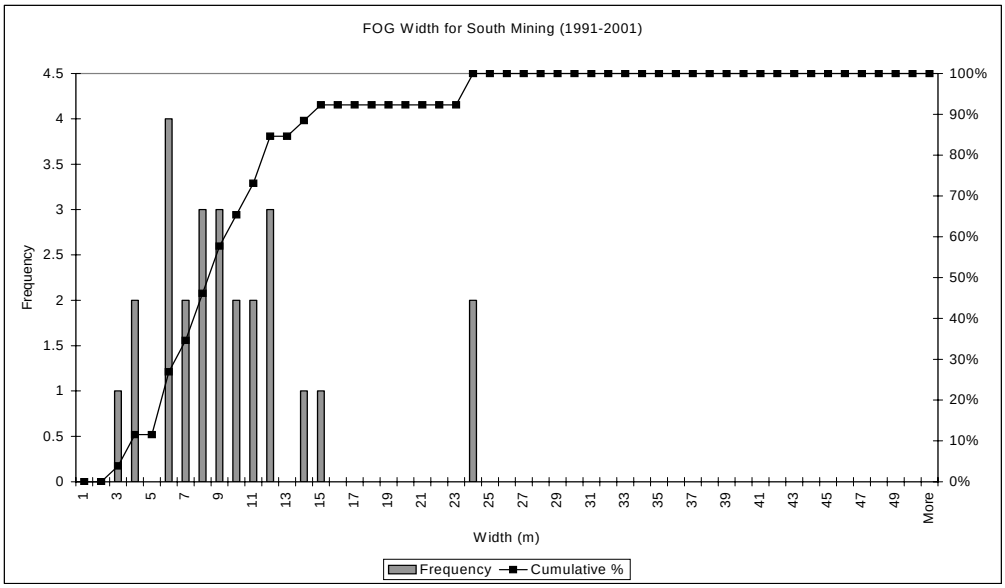

Figure E5 FOG width frequency and cumulative percentage for south mining (1991-2001)

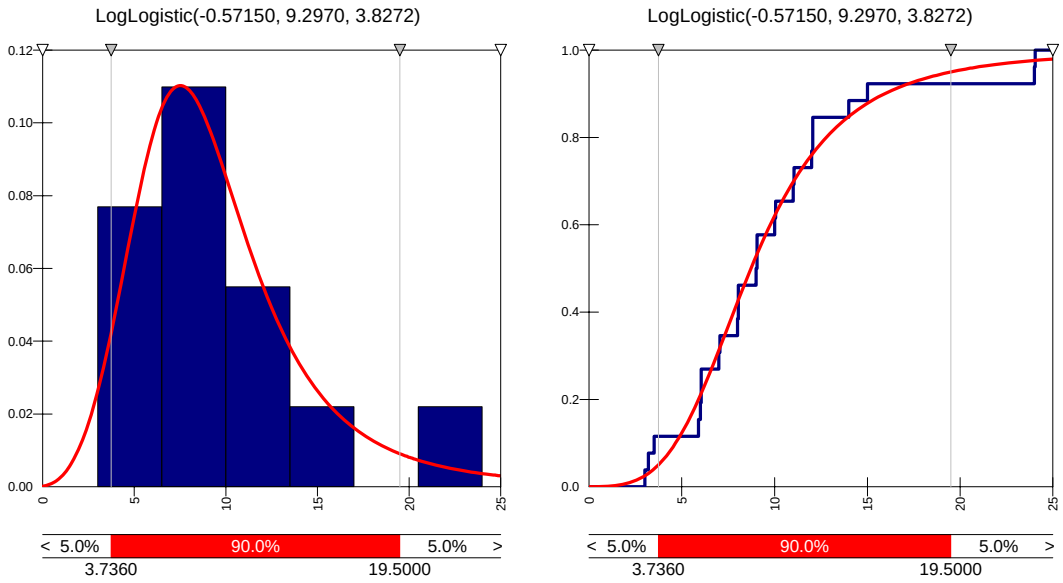

Figure E6 FOG width PDF and cumulative distribution for south mining (1991-2001)

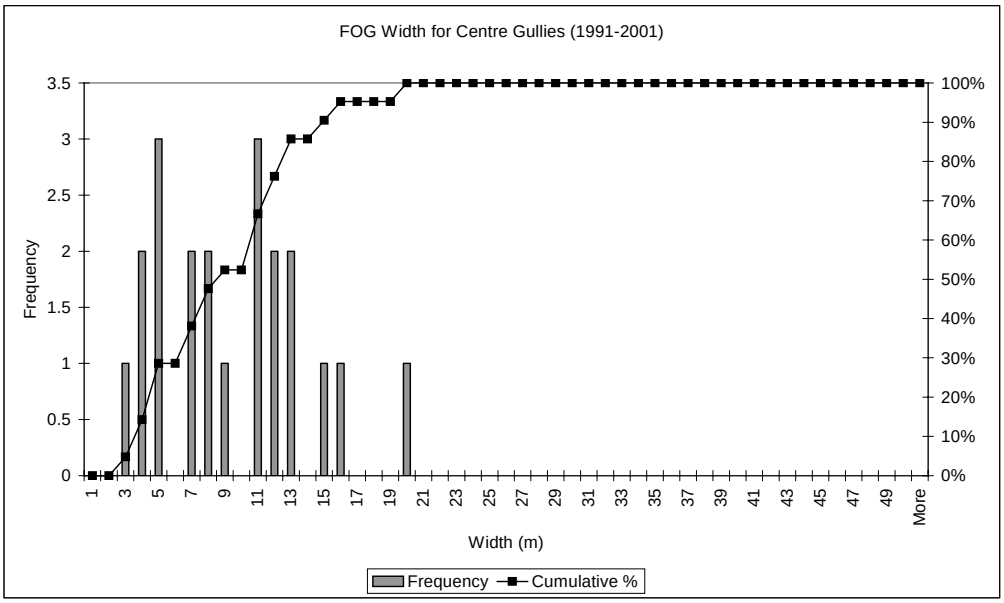

Figure E7 FOG width frequency and cumulative percentage for centre gullies (1991-2001)

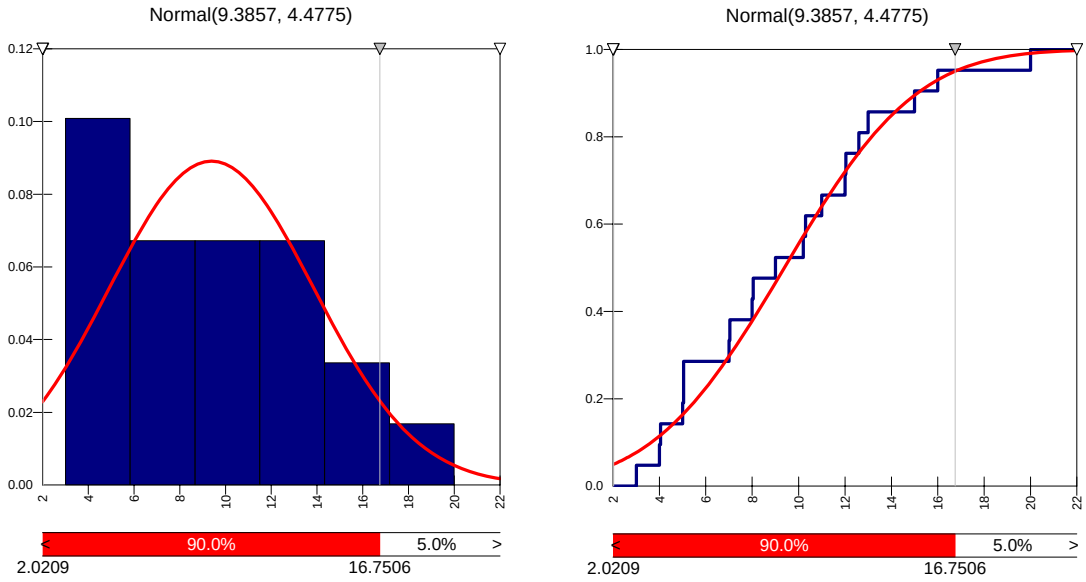

Figure E8 FOG width PDF and cumulative distribution for centre gullies (1991-2001)

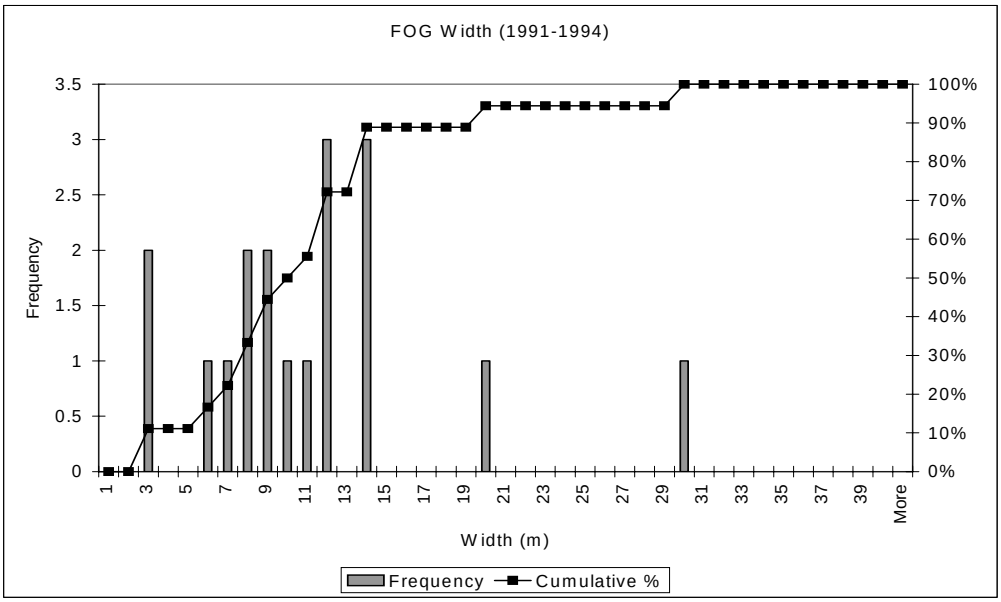

Figure E9 FOG width frequency and cumulative percentage (1991-1994)

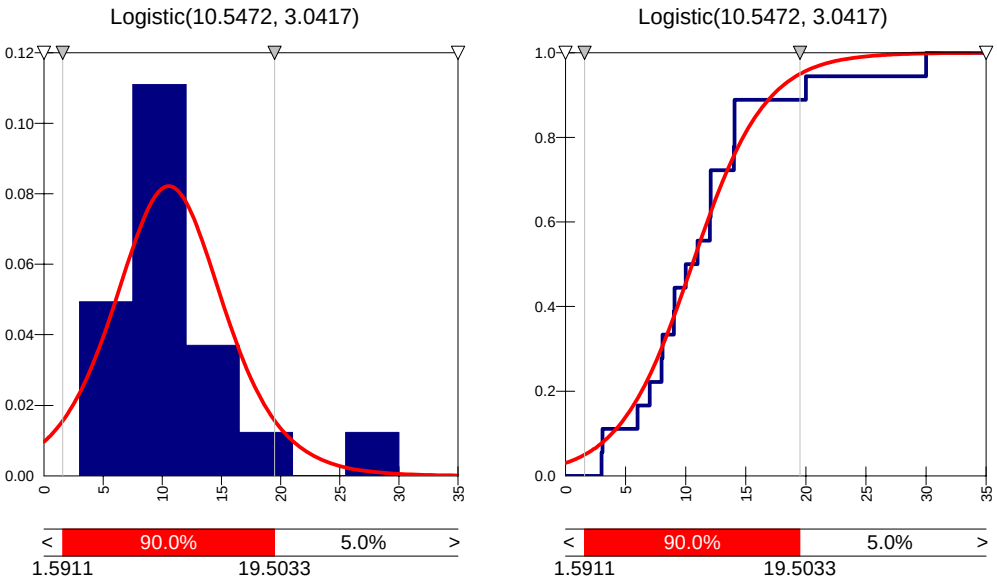

Figure E10 FOG width PDF and cumulative distribution (1991-1994)

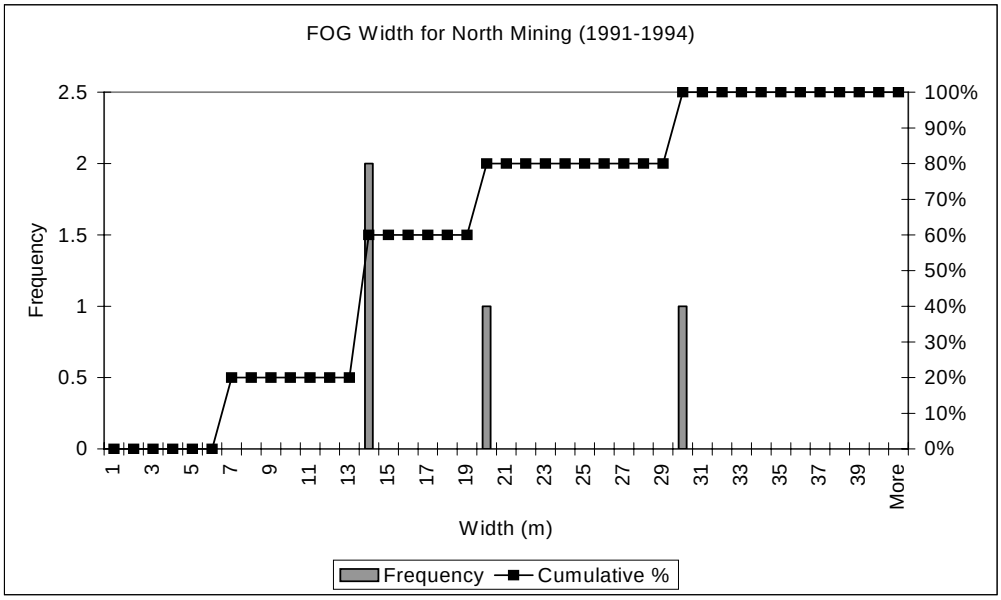

Figure E11 FOG width frequency and cumulative percentage for north mining (1991-1994)

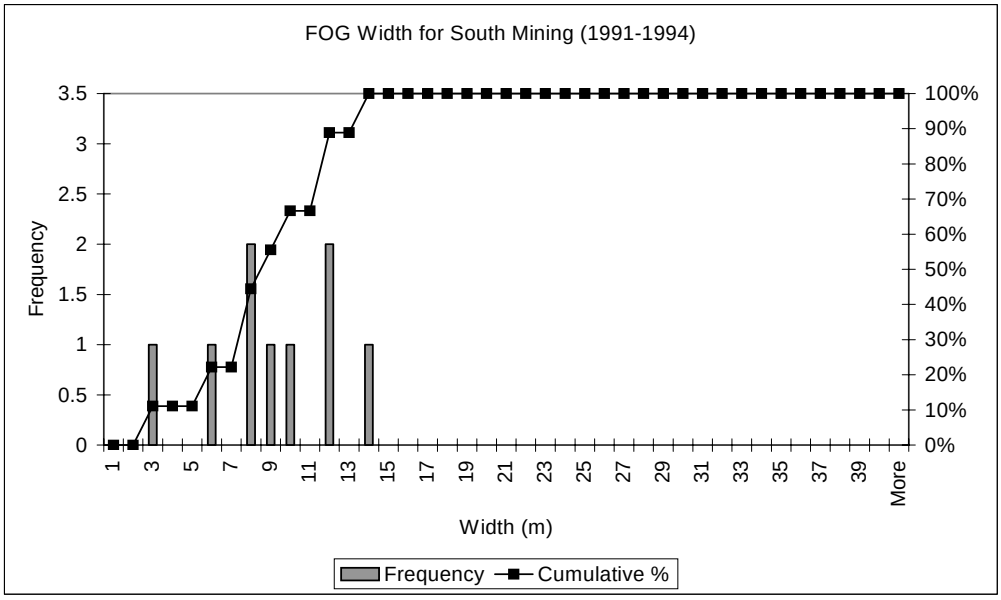

Figure E12 FOG width frequency and cumulative percentage for south mining (1991-1994)

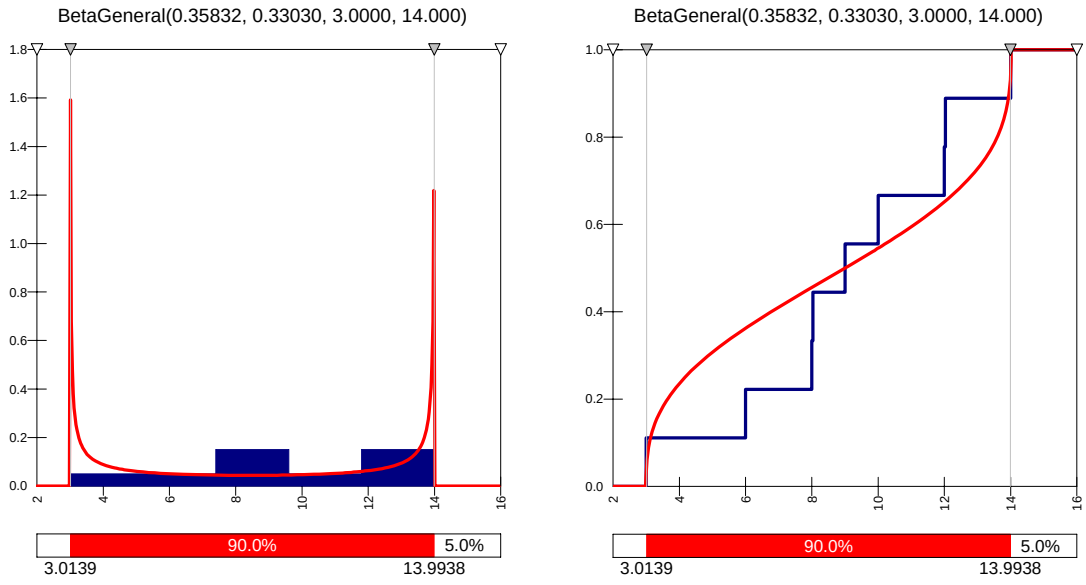

Figure E13 FOG width PDF and cumulative distribution for south mining (1991-1994)

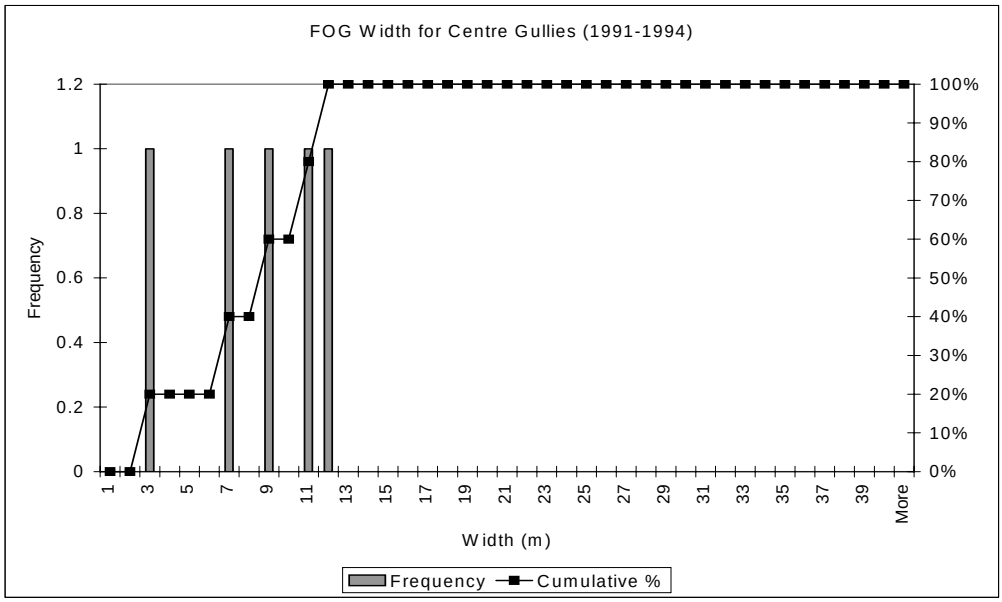

Figure E14 FOG width frequency and cumulative percentage for centre gullies (1991-1994)

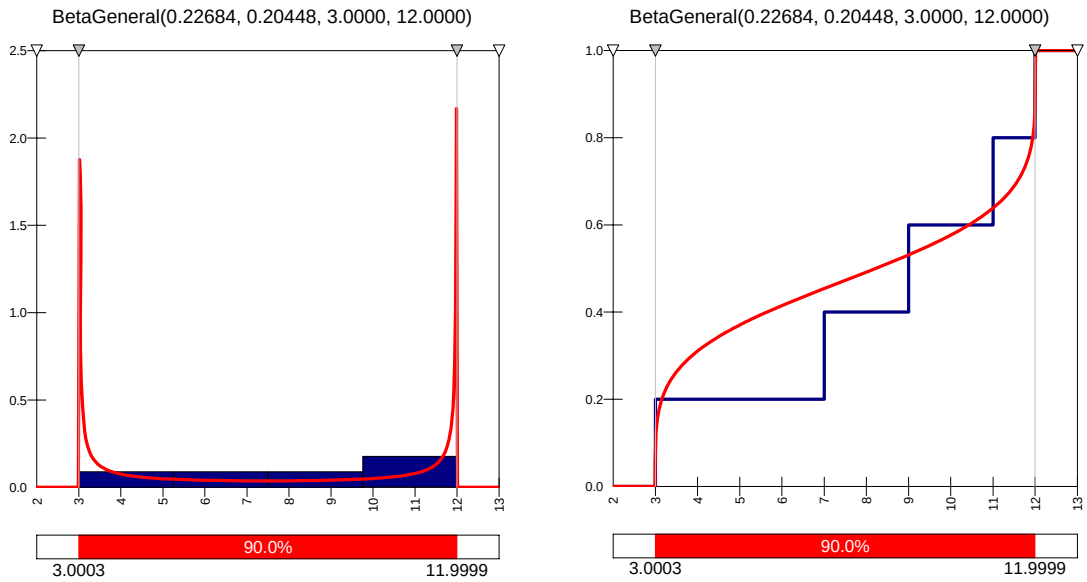

Figure E15 FOG width PDF and cumulative distribution for centre gullies (1991-1994)

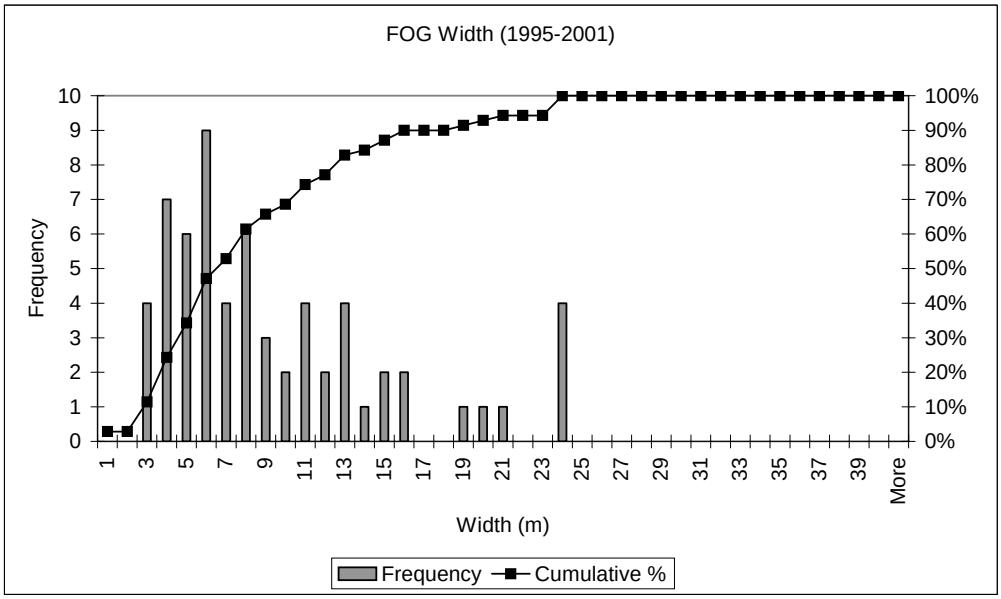

Figure E16 FOG width frequency and cumulative percentage (1995-2001)

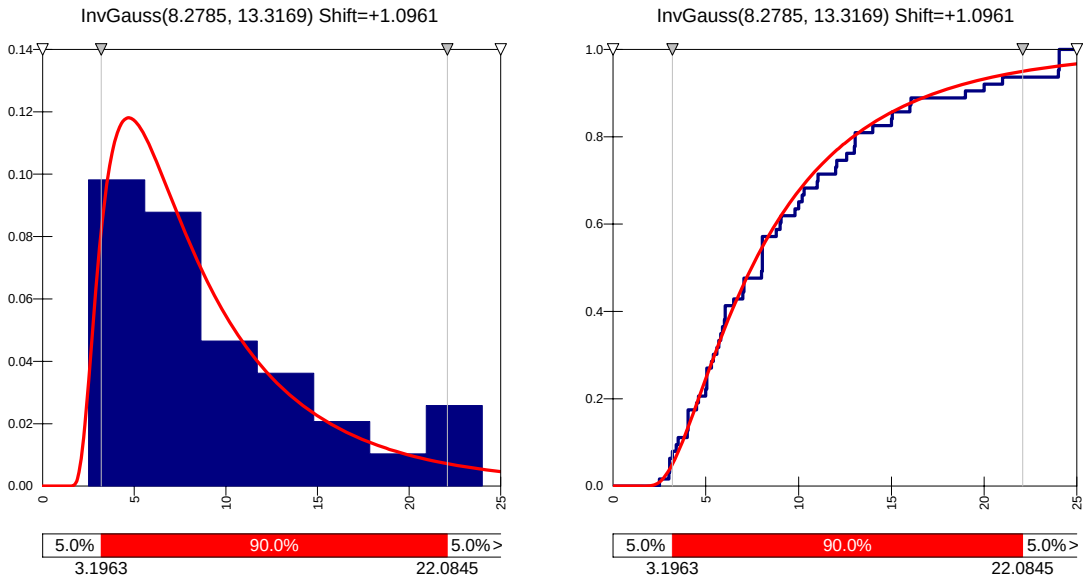

Figure E17 FOG width PDF and cumulative distribution (1995-2001)

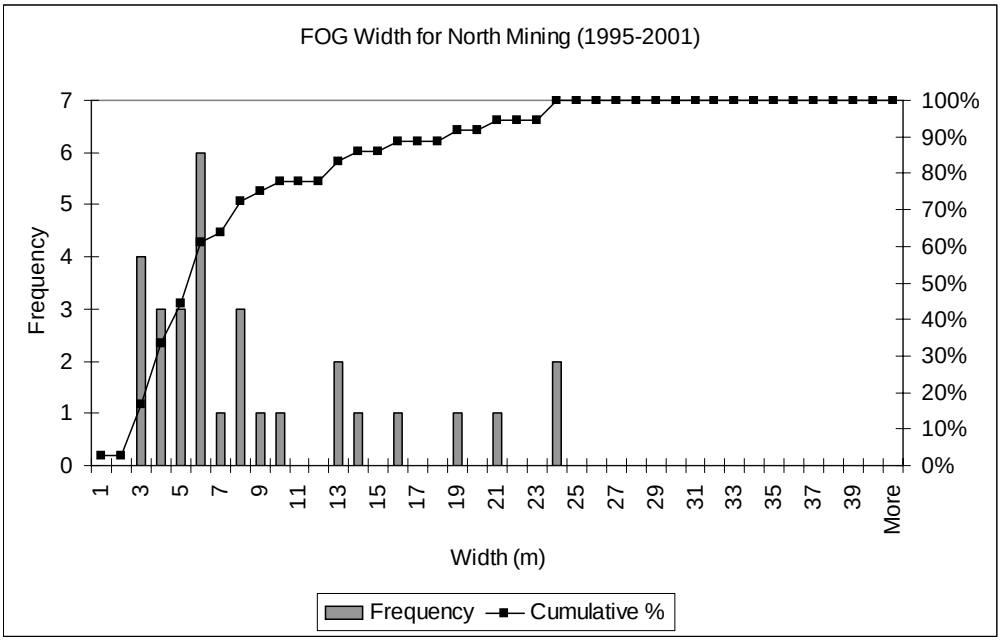

Figure E18 FOG width frequency and cumulative percentage for north mining (1995-2001)

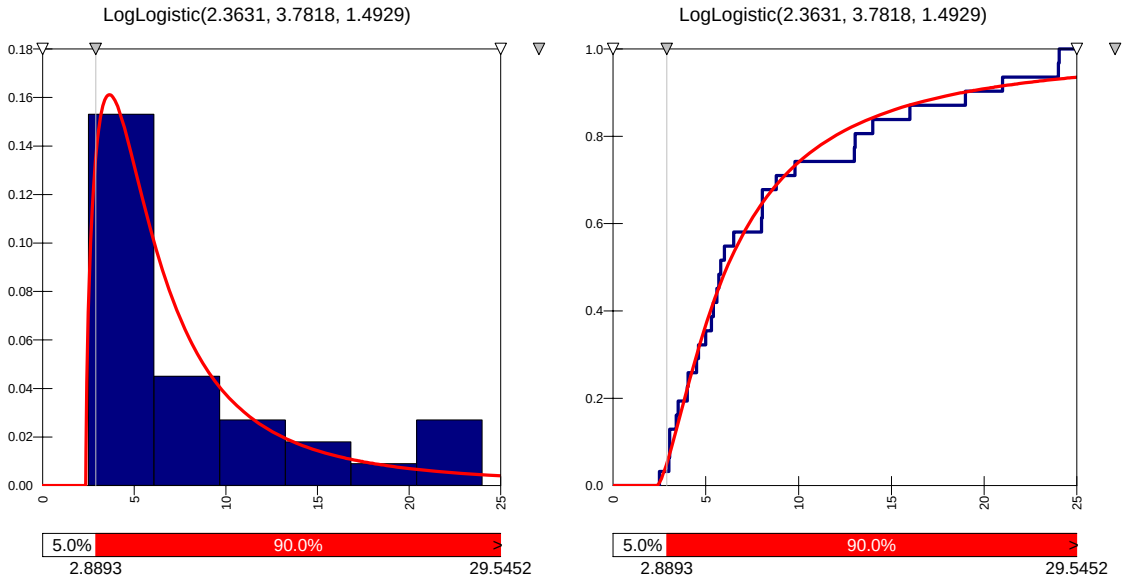

Figure E19 FOG width PDF and cumulative distribution for north mining (1995-2001)

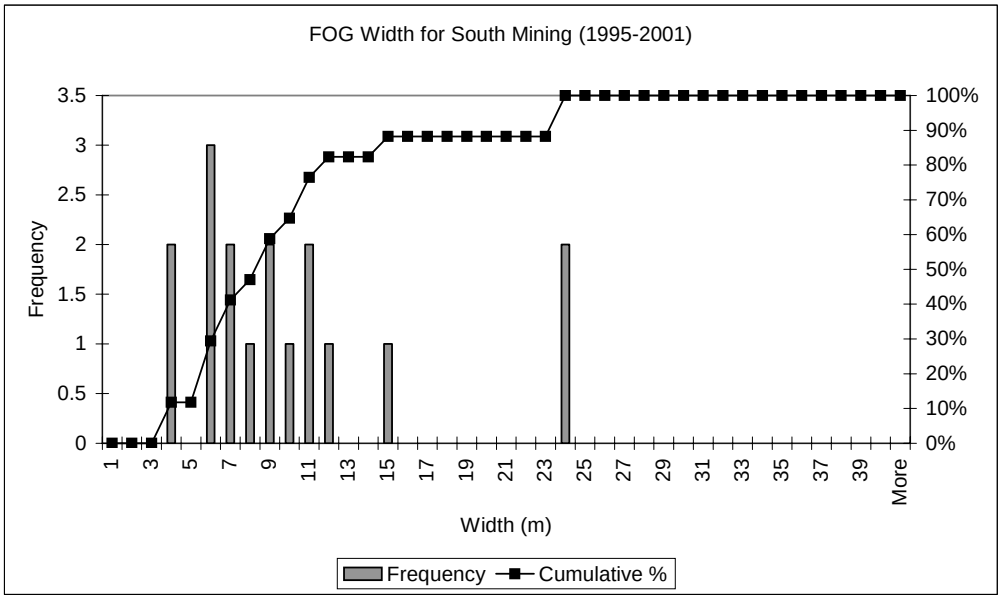

Figure E20 FOG width frequency and cumulative percentage for south mining (1995-2001)

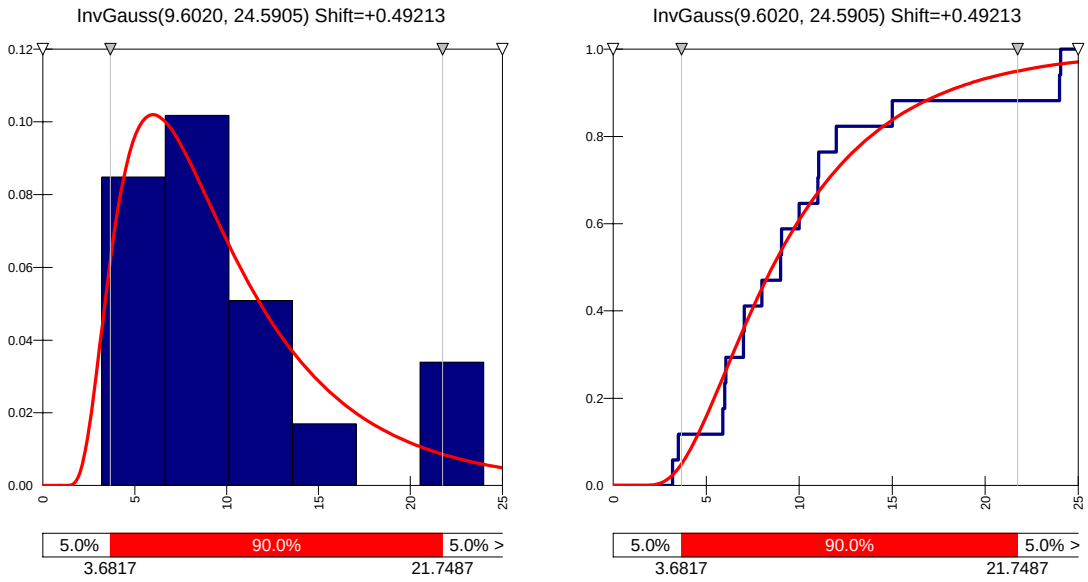

Figure E21 FOG width PDF and cumulative distribution for south mining (1995-2001)

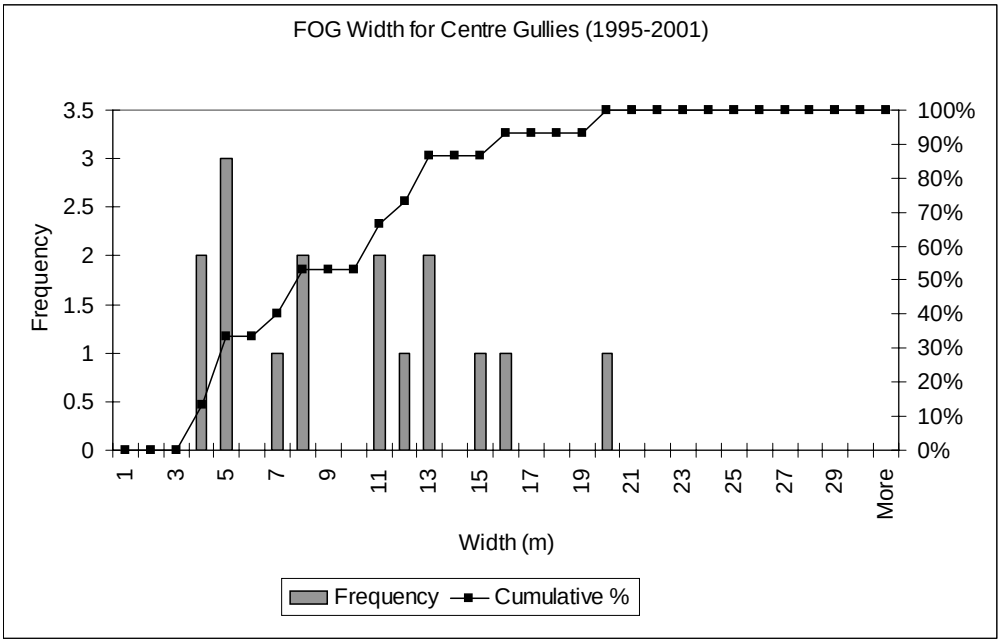

Figure E22 FOG width frequency and cumulative percentage for centre gullies (1995-2001)

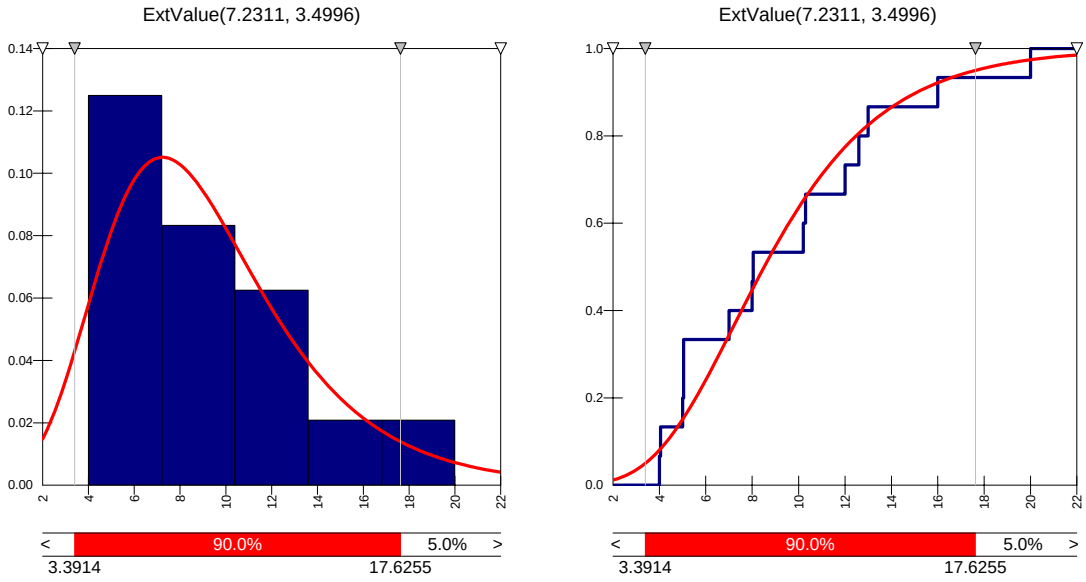

Figure E23 FOG width PDF and cumulative distribution for centre gullies (1995-2001)

APPENDIX F

FOG DIMENSION (FIGURES F1-F23)

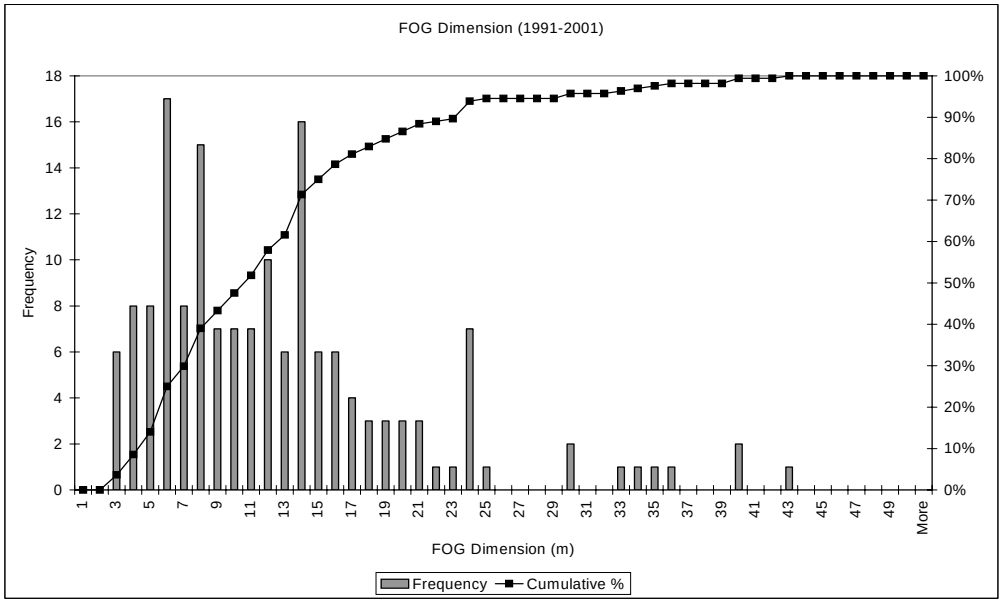

Figure F1 FOG Dimension frequency and cumulative percentage (1991-2001)

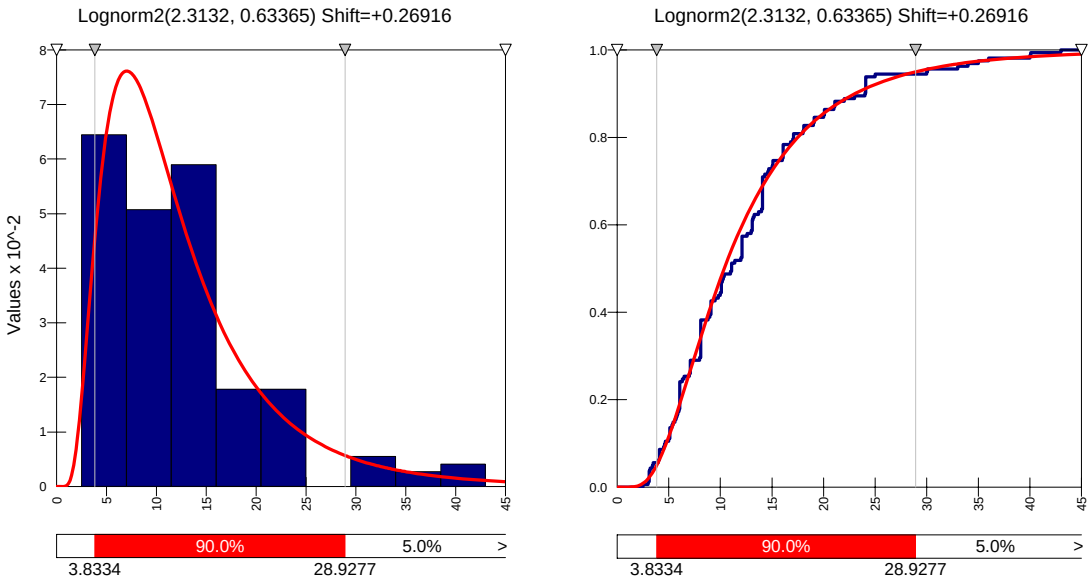

Figure F2 FOG Dimension PDF and cumulative distribution (1991-2001)

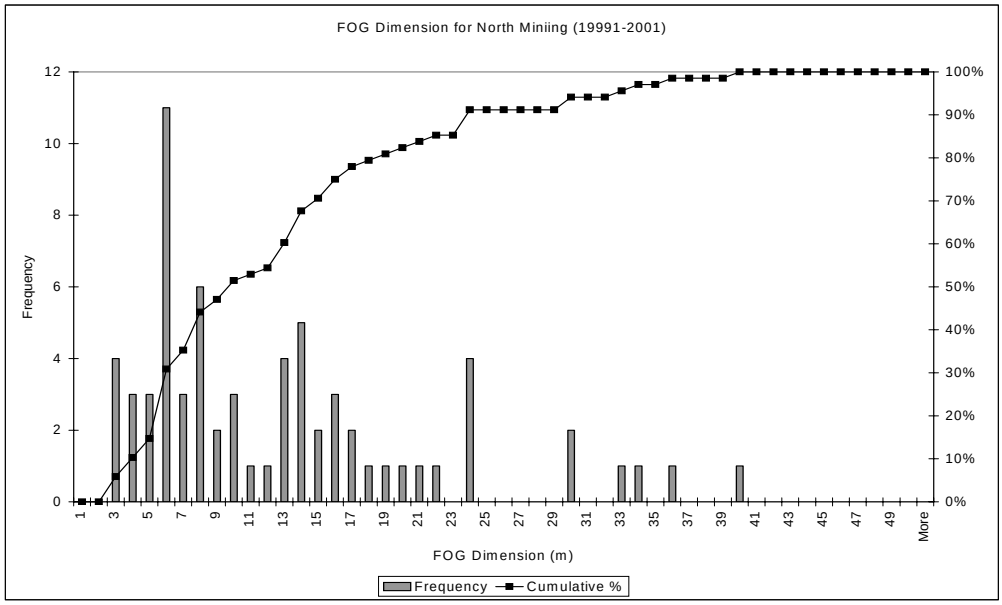

Figure F3 FOG Dimension frequency and cumulative percentage for north mining (1991-2001)

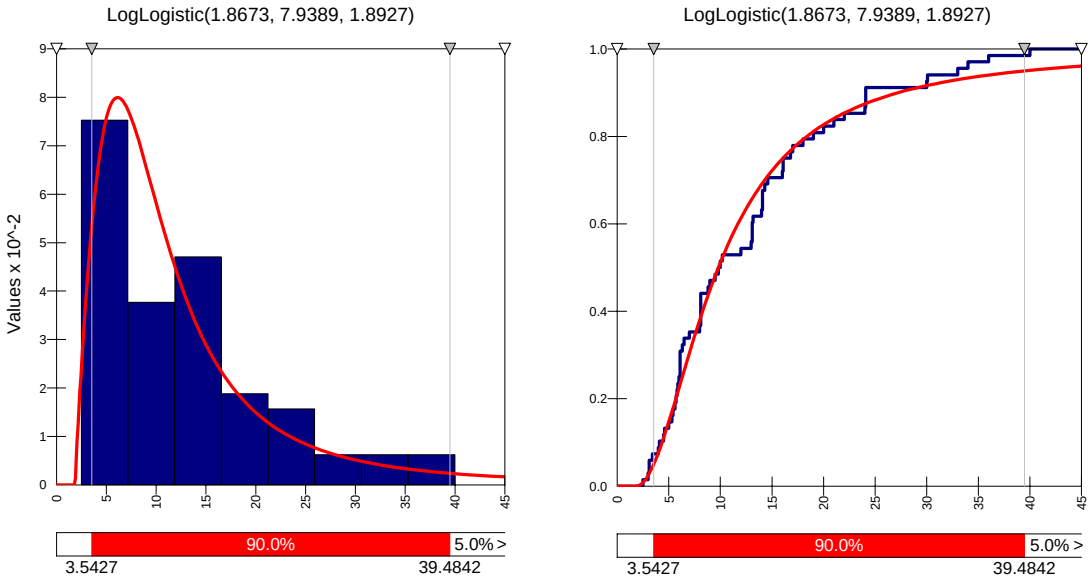

Figure F4 FOG Dimension PDF and cumulative distribution for north mining (1991-2001)

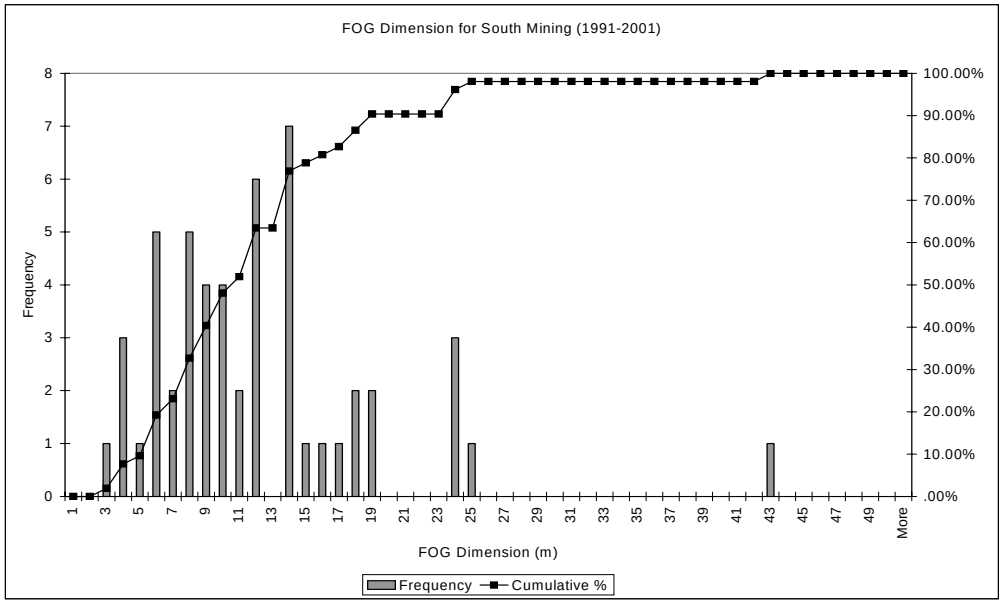

Figure F5 FOG Dimension frequency and cumulative percentage for south mining (1991-2001)

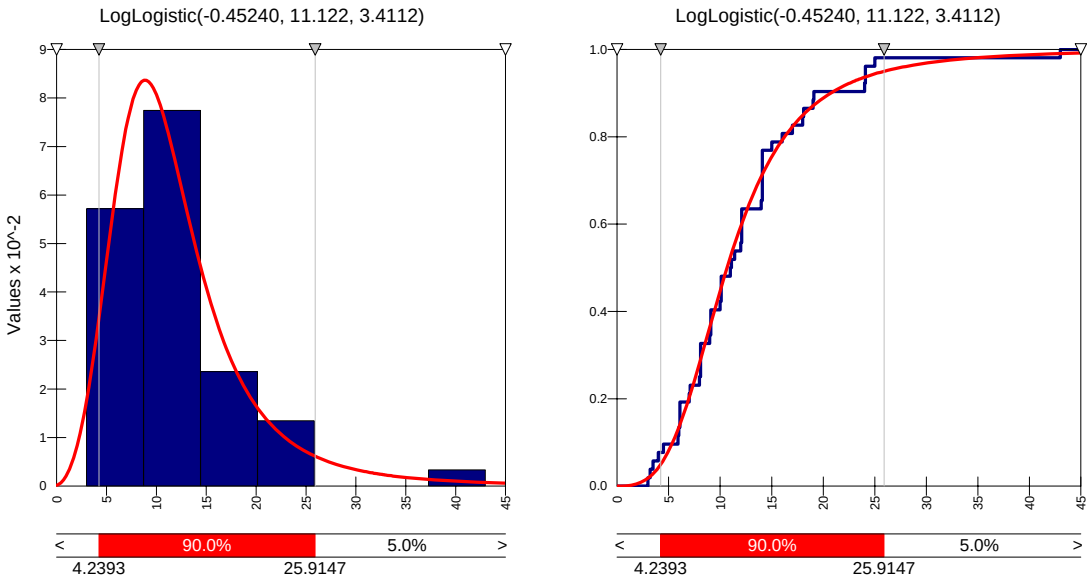

Figure F6 FOG Dimension PDF and cumulative distribution for south mining (1991-2001)

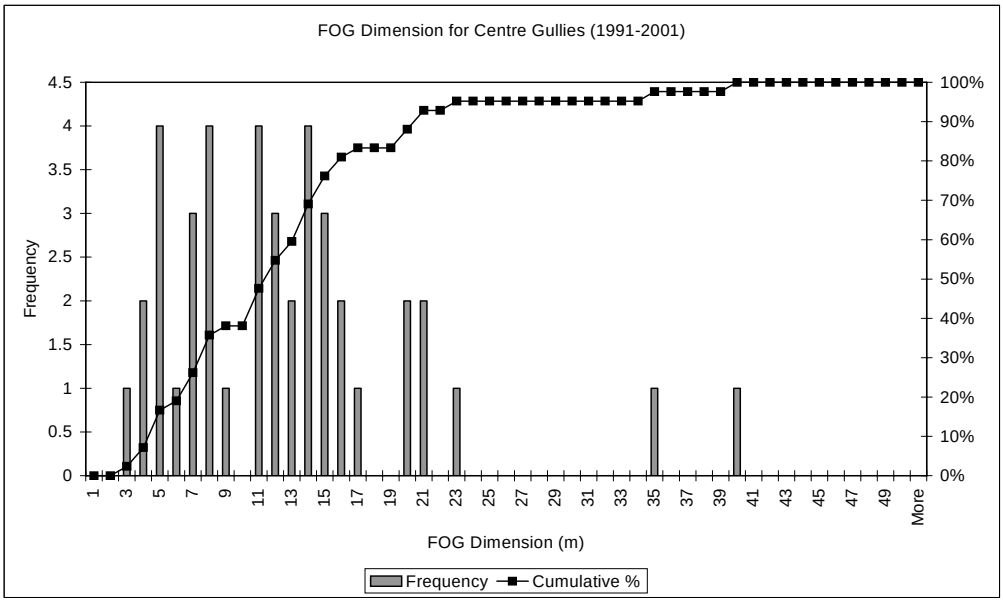

Figure F7 FOG Dimension frequency and cumulative percentage for centre gullies (1991-2001)

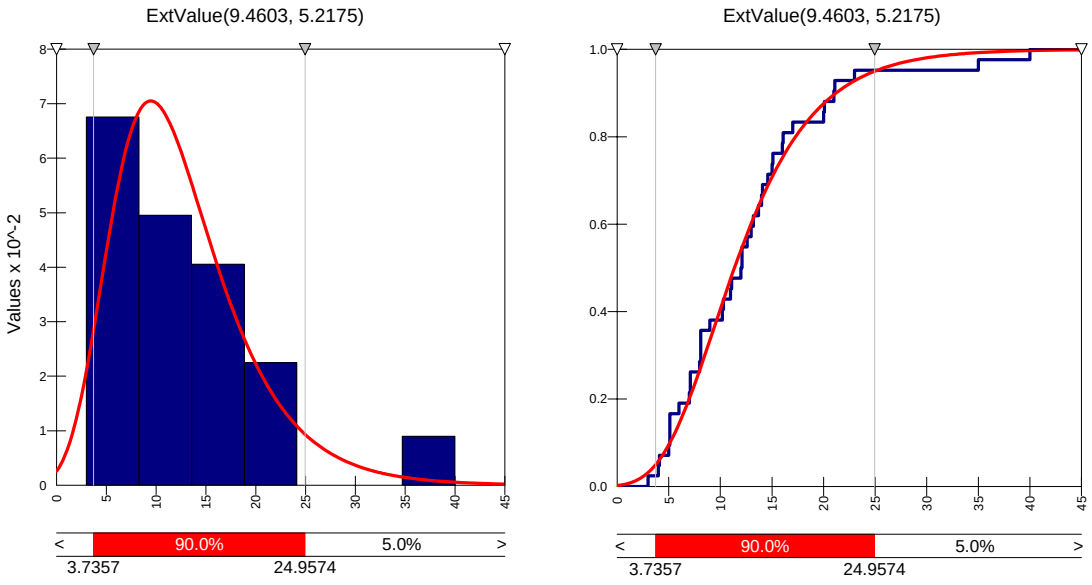

Figure F8 FOG Dimension PDF and cumulative distribution for centre gullies (1991-2001)

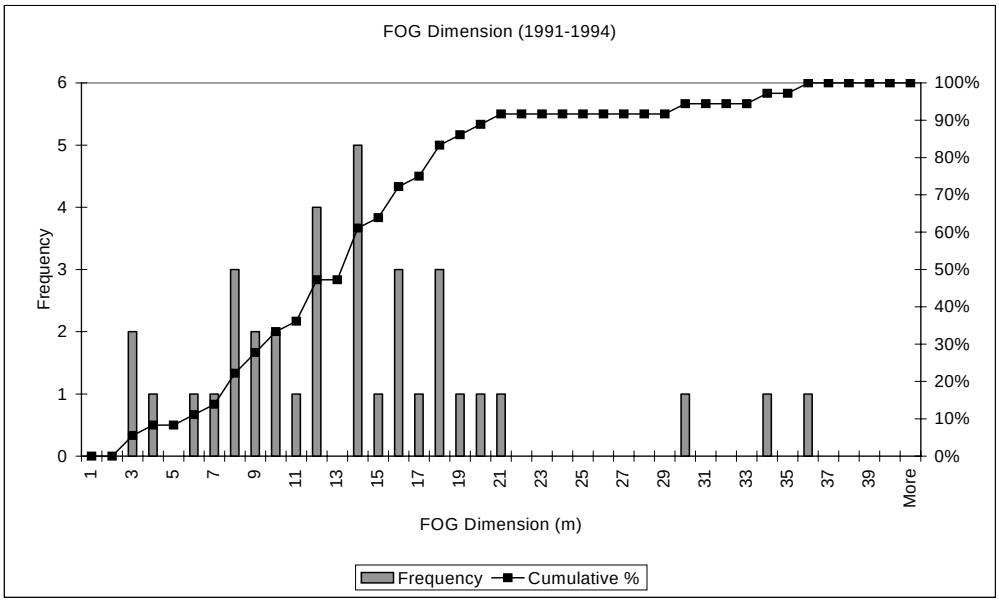

Figure F9 FOG Dimension frequency and cumulative percentage (1991-1994)

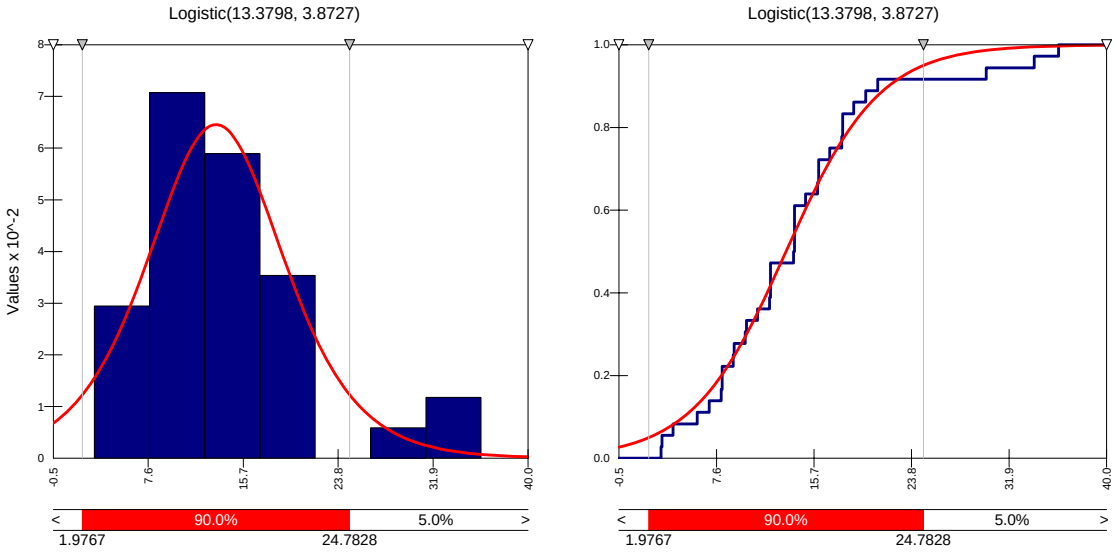

Figure F10 FOG Dimension PDF and cumulative distribution (1991-1994)

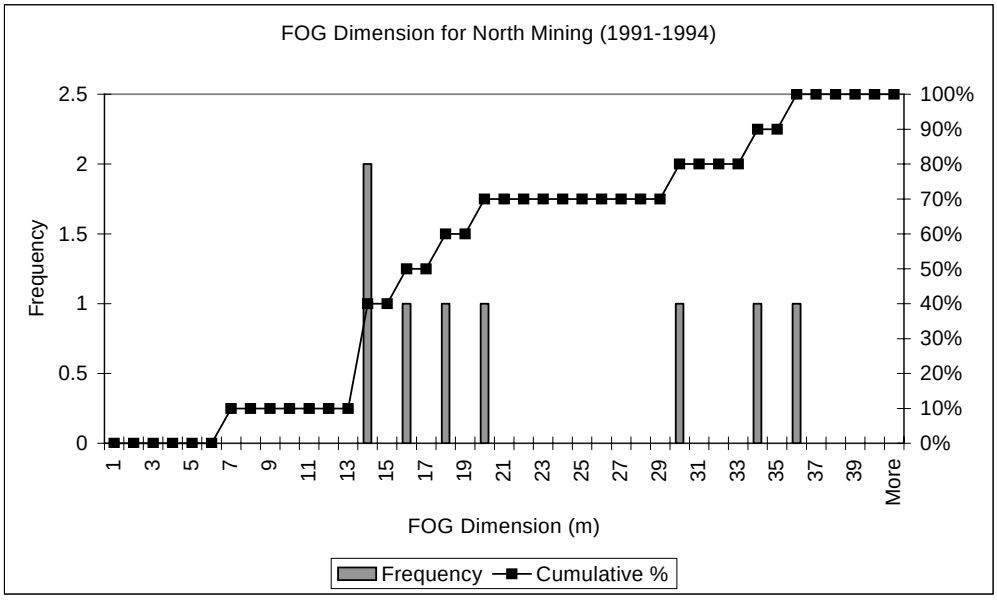

Figure F11 FOG Dimension frequency and cumulative percentage for north mining (1991-1994)

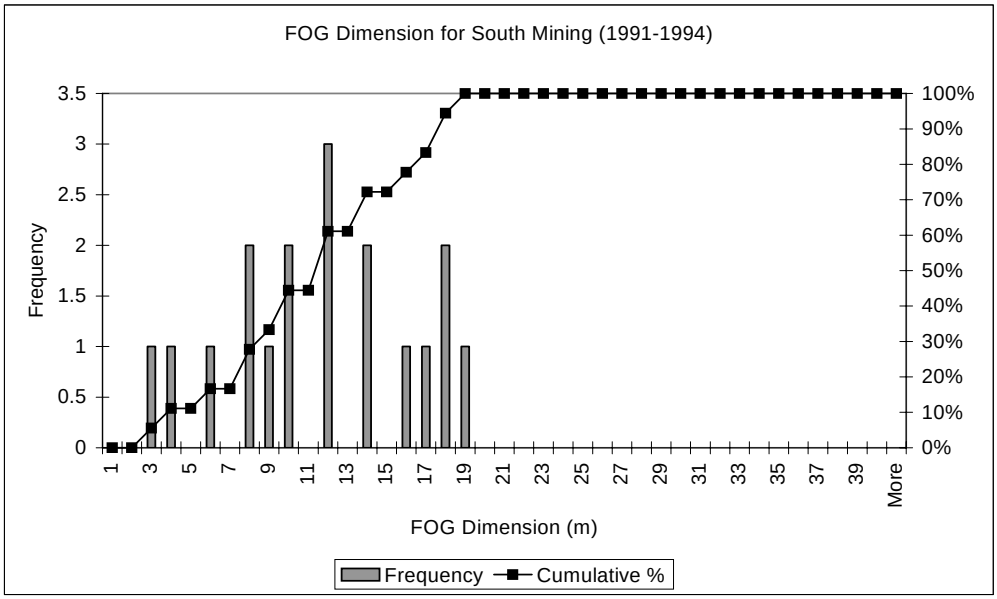

Figure F12 FOG Dimension frequency and cumulative percentage for south mining (1991-1994)

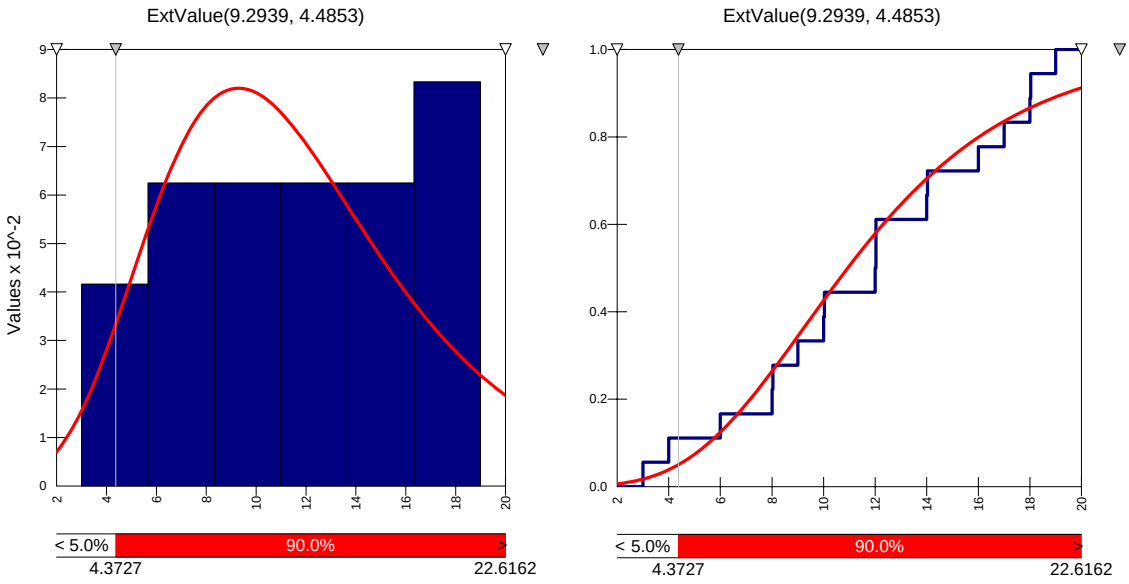

Figure F13 FOG Dimension PDF and cumulative distribution for south mining (1991-1994)

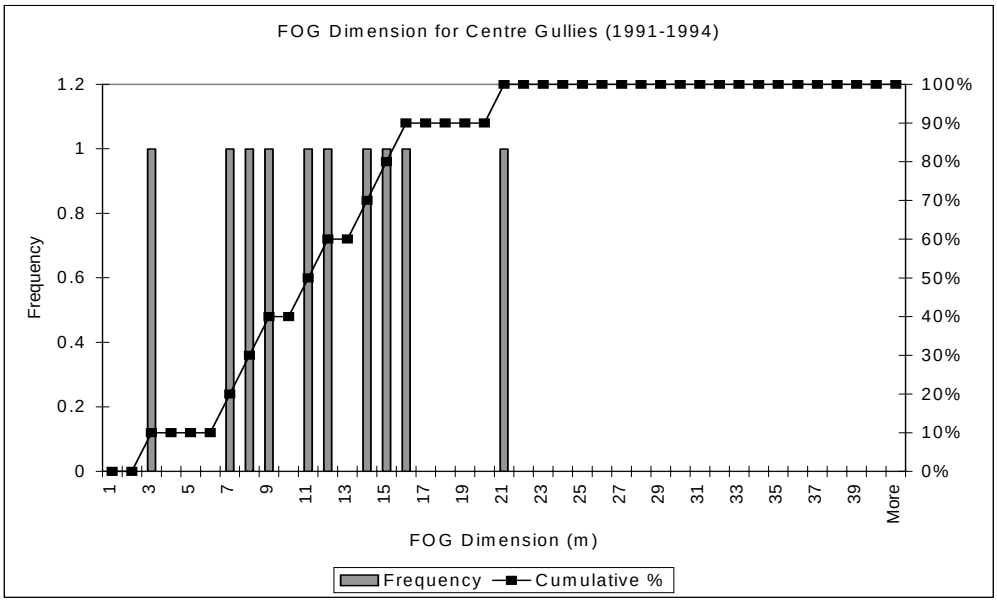

Figure F14 FOG Dimension frequency and cumulative percentage for centre gullies (1991-1994)

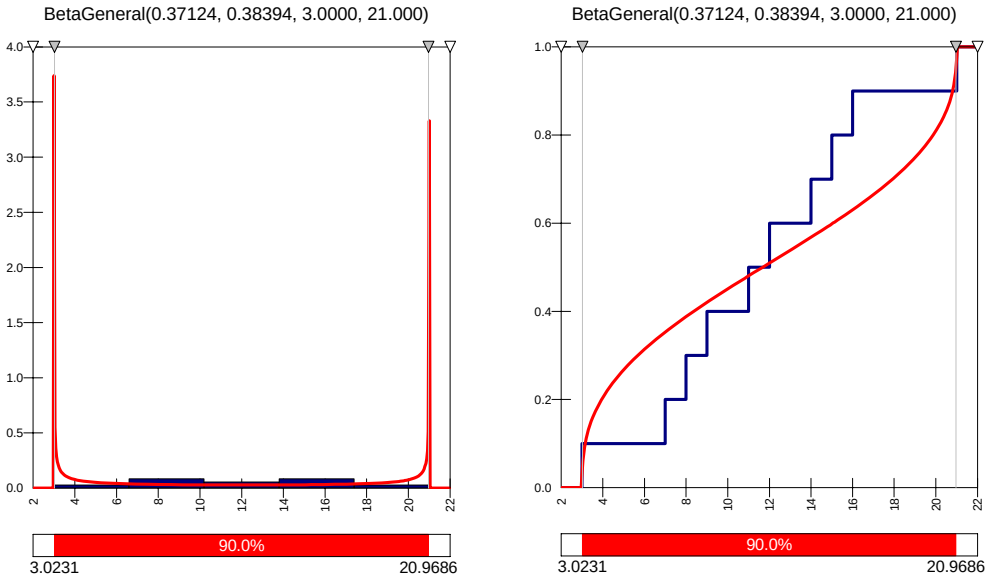

Figure F15 FOG Dimension PDF and cumulative distribution for centre gullies (1991-1994)

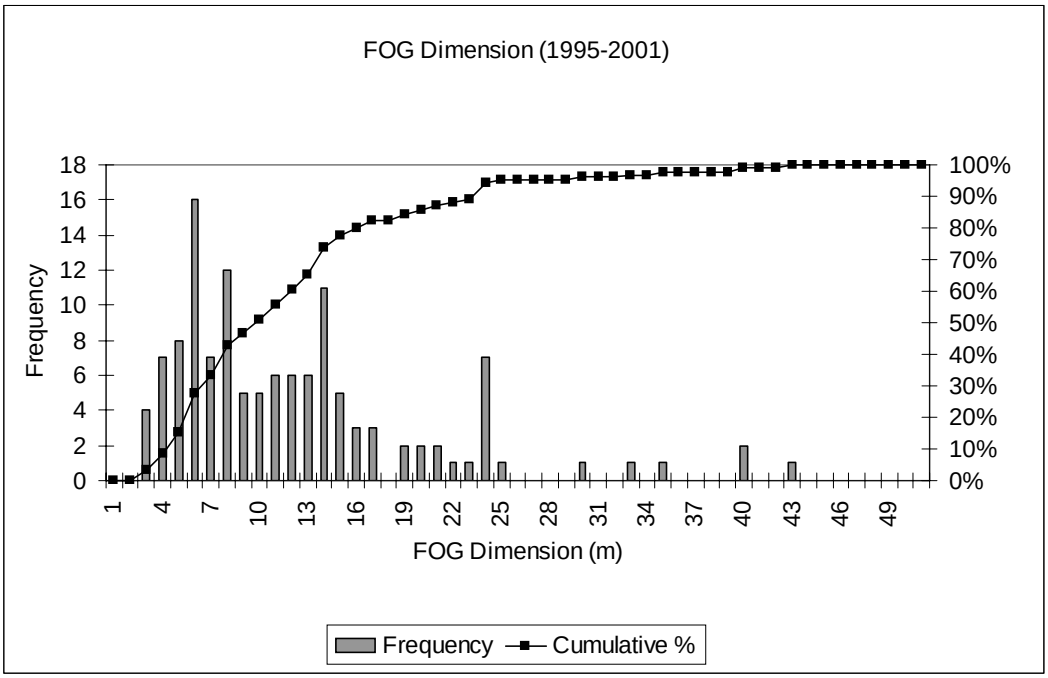

Figure F16 FOG Dimension frequency and cumulative percentage (1995-2001)

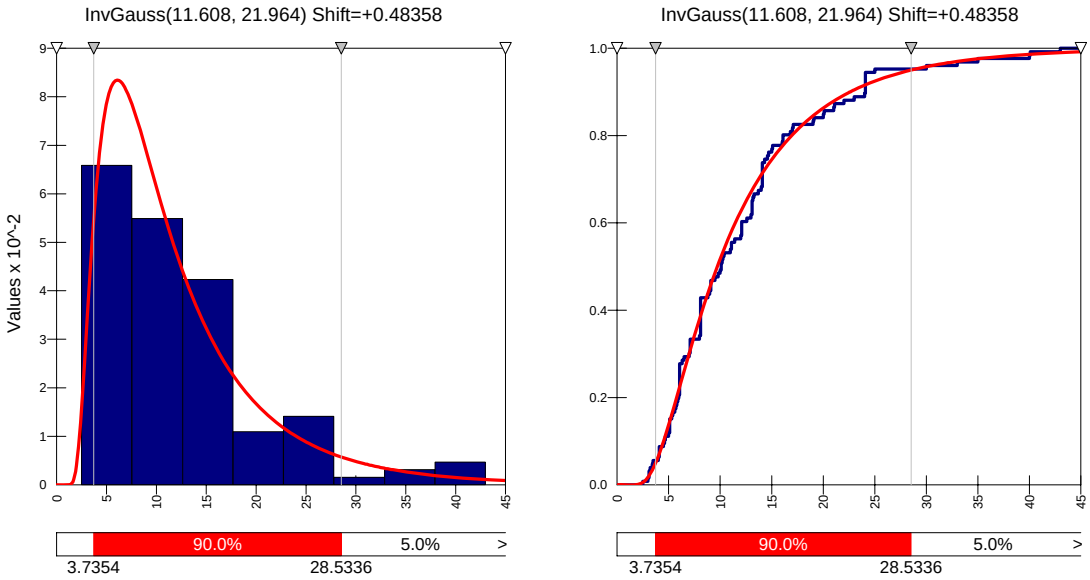

Figure F17 FOG Dimension PDF and cumulative distribution (1995-2001)

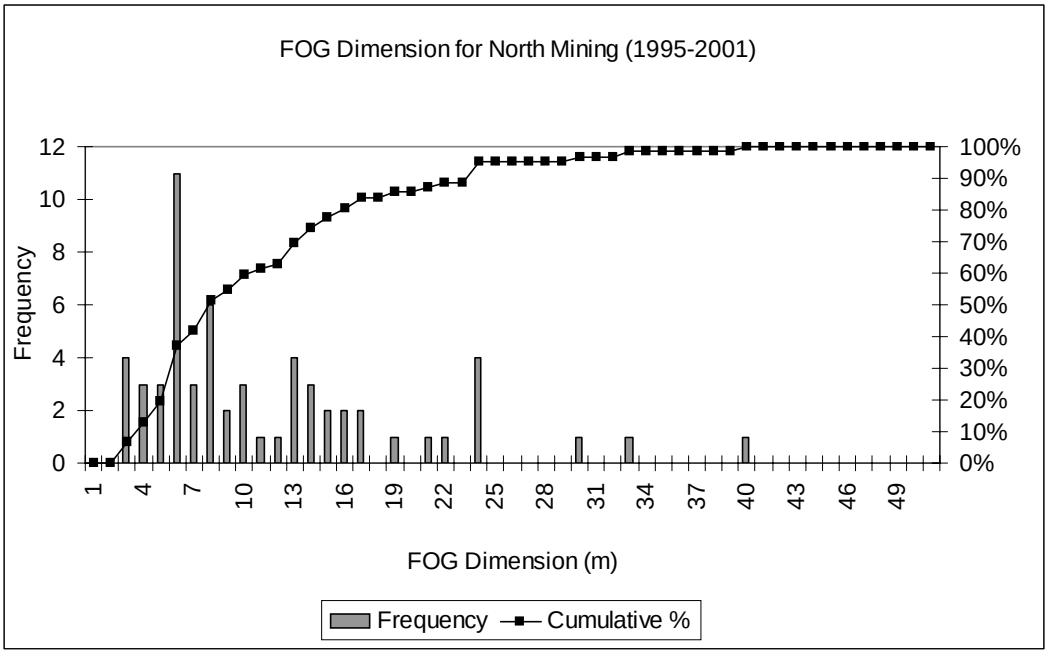

Figure F18 FOG Dimension frequency and cumulative percentage for north mining (1995-2001)

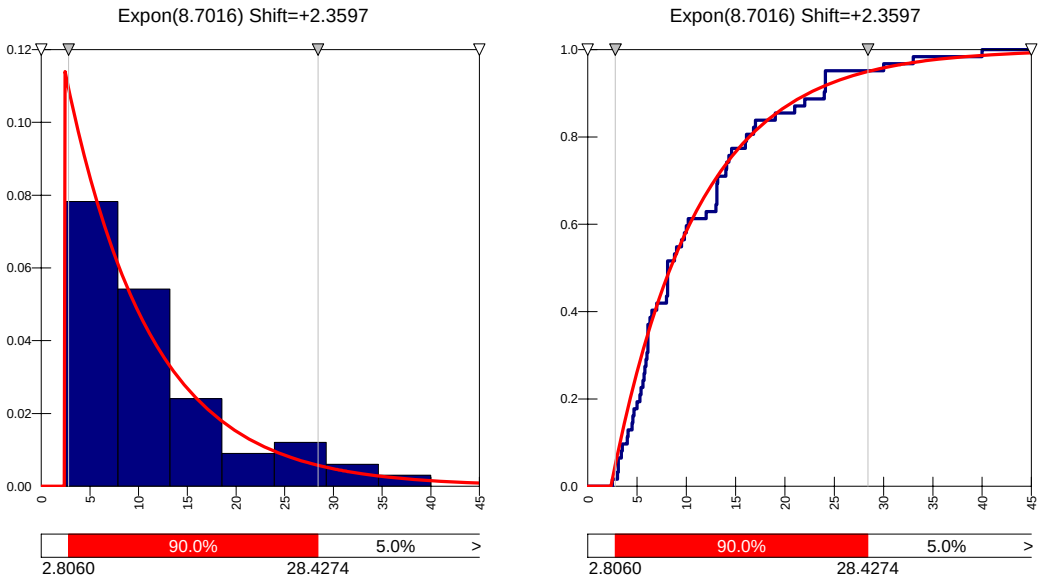

Figure F19 FOG Dimension PDF and cumulative distribution for north mining (1995-2001)

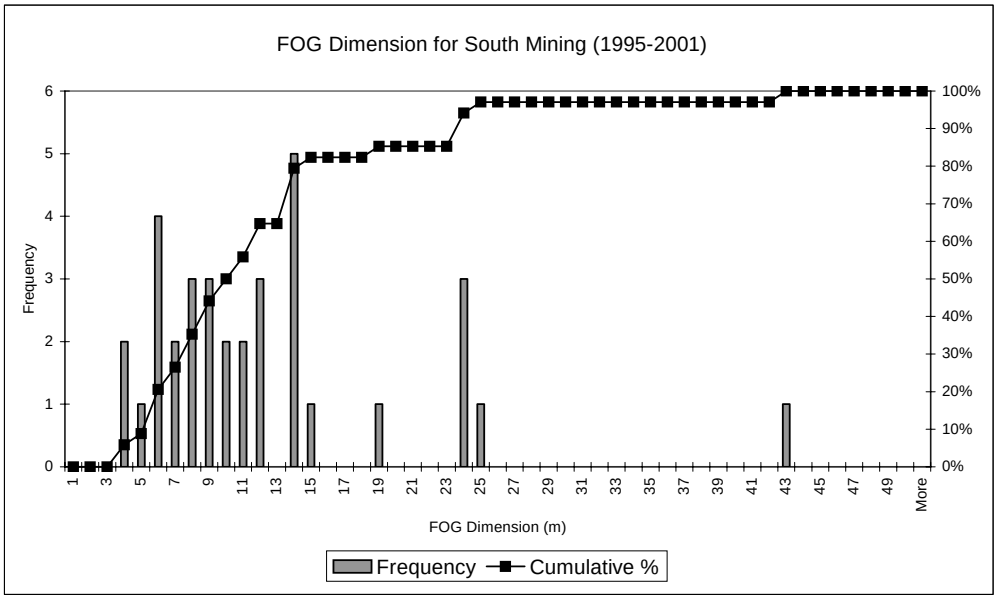

Figure F20 FOG Dimension frequency and cumulative percentage for south mining (1995-2001)

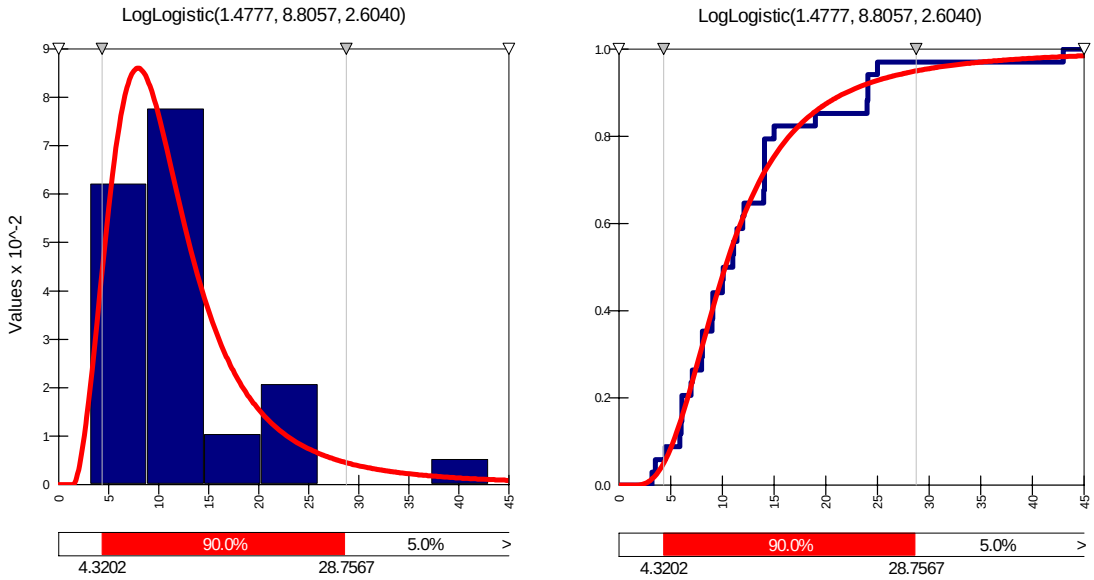

Figure F21 FOG Dimension PDF and cumulative distribution for south mining (1995-2001)

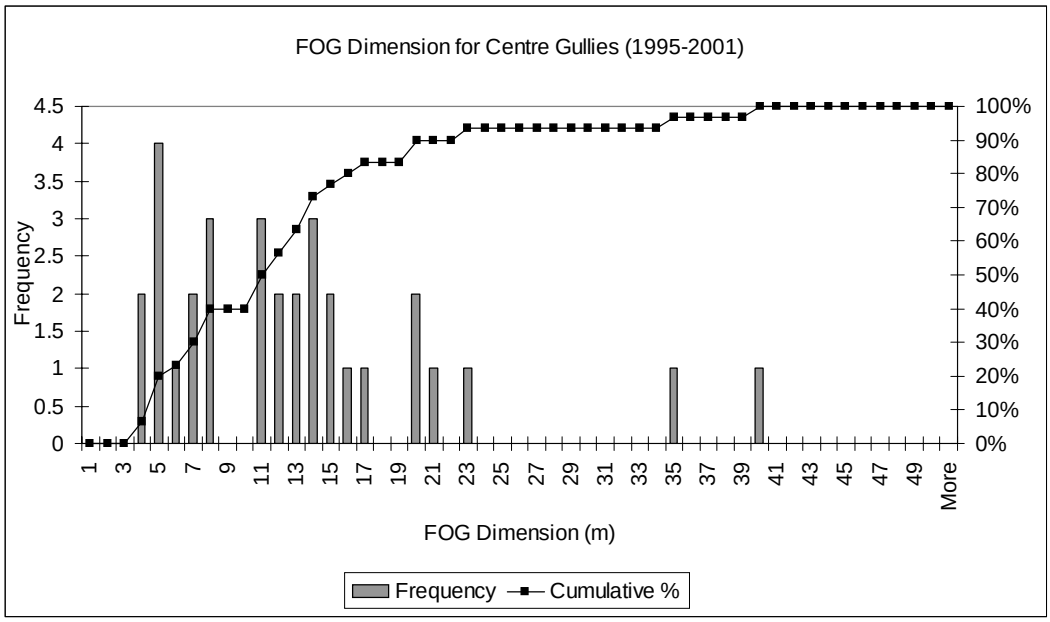

Figure F22 FOG Dimension frequency and cumulative percentage for centre gullies (1995-2001)

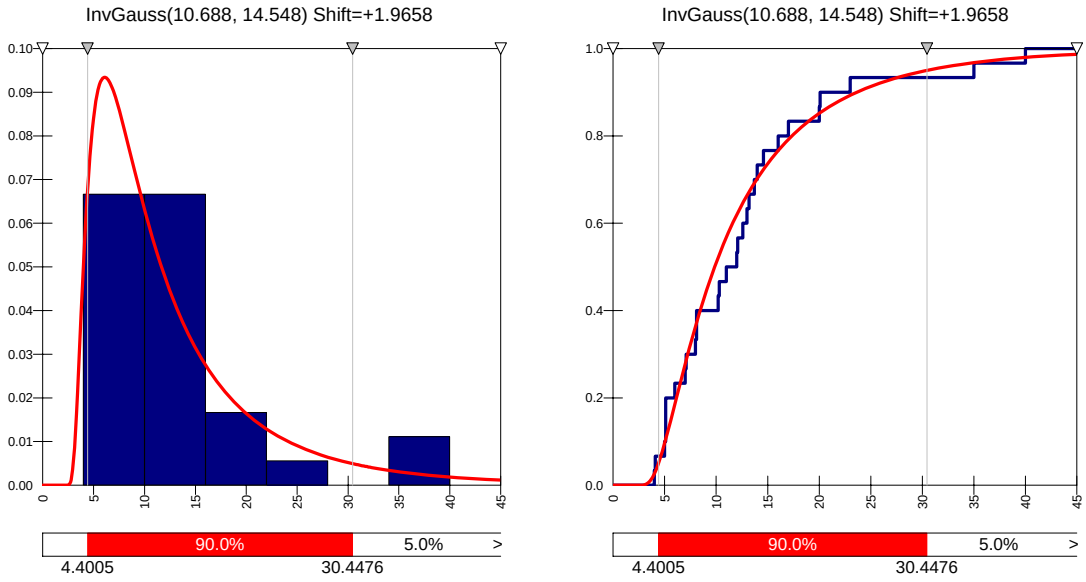

Figure F23 FOG Dimension PDF and cumulative distribution for centre gullies (1995-2001)

APPENDIX G

FOG STOPING WIDTH (FIGURES G1-G23)

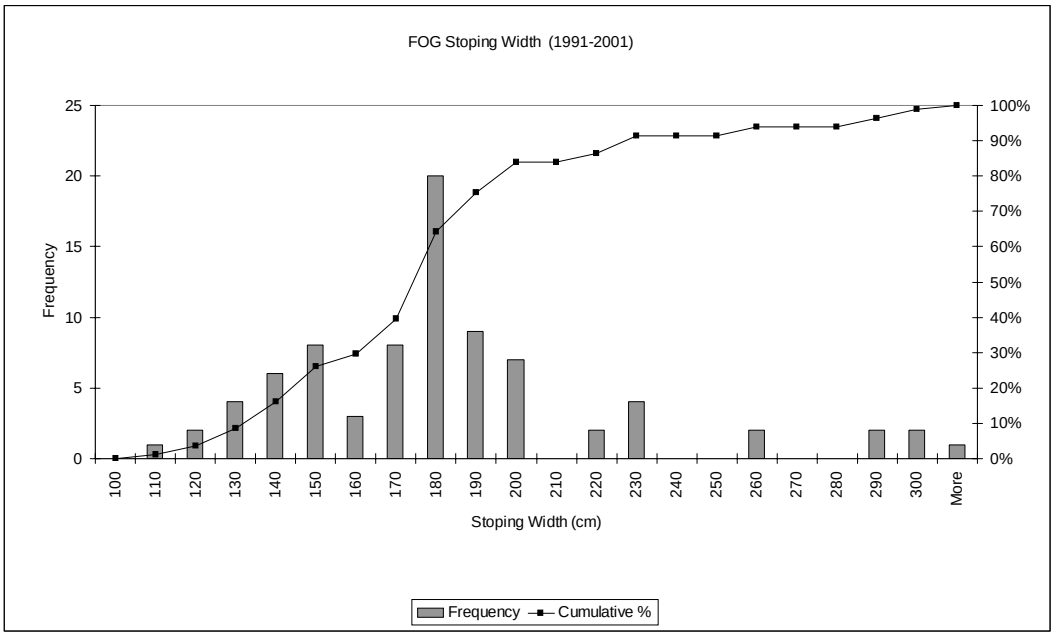

Figure G1 FOG stoping width frequency and cumulative percentage (1991-2001)

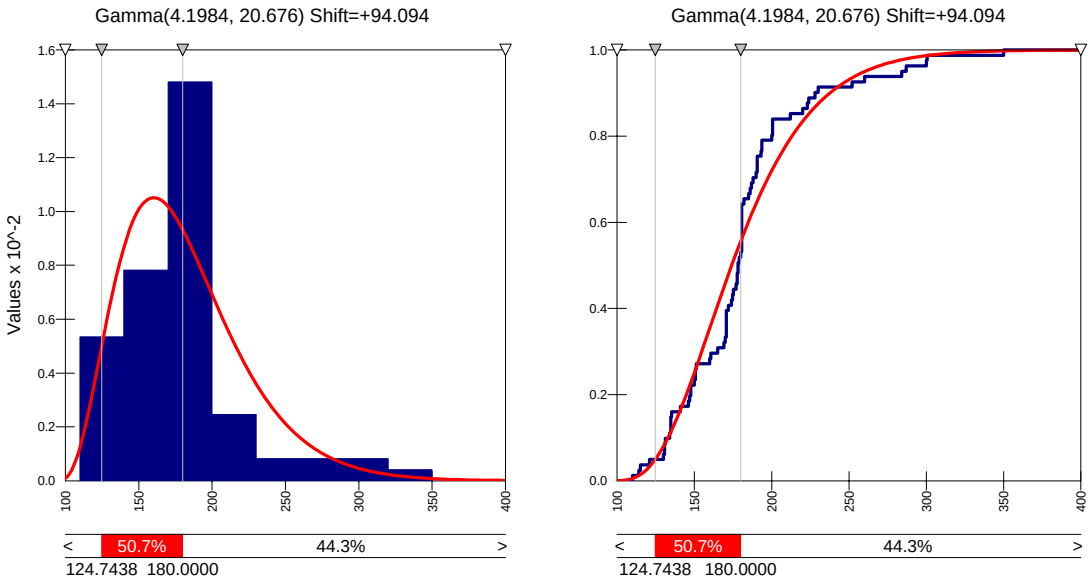

Figure G2 FOG stoping width PDF and cumulative distribution (1991-2001)

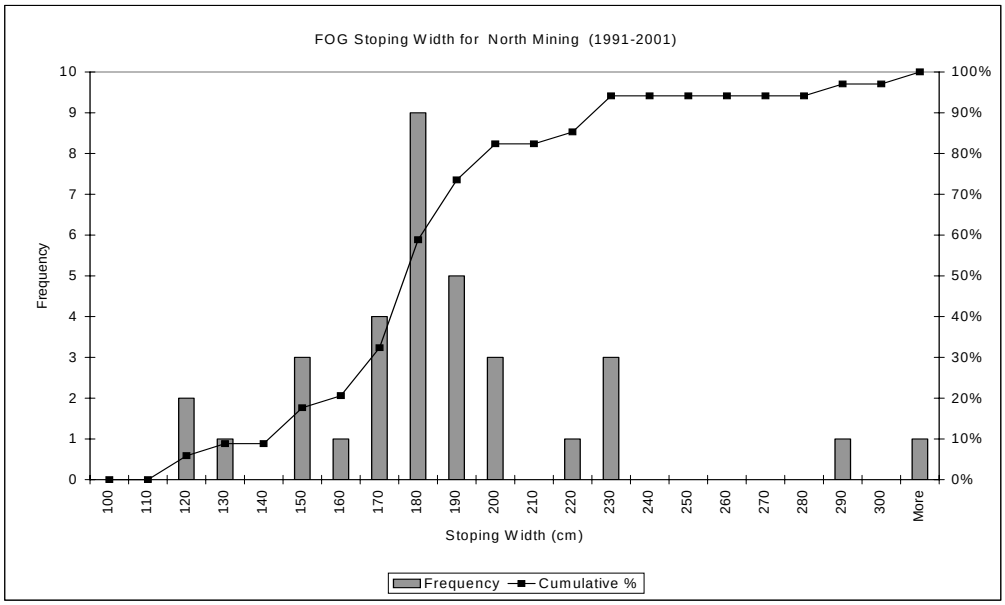

Figure G3 FOG stoping width frequency and cumulative percentage for north mining (1991-2001)

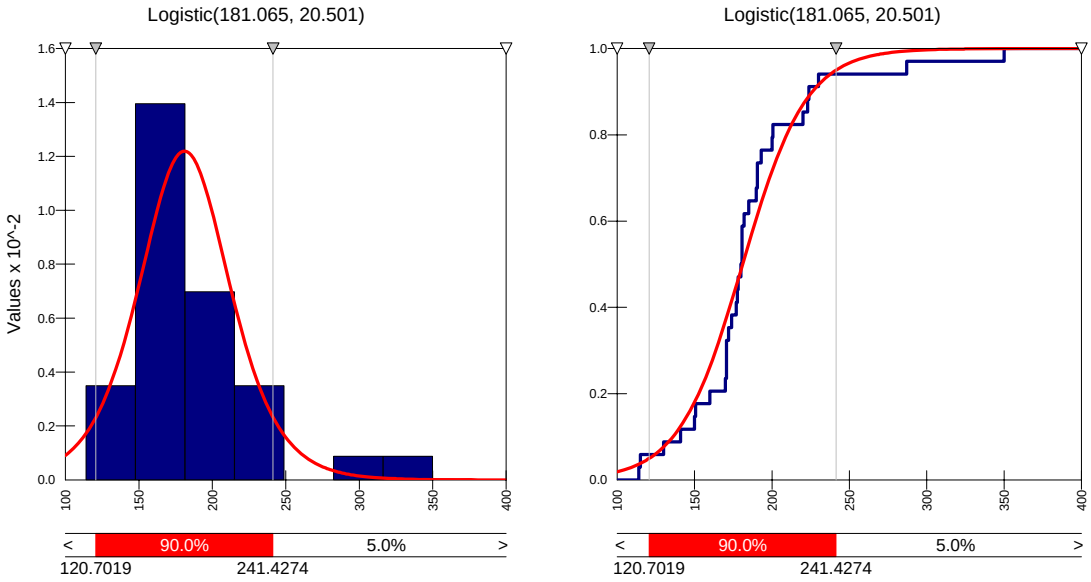

Figure G4 FOG stoping width PDF and cumulative distribution for north mining (1991-2001)

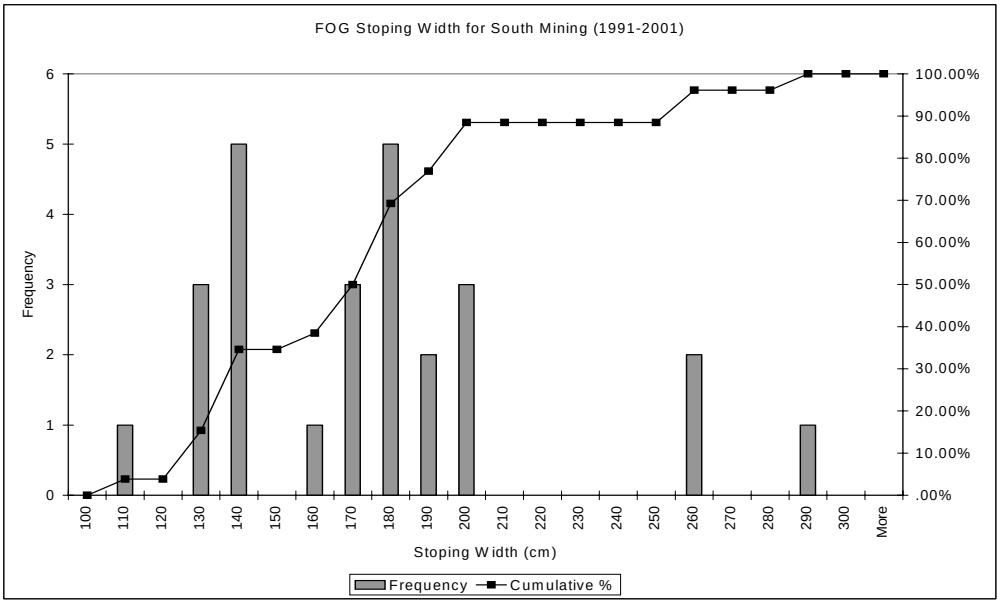

Figure G5 FOG stoping width frequency and cumulative percentage for south mining (1991-2001)

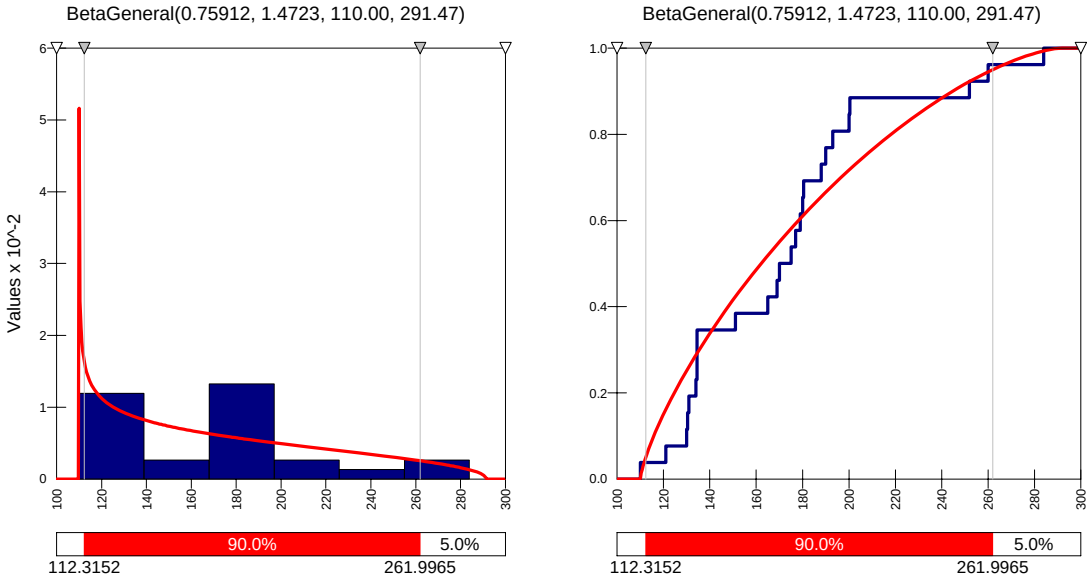

Figure G6 FOG stoping width PDF and cumulative distribution for south mining (1991-2001)

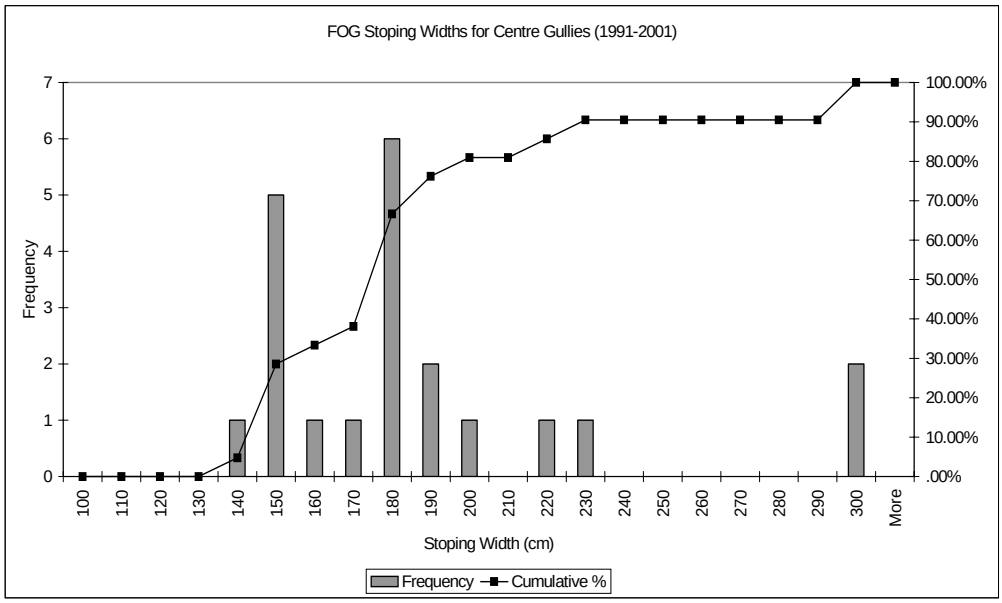

Figure G7 FOG stoping width frequency and cumulative percentage for centre gullies (1991-2001)

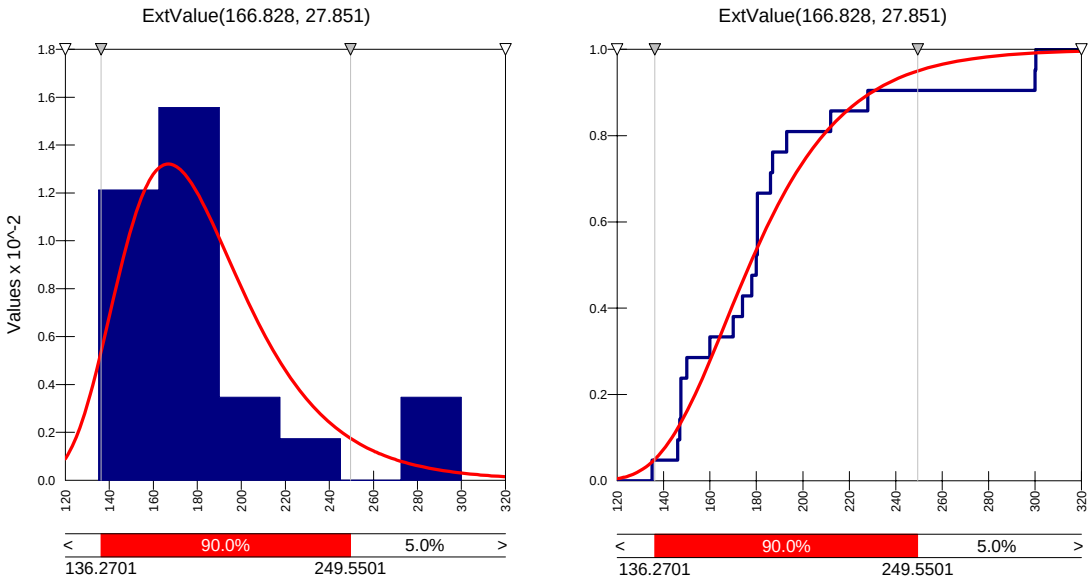

Figure G8 FOG stoping width PDF and cumulative distribution for centre gullies (1991-2001)

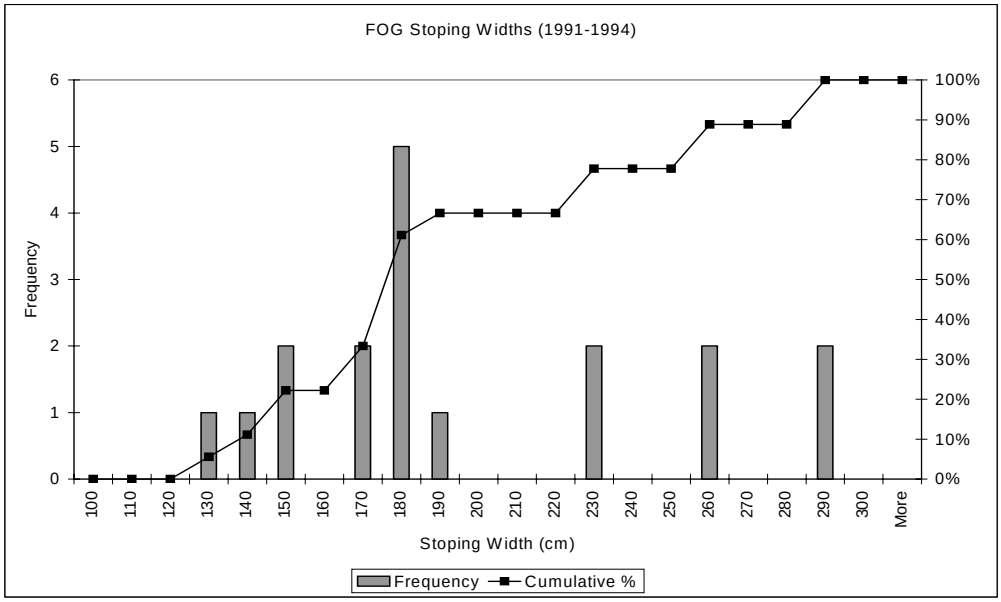

Figure G9 FOG stoping width frequency and cumulative percentage (1991-1994)

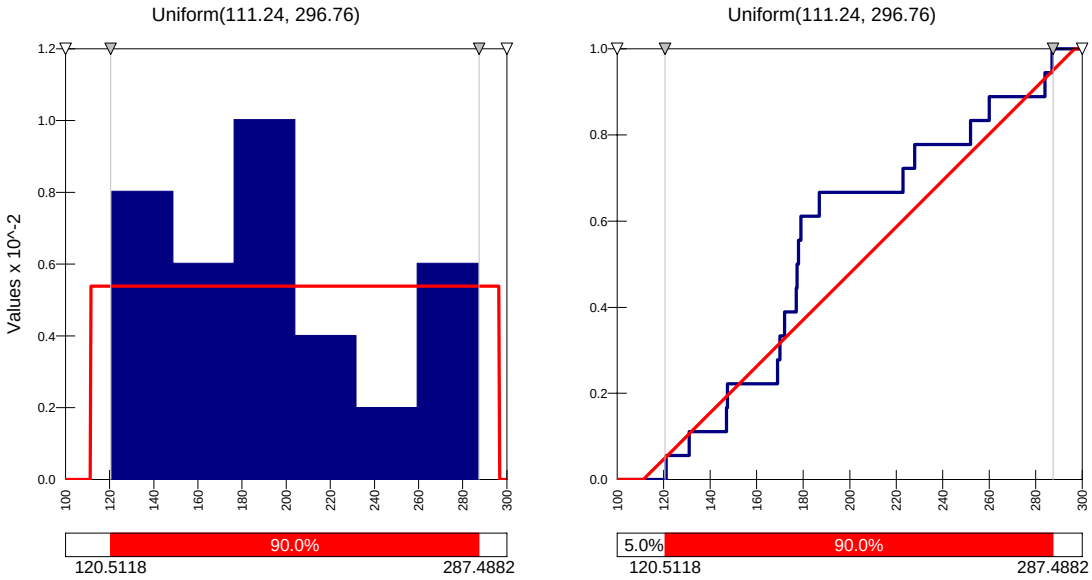

Figure G10 FOG stoping width PDF and cumulative distribution (1991-1994)

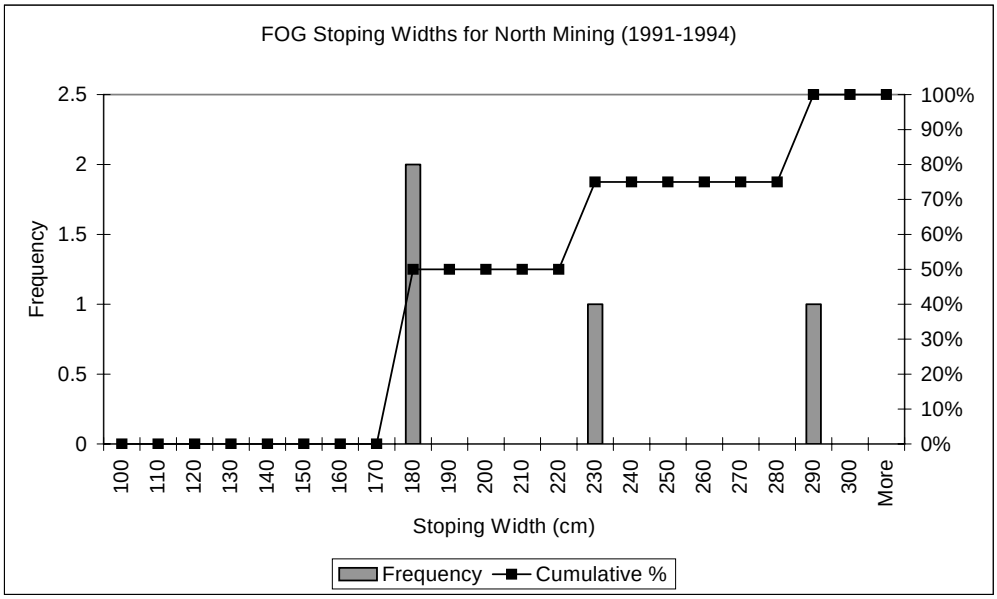

Figure G11 FOG stoping width frequency and cumulative percentage for north mining (1991-1994)

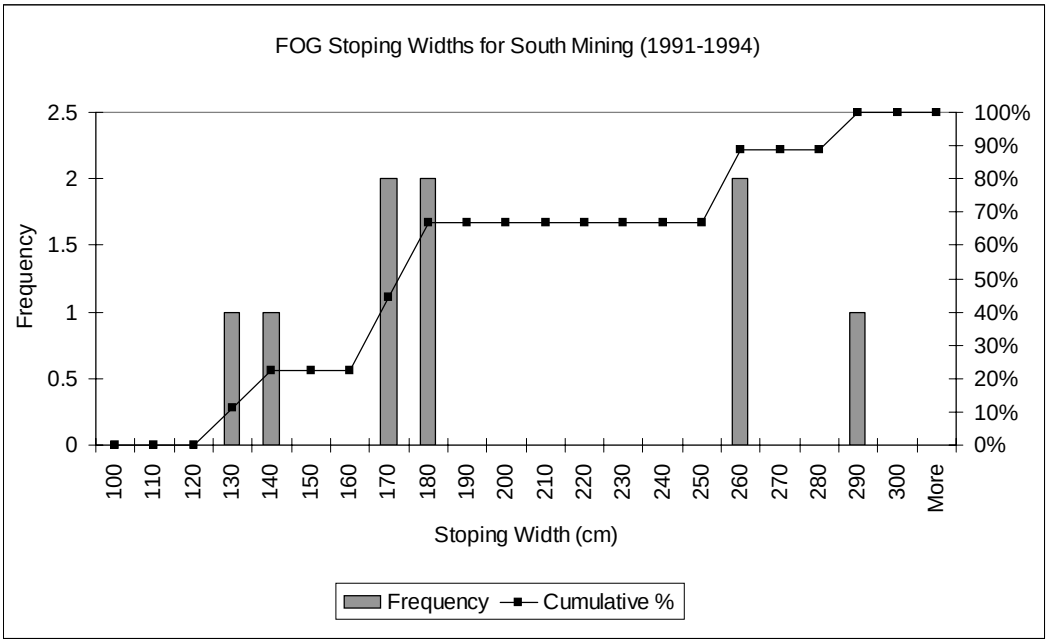

Figure G12 FOG stoping width frequency and cumulative percentage for south mining (1991-1994)

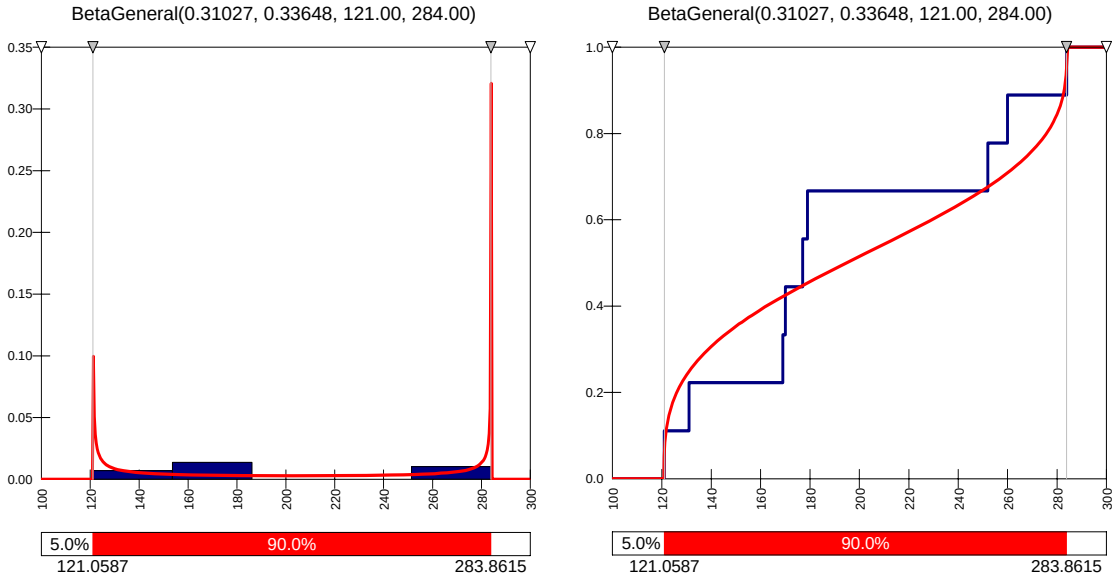

Figure G13 FOG stoping width PDF and cumulative distribution for south mining (1991-1994)

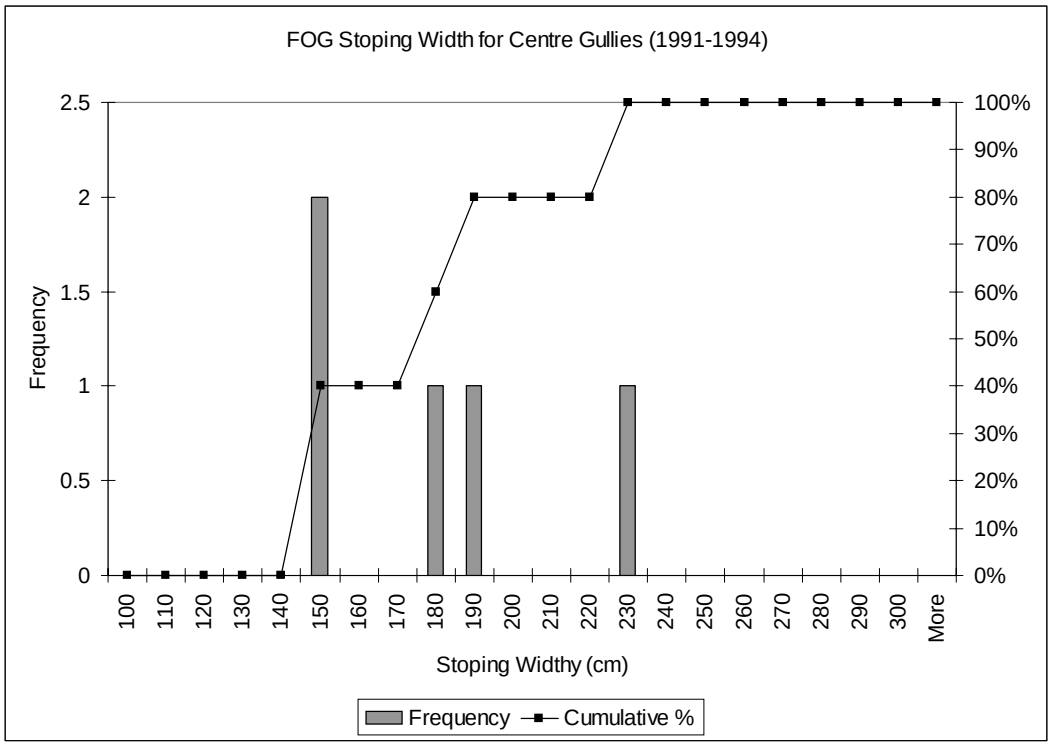

Figure G14 FOG stoping width frequency and cumulative percentage for centre gullies (1991-1994)

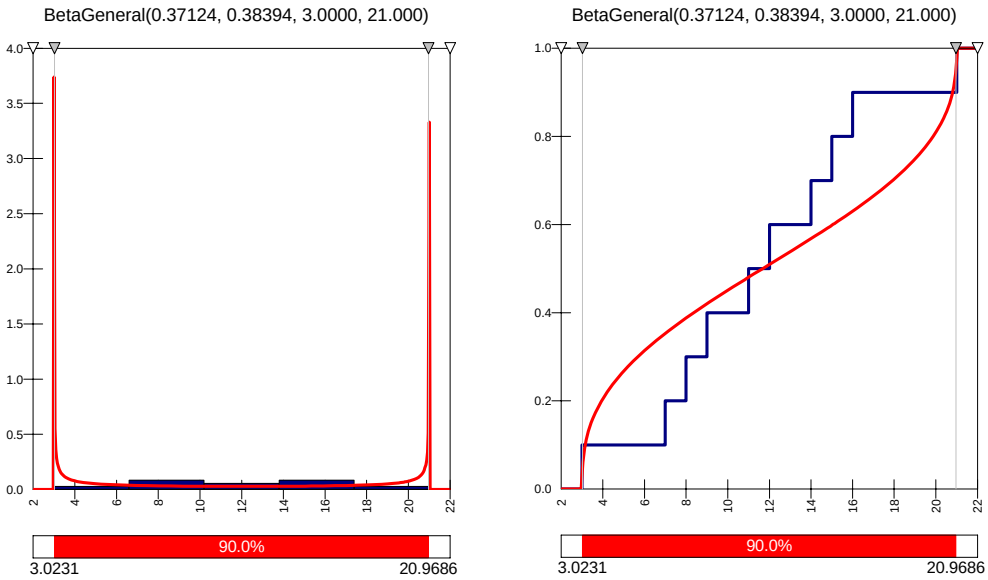

Figure G15 FOG stoping width PDF and cumulative distribution for centre gullies (1991-1994)

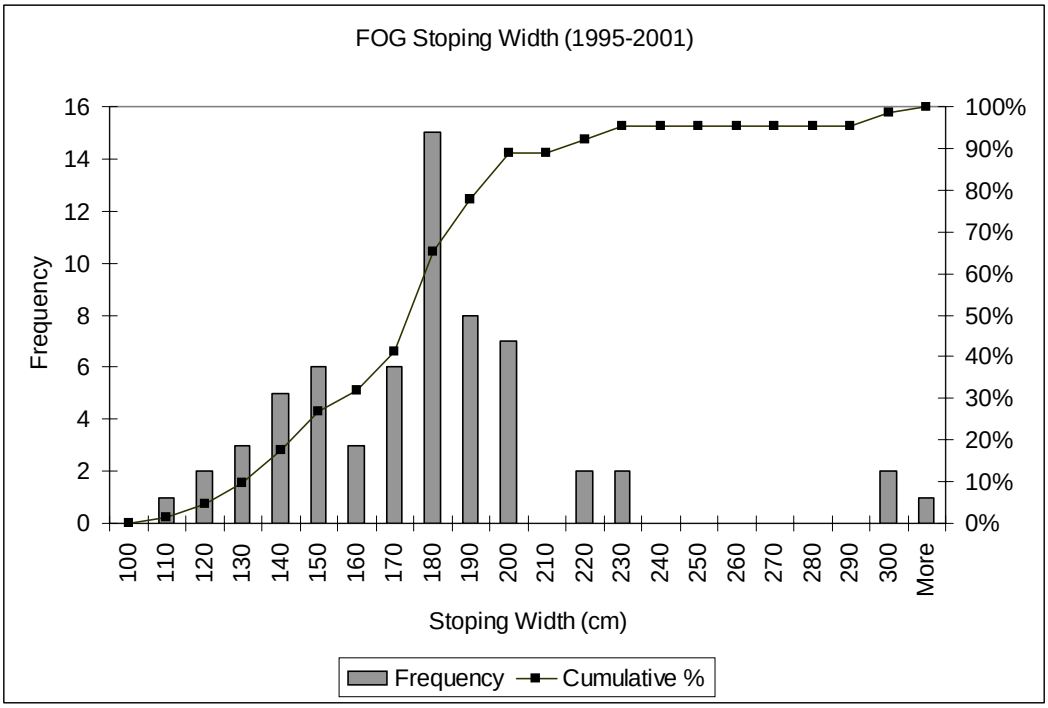

Figure G16 FOG stoping width frequency and cumulative percentage (1995-2001)

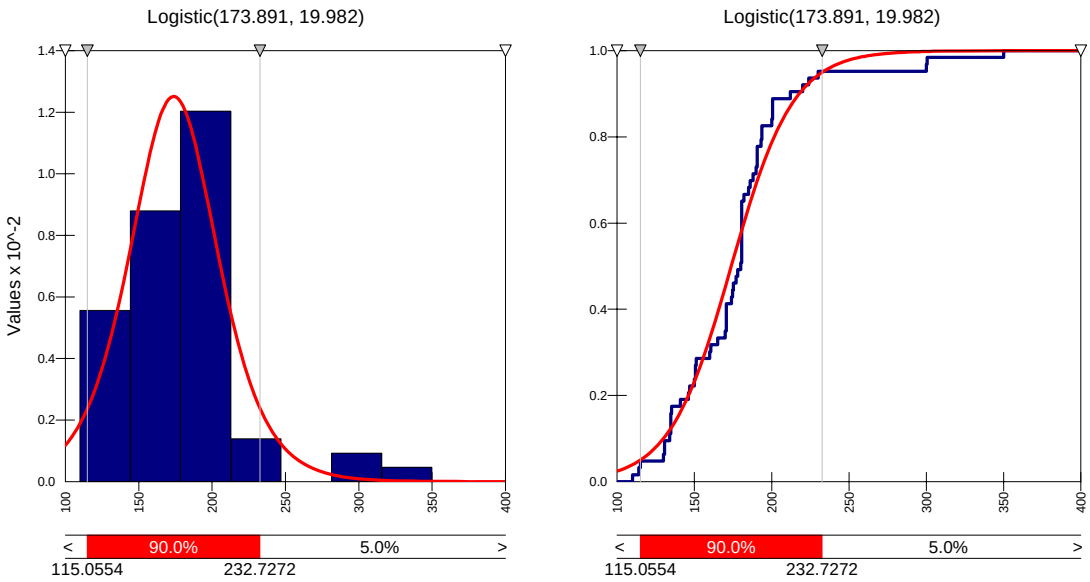

Figure G17 FOG stoping width PDF and cumulative distribution (1995-2001)

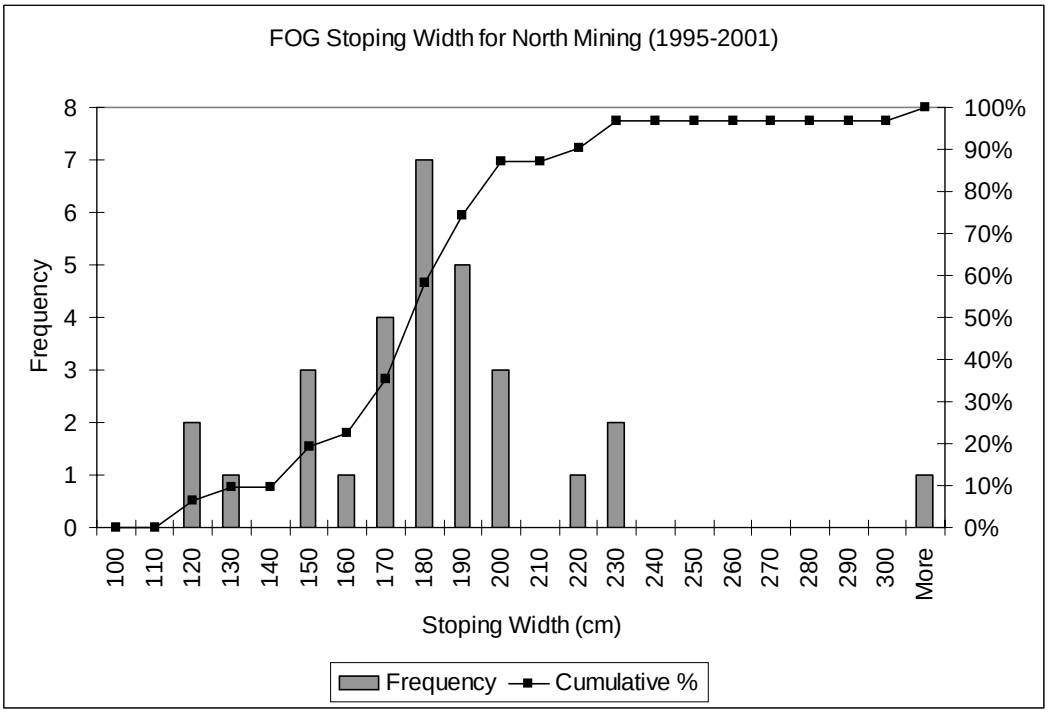

Figure G18 FOG stoping width frequency and cumulative percentage for north mining (1995-2001)

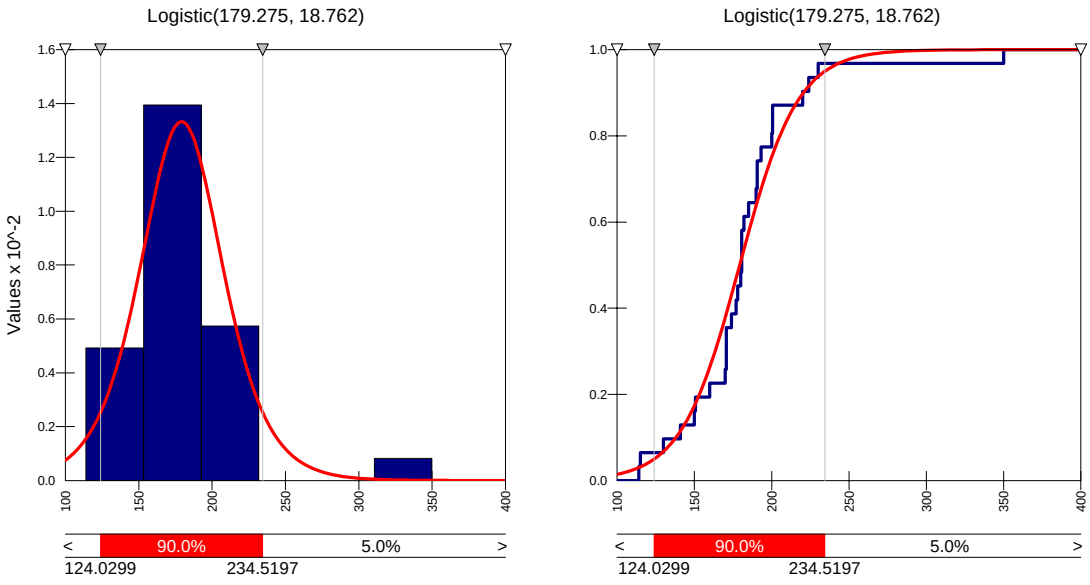

Figure G19 FOG stoping width PDF and cumulative distribution for north mining (1995-2001)

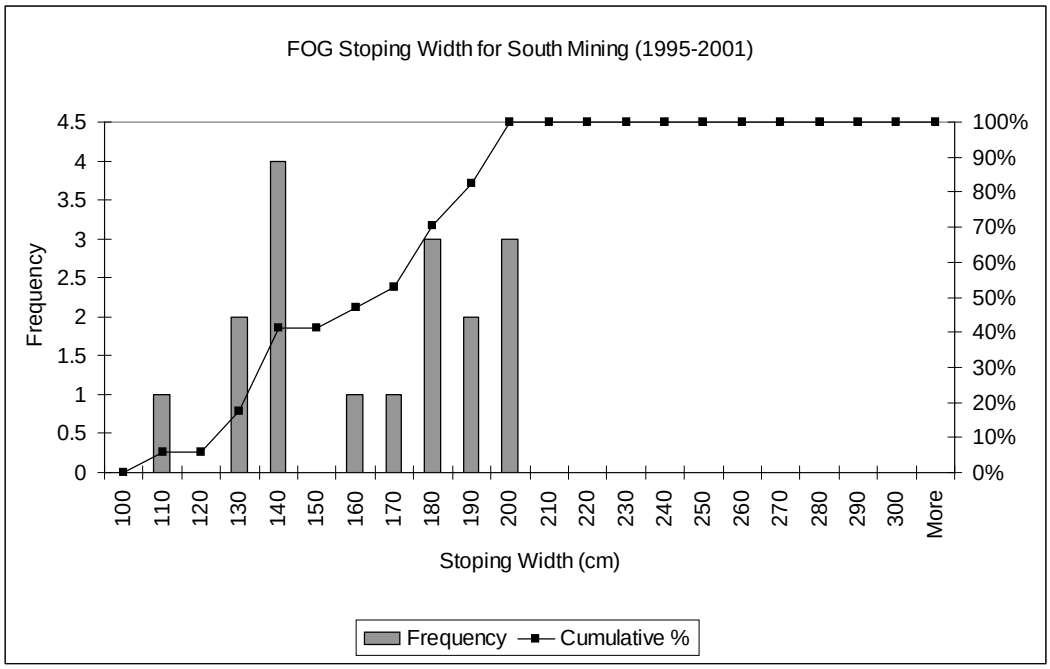

Figure G20 FOG stoping width frequency and cumulative percentage for south mining (1995-2001)

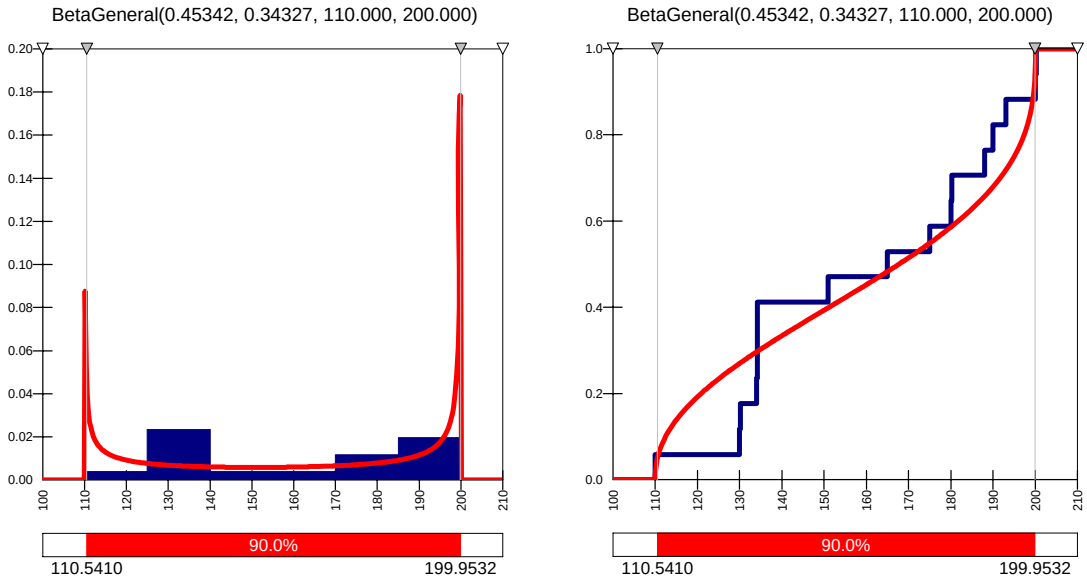

Figure G21 FOG stoping width PDF and cumulative distribution for south mining (1995-2001)

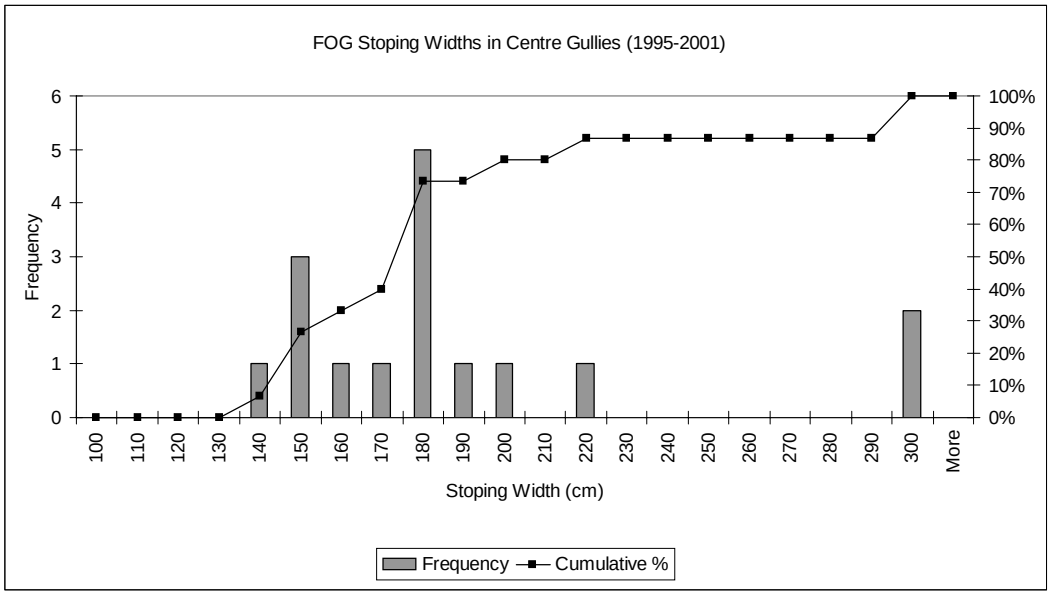

Figure G22 FOG stoping width frequency and cumulative percentage for centre gullies (1995-2001)

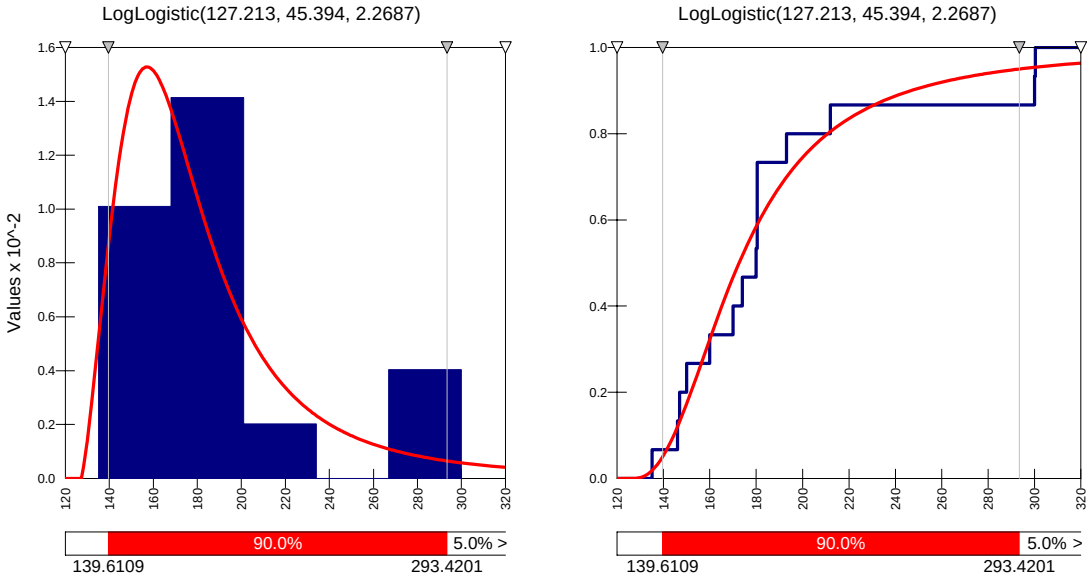

Figure G23 FOG stoping width PDF and cumulative distribution for centre gullies (1995-2001)

APPENDIX H

FOG PILLAR SPANS (FIGURES H1-H23)

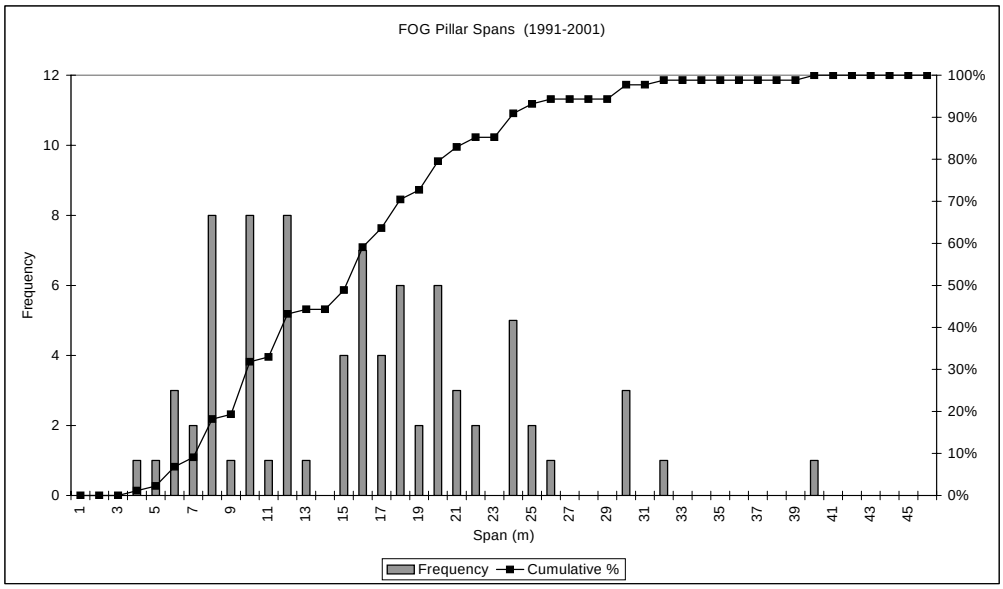

Figure H1 FOG pillar spans frequency and cumulative percentage (1991-2001)

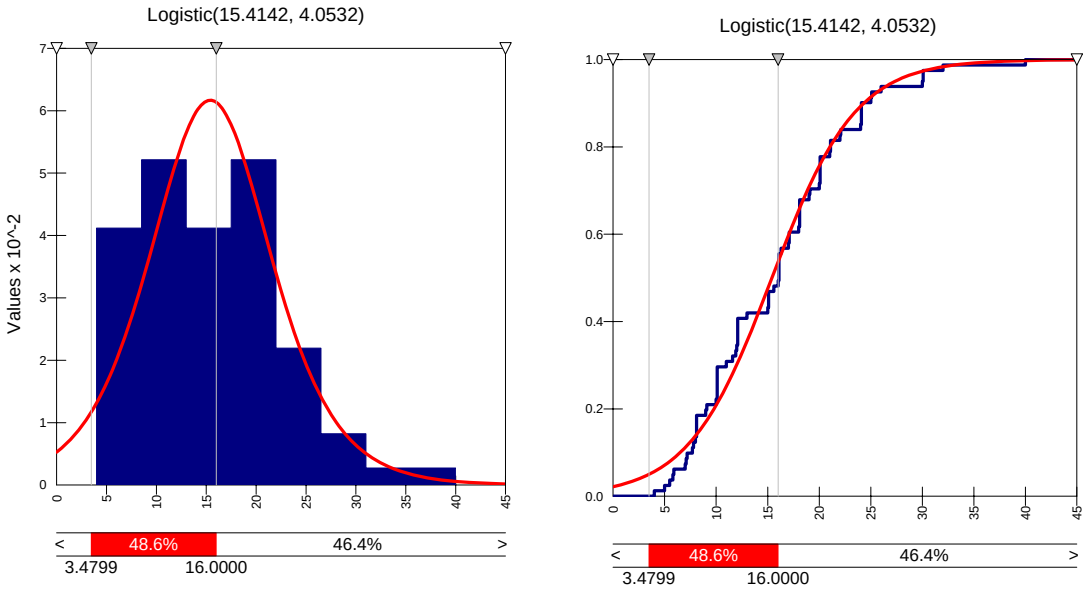

Figure H2 FOG pillar spans PDF and cumulative distribution (1991-2001)

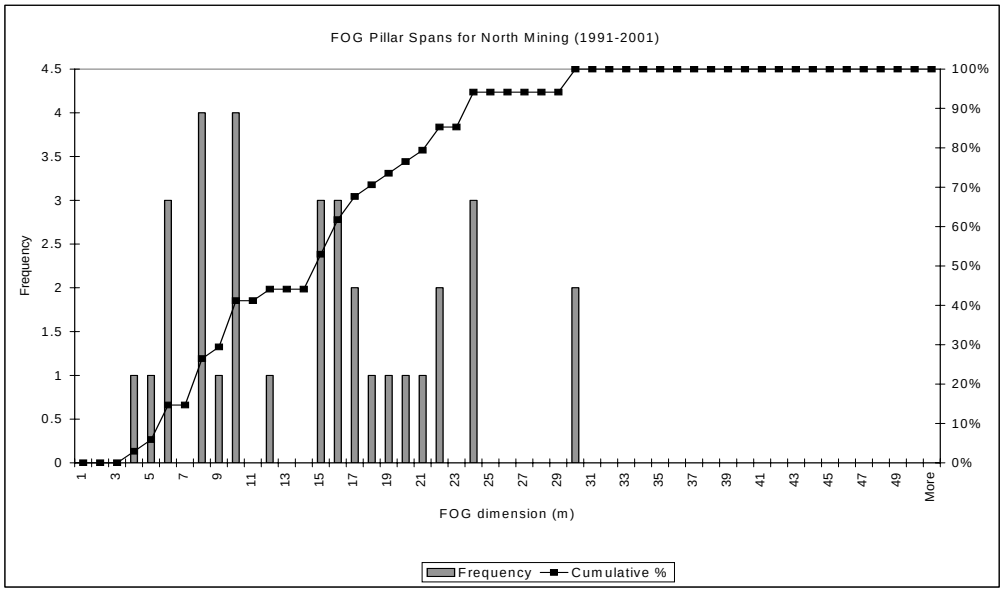

Figure H3 FOG pillar spans frequency and cumulative percentage for north mining (1991-2001)

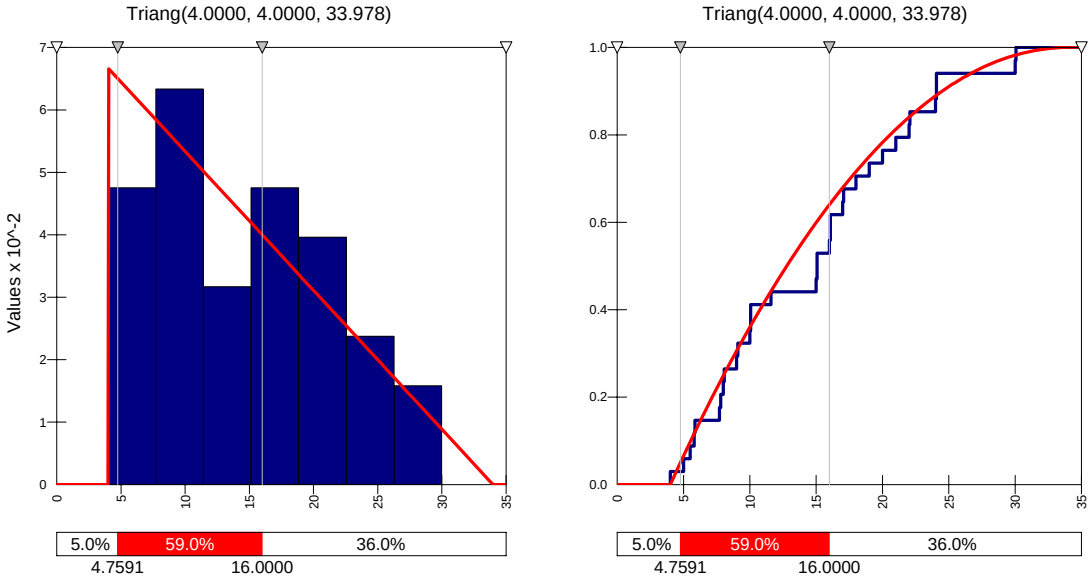

Figure H4 FOG pillar spans PDF and cumulative distribution for north mining (1991-2001)

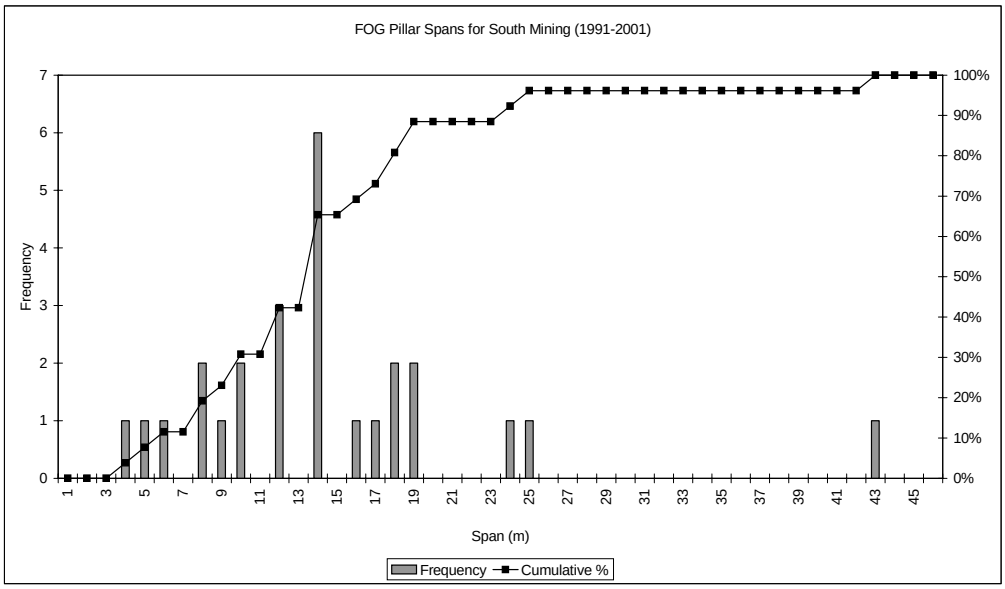

Figure H5 FOG pillar spans frequency and cumulative percentage for south mining (1991-2001)

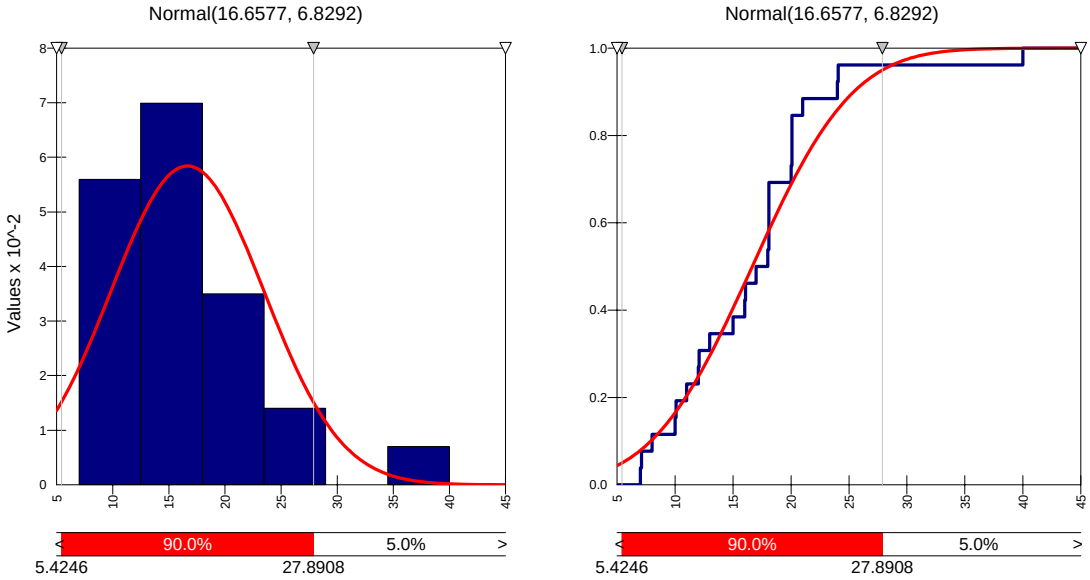

Figure H6 FOG pillar spans PDF and cumulative distribution for south mining (1991-2001)

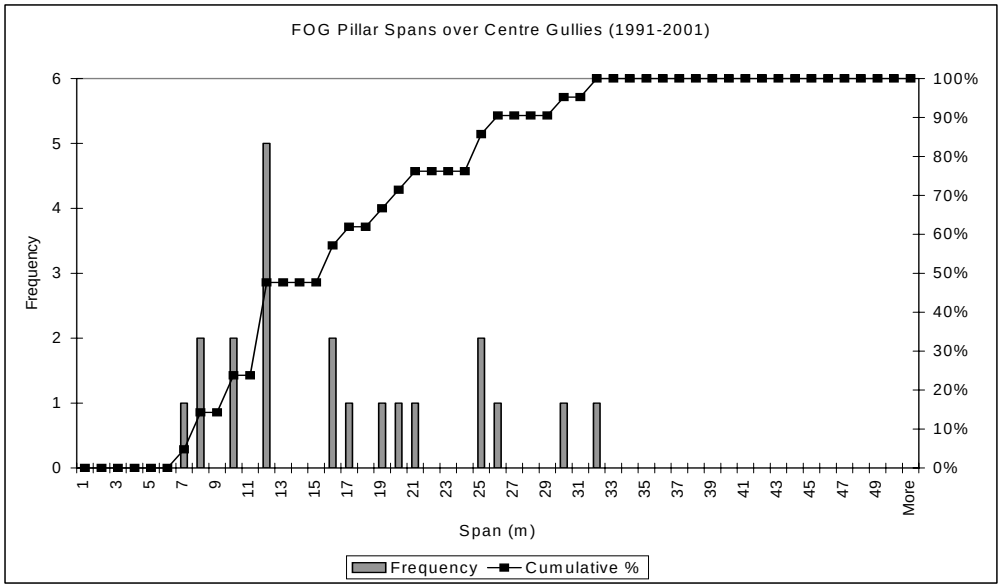

Figure H7 FOG pillar spans frequency and cumulative percentage for centre gullies (1991-2001)

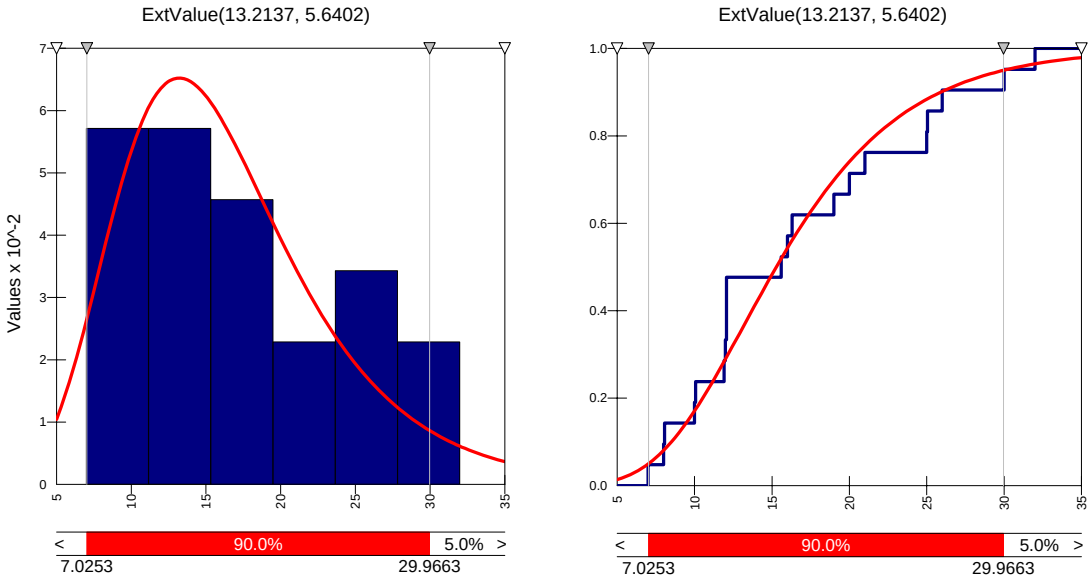

Figure H8 FOG pillar spans PDF and cumulative distribution for centre gullies (1991-2001)

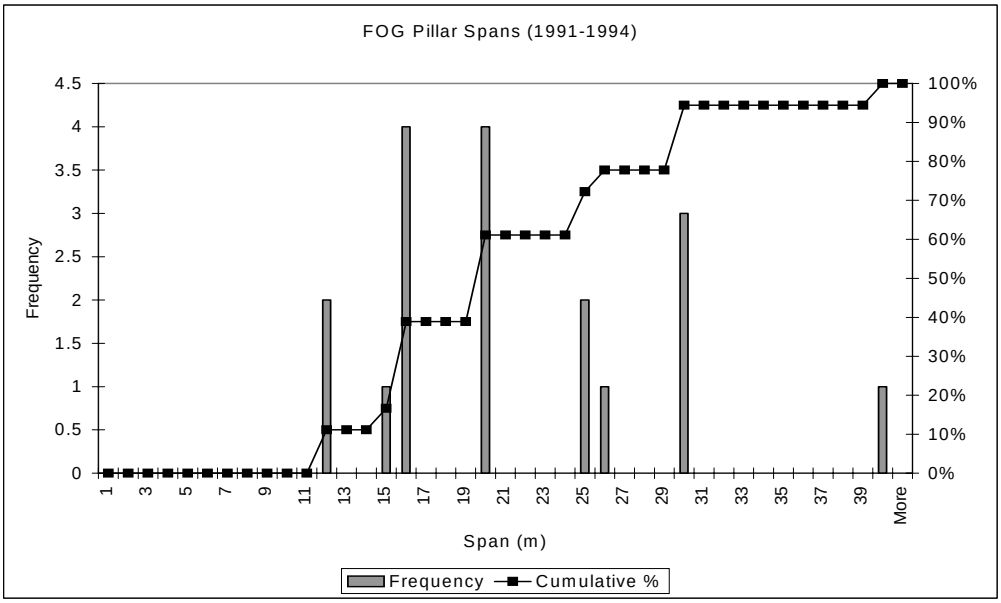

Figure H9 FOG pillar spans frequency and cumulative percentage (1991-1994)

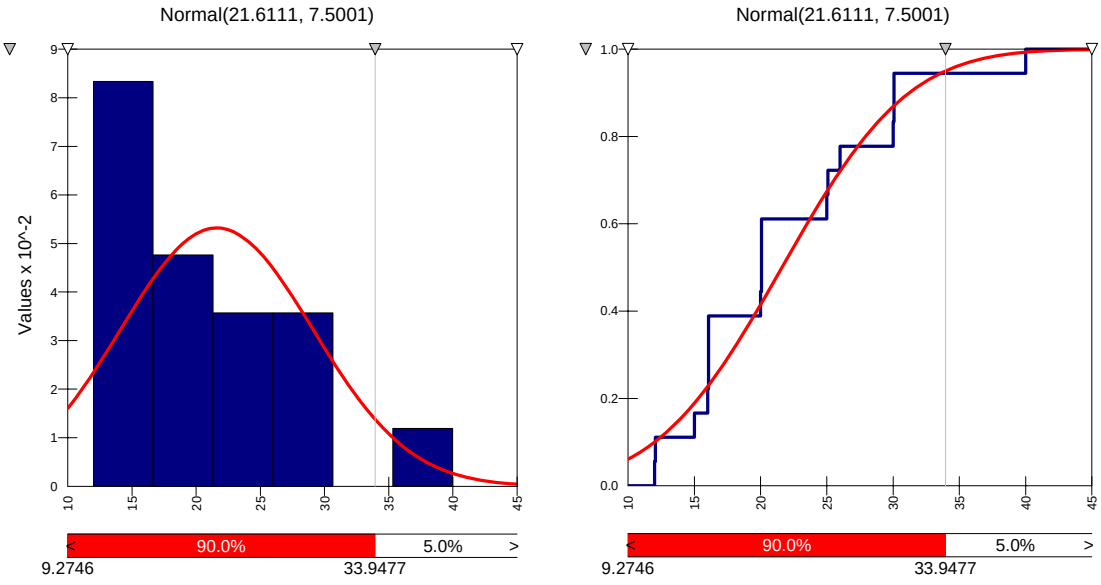

Figure H10 FOG pillar spans PDF and cumulative distribution (1991-1994)

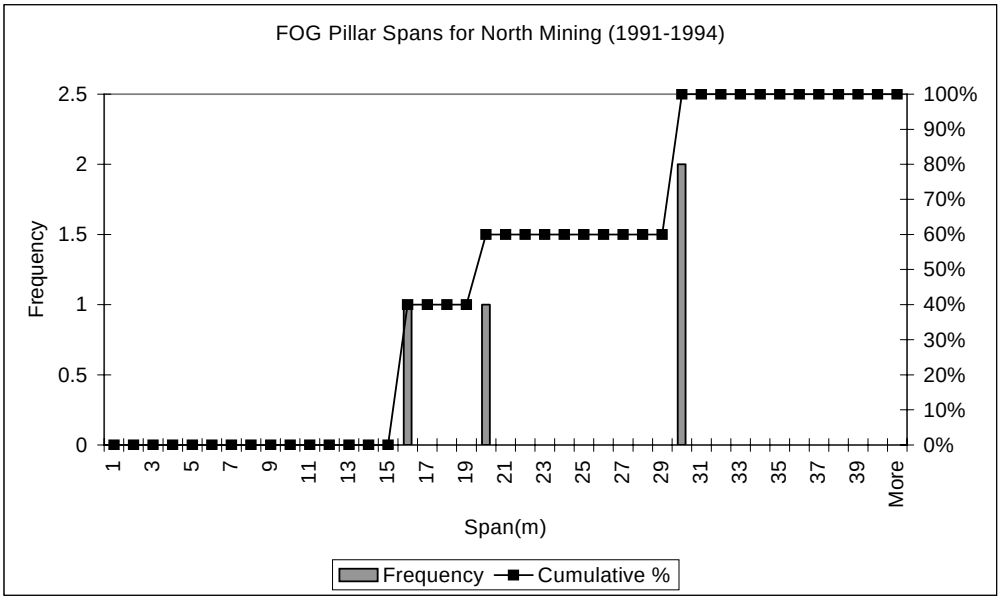

Figure H11 FOG pillar spans frequency and cumulative percentage for north mining (1991-1994)

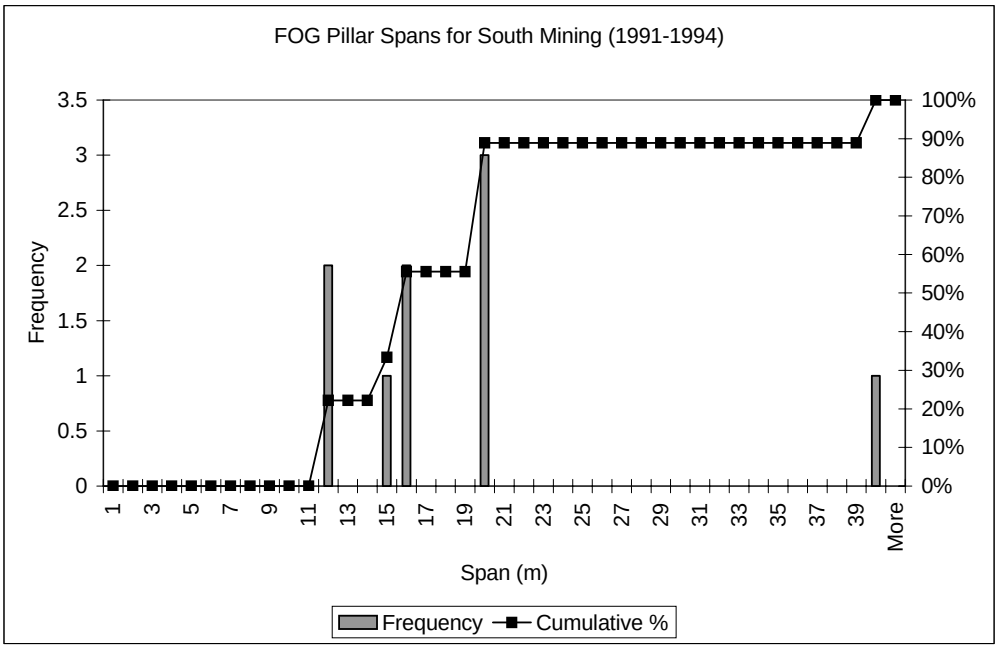

Figure H12 FOG pillar spans frequency and cumulative percentage for south mining (1991-1994)

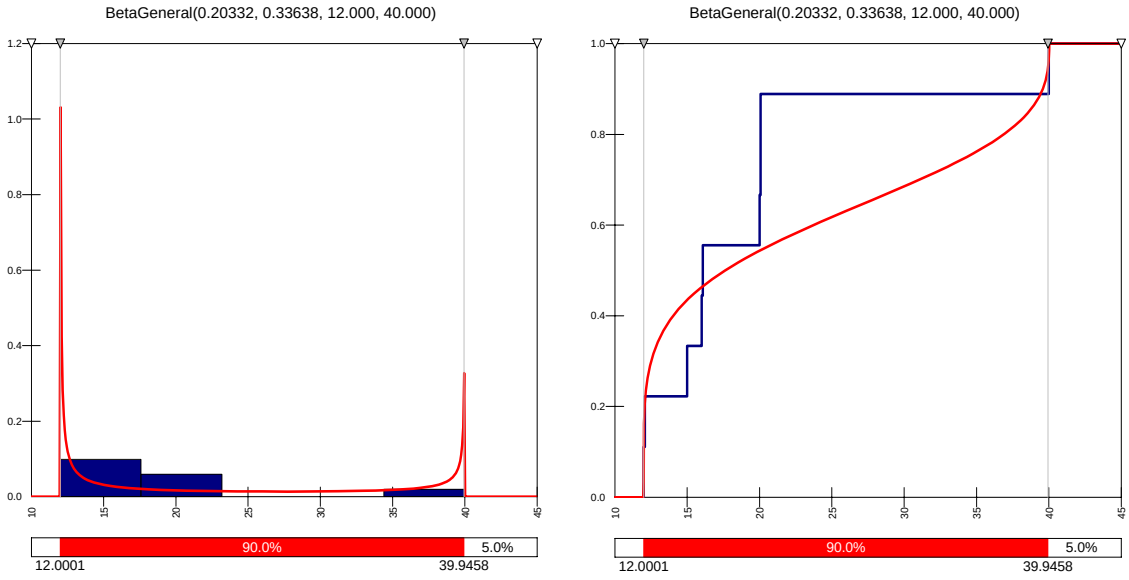

Figure H13 FOG pillar spans PDF and cumulative distribution for south mining (1991-1994)

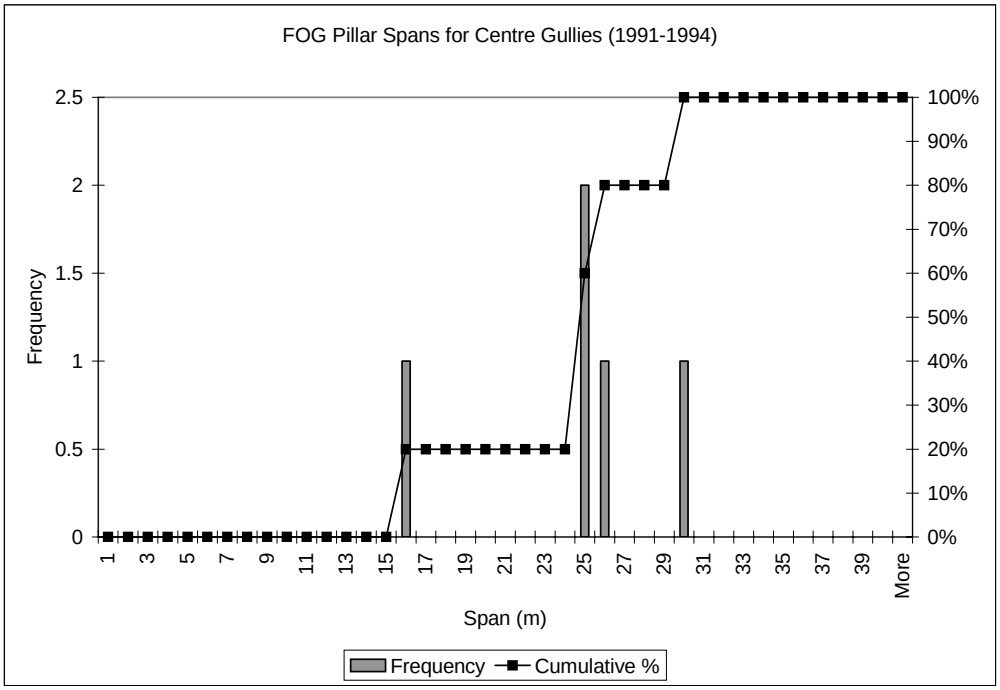

Figure H14 FOG pillar spans frequency and cumulative percentage for centre gullies (1991-1994)

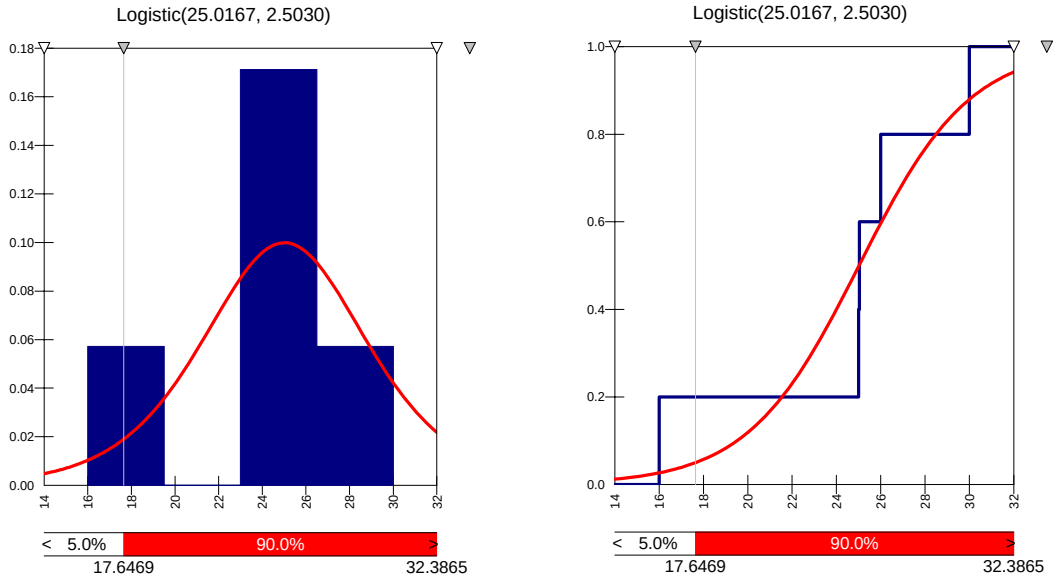

Figure H15 FOG pillar spans PDF and cumulative distribution for centre gullies (1991-1994)

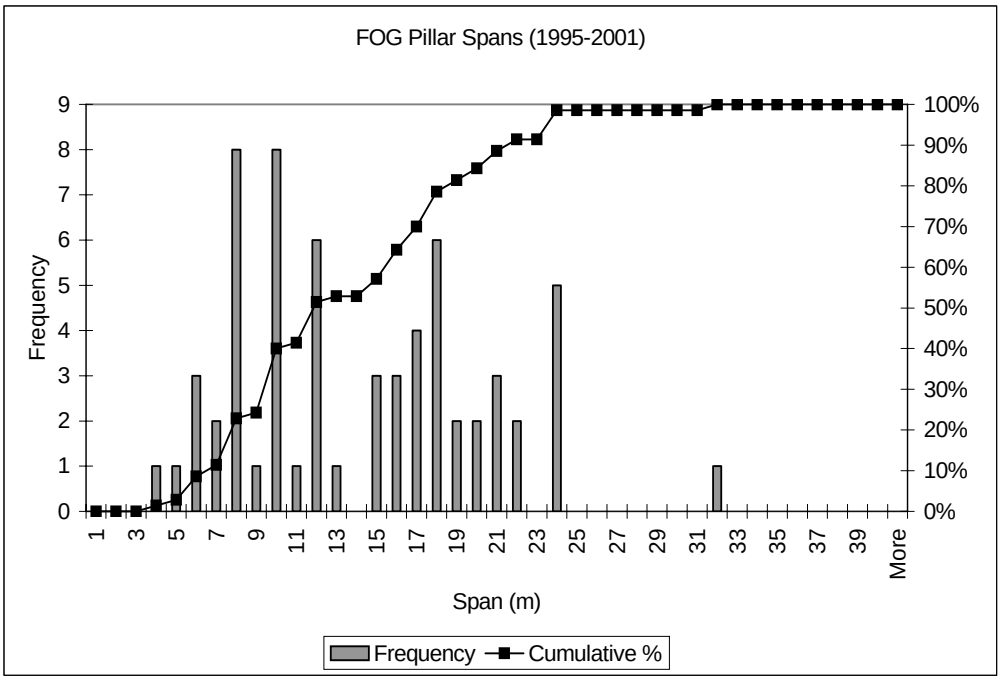

Figure H16 FOG pillar spans frequency and cumulative percentage (1995-2001)

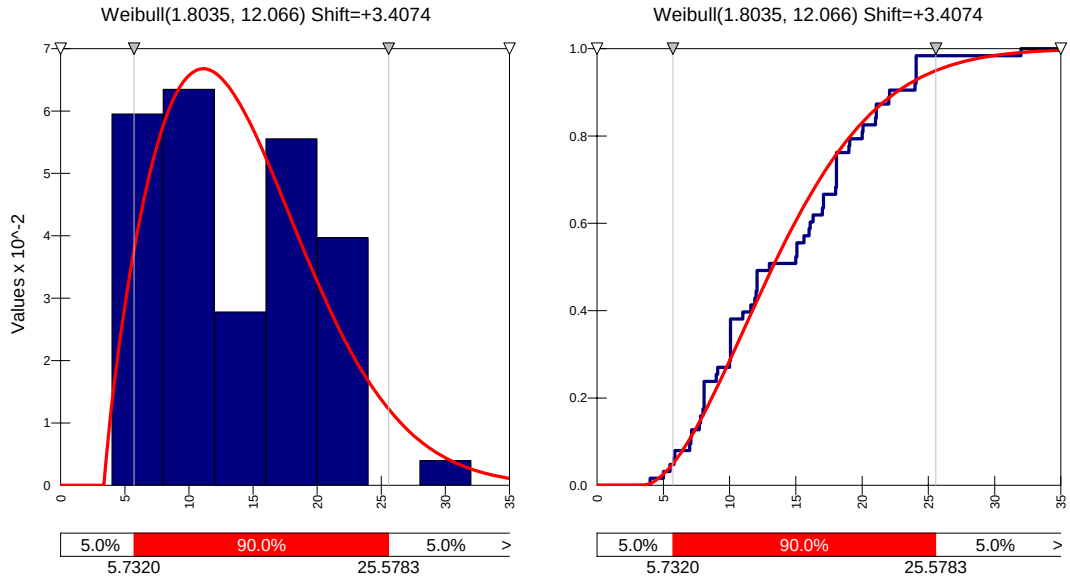

Figure H17 FOG pillar spans PDF and cumulative distribution (1995-2001)

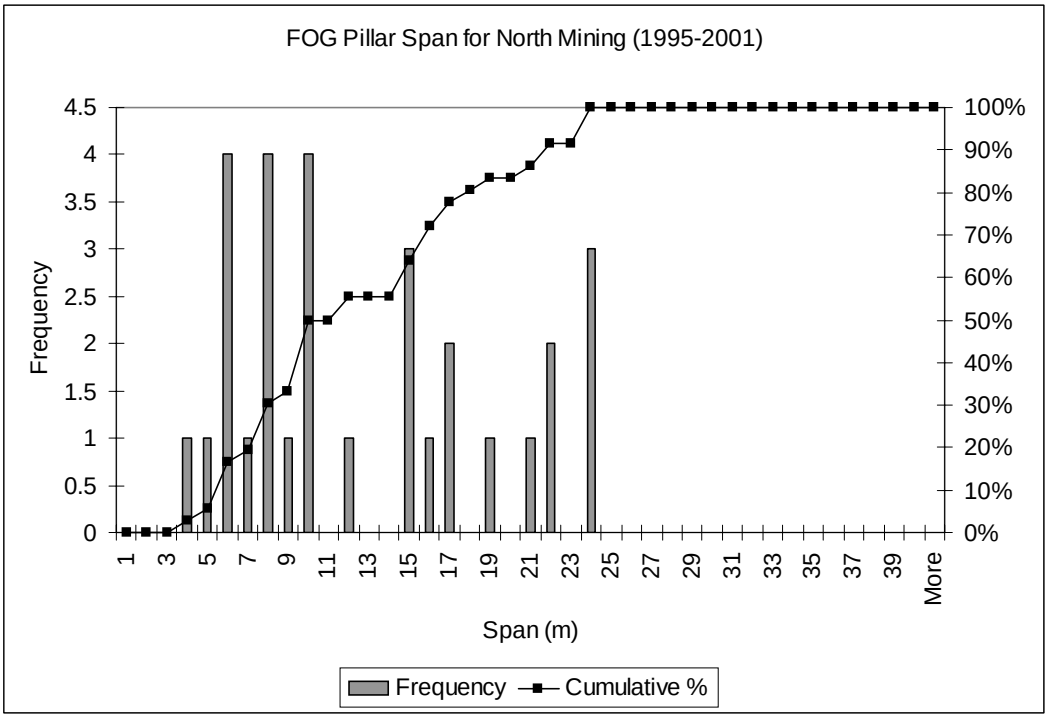

Figure H18 FOG pillar spans frequency and cumulative percentage for north mining (1995-2001)

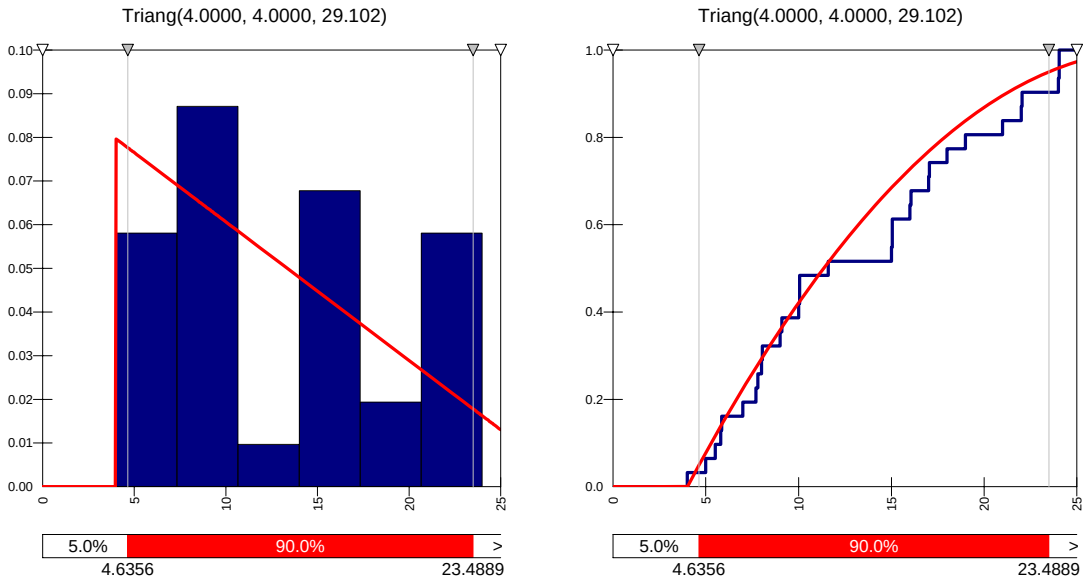

Figure H19 FOG pillar spans PDF and cumulative distribution for north mining (1995-2001)

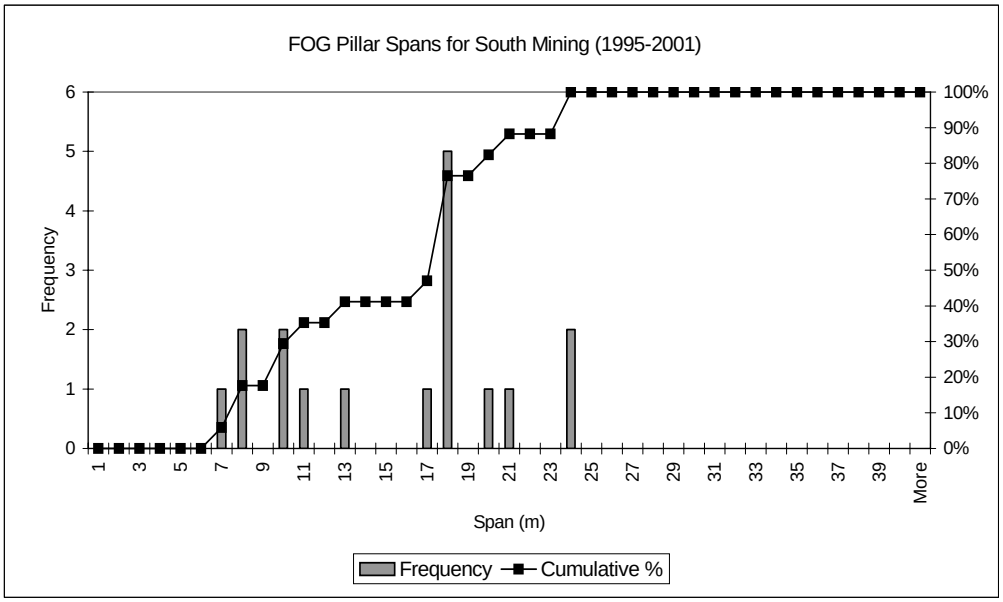

Figure H20 FOG pillar spans frequency and cumulative percentage for south mining (1995-2001)

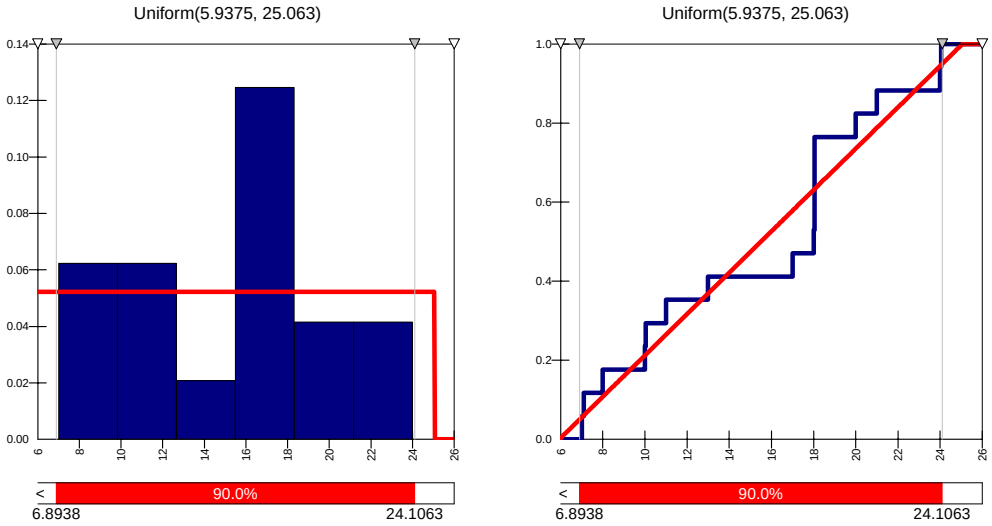

Figure H21 FOG pillar spans PDF and cumulative distribution for south mining (1995-2001)

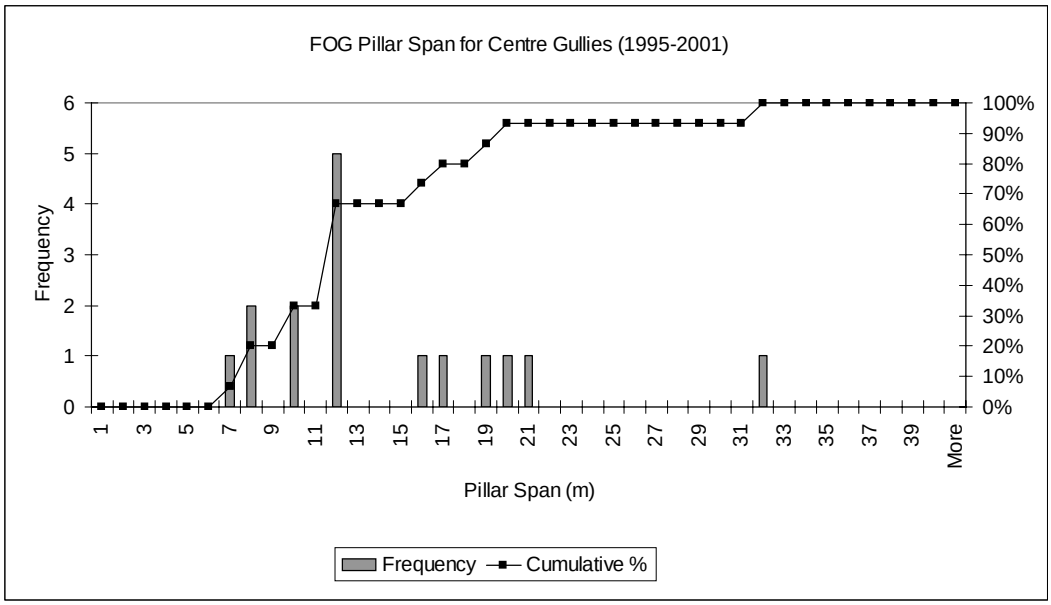

Figure H22 FOG pillar spans frequency and cumulative percentage for centre gullies (1995-2001)

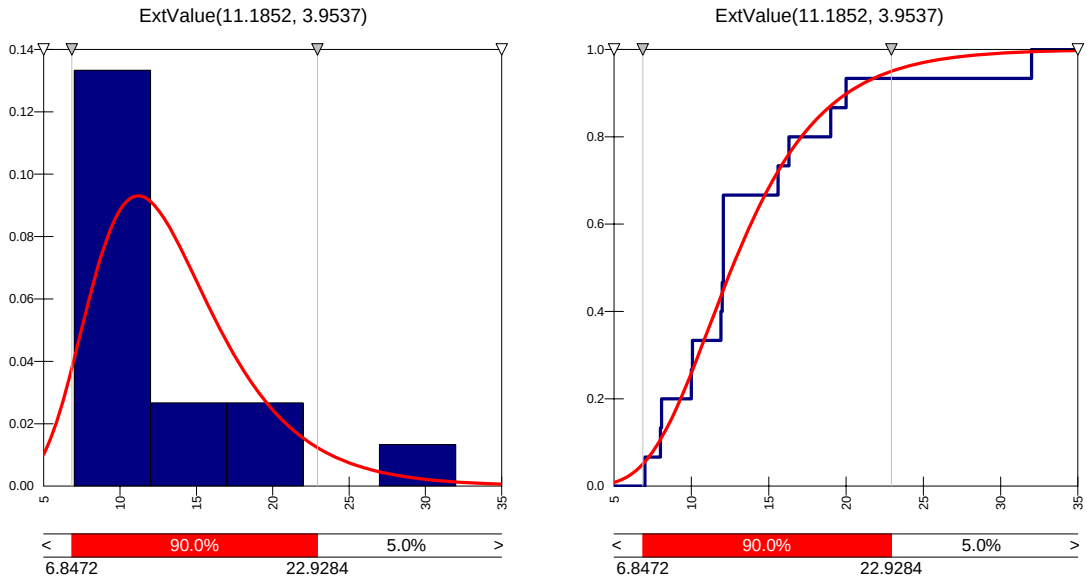

Figure H23 FOG pillar spans PDF and cumulative distribution for centre gullies (1995-2001)